

THE UNIVERSITY OF MANITOBA

**A NEW SHUNT STATIC REACTIVE POWER
CONTROL DEVICE AND ITS APPLICATIONS**

**BY
ADEL EZZAT A.M. HAMMAD**

A Thesis

*Submitted to the Faculty of Graduate Studies
in Partial Fulfilment of the Requirements for the Degree
of Doctor of Philosophy*

DEPARTMENT OF ELECTRICAL ENGINEERING

WINNIPEG, MANITOBA R3T 2N2

CANADA

March 1978

A NEW SHUNT STATIC REACTIVE POWER
CONTROL DEVICE AND ITS APPLICATIONS

BY

ADEL EZZAT A.M. HAMMAD

A dissertation submitted to the Faculty of Graduate Studies of
the University of Manitoba in partial fulfillment of the requirements
of the degree of

DOCTOR OF PHILOSOPHY

© 1978

Permission has been granted to the LIBRARY OF THE UNIVERSITY OF MANITOBA to lend or sell copies of this dissertation, to the NATIONAL LIBRARY OF CANADA to microfilm this dissertation and to lend or sell copies of the film, and UNIVERSITY MICROFILMS to publish an abstract of this dissertation.

The author reserves other publication rights, and neither the dissertation nor extensive extracts from it may be printed or otherwise reproduced without the author's written permission.



To my parents

ABSTRACT

Static shunt reactive power compensation schemes are being more and more widely considered for VAR control in power systems. They form in large a natural replacement for the traditional synchronous compensators with the promise of benefits in performance, reliability and cost.

A new generalized concept for static shunt VAR compensation is proposed which permits selection of an optimum design. With a slight increase in the VAR rating of the reactors this novel scheme should overcome the harmonics and thyristors rating problems of the existing devices.

A faithful analytical comparison with other known devices is made to show the superiority of the new device with respect to harmonics generation, control range and thyristor stresses during steady-state and overvoltage transient conditions.

In order to be able to verify the feasibility and the advantages of using thyristor controlled reactors in ac systems and at HVDC terminals different models are developed for the fundamental current behavior of these systems. A large scale load flow and transient stability program is developed based on these models and with unique features for the simulation of multi-terminal HVDC schemes and for ac/dc network solution algorithms. The program is then applied to various practical problems such as MANDAN to demonstrate the ability of static means for VAR control to enhance the performance of weak ac systems when connected to HVDC converters.

The application of thyristor controlled reactors at the terminals of superconducting generators is, for the first time, suggested and fully analysed.

The results of all the studies prove that the application of static reactive power schemes in ac and HVDC transmission systems do solve or reduce the major transmission problems; voltage control, and stability.

ACKNOWLEDGEMENTS

The author expresses deep gratitude to Professors R. M. Mathur and M. Z. Tarnawecky, Dr. P. C. S. Krishnayya and Mr. W. J. Tishinski for serving on his Advisory Committee. Special acknowledgement goes to Dr. P. K. Dash, former visiting professor with the Department of Electrical Engineering, University of Manitoba, for his valuable guidance and assistance in some parts of the research.

A very special word of thanks is reserved for Dr. R. M. Mathur, committee chairman, for his contagious enthusiasm as a scholar and educator. The author has benefited immensely from his association with Dr. Mathur and will appreciate such a relationship for many years to come.

The author also wishes to thank Dean L. M. Wedepohl of the University of Manitoba and Messrs. C. V. Thio and D. A. Woodford of Manitoba Hydro for their understanding and encouragement. Special appreciation is due to Mrs. M. Derry for her untiring effort in expertly typing the manuscript.

Thanks are also due to the National Research Council of Canada, the University of Manitoba and Manitoba Hydro Electric Board for a partial support and cooperation during the course of this research.

Finally, the author expresses sincere appreciation to his parents and his sisters Azza and Soumaya for their patience, interest, encouragement and love.

TABLE OF CONTENTS

		Page
	ABSTRACT	iii
	ACKNOWLEDGEMENTS	iv
	TABLE OF CONTENTS	v
	LIST OF FIGURES	vii
	LIST OF TABLES	xiv
	LIST OF MOST-USED SYMBOLS	xv
 Chapter		
<i>one</i>	INTRODUCTION	1
	1.1 General	1
	1.2 Reactive Power Systems, Critical Evaluation . .	4
	1.3 Reactive Power Control for ac Transmission Systems	15
 <i>two</i>	 A NOVEL DESIGN FOR THYRISTOR CONTROLLED VAR COMPENSATORS	 27
	2.1 Introduction	27
	2.2 Generalized System Equations	32
	2.3 Steady State Performance	33
	2.4 Fundamental Current and Reactors Rating	46
	2.5 Harmonic Analysis	49
	2.6 Overvoltage Transient Performance	63
	2.7 Guide Lines for the Selection of an Optimum Design	81
	2.8 Modeling For System Studies	85

Chapter	Page
<i>three</i> STATIC REACTIVE POWER CONTROL WITH HVDC SYSTEMS . . .	88
3.1 Reactive Power Control at ac/dc Junction Terminal	88
3.2 Short-Term Regulation Characteristics of ac/dc Junction Terminal	90
3.3 Application of Thyristor Controlled Reactors at the Terminals of HVDC Systems	108
3.4 AC Voltage Control Using a HVDC Converter Terminal	110
3.5 Conclusions	122
<i>four</i> APPLICATION OF THYRISTOR CONTROLLED REACTOR SYSTEMS WITH SUPER CONDUCTING GENERATORS	124
4.1 Introduction	124
4.2 System Under Study	126
4.3 Mathematical Modelling	128
4.4 Load Rejection Study	139
4.5 Small Signal Dynamic Stability	140
4.6 Large Signal Transient Stability	154
4.7 Conclusions	159
<i>five</i> MAJOR CONTRIBUTIONS	161
Appendix A: Power System Digital Simulation Program (A Load Flow and Transient Stability Program for Power Systems with Multi-Terminal HVDC Schemes and Static VAr Compensators)	163
BIBLIOGRAPHY	177

LIST OF FIGURES

Figure	Page
1.1 Gap Connected Reactors	7
1.2 Single Phase Transductor Schematic Diagram	7
1.3 Saturated Reactor Scheme	10
1.4 Saturated Reactor Steady State Characteristics	10
1.5 Thyristor Switched Reactors	13
1.6 Thyristor Switched Capacitors Scheme	13
1.7 Power Frequency Voltage Profile (Line opened at Dorsey).	19
1.8 Power Frequency Voltage Profile (DC commutation failure at Dorsey)	20
1.9 Transmission System Models	
(a) System with fixed compensation	22
(b) System with controlled static compensation	22
1.10 Power Angle Characteristics	23
1.11 Phase-Plane of System (a) Fixed Reactors	24
1.12 Phase-Plane of System (b) Static Compensator	25
1.13 Swing Curves for 75.0 msec. Line Reclosure for Systems (a) and (b)	26
2.1 Single-Phase Schematic of a Known Design of a Controlled Reactor	29
2.2 Voltage and Currents for the Scheme in Figure 2.1	29
2.3 Basic Realization of UM-Concept	29
2.4 Voltage and Currents for the Scheme in Figure 2.3	29
2.5 Arrangement of the Proposed UM-Concept	29

Figure	Page
2.6 Schematic Diagram for the Generalized UM-Concept for a 3-phase Reactor Compensator	30
2.7 Voltage and Currents for One Phase, $\alpha = 130^\circ, y = 0, z = 0$	42
2.8 Voltage and Currents for One Phase, $\alpha = 130^\circ, y = 0, z = 1$	42
2.9 Voltage and Currents for One Phase, $\alpha = 130^\circ, y = 0.3, z = 0.7$	43
2.10 Voltage and Currents for One Phase, $\alpha = 80^\circ, y = 0.3, z = 0.7$	43
2.11 Voltage and Currents for One Phase, $\alpha = 80^\circ, y = 0.0, Z = 0.0$	45
2.12 Voltage and Currents for One Phase, $\alpha = 110^\circ, y = 0.0, z = 1.0$	45
2.13 Variation of Reactive Power with Control Angle for Various Designs	48
2.14 Total Rating of Reactors for Various Designs	50
2.15 Magnitude of Harmonics in Line Current for: $y=0, z=0$	54
2.16 Magnitude of Harmonics in Line Current for: $y=0, z=1$	54
2.17 Magnitude of Harmonics in Line Current for: $y=0.3, z=0.7$	55
2.18 Magnitude of Harmonics in Line Current for: $y=0.1, z=0.9$	55
2.19 Magnitude of Harmonics in Line Current for: $y=0.2, z=0.8$	56

Figure	Page
2.20 Magnitude of Harmonics in Line Current for: y=0.4, z=0.6	56
2.21 Magnitude of Harmonics in Line Current for: y=0.5, z=0.5	57
2.22 Magnitude of Harmonics in Line Current for: y=0.6, z=0.4	57
2.23 Magnitude of Harmonics in Line Current for: y=0.8, z=0.2	58
2.24 Magnitude of Harmonics in Line Current for: y=1.0, z=0.0	58
2.25 Peak Value of the 5th Harmonic Current for Various Designs	59
2.26 Peak Value of the 7th Harmonic Current for Various Designs	60
2.27 Presence of a 5th Harmonic Current Magnitude Over a Percentage of the Operating Range for Various Designs	61
2.28 Presence of a 7th Harmonic Current Magnitude Over a Percentage of the Operating Range for Various Designs	62
2.29 Description of the Assumed Overvoltage	65
2.30 Maximum Peak of Transient Valve Current for Sudden and Assumed Overvoltages (1.70 p.u.)	65
2.31 Maximum Peak of Transient Valve Current for Different Initial Control Angles	66

Figure	Page
2.32 Transient Performance Subsequent to Overvoltage for $\alpha = 180^\circ, y=0, z=0$	
(a) Valve voltages	68
(b) Valve currents	69
(c) Line currents ($y=0, z=0$)	70
(d) Line currents ($y=0, z=1.0$)	71
2.33 Transient Performance Subsequent to Overvoltage for $\alpha = 180^\circ, y=1, z=0$	
(a) Valve voltages	72
(b) Valve voltages	73
(c) Valve currents	74
(d) Line currents	75
2.34 Transient Performance Subsequent to Overvoltage for $\alpha_0 = 180^\circ, y=0.3, z=0.7$	
(a) Valve voltages	76
(b) Valve voltages	77
(c) Valve currents	78
(d) Line currents	79
2.35 System model of a Thyristor Controlled Reactor	86
3.1 (a) System model	91
(b) Synchronous compensators stability regions	91
3.2 Equivalent Circuit Diagram of a HVDC Inverter Terminal Station in a 3-phase System	94
3.3 Short-term Inverter Regulation Characteristics (S.C.R. = 2.0)	99

Figure	Page
3.4 Short-term Inverter Regulation Characteristics (S.C.R. = 2.0)	100
3.5 Short-term Inverter Reactive Load Characteristics (S.C.R. = 2.0)	101
3.6 Regulation Characteristics for S.C.R. = 4.0	102
3.7 Short-term Regulation Characteristics for Different Values of Short Circuit Ratio	103
3.8 Reactive Power Characteristics for an Inverter Terminal with Constant Extinction Angle of 18°	104
3.9 Short-term Regulation Characteristics with a System S.C.R. = 1.0 and a Static Compensator of 10% Effective Reactance Slope	105
3.10 AC Terminal Voltage Time Response for a 50% dc Load Rejection	107
3.11 MANDAN Transmission Scheme, ac/dc Alternative	111
3.12 AC Voltage at Fargo for a 3 ϕ Fault at Center	112
3.13 Machine Rotor Angle at Center	112
3.14 MANDAN Transmission Scheme, dc Alternative with Tapping at Fargo	113
3.15 AC Voltage at Fargo for a 3 ϕ Fault at Center	114
3.16 Machine Rotor Angle at Center	114
3.17 A 3-Terminal HVDC Alternative for MANDAN Transmission Scheme	117
3.18 Steady State Characteristics for Dorsey Rectifier with dc Current Control	118

Figure	Page
3.19 Steady State Characteristics for Dorsey Rectifier with DC Voltage Control	118
3.20 AC Voltage at Dorsey Following Blocking of BP1	119
3.21 Machine Rotor Angle at Dorsey Following Blocking of BP1	119
3.22 Reactive Power Absorbed by MANDAN Rectifier at Dorsey	120
3.23 DC Power of MANDAN Rectifier at Dorsey	120
3.24 DC Voltage of MANDAN Rectifier at Dorsey	121
3.25 Firing Angle of MANDAN Rectifier at Dorsey	121
4.1 Super-conducting Machine System	127
4.2 Thyristor-controlled Reactor Model	130
4.3 Voltage Regulator for Field Forcing	141
4.4 Terminal Voltage Response Following Load Rejection	141
4.5 Machine Rotor Speed Deviation Following Load Rejection	142
4.6 Field Voltage Response for Various Control Methods	143
4.7 Reactive Power Absorbed by the Static Compensator	144
4.8 Dominant Eigenvalues for Variations in τ_p and τ_s with Field Forcing:	
(a) for stabilizer gain $K_{we} = 0.0$	147
(b) for stabilizer gain $K_{we} = 0.1$	147
4.9 System Dominant Eigenvalues for Variations in τ_p and τ_s with Static Compensator:	

Figure	Page
4.9 (Continued)	
(a) for stabilizer gain $K_w = 0.0$	148
(b) for stabilizer gain $K_w = 0.1$	148
4.10 System Damping with:	
(a) Field forcing, $K_{we} = 0.1$	149
(b) Static compensator, $K_w = 0.1$	150
(c) Static compensator, $K_w = 0.2$	151
4.11 Small Signal Dynamic Response for:	
(a) $\tau_p = 0.5, \tau_s = 0.2$	152
(b) $\tau_p = 2.0, \tau_s = 0.5$	153
4.12 Variation in Rotor Angle for 3-phase Fault,	
$\tau_p = 2.0, \tau_s = 0.5$	155
4.13 Variation of Field Current for 3-phase Fault	156
4.14 Variation in the Total Reactive Power of the	
Compensator	157
4.15 Variation in the Generator Terminal Voltage	158
A.1 Simplified Flow Chart of ac/dc Transient	
Stability Program	165
A.2 Functional Diagram of Local and Central Controllers	
of a HVDC Scheme	171
A.3 Generalized Model for Static VAr Compensators	172

LIST OF TABLES

Table	Page
2.I Expressions for Steady-state Currents and Voltages:	
(a) $0^\circ \leq \alpha \leq 30^\circ$	36
(b) $30^\circ \leq \alpha \leq 60^\circ$	37
(c) $60^\circ \leq \alpha \leq 90^\circ$	38
(d) $90^\circ \leq \alpha \leq 120^\circ$	39
(e) $120^\circ \leq \alpha \leq 150^\circ$	40
(f) $150^\circ \leq \alpha \leq 180^\circ$	41
2.II Per-unit Fundamental and Harmonic Components of Line Current	52
2.III A Comparative Evaluation of Key Performance Indices of Various Designs	82

LIST OF MOST-USED SYMBOLS

E_T	Synchronous or static VAR compensator model source Voltage (p.u.)
e_d, e_q	Direct and quadrature components of terminal voltage (p.u.)
e_f	Super conducting field voltage (p.u.)
f_0	Rated synchronous frequency (Hz)
G	Conductance (p.u.)
H	Inertia constant (sec.)
I_1	Magnitude of fundamental component of line current (p.u.)
I_n	Magnitude of nth harmonic component of line current (p.u.)
i_1, i_2, \dots	Instantaneous currents of thyristors T_1, T_2, \dots
i_A, i_B, i_C	Instantaneous 3-phase line currents (p.u.)
i_{dL}, i_{qL}	Direct and quadrature components of load current (p.u.)
i_d, i_q	Direct and quadrature armature current components (p.u.)
i_f	Super conducting field current (p.u.)
$i_{pd}, i_{pq}, i_{sd}, i_{sq}$	Direct and quadrature currents of screening and damping shields (p.u.)
K_α, K_w	Controller and stabilizer gains of a static compensator
K_e, K_{we}	Field forcing regulator and stabilizer gains
L	Inductance (p.u.)
N	Number of series bridges of a HVDC converter
n	Harmonic order
P_d	DC power (p.u.)
P_m	Mechanical power (p.u.)
p	d/dt operator

Q_c	Reactive power of a shunt capacitor (p.u.)
Q_d	Reactive power absorbed by a HVDC converter (p.u.)
Q_r	Reactive power absorbed by a thyristor controlled reactor (p.u.)
R	Resistance (p.u.)
T	HVDC converter transformer taps
T_e, T_m	Electrical and mechanical torques (p.u.)
t	Time (sec.)
V_a	RMS ac voltage (p.u.)
V_b	RMS ideal supply voltage (p.u.)
V_T	RMS terminal ac voltage (p.u.)
V_d	DC voltage (p.u.)
V_{ref}	Reference voltage (p.u.)
V_A, V_B, V_C	Instantaneous 3-phase line voltages (p.u.)
X or X_T	Total reactance of thyristor controlled reactor (p.u.)
X_s	Synchronous or static compensator model reactance (p.u.)
X_e	Equivalent reactance of an ac system (p.u.)
x_1, x_2, x_3	Reactors of a Generalized UM-Concept for thyristor controlled reactors
x_d, x_q	Direct and quadrature armature reactances of a generator (p.u.)
x'_d, x''_d, x'''_d	Transient and subtransient reactances of a super conducting turbo generator (p.u.)
x_f, x_p, x_s	Reactances of field & screening and damping shields of a super conducting turbo generator (p.u.)
Y	Admittance (p.u.)

α	Firing (or control) angle of thyristor
β	Advance angle of an inverter
γ	Extinction angle of a HVDC inverter
δ	Rotor angle
θ	Voltage angle
ϕ	Power factor angle of a dc converter
ψ_d, ψ_q	Direct and quadrature components of flux linkages
ψ_f	Super conducting field flux linkage
$\psi_{pd}, \psi_{pq}, \psi_{sd}, \psi_{sq}$	Direct and quadrature flux of screening and damping shields
τ_α	Controller time constant of a static compensator system
τ_f, τ_p, τ_s	Time constants of field, screening and damping shields
ω	Angular speed (rad/sec)
ω_0	Rated synchronous angular speed (rad/sec)
ζ	Damping ratio
Δ	A small change in a variable

chapter one

INTRODUCTION

1.1 General

Controlling the reactive power generation and flow in an energy transmission system is of an immense importance. The influence of the balance and flow of reactive power in EHV transmission lines in terms of voltage is easy to visualize. External sources and sinks of reactive power provided at chosen points in a transmission network are therefore used for controlling the voltage and the power transmission efficiency and capability. Fixed elements (capacitors or reactors) have an inherent generation or absorption characteristics dependent upon terminal voltage and hence are of limited effectiveness. The availability of fully controllable VAR systems multiplies the value of reactive power control by providing an alternative method of system stabilization in addition to an optimum control of voltage and power transmission capability.

While the virtue of reactive power control is easy to visualize for an ac transmission system it is not very difficult to see its value for an ac/dc system. A HVDC converter requires, for its commutation process, an amount of reactive power which is dependent upon the active power transmitted on the dc side and which must be supplied from the ac side. Fully controllable reactive power sources at the HVDC converter terminals are, therefore, the best choice to enhance the performance of both ac and dc systems.

Up till now synchronous compensators have been the major

fully controllable reactive power device. However, during the last few years a number of static reactive power compensators have emerged which appear to be technically superior to the traditional synchronous compensators in many ways and are economical too. Hence, a systematic evaluation of the performance of the static VAr controlling devices and that of the system in which they are employed is very timely and much needed.

The research work described in this thesis is devoted to this end and has resulted in the following major contributions:

- (1) A new design of thyristor phase-controlled static VAr compensator has been invented which upon analysis is shown to be superior when compared to those available. In this connection a generalized concept has been put forward which permits selection of an optimum design.
- (2) The application of static VAr compensation systems at the converter terminals of interconnected ac/dc networks has been thoroughly investigated and in the process a large scale load flow and transient stability program for power systems incorporating multiterminal dc schemes has been developed.
- (3) While investigating the application of static VAr compensators, for the first time a suggestion has been made and fully analysed for their application at the terminals of a superconducting alternator.

The major emphasis of the thesis is, thus, on the development of a new type of compensator and its novel applications.

In Section 1.2 of this chapter a summary and brief critical evaluation of available VAR compensators are presented. Section 1.3 deals briefly with the application of VAR compensators in ac transmission systems. This part of the investigation has been kept very brief on purpose keeping in view the reporting of the major contributions.

Chapter 2 is devoted to the development and analysis of the new type of thyristor phase controlled VAR compensator.

Chapters 3 and 4 investigate the impact of applications of static means of reactive power control at the terminals of HVDC converters and superconducting alternators respectively. The overall conclusions and major contributions achieved in the thesis are summarized in Chapter 5.

1.2 Reactive Power Systems; Critical Evaluation

In the following an evaluation of the known types of reactive power systems is undertaken.

1.2.1 Rotating Synchronous Machines^{2,3,4}

Excitation control of a synchronous machine connected to an ac bus allows a controlled reactive power supply. The machines specially designed for the control of reactive power are known as synchronous compensators.

Typically a synchronous compensator when under-excited can absorb about half of its over-excited MVA rating.

The response time for changing its output from no-load to rated reactive load is generally in the range from 0.10 to 2.00 seconds depending on the field time constant, excitation system and voltage regulator of the machine and the nature of the network disturbance initiating the change.

Unlike static devices, synchronous compensators have stored kinetic energy in their rotors, and hence can exhibit transient oscillations of real power about a mean value of zero, during or following disturbances.

However, starting of such a machine can create a substantial voltage dip, and when running, the synchronous compensator due to its inertia has its own stability problem in the event of a system fault.

A synchronous compensator reduces the system reactance while it regulates the reactive power.⁶

Reduction of system equivalent Thevenin's reactance minimizes the alternating voltage phase angle fluctuations in case of any disturbance, it, however, causes an increased short circuit level and circuit breaker duty.

The high capital investment, running and maintenance costs and losses of a synchronous compensator add to its shortcomings and must also be taken into account for the selection of compensators.

1.2.2 Static Compensators^{1,5}

Generally these types of shunt VAR compensators do not contribute to the system short circuit capacity, have lower initial investment and losses per KVAR and are less costly to operate and maintain compared to synchronous compensators. Static compensators can be divided into two main classes: Fixed Elements and Controllable Devices.

i. Fixed Elements

(a) Shunt Capacitors:⁷

Shunt Capacitor banks are used with mechanical switches to compensate the inductive reactive power at HVDC terminals or major load terminals in order to maintain the ac voltage at the rated value.

It may however lead to excessive voltage rise on account of a sudden loss of load.

(b) Linear Shunt Reactors:^{7,8}

The inductance of these reactors is independent of their loading. They often are air-cored or gapped type reactors.

Permanently connected linear reactors are used to compensate the excessive capacitive reactive power on long ac transmission

lines and thus suppressing the voltage along the line and its terminals under light load conditions. This, however, reduces the maximum power transfer capability of the line.

Optimum line compensation requires shunt reactors to be switched out of service under heavy load transmission. This leaves the system open to transient overvoltages in case of a severe loss of load in addition to an undesirable step voltage variation due to switching-in of the reactors.

(c) Saturable (or Saturation) Shunt Reactors:^{9,10}

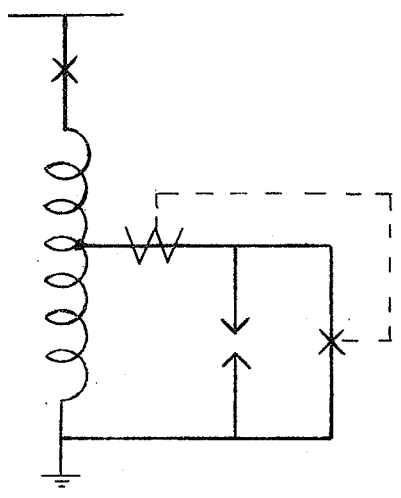
This refers to the EHV line connected reactors with a saturation knee at 1.1 the normal system voltage, thus restricting power frequency overvoltages under abnormal conditions.

The non-linear reactor is less effective in limiting instantaneous overvoltages than it might seem, since a specific voltage-time area is required for changing the reactor magnetic state. Furthermore, with linear transmission systems this type of reactor, in conjunction with the saturation effects of transformers, introduces some risk of sub-harmonic instabilities because overvoltages are possible due to partial shunt compensation not eliminating the Ferranti effect under light-load conditions.

(d) Gap-Connected Shunt Reactors:¹¹

An arc gap is used to either switch a line shunt reactor in or out. The reactor assembly may take either form (a) or (b) as shown in Figure 1.1. The gaps are shunted by circuit breakers which are switched on by a trigger derived from the gap breakdown current.

(a)



(b)

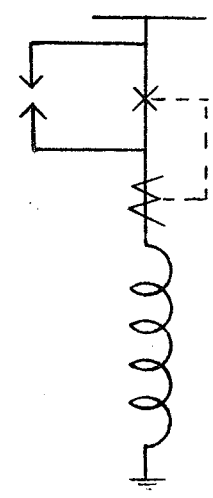


Figure 1.1 Gap connected reactors

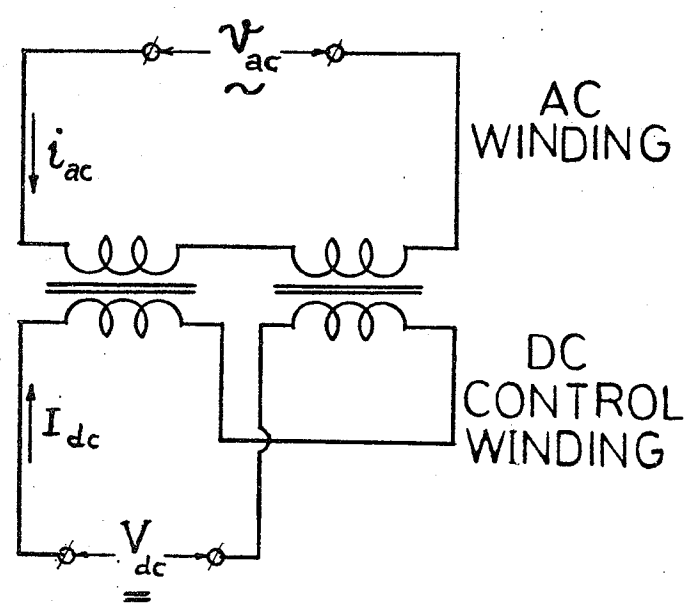


Figure 1.2 Single phase transductor schematic diagram

At first sight such a device may appear trivial. However, a number of studies (as will be discussed in Chapter 4) show that in many applications, involving severe disturbances, even controllable static VAR compensators behave in a bang-bang fashion.

Gap connected reactors provide an economic but crude compensation means.

ii. Controllable Devices

(a) Transductors:^{12,15}

A transductor is a reactor with direct current controlled saturation, i.e. the effective reactor impedance and the primary alternating current are controlled by a direct current fed into a separate winding. (Figure 1.2)

The increase of direct current causes an increase of the unidirectional flux in the reactor iron cores. As a consequence the superimposed alternating flux tops are raised beyond the magnetic saturation limits giving rise to the fundamental alternating current nearly proportional to the dc current.

Odd current harmonics are generated in the ac circuit while even harmonics are produced in the dc control circuit.

Another device can be used utilizing the principle of a rotating magnetic field created by a 3-phase wound stator.¹³ The saturation level of the magnetic circuit of the stationary rotor is controlled by dc winding.

The stator windings and slots are arranged in such a way that the alternating current contains minimum amount of harmonics.

The above controlled saturation compensators have the major drawback of slow response compared to the other types of controllable compensators due to the dc circuit time constant and the dead time required to build up the direct flux in the magnetic core. However, when a thyristor rectifier with a high ceiling voltage for forcing the control current is used, total time to change the primary ac current can be substantially reduced.

Unfortunately, under system fault conditions the dc control winding is difficult to protect.

(b) Saturated Reactors: (inherently controlled devices)¹³⁻²⁹

The saturated reactor is designed to operate in the saturated region at normal operating voltages. With a series and shunt capacitors combination it automatically varies the reactive power output over a wide range and holds the terminal voltage constant.

The device elements and the corresponding V-I characteristics are illustrated in Figures 1.3 and 1.4 respectively.

Special measures must be taken; especially for applications in weak ac systems, to decrease the high current harmonic content due to the saturated reactor and to avoid the possibility of ferroresonant sub-harmonic instability arising from the presence of the slope correcting series capacitor.

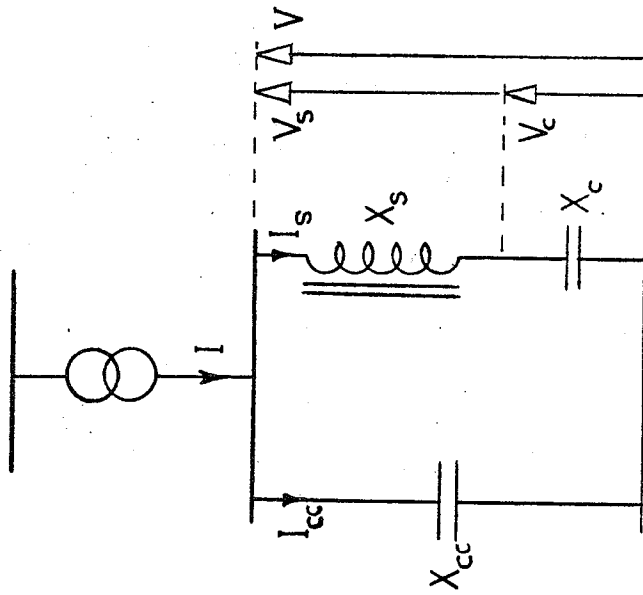


Figure 1.3 Saturated reactor scheme

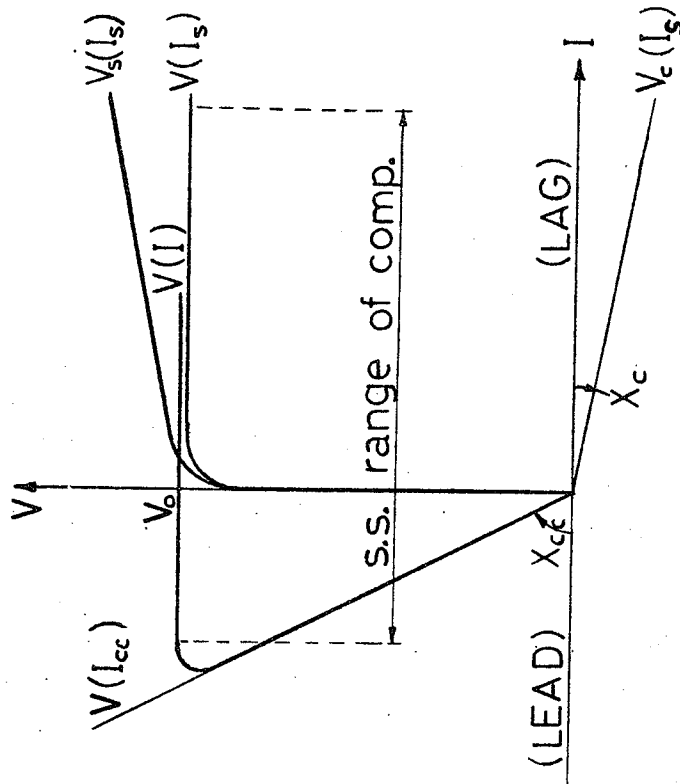


Figure 1.4 Saturated reactor steady state characteristics

In this regard, techniques employing complex multi-core, multi-winding designs are used to cancel the current harmonics internally by suitable choice of the flux phase-shifts between cores and by an appropriate flow of the magnitude of triplen harmonic currents in the secondary windings. (e.g. Quin, Twin-tripler and treble-tripler types of harmonic compensated ac saturated reactors.)

However this multiphase construction reduces the potentiality of the device for unsymmetrical compensation of unbalanced loads. Although the transient response of the compensator is of the order of one to two cycles of the supply voltage, capacitive compensation of the slope reactance introduces transiently higher reactances. When the current through the slope correcting capacitor exceeds a predetermined value, during a transient overvoltage condition, part or all of the latter may be short circuited, thus increasing the slope of the compensator from $(X_S - X_C)$ to X_S (in Figures 1.3 and 1.4) or to some intermediate value.⁵

(c) Thyristor-Switched Shunt Reactors:

Thyristor valves are used as fast switches to connect, in a coordinated manner, a number of shunt reactors in small steps (Figure 1.5). The switching is performed at voltage peaks to avoid dc current components injected into the ac system. This form of discrete control requires a large number of components and hence increases the cost and deteriorates the reliability of the device.

(d) Thyristor Phase-Controlled Reactors:³⁰⁻³⁸

A smoother control of reactive power is achieved by using thyristor phase-angle control of current through a linear reactor. In an alternative design, the linear reactor is an integral part of the connecting transformer (Reactor Transformer). This type of compensator is of major interest in this investigation and is dealt with in greater detail in Chapter 2.

(e) Thyristor-Switched Capacitors:^{39,40}

Generally, transient inrush currents and high harmonic generation preclude the use of phase-angle control of a shunt capacitor. Instead, the capacitor bank is split into a number of small units which are switched individually on or off by thyristors.

The scheme as shown in Figure 1.6 employs the following elements:

- In series with each switched capacitor bank there is a small air-cored reactor to limit the rate of rise of the current through the thyristors depending on misfiring and to avoid resonance with the network.
- In parallel with the switched capacitor banks fixed capacitor and reactor are installed to give optimum operating range.

When capacitors are not connected, they are maintained charged to the positive or negative peak value of the voltage by regularly switching them in for very short durations.

The switching instant is selected at the time when the network voltage across each arm corresponds to the magnitude

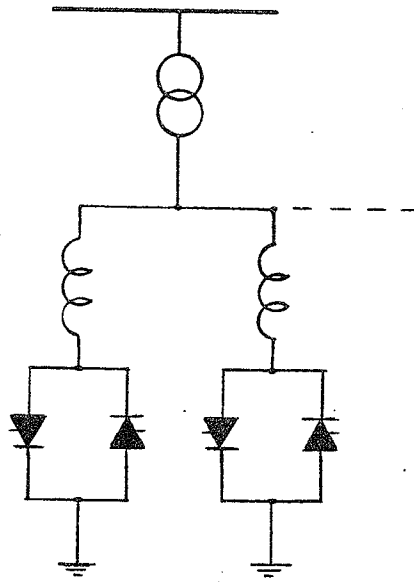


Figure 1.5 Thyristor switched reactors

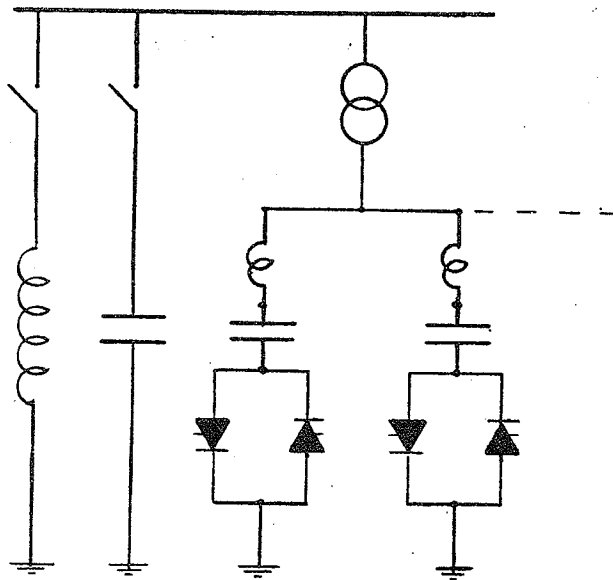


Figure 1.6 Thyristor switched capacitors scheme

and polarity of the capacitor voltage. This ensures that the connection takes place at the natural zero crossing of the capacitor current.

The capacitor is disconnected through the suppression of the gate trigger pulses of the thyristors so that the thyristors carrying current will block as soon as the current becomes zero.

This type of compensator has the following major drawbacks:

- 1) The capacitors are kept charged at the peak value of "normal" voltage so when system voltage reduction occurs and VAR assistance is needed, the charged capacitors have to be switched in to a lower voltage resulting in an injection of transient inrush currents and harmonics in the faulted system.
- 2) In the case of a complete collapse of ac voltage at the compensator terminals for a period of time, long enough to discharge the capacitors, problems of switching transients arise when the system is energized.
- 3) The capacitors used are of the ac type which are less suitable for direct voltage but are subjected to dc voltage in the stand-by state; therefore provisions have to be made to repolarise them at regular intervals simulating a low frequency alternating voltage, which complicates the controls of the thyristor valves.

Generally, controlled static VAR compensators, except the saturated reactor, provide possibilities for various forms of control signals based on voltage, current and active and reactive power flow at one or more points of the line as well as on their individual or combined functions.^{31,32-40}

A reactive power compensation scheme employing thyristor controlled reactor although has no reactance slope correction capacitors, the function of its control system is essentially one of slope correction. Such a scheme has the advantage that effective reactance slope correction is obtained at very low electronic circuit power levels rather than at higher power levels in case of dc controlled saturation reactors or even at the full power rating of the compensator as in the case of saturated reactors.

The uncompensated slope reactance of the thyristor controlled reactor is 1.0 p.u. as compared to a typical value of 0.12 p.u. for a saturated reactor and therefore the sub-transient reactance effect may be more significant in the former case.²⁹ However, the slope correcting capacitor used in series with the saturated reactor can cause sub-synchronous resonance by making the natural frequency of the compensated line match with one of the sub-synchronous natural frequencies of the machines connected to it.^{28,29}

Also there is a time lag of about 0.02 sec for the slope correcting capacitor which is, generally, required to be switched off when its current (or voltage) exceeds a certain limit during a transient over-voltage condition thus increasing the slope reactance of the device.⁵

1.3 Reactive Power Control for AC Transmission Systems

Many problems, in the steady or the dynamic state, are intimately connected with the balance and flow of reactive power in EHV ac energy transmission systems. Consequently it is one of the major duties of the reactive power compensation scheme to control the VAR flow

during steady state condition to provide an optimum voltage profile of the system with respect to the transmission losses and maintain voltage limits at individual network nodes.

In order to avoid temporary excess voltage, e.g. transient and dynamic overvoltages on EHV long line terminating components arising from line energization, re-energization and load rejection or on the ac side of a dc converter station during load rejection, steady state reactive power flow conditions should be maintained as far as possible or restored as quickly as possible.⁴²

With the limited availability of rights-of-way and also owing to the cost of lines, keeping the transfer capability of the system as high as possible is a main objective for any designer.

Therefore, another duty of reactive power compensators in EHV systems is to adjust the VAR infeed in such a way that the active power transmission capability of the lines, particularly when long lines are involved, is utilized to an optimum. This also requires correct voltage maintenance at the delivery end and, if necessary, at substations along the line.⁴¹ This is achieved through the availability, during maximum loading, of enough VAR's such that system frequency voltage variations could be limited in cases of transient power fluctuations, switching surges or faulted conditions.

Until very recently, generators in power transmission systems were used to control the reactive power infeed. However, dynamic overvoltages associated with load rejections are essentially caused by high machine internal voltage and may be aggravated by the generator overspeed. Self-excitation problems can appear if reactive generation of the line

exceeds the reactive absorption capability of the machines connected to the sending end. The overvoltages resulting from self-excitation are dangerous not only for the system but also to the machines and transformers. This condition must definitely be avoided either by increasing the generating capacity or, simply, by line shunt compensation.

Dynamically any system running near the peak of a steady state stability limit will become unstable under the impact of short circuits which will produce phase angles in the range beyond this limit.² Due to the inertias involved at both ends of the line, for dynamic stability to be secured, the lines should be made capable of transmitting more than the pre-fault power up to the point of maximum angular overswing. This implies that it is generally necessary that the voltage along a very long line can recover near to its normal value after the fault is removed.^{4,3} This is possible only if sufficient shunt capacitive power is supplied to compensate for the increased line reactive power consumption caused by the greatly increased line current at large phase angles. This can be achieved either by operating the line sufficiently below its surge impedance power - which is an uneconomical solution - or by adding capacitive power transiently for the period in which the phase angle across the line will be abnormally increased.^{1,6} However, without adequately fast VAR control either solution can lead to dangerous overvoltages particularly under the conditions of a severe "back-swing", i.e. a phase condition when the power transmitted is much less than the pre-fault level.

If non-controllable compensating equipment is used for obtaining a favourable reactive power flow in the steady-state it has an

adverse effect on the system under transient conditions and vice versa.

Two digital computer studies have been carried out to illustrate the positive effects of employing static shunt reactive power controllers in ac transmission systems.

- (1) Using Manitoba-U.S. interconnected system as a model, an evaluation of different alternative shunt compensation schemes was investigated based on the dynamic overvoltages arising from full load rejection through the main ac tie line or commutation failure of the interconnected dc link inverter terminal.⁴⁴

Figures 1.7 and 1.8 show some sample results.

The main conclusion of the study is that static shunt compensators are inherently effective in limiting overvoltages. They not only give an optimum voltage profile at all loads, but also make maximum use of long lines capacitance and permit the addition of shunt capacitors to boost maximum power. Also, the appropriate location of the compensator is of particular value.

- (2) The two machine system model shown in Figure 1.9 has been used to study qualitatively the effect of static reactive power shunt compensation on the steady-state, transient and dynamic stability of a long ac tie line, irrespective of the type of compensator used.

It is apparent from the resulting Power/Angle characteristics shown in Figure 1.10 that the steady-state stability limit is increased and an improvement in the transient stability limit (evaluated by the equal area criteria)²¹ is possible in case of static VAR compensation schemes.^{29,41} However, the gain achieved is limited by the finite rating of the compensator in the capacitive range compared

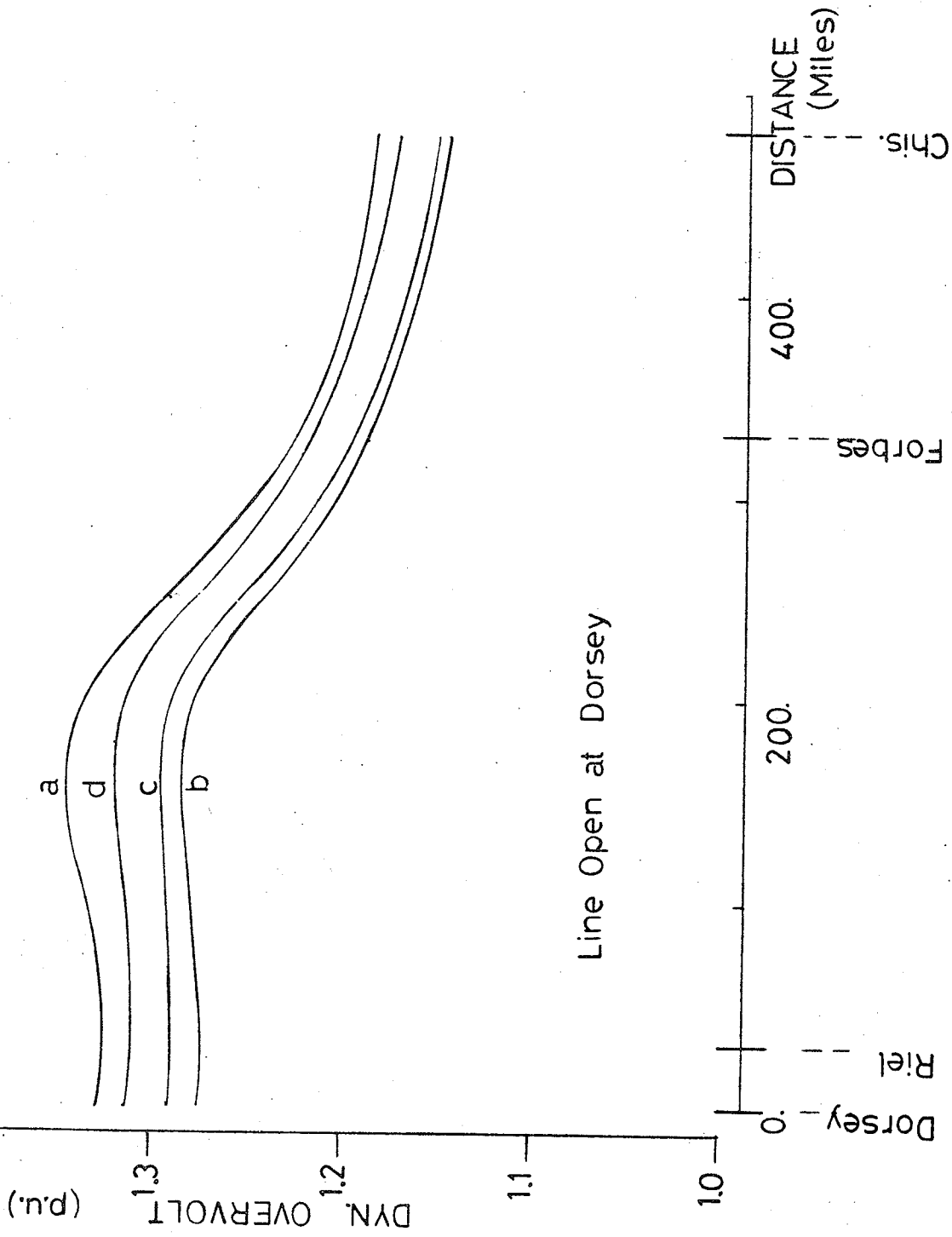


Figure 1.7 Power frequency voltage profile (line opened at Dorsey)

- (a) - Fixed Line reactor at Riel
- (b) - Saturated reactor at Riel
- (c) - Thyristor Cont. reactor at Riel
- (d) - Thy. switched cap. at Dorsey and line reactor at Riel

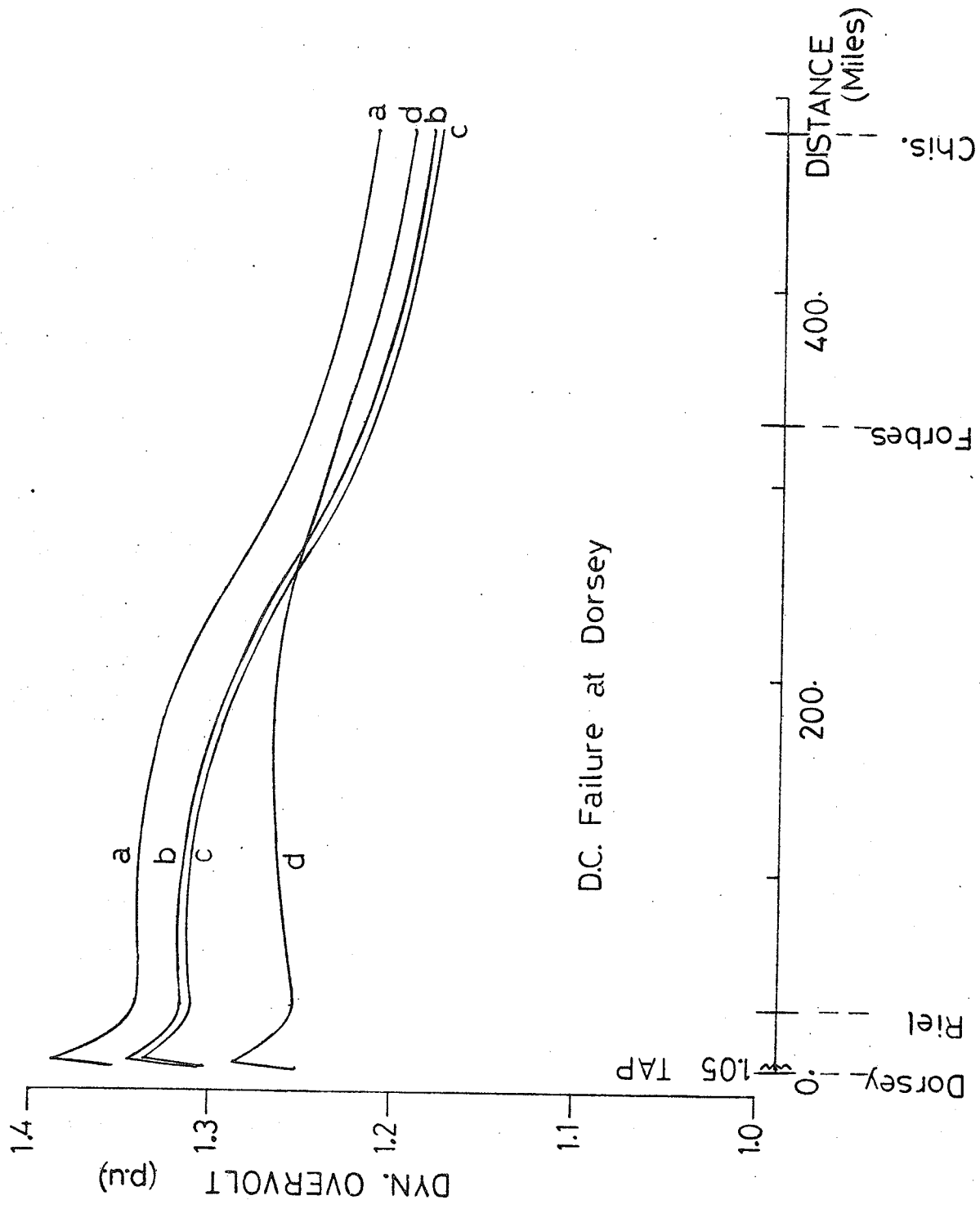


Figure 1.8 Power frequency voltage profile (DC commutation failure at Dorsey)

- (a) - Fixed Line reactor at Riel
- (b) - Saturated reactor at Riel
- (c) - Thyristor cont. reactor at Riel
- (d) - Thy. switched cap. at Dorsey and line reactor at Riel

with an ideal compensator.⁴¹ The dynamic stability has been investigated using the phase-plane technique as follows:

For the system model in Figure 1.9, if H and D are the equivalent inertia constant and damping of the two machines, the swing equation can be written in the form:²

$$\frac{d^2\theta}{dt^2} \left(1 + \frac{1}{\omega_0} \frac{d\theta}{dt}\right) = \frac{\pi f_0}{H} \left(P_m - \frac{D}{\omega_0} \frac{d\theta}{dt} - \frac{V_1 V_2}{X_e} \sin\theta\right)$$

where, θ is the equivalent deviation angle from a reference bus and X_e is the equivalent reactance of the connecting system (all values are expressed in per unit on the equivalent machine rating).

Defining new parameters:

$$\begin{aligned} \omega_N &= \pi f_0 / H && : \text{natural angular frequency} \\ \tau &= \omega_N t && : \text{normalized time} \\ \gamma &= d\theta/d\tau = \omega/\omega_N && : \text{normalized angular velocity deviation} \end{aligned}$$

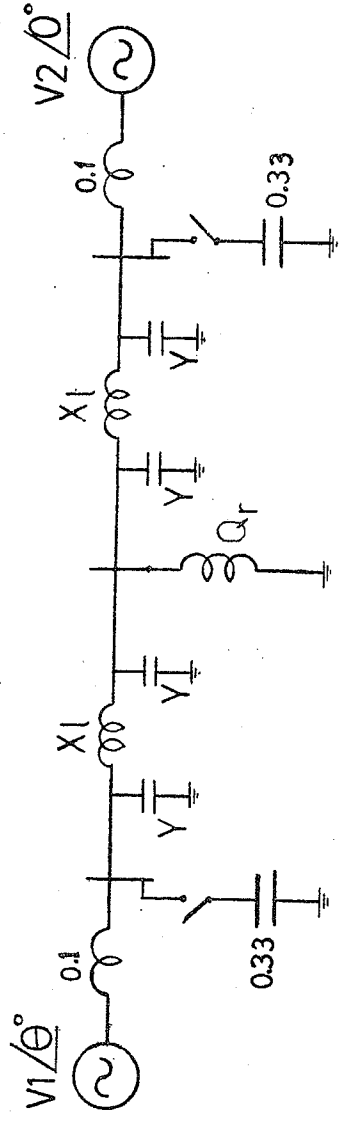
the swing equation can be rewritten as:

$$\gamma \frac{d\gamma}{d\theta} \left(1 + \frac{\omega_N}{\omega_0} \gamma\right) = P_m - D \frac{\omega_N}{\omega_0} \gamma - \frac{V_1 V_2}{X_e} \sin\theta$$

The well known phase-plane technique can be applied in a straight forward manner for a plot of γ versus θ (for $H=100$ and $D=10$).

Resulting phase-planes (Figures 1.11 and 1.12) and corresponding rotor angle swing curves (Figure 1.13) for the different schemes illustrate, clearly, the favourable effect of the static compensator on the rotor motion subsequent to the first swing after the disturbance.

a)



$XI = 0.65$
 $Y = 0.24$

b)

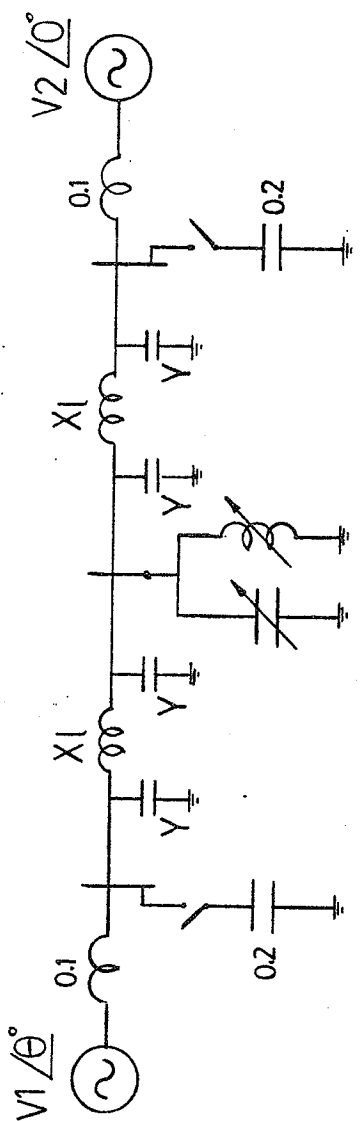


Figure 1.9 Transmission System Models
 (a) System with fixed compensation
 (b) System with controlled static compensation
 (all values are in per-unit)

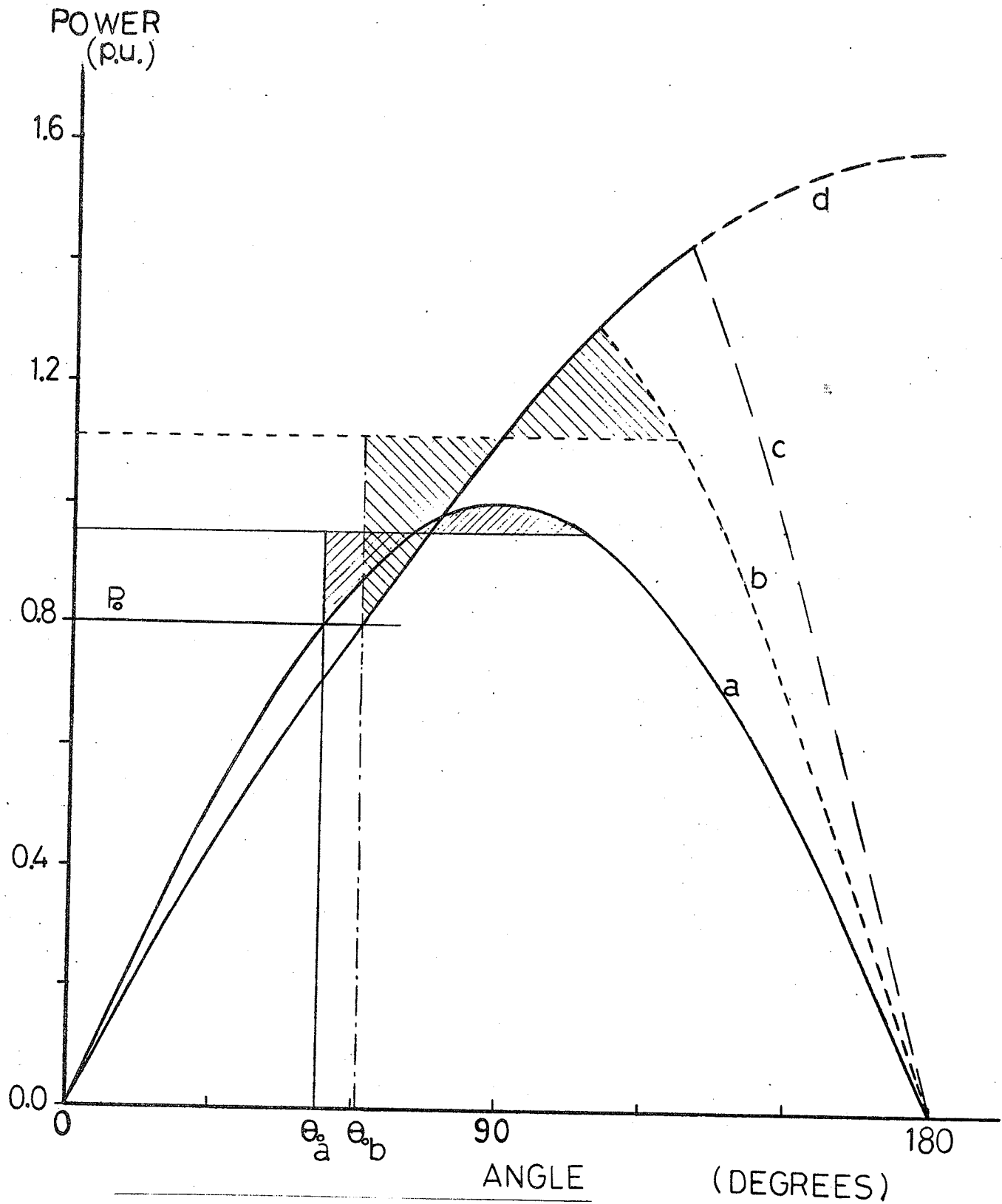


Figure 1.10 Power angle characteristics

- a) System a, fixed compensation ($Q_r = 0.25$ p.u.)
- b) System b, static compensator (0.60 p.u. capacitive range)
- c) System b, static compensator (1.00 p.u. capacitive range)
- d) Ideal compensator (infinite capacitive rating).

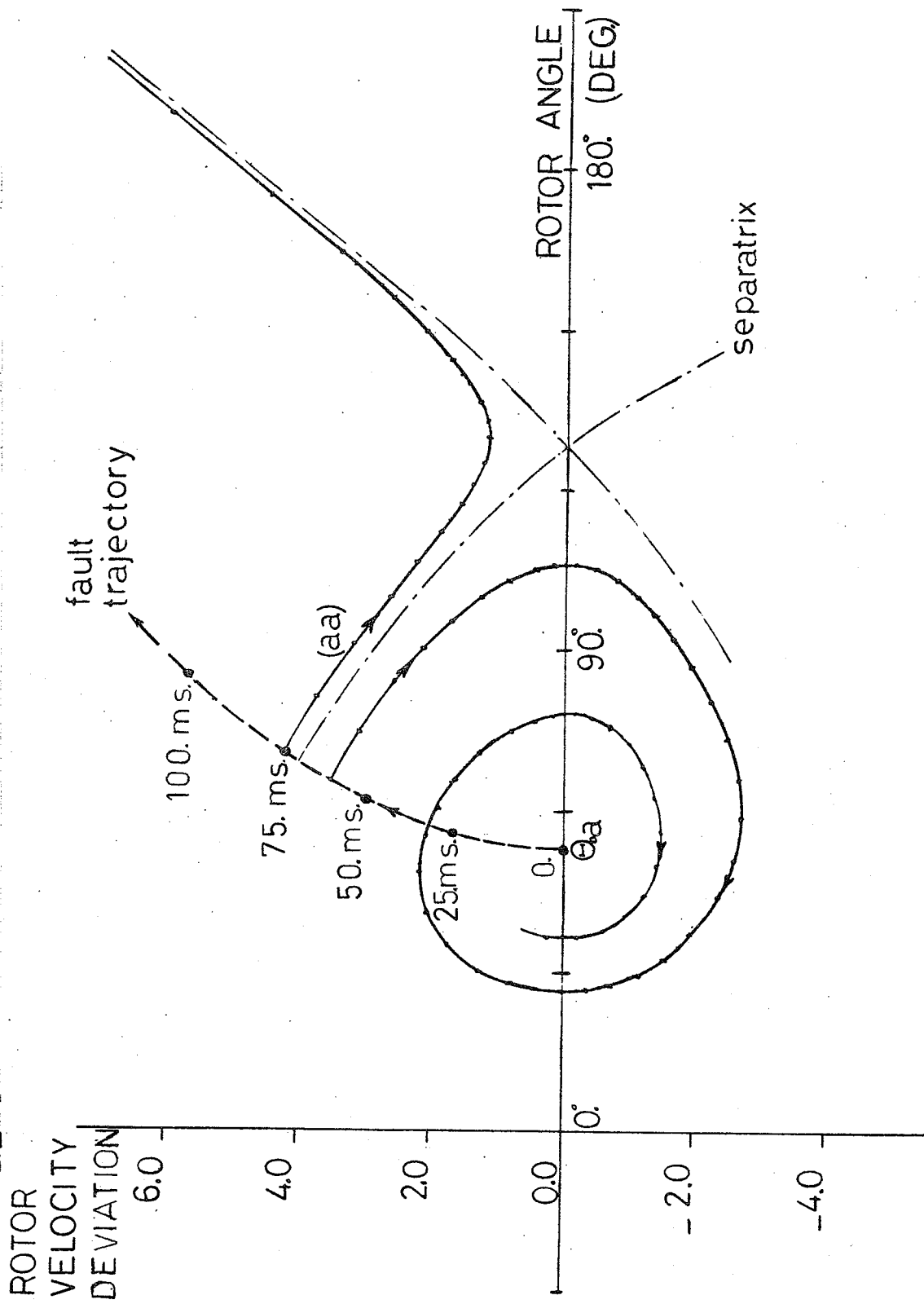


Figure 1.11 Phase-plane of system (a)

(fixed reactor, $Q_r = 0.25$ p.u.)
Time interval = 25.0 m Sec.

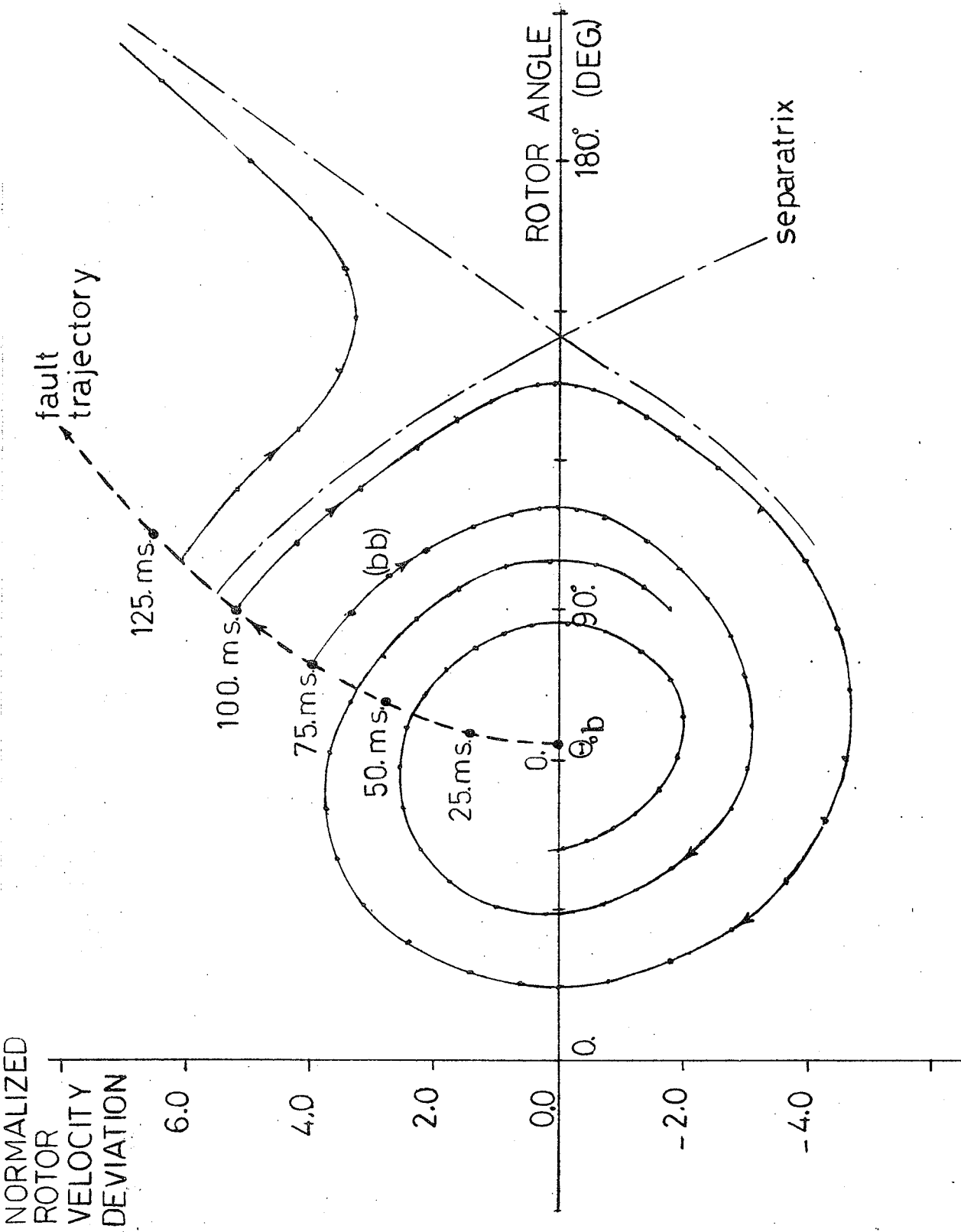


Figure 1.12 Phase-plane of system. (b)

(static compensator, capacitive range = 0.60 p.u.)
 Time interval = 25.0 m Sec.

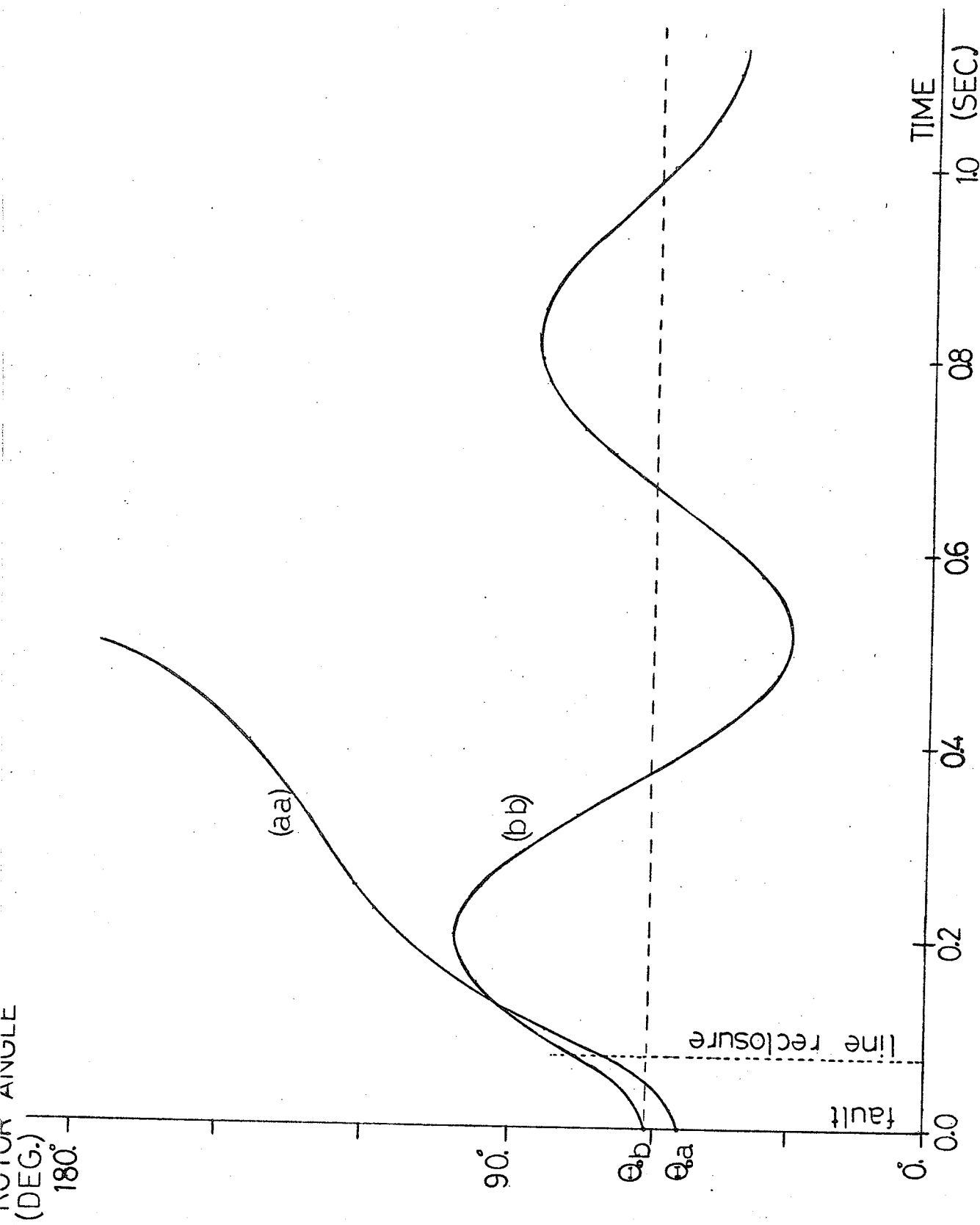


Figure 1.13 Swing curves for 75.0 msec. line reclosure

(aa) for case a) in Figure 1.11

(bb) for case b) in Figure 1.12

chapter two

A NOVEL DESIGN FOR THYRISTOR CONTROLLED VAR COMPENSATORS

2.1 Introduction

Among other types of static shunt VAR compensation systems, thyristor phase-controlled reactors offer more flexibility in terms of external system stabilizing signals, smoother operation in terms of reactive power variations and with recent advances in solid state technology have become cost effective. However, they suffer from high harmonic current generation under steady-state conditions and high current rating of thyristor valves under transient overvoltage conditions. ³¹⁻³⁷ Such problems can decrease the cost benefits offered by these systems.

The novelty of a new design concept can be best demonstrated by comparing Figures 2.1 to 2.4. Figure 2.1 shows a single phase schematic diagram for a known ^{12,34-37} design of thyristor phase controlled reactor. Figure 2.2 shows the voltage and resulting current waveforms for a firing angle α . Because of the anti-parallel connection of the thyristor pair, it is easy to understand that $\alpha=90^\circ$ gives rise to a maximum current through the reactor and that a value lower than this would result in an unsatisfactory operation without affecting the fundamental component of this maximum current as will be shown in Section 2.3. In Figure 2.3 the required reactance X is split into two, each of value $2X$. A thyristor is used in each arm such that each of the paralleled

branches has a reverse biased thyristor.⁴⁵⁻⁴⁷ The operation of this circuit is not different from that described in Figure 2.1 for $90^\circ \leq \alpha \leq 180^\circ$. However, it is now possible to operate this circuit at any value of α from 0° to 180° .

For $0^\circ \leq \alpha \leq 90^\circ$ there are periods when both thyristors of a circuit (per phase) conduct, thereby, causing a circulating current in the paralleled branches. The very first reaction is, therefore, that the reactors and thyristors both have to be of a higher rating as compared to the arrangement in Figure 2.1. This conclusion is partly true. Reactor ratings are discussed in Section 2.4 and the thyristor valve dimensioning is discussed in Section 2.6.

One of the benefits arising from the proposed arrangement is easily understood when one considers the harmonic currents injected into the system due to discontinuous conduction of thyristors. For an equal maximum rating of the phase controlled reactors of Figure 2.1 and Figure 2.3 the values of the reactances have to be as shown in the figures. Since for the arrangement of Figure 2.3 the series reactor is of twice the magnitude, the harmonic currents generated would be half of that for the arrangement in Figure 2.1 when the circuits are connected to the same supply voltage and are operated at an equal firing angle α . This result has far reaching consequences and will be discussed in detail in the rest of this chapter.

The arrangement of Figure 2.3 has a drawback in that the thyristors are not protected from overvoltage stresses. It has become a regular practice to protect thyristors from overvoltage stresses by putting them into conducting mode by emergency firing (BOD firing).⁵¹

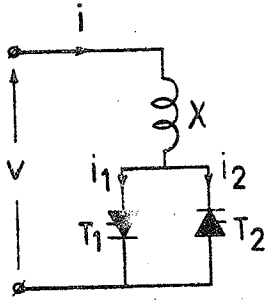


Figure 2.1 Single-phase schematic of a known design of a controlled reactor

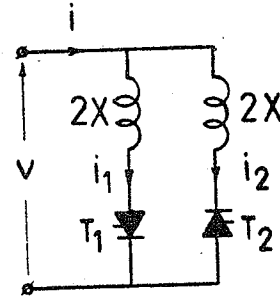


Figure 2.3 Basic realization of UM-Concept

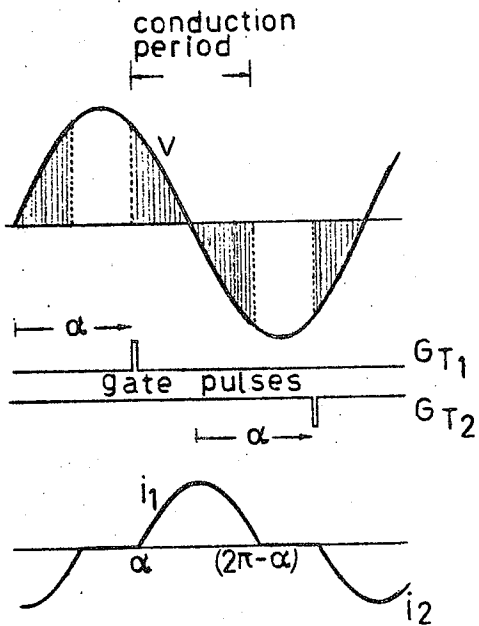


Figure 2.2 Voltage and currents for the scheme in Figure 2.1

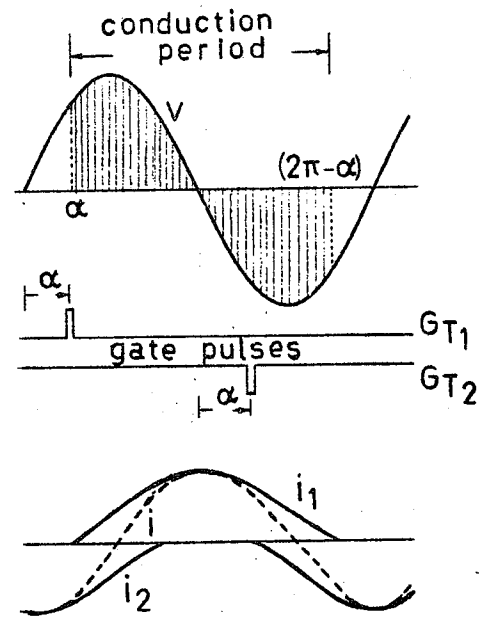


Figure 2.4 Voltage and currents for the scheme in Figure 2.3

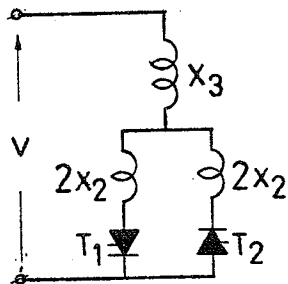


Figure 2.5 Arrangement of the proposed UM-Concept

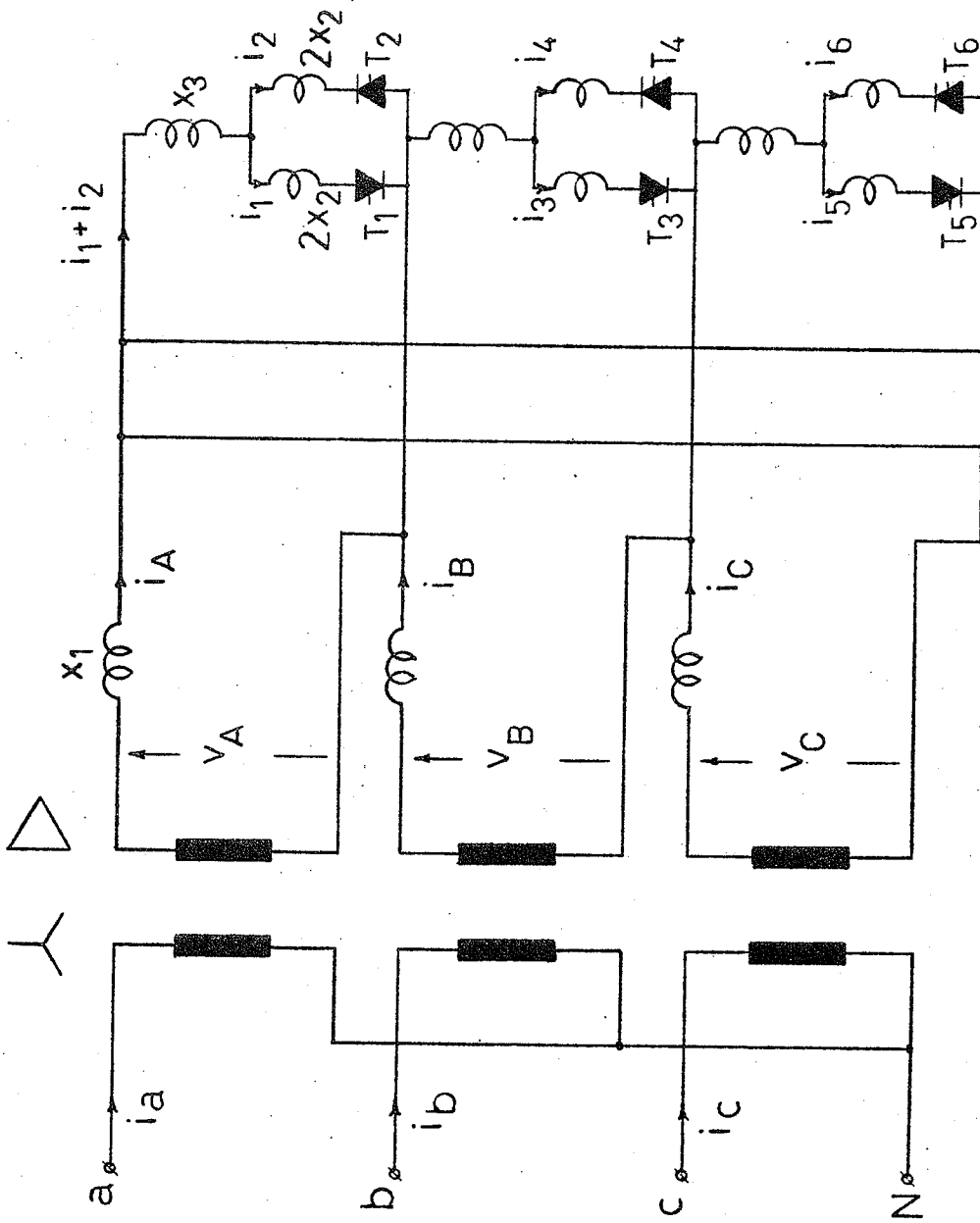


Figure 2.6 Schematic diagram for the generalized UM-Concept for a 3-phase reactor compensator

Fortunately this is the best course of action for the reactor compensators because the insertion of shunt reactors, due to emergency firing of the thyristors, on a bus experiencing overvoltage, is the desired corrective action. For the arrangement of anti-parallel thyristors in Figure 2.1, when the forward biased thyristor starts conducting, the reverse biased thyristor experiences only the forward voltage drop of the other thyristor and, hence, is protected. An emergency firing for the arrangement of Figure 2.3 will protect only the forward biased thyristor and may cause a voltage breakdown of the other. Figure 2.5 is, therefore, proposed to overcome this problem. This new configuration causes a reduced voltage to appear across the non-conducting thyristor due to a voltage drop in the series reactor. The arrangement of Figure 2.5 will be referred to as the Generalized UM-Concept.⁴⁸⁻⁵⁰ The addition of a series reactor brings to mind an enormous number of combinations of x_2 and x_3 possible for a given value of the maximum rating of the reactive compensator. The remaining part of this chapter is devoted to a systematic analysis of this configuration. The UM-Concept presents a generalized arrangement of which the designs of Figure 2.1 and Figure 2.3 are special cases when the value of x_2 or x_3 is reduced to zero respectively. For completeness a further addition to the description of the UM concept is required, considering that for HV systems the compensating equipment may be connected via a transformer. A complete arrangement is shown in Figure 2.6 where the leakage reactance of the transformer is referred to the low voltage side (x_1).

2.2 Generalized System Equations

A number of simplifying assumptions are made in the following analysis in order to be able to obtain simple final algebraic expressions and to keep the basic physical behavior of the system in sight to gain a feel for major design changes.

- (a) The resistance of all inductors and transformer windings is ignored. This assumption is very reasonable since such a device has a very high Q factor in general.
- (b) The magnetic non-linearity of the connecting transformer is ignored. The analysis of the saturation in the flux path of the transformer, in Reference [38], indicates that it would increase the peak valve currents by about 11% for a case with $x_2=x_3=0$.
- (c) The thyristors are represented as ideal switches ignoring their forward voltage drop, which is usually very small, and di/dt, dv/dt protection circuits.
- (d) The analysis also ignores the presence of stray capacitance effects, protection surge arrestors, etc. which have been found [38] to produce negligible influence on the performance.

For the system described in Figure 2.6 we have the following set of equations:

$$L_1 \left(\frac{di_A}{dt} + \frac{di_B}{dt} + \frac{di_C}{dt} \right) = v_A + v_B + v_C \quad (2.1)$$

$$i_A - i_B - i_1 - i_2 + i_3 + i_4 = 0 \quad (2.2)$$

$$i_A - i_C - i_1 - i_2 + i_5 + i_6 = 0 \quad (2.3)$$

Considering all thyristors in a conducting mode the voltage equations for phase A are:

$$L_1 \frac{di_A}{dt} + L_3 \left(\frac{di_1}{dt} + \frac{di_2}{dt} \right) + 2L_2 \frac{di_1}{dt} = v_A \quad (2.4)$$

$$L_1 \frac{di_A}{dt} + L_3 \left(\frac{di_1}{dt} + \frac{di_2}{dt} \right) + 2L_2 \frac{di_2}{dt} = v_A \quad (2.5)$$

Voltage equations for phases B and C are similarly obtained.

In the above, L_1 , L_2 & L_3 are the inductances of reactors x_1 , x_2 and x_3 respectively.

2.3 Steady State Performance

For the prediction of the currents and therefore reactive power absorption by the thyristor phase-controlled reactor and also voltage stresses across the valves under steady state operating conditions the following procedure is employed.

Since the model in Figure 2.6 is purely inductive it is possible to determine uniquely the conduction period of each thyristor for a given value of firing angle α (from α to $180^\circ - \alpha$ with respect to the voltage across it). Conduction states of thyristors give rise to a number of different operating modes, per cycle, of the system, which are recognized and recorded.

For the solution of currents during a particular operating mode, a set of simultaneous equations is formed by equations (2.1), (2.2), (2.3), and some others from the voltage equations of the type (2.4) and (2.5), based on the criteria explained below:

Consider the operating modes related to phase A:

- (a) when thyristor T_1 conducts and T_2 does not, use equation (2.4) with $\frac{di_2}{dt} = 0$;

- (b) when thyristor T_2 conducts and T_1 does not, use equation (2.5) with $\frac{di_1}{dt} = 0$, and
- (c) When both T_1 and T_2 conduct, use both equations (2.4) and (2.5).

Selection of voltage equations for phases B and C are made on a similar basis. With the knowledge of voltages v_A , v_B , and v_C at any instant, system equations are solved by Gauss Elimination method giving the corresponding values of di/dt . By integrating di/dt , currents in all parts are then evaluated.

From the values of di/dt voltage across any component can be calculated. e.g. the voltage across thyristor valve T_1 is:

$$v_{T_1} = v_A - L_1 di_A/dt - L_3(di_1/dt + di_2/dt) - 2L_2 di_1/dt \quad (2.6)$$

where di_1/dt and $di_2/dt = 0$ when T_1 or T_2 is not conducting respectively.

For secondary phase voltages defined as:

$$v_A = \hat{V} \sin(\omega t) \quad (2.7)$$

$$v_B = \hat{V} \sin(\omega t - 120^\circ) \quad (2.8)$$

$$v_C = \hat{V} \sin(\omega t + 120^\circ) \quad (2.9)$$

where \hat{V} is taken 1.0 p.u., the final general expressions for a line current (i_A), valve current (i_1) and voltage across that valve (v_{T_1}) are given in per unit, for all possible ranges of control angle α , in

Table 2.I.

Ratios y and z are defined as key functions to determine the values of x_1 , x_2 and x_3 to make up a given total value X in all cases.

$$X = x_1 + x_2 + x_3 \quad (2.10)$$

$$z = \frac{x_1}{X} \quad (2.11)$$

$$y = \frac{x_2}{X} \quad (2.12)$$

For simplified expressions in Table 2.I, the following substitutions are made:

$$c_1 = 1 + y \quad (2.13)$$

$$c_2 = c_1 - z \quad (2.14)$$

$$c_3 = c_1 + c_2 \quad (2.15)$$

$$c_4 = c_1 + c_3 \quad (2.16)$$

$$c_5 = c_1 + c_4 \quad (2.17)$$

$$c_6 = 3c_2 - y \quad (2.18)$$

$$c_7 = 3c_2 - yz \quad (2.19)$$

$$c_8 = 3c_2 - 2yz \quad (2.20)$$

Also,

$$h_1 = \cos(\omega t) \quad (2.21)$$

$$h_2 = \cos(\omega t - 120^\circ) \quad (2.22)$$

$$h_3 = \cos(\omega t + 120^\circ) \quad (2.23)$$

and

$$k_1 = \cos(\alpha) \quad (2.24)$$

$$k_2 = \cos(\alpha - 120^\circ) \quad (2.25)$$

$$k_3 = \cos(\alpha + 120^\circ) \quad (2.26)$$

Some results, using the expressions in Table 2.I, are drawn to bring out the important aspects of operation.

Table 2.1

Expressions for Steady-state Currents and Voltages

(a) $0^\circ < \alpha \leq 30^\circ$

Angle, ωt	Line current, i_A	Valve current, i_1	Valve voltage, v_{T1}
$\alpha < \omega t \leq (60^\circ - \alpha)$	$-I_{P13}^-(h_1 - k_1)$	$-(h_1 - k_1)/2$	$(1-z)v_A$
$(60^\circ - \alpha) < \omega t \leq (60^\circ + \alpha)$	$-I_{P12}^-(h_1 + k_3) - y(1-z)(h_3 + k_1)/C_8$	$I_{V11}^-(h_1 + k_3)/2 - yz(h_3 + k_1)/2C_8$	$(1-z)(v_A - yz v_C/C_8)$
$(60^\circ + \alpha) < \omega t \leq (120^\circ - \alpha)$	$-h_1$	$I_{V12}^-(h_1 + k_2)/2$	$(1-z)v_A$
$(120^\circ - \alpha) < \omega t \leq (120^\circ + \alpha)$	$I_{P11}^-(h_1 - k_2) - y(1-z)(h_2 - k_1)/C_8$	$I_{V13}^-(h_1 - k_2)/2 + yz(h_2 - k_1)/2C_8$	$(1-z)(v_A - yz v_B/C_8)$
$(120^\circ + \alpha) < \omega t \leq (180^\circ - \alpha)$	$I_{P12}^-(h_1 - k_3)$	$I_{V14}^-(h_1 - k_3)/2$	$(1-z)v_A$
$(180^\circ - \alpha) < \omega t \leq (180^\circ + \alpha)$	$I_{P13}^-(C_6 - y)(h_1 + k_1)/C_8$	$I_{V15}^-3(1-z)(h_1 + k_1)/C_8$	$3(1-z)v_A C_2/C_8$
$(180^\circ + \alpha) < \omega t \leq (240^\circ - \alpha)$	$I_{P13}^-(h_1 + k_1)$	$I_{V15}^-(h_1 + k_1)/2$	$(1-z)v_A$
$(240^\circ - \alpha) < \omega t \leq (240^\circ + \alpha)$	$I_{P12}^-(h_1 - k_3) - y(1-z)(h_3 - k_1)/C_8$	$I_{V14}^-(h_1 - k_3)/2 + yz(h_3 - k_1)/2C_8$	$(1-z)(v_A - yz v_C/C_8)$
$(240^\circ + \alpha) < \omega t \leq (300^\circ - \alpha)$	$I_{P11}^-(h_1 - k_2)$	$I_{V13}^-(h_1 - k_2)/2$	$(1-z)v_A$
$(300^\circ - \alpha) < \omega t \leq (300^\circ + \alpha)$	$-I_{P11}^-(h_1 + k_2) - y(1-z)(h_2 + k_1)/C_8$	$I_{V12}^-(h_1 + k_2)/2 + yz(h_2 + k_1)2C_8$	$(1-z)(v_A - yz v_B/C_8)$
$(300^\circ + \alpha) < \omega t \leq (360^\circ - \alpha)$	$-I_{P12}^-(h_1 + k_3)$	$I_{V11}^-(h_1 + k_3)/2$	$(1-z)v_A$

where

$$I_{P11}^- = -k_2, \quad I_{P12}^- = -k_3, \quad I_{P13}^- = k_1$$

$$I_{V11}^- = -k_2/2, \quad I_{V12}^- = -k_3/2, \quad I_{V13}^- = (k_1 - k_2)/2, \quad I_{V14}^- = (k_1 - k_3)/2, \quad I_{V15}^- = k_1$$

Table 2.1

Expressions for Steady-state Currents and Voltages

(b) $30^\circ \leq \alpha \leq 60^\circ$

Angle, ωt	Line current, i_A	Valve current, i_I	Valve voltage, v_{TI}
$\alpha \leq \omega t \leq (120^\circ - \alpha)$	$-I_{P21}^-(h_1 - k_1) - y(1-z)(h_3 - k_3)/C_8$	$-(h_1 - k_1)/2 + yz(h_3 - k_3)/2C_8$	$(1-z)(v_A - yz v_C/C_8)$
$(120^\circ - \alpha) \leq \omega t \leq (60^\circ + \alpha)$	$-h_1 C_6/C_7$	$-I_{V21} - 3C_2(h_1 - k_2)/2C_7$	$3(1-z)v_A C_2/C_7$
$(60^\circ + \alpha) \leq \omega t \leq (180^\circ - \alpha)$	$I_{P21}^-(h_1 + k_2) - y(1-z)(h_2 + k_3)/C_8$	$I_{V22}^-(h_1 + k_2)/2 + yz(h_2 + k_3)/2C_8$	$(1-z)(v_A - yz v_B/C_8)$
$(180^\circ - \alpha) \leq \omega t \leq (120^\circ + \alpha)$	$I_{P22}^-(h_1 + k_1)/C_1 + yC_2(h_3 + k_2)/C_1 C_7$	$I_{V23}^-(h_1 + k_1)/C_1 - yz(h_3 + k_2)/C_1 C_7$	$(v_A + yz v_C/C_7)C_2/C_1$
$(120^\circ + \alpha) \leq \omega t \leq (240^\circ - \alpha)$	$I_{P23}^-(C_6 - y)(h_1 - k_3)/C_8$	$I_{V24} - 3(1-z)(h_1 - k_3)/C_8$	$3(1-z)v_A C_2/C_8$
$(240^\circ - \alpha) \leq \omega t \leq (180^\circ + \alpha)$	$I_{P23}^-(h_1 - k_3)/C_1 + yC_2(h_2 - k_2)/C_1 C_7$	$I_{V24}^-(h_1 - k_3)/C_1 - yz(h_2 - k_2)/C_1 C_7$	$(v_A + yz v_B/C_7)C_2/C_1$
$(180^\circ + \alpha) \leq \omega t \leq (300^\circ - \alpha)$	$I_{P22}^-(h_1 + k_1) - y(1-z)(h_3 + k_3)/C_8$	$I_{V23}^-(h_1 + k_1)/2 + yz(h_3 + k_3)/2C_8$	$(1-z)(v_A - yz v_C/C_8)$
$(300^\circ - \alpha) \leq \omega t \leq (240^\circ + \alpha)$	$-h_1 C_6/C_7$	$I_{V22} - 3C_2(h_1 + k_2)/2C_7$	$3(1-z)v_A C_2/C_7$
$(240^\circ + \alpha) \leq \omega t \leq (360^\circ - \alpha)$	$-I_{P21}^-(h_1 - k_2) - y(1-z)(h_2 - k_3)/C_8$	$I_{V21}^-(h_1 - k_2)/2 + yz(h_2 - k_3)/2C_8$	$(1-z)(v_A - yz v_B/C_8)$

where

$$I_{P21} = k_2 C_6/C_7, \quad I_{P22} = I_{P21} + (k_1 - k_2),$$

$$I_{V21} = (k_1 - k_2)/2, \quad I_{V22} = I_{V21} + 3k_2 C_2/C_7, \quad I_{V23} = I_{V21} + I_{V22}, \quad I_{V24} = I_{V23} + 3(1-z)k_2/C_7,$$

Table 2.1

Expressions for Steady-state Currents and Voltages

(c) $60^\circ \leq \alpha \leq 90^\circ$

Angle, ωt	Line current, i_A	Valve current, i_1	Valve voltage, v_{T1}
$\alpha \leq \omega t \leq (180^\circ - \alpha)$	$-h_1 C_6 / C_7$	$-3C_2(h_1 - k_1) / 2C_7$	$3(1-z)v_A C_2 / C_7$
$(180^\circ - \alpha) \leq \omega t \leq (60^\circ + \alpha)$	$IP_{31} - (h_1 + k_1) / C_1$	$Iv_{31} - (h_1 + k_1) / C_1$	$v_A C_2 / C_1$
$(60^\circ + \alpha) \leq \omega t \leq (240^\circ - \alpha)$	$IP_{32} - (h_1 + k_2) / C_1 + yC_2(h_3 + k_1) / C_1 C_7$	$Iv_{32} - (h_1 + k_2) / C_1 - yz(h_3 + k_1) / C_1 C_7$	$(v_A + yzv_C / C_7) C_2 / C_1$
$(240^\circ - \alpha) \leq \omega t \leq (120^\circ + \alpha)$	$IP_{33} - (h_1 - k_3) / C_1$	$Iv_{33} - (h_1 - k_3) / C_1$	$v_A C_2 / C_1$
$(120^\circ + \alpha) \leq \omega t \leq (300^\circ - \alpha)$	$IP_{33} - (h_1 - k_3) / C_1 + yC_2(h_2 - k_1) / C_1 C_7$	$Iv_{33} - (h_1 - k_3) / C_1 - yz(h_2 - k_1) / C_1 C_7$	$(v_A + yzv_B / C_7) C_2 / C_1$
$(300^\circ - \alpha) \leq \omega t \leq (180^\circ + \alpha)$	$IP_{32} - (h_1 + k_2) / C_1$	$Iv_{32} - (h_1 + k_2) / C_1$	$v_A C_2 / C_1$
$(180^\circ + \alpha) \leq \omega t \leq (360^\circ - \alpha)$	$-h_1 C_6 / C_7$	$-3C_2(h_1 - k_1) / 2C_7$	$3(1-z)v_A C_2 / C_1$

where

$$IP_{31} = k_1 C_6 / C_7, \quad IP_{32} = IP_{31} + (k_2 - k_1) / C_1, \quad IP_{33} = IP_{32} + k_1(C_2(3+2y) - yz) / C_1 C_7$$

$$Iv_{31} = 3k_1 C_2 / C_7, \quad Iv_{32} = Iv_{31} + (k_2 - k_1) / C_1, \quad Iv_{33} = Iv_{32} + 3k_1(C_2 - yz) / C_1 C_7$$

Table 2.1

Expressions for Steady-state Currents and Voltages

(d) $90^\circ \leq \alpha \leq 120^\circ$

Angle, ωt	Line current, i_A	Valve current, i_1	Valve voltage, v_{T1}
$(180^\circ - \alpha) \leq \omega t \leq \alpha$	$-h_1 / (C_4 - z)$	0.0	$3v_A C_2 / (C_4 - z)$
$\alpha \leq \omega t \leq (240^\circ - \alpha)$	$IP_{41} - (h_1 - k_1) / C_1$	$-(h_1 - k_1) / C_1$	$v_A C_2 / C_1$
$(240^\circ - \alpha) \leq \omega t \leq (60^\circ + \alpha)$	$IP_{42} - (C_3(h_1 - k_3) - C_2(h_2 - k_2)) / (C_4 - z) C_1$	$IV_{41} - (C_4(h_1 - k_3) + z(h_2 - k_2)) / (C_4 - z) C_1$	$(C_4^v + zv_B) C_2 / (C_4 - z) C_1$
$(60^\circ + \alpha) \leq \omega t \leq (300^\circ - \alpha)$	$IP_{43} - (h_1 + k_2) / C_1$	$IV_{42} - (h_1 + k_2) / C_1$	$v_A C_2 / C_1$
$(300^\circ - \alpha) \leq \omega t \leq (120^\circ + \alpha)$	$IP_{43} - (C_3(h_1 + k_2) - C_2(h_3 + k_3)) / (C_4 - z) C_1$	$IV_{42} - (C_4(h_1 + k_2) + z(h_3 + k_3)) / (C_4 - z) C_1$	$(C_4^v + zv_C) C_2 / (C_4 - z) C_1$
$(120^\circ + \alpha) \leq \omega t \leq (360^\circ - \alpha)$	$IP_{41} - (h_1 - k_1) / C_1$	$-(h_1 - k_1) / C_1$	$v_A C_2 / C_1$
$(360^\circ - \alpha) \leq \omega t \leq (180^\circ + \alpha)$	$-h_1 / (C_4 - z)$	0.0	$3v_A C_2 / (C_4 - z)$

where

$$IP_{41} = -k_1 / (C_4 - z), \quad IP_{42} = IP_{41} + (k_1 - k_3) / C_1, \quad IP_{43} = IP_{41} + IP_{42}$$

$$IV_{41} = (k_1 - k_3) / C_1, \quad IV_{42} = IV_{41} - 3k_1 / (C_4 - z)$$

Table 2.I

Expressions for Steady-state Currents and Voltages

(e) $120^\circ \leq \alpha \leq 150^\circ$

Angle, ωt	Line current, i_A	Valve current, i_1	Valve voltage, v_{T1}
$(\alpha - 60^\circ) \leq \omega t \leq (240^\circ - \alpha)$	$-h_1 / (C_4 - z)$	0.0	$3v_A C_2 / (C_4 - z)$
$(240^\circ - \alpha) \leq \omega t < \alpha$	$Ip_{51} + (h_2 - k_2) / C_4$	0.0	$v_A + zv_B / C_4$
$\alpha \leq \omega t \leq (300^\circ - \alpha)$	$Ip_{51} - (C_3(h_1 - k_1) - C_2(h_2 - k_2)) / (C_4 - z) C_1$	$-(C_4(h_1 - k_1) + z(h_2 - k_2)) / (C_4 - z) C_1$	$(C_4 v_A + zv_B) C_2 / (C_4 - z) C_1$
$(300^\circ - \alpha) \leq \omega t \leq (60^\circ + \alpha)$	$Ip_{52} - 2(h_1 + k_2) / C_4$	$Iv_{51} - 3(h_1 + k_2) / C_4$	$3v_A C_2 / C_4$
$(60^\circ + \alpha) \leq \omega t \leq (360^\circ - \alpha)$	$Ip_{52} - (C_3(h_1 + k_2) - C_2(h_3 + k_1)) / (C_4 - z) C_1$	$Iv_{51} - (C_4(h_1 + k_2) + z(h_3 + k_1)) / (C_4 - z) C_1$	$(C_4 v_A C_2) / (C_4 - z) C_1$
$(360^\circ - \alpha) \leq \omega t \leq (120^\circ + \alpha)$	$Ip_{51} + (h_3 - k_2) / C_4$	0.0	$v_A + zv_C / C_4$
$(120^\circ + \alpha) \leq \omega t \leq (420^\circ - \alpha)$	$-h_1 / (C_4 - z)$	0.0	$3v_A C_2 / (C_4 - z)$

where

$$Ip_{51} = -k_3 / (C_4 - z) \quad , \quad Ip_{52} = 2Ip_{51}$$

$$Iv_{51} = -3k_3 / (C_4 - z)$$

Table 2.I

Expressions for Steady-state Currents and Voltages

(f) $150^\circ \leq \alpha \leq 180^\circ$

Angle, ωt	Line current, i_A	Valve current, i_1	Valve voltage, v_{T1}
$(240^\circ - \alpha) \leq \omega t \leq (\alpha - 60^\circ)$	0.0	0.0	v_A
$(\alpha - 60^\circ) \leq \omega t \leq (300^\circ - \alpha)$	$(h_2 + k_1)/C_4$	0.0	$v_A + z v_B / C_4$
$(300^\circ - \alpha) \leq \omega t \leq \alpha$	0.0	0.0	v_A
$\alpha \leq \omega t \leq (360^\circ - \alpha)$	$-2(h_1 - k_1)/C_4$	$-3(h_1 - k_1)/C_4$	$3v_A C_2 / C_4$
$(360^\circ - \alpha) \leq \omega t \leq (60^\circ + \alpha)$	0.0	0.0	v_A
$(60^\circ + \alpha) \leq \omega t \leq (420^\circ - \alpha)$	$(h_3 + k_1)/C_4$	0.0	$v_A + z v_C / C_4$
$(420^\circ - \alpha) \leq \omega t \leq (120^\circ + \alpha)$	0.0	0.0	v_A

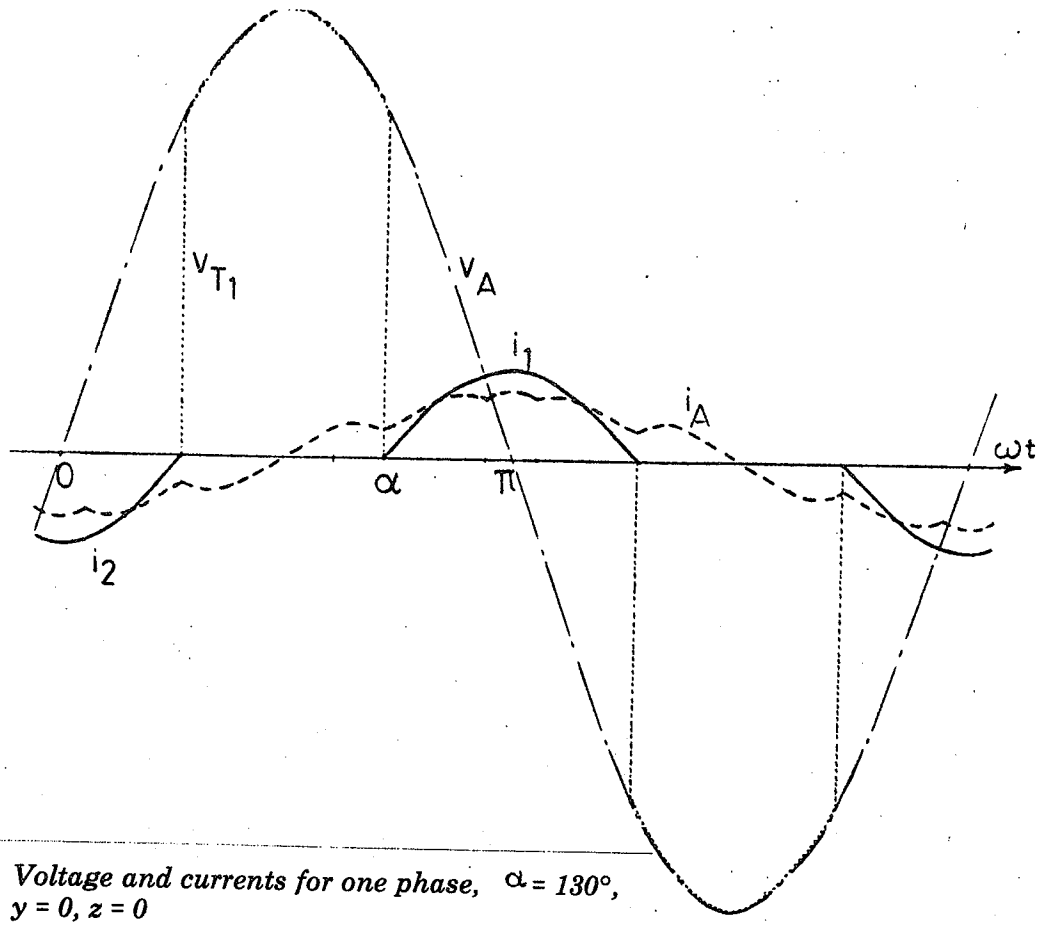


Figure 2.7 Voltage and currents for one phase, $\alpha = 130^\circ$, $y = 0, z = 0$

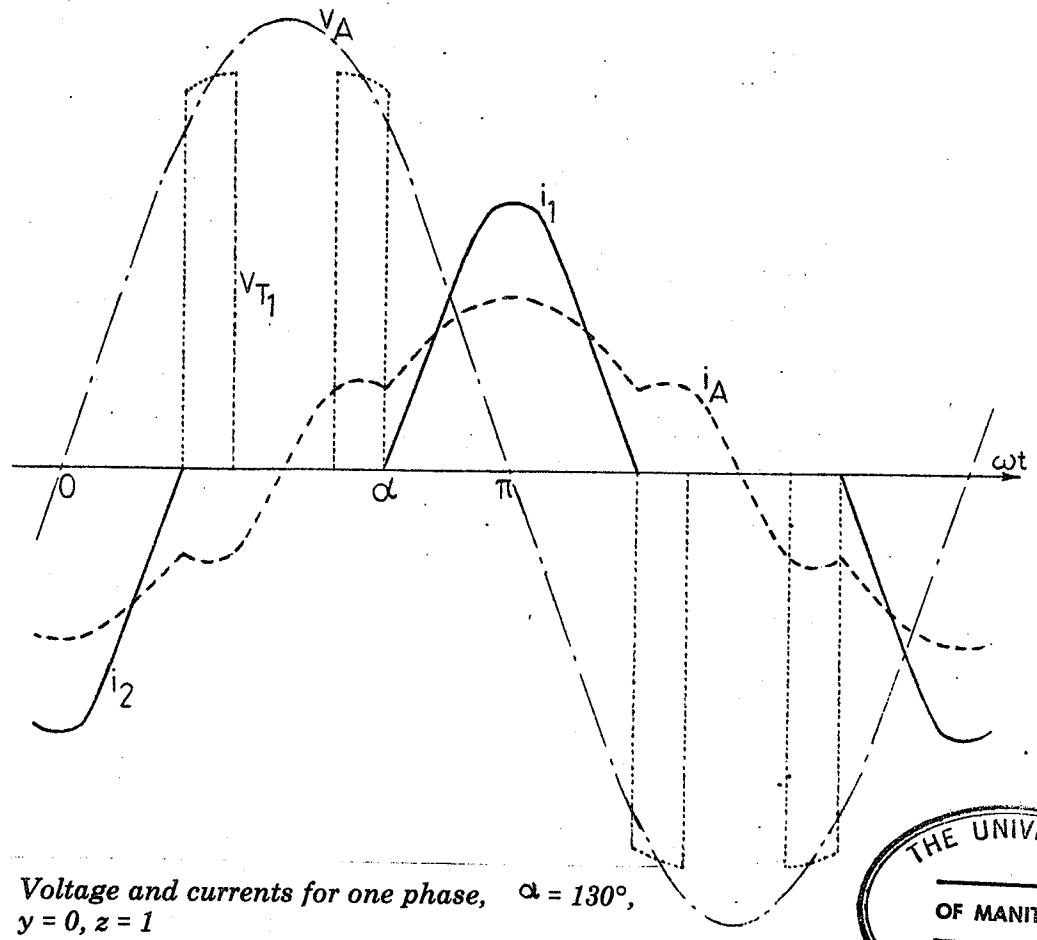
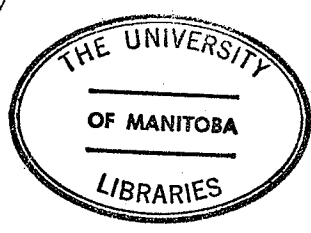


Figure 2.8 Voltage and currents for one phase, $\alpha = 130^\circ$, $y = 0, z = 1$



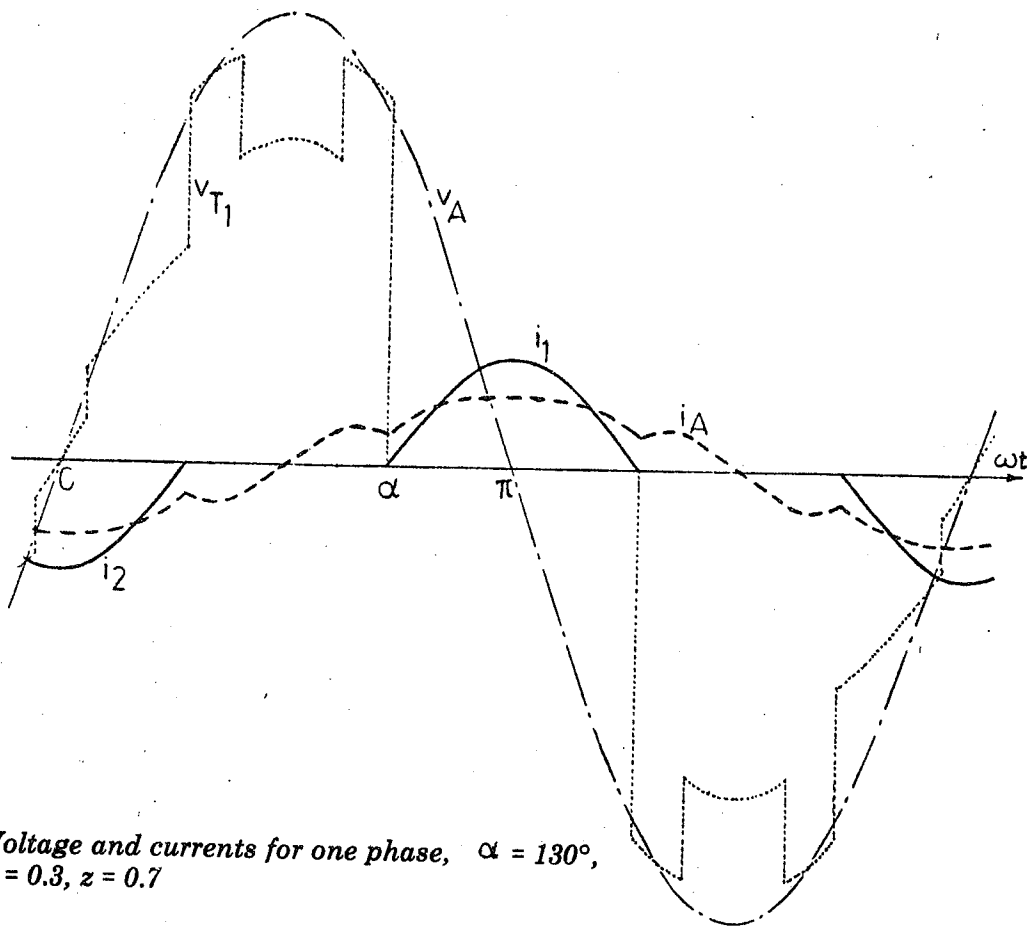


Figure 2.9 Voltage and currents for one phase, $\alpha = 130^\circ$, $y = 0.3$, $z = 0.7$

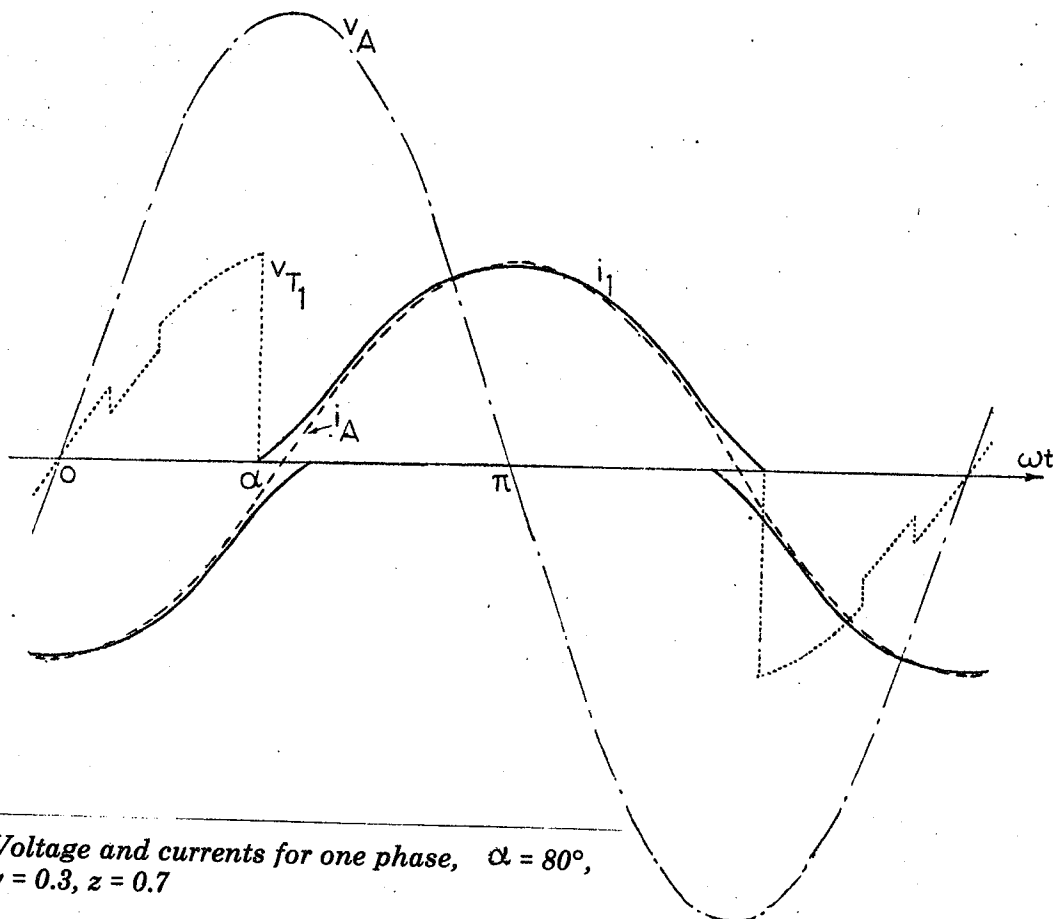


Figure 2.10 Voltage and currents for one phase, $\alpha = 80^\circ$, $y = 0.3$, $z = 0.7$

Figures 2.7 to 2.10 are included to show the basic influence of configurations. Results of Figures 2.7, 2.8 and 2.9 correspond to the layout in Figure 2.6, and are for:

Case 1: $y = 0, z = 0$ (i.e. all reactance is lumped into the separate reactor x_3) This design is reported by General Electric and Westinghouse;^{34-37,52}

Case 2: $y = 0, z = 1$ (i.e. all reactance is included in the transformer leakage). This design is reported by BBC;^{30-33,38} and

Case 3: $y = 0.3$ and $z = 0.7$ as an example arbitrarily chosen to illustrate the behaviour of the Generalized UM-Concept.

Each figure shows voltage on the secondary side (v_A), voltage across a valve (v_{T1}) currents through the valves (i_1, i_2) and current on the primary side (i_A) for one phase, for $\alpha = 130^\circ$. The following observations are noteworthy:

- (a) $\alpha = 130^\circ$ does not correspond to the same reactive power loading for all three cases. This is because of the differences in the ranges of α control, as will be shown later.
- (b) The peak voltage appearing across a valve is always equal to the peak secondary line voltage in case 1, whereas in other cases it is reduced to a lower voltage.

Since in the UM-Concept (case 3) it is possible to operate for $\alpha < 90^\circ$, Figure 2.10 is included to show current and voltage waveforms for $\alpha = 80^\circ$. It is to be noted that the line current is nearly sinusoidal and that the peak voltage across the valves is substantially reduced.

Figures 2.11 and 2.12 are included to show cases of abnormal operation for known designs. Figure 2.11 is for case 1 ($y=0, z=0$), with

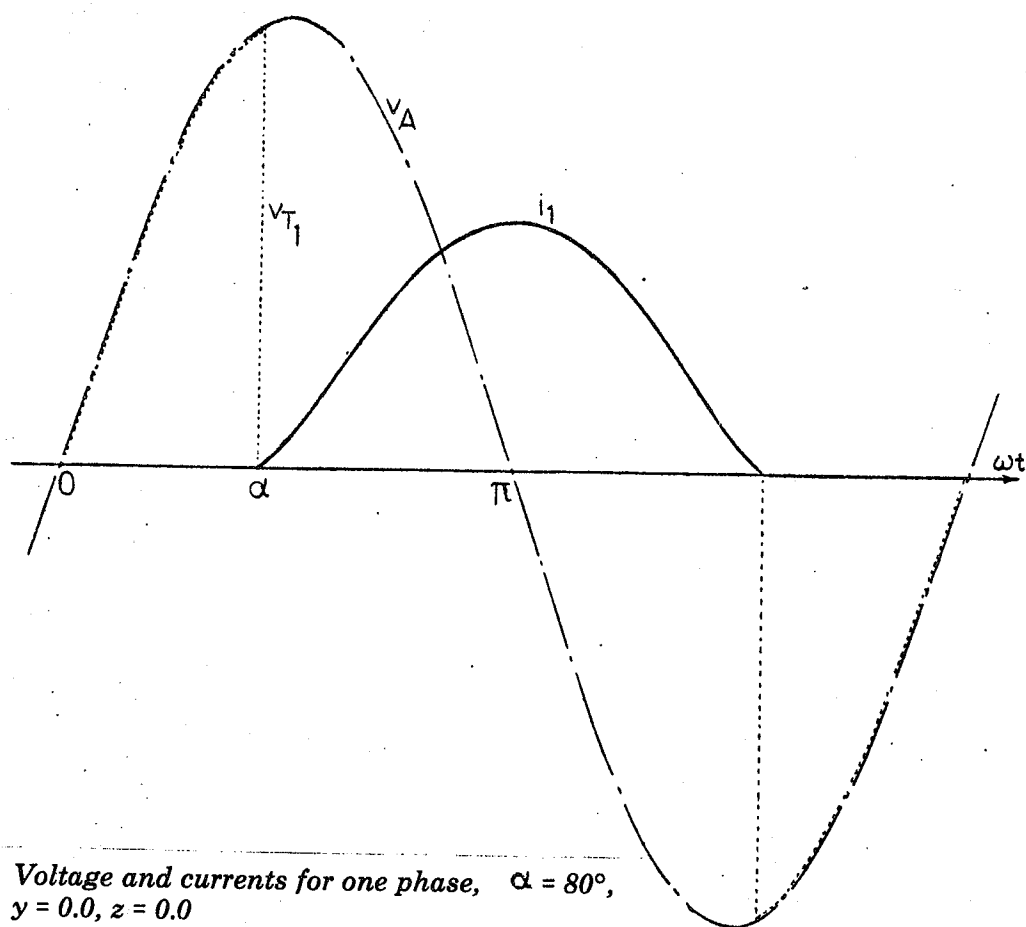


Figure 2.11 Voltage and currents for one phase, $\alpha = 80^\circ$,
 $y = 0.0, z = 0.0$

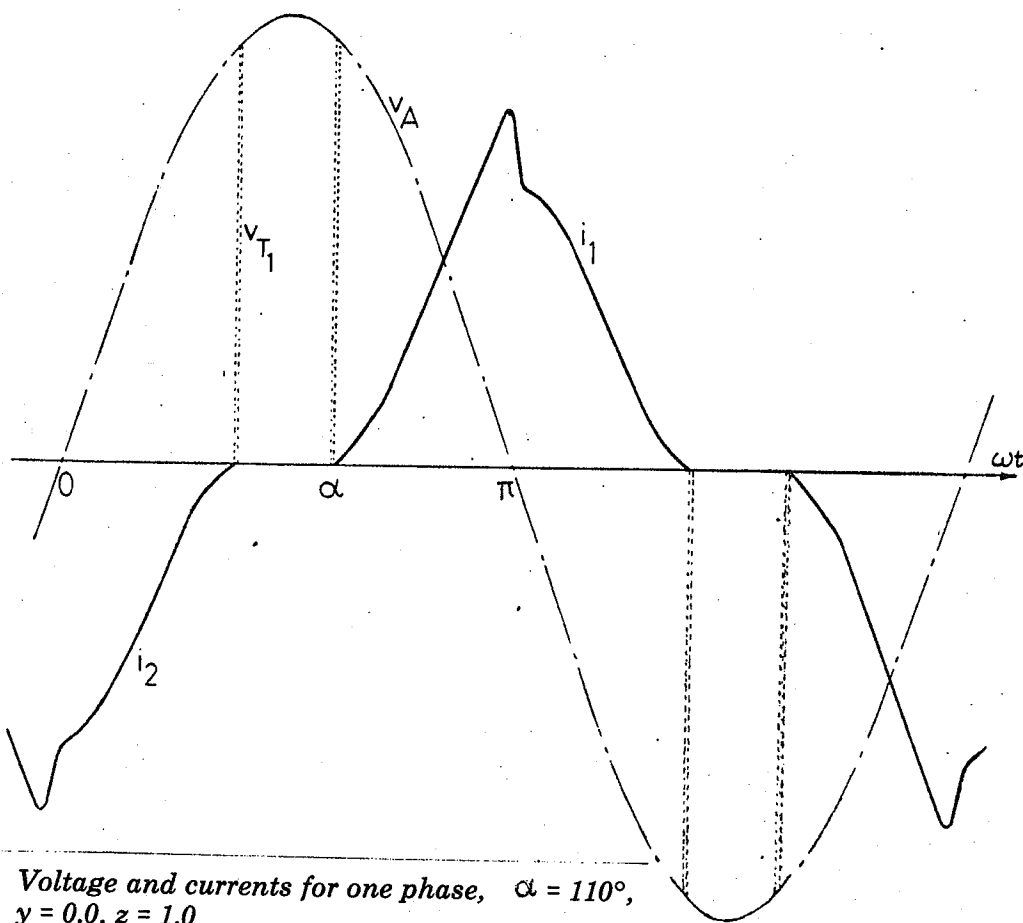


Figure 2.12 Voltage and currents for one phase, $\alpha = 110^\circ$,
 $y = 0.0, z = 1.0$

$\alpha=80^\circ$. When the triggering pulse is applied to thyristor T_2 the voltage across it is very small since T_1 is still in conduction mode and therefore would not conduct. However, when a high voltage appears across T_2 , at the instant T_1 stops conducting, there would be no pulses applied to T_2 and therefore conduction would not take place. Hence we end up with one thyristor conducting per phase and this results in a distorted line current with a high dc component. However for practical applications there is usually a small non-linear reactor in series with each thyristor valve for di/dt protection. This small reactor may cause the two thyristors/phase to conduct simultaneously. In Figure 2.12, Case 2 ($y=0, z=1$) was examined for a firing angle $\alpha = 110^\circ$. The high current through T_1 is due to the fact that when two phases are conducting, in this configuration, the voltage appearing across the third phase is very small. However when voltage across one of the conducting phases becomes small (near its zero crossing), there is a chance that a thyristor in the third phase would conduct provided that the triggering pulse is still applied to it. The current and voltage waveforms appearing in Figure 2.12 do match to a great extent the results in Reference [38] given for an actual reduced scale physical model.

2.4 Fundamental Current and Reactors Rating

In order to study the characteristic performance of the device in the steady state it is important to derive a direct relationship between its input parameter (control angle α) and its output quantity (reactive power). The effective reactive power of the thyristor controlled reactor is directly proportional to the power frequency component of its line current and, in per unit, they both are equal. In per-unit

values i_A , i_B and i_C represent these currents.

The magnitude of the fundamental component of line current i_A is given by:

$$I_{A1} = \frac{2}{\pi} \int_{\pi/2}^{3\pi/2} i_A(\omega t) \cdot \cos(\omega t) \cdot d(\omega t) \quad (2.27)$$

where $i_A(\omega t)$ is given in Table 2.I.

The final expressions for this fundamental current, in per unit, over different operating ranges of control angle α are given in Table 2.II. Figure 2.13 shows the p.u. reactive power variation with α for various designs. Known designs of Cases 1 and 2 provide an effective control range of α from 90° to 180° and 120° to 180° respectively. Other combinations of y and z provide a whole new range of alternative designs - some of which appear superior to the known ones in an over-all assessment.

Non-zero values of y spread the control range from 0° to 180° . The value of z , however, has no influence on the reactive power for $\alpha < 90^\circ$. As the value of y increases the sensitivity of reactive power to small deviations of control angle α is reduced, which would have a favourable effect on the stability of α control.

One other criterion for comparing various designs is the total MVA rating of all reactors forming a compensator. At full load ($\alpha = 0^\circ$) p.u. valve current i_1 , from Table 2.I, is given by:

$$i_1 = (1 - \cos(\omega t)) / 2 \quad \text{for } 0 \leq \omega t \leq 2\pi \quad (2.28)$$

therefore the p.u. rms value is:

$$I_1 = \sqrt{\frac{1}{2\pi} \int_0^{2\pi} i_1^2 d(\omega t)} = \sqrt{\frac{3}{2}} \quad (2.29)$$

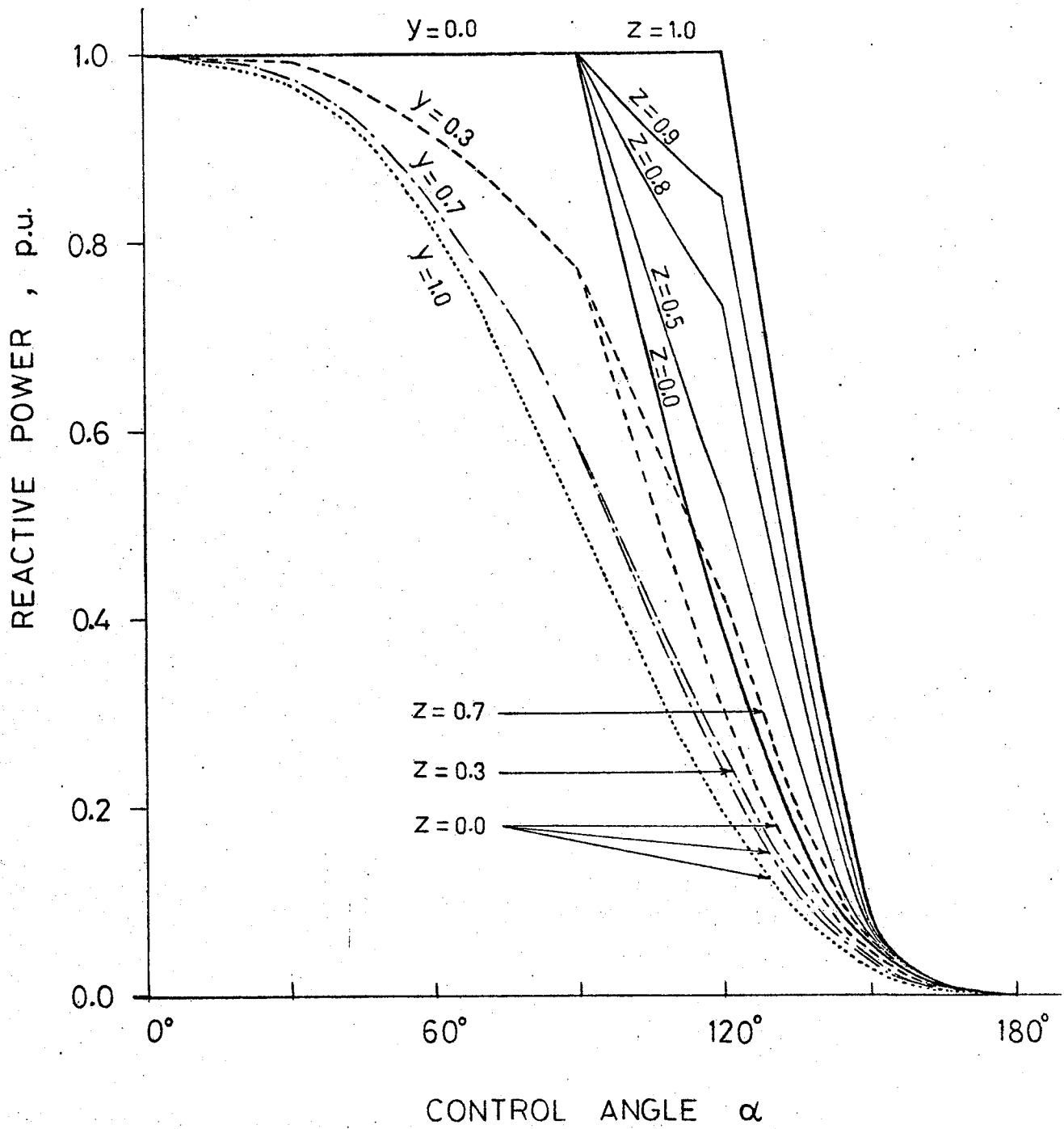


Figure 2.13 Variation of reactive power with control angle for various designs

At $\alpha = 0^\circ$ all valve currents are equal in magnitude, and the line current in p.u. = 1.0. Under this condition, the value of current through reactor x_3 in Figure 2.6 equals to that of line current. Hence the per unit total rating of all reactors/phase is;

$$\begin{aligned} Q_r &= \frac{x_1}{X} + \frac{x_3}{X} + \left(\frac{\sqrt{3}}{2}\right)^2 \frac{2x_2}{X} + \left(\frac{\sqrt{3}}{2}\right)^2 \frac{2x_2}{X} \\ &= \frac{x_1 + x_2 + x_3}{X} + 2\frac{x_2}{X} \\ &= 1 + 2y \end{aligned} \quad (2.30)$$

The rating Q_r is increased as a higher value of y is chosen as shown in Figure 2.14. However, selection of z does not influence the installed capacity of the reactors. Therefore for the three cases considered before:

Case 1 ($y=0.0, z=0.0$):	$Q_r = 1.0$ p.u.
Case 2 ($y=0.0, z=1.0$):	$Q_r = 1.0$ p.u.
Case 3 ($y=0.3, z=0.7$):	$Q_r = 1.6$ p.u.

2.5 Harmonic Analysis

Harmonics generated by the static compensators form by far the most important concern in their application for power systems. It is, therefore, only reasonable to search for designs which produce low level of harmonic content and also result in a saving in the cost of filtering equipment. The Generalized UM-Concept offers such possibilities. From harmonic consideration the major interest lies in the line currents. Since these currents are periodic and of odd function behaviour, as seen from Figures 2.7 to 2.10, they can be resolved into odd harmonics.

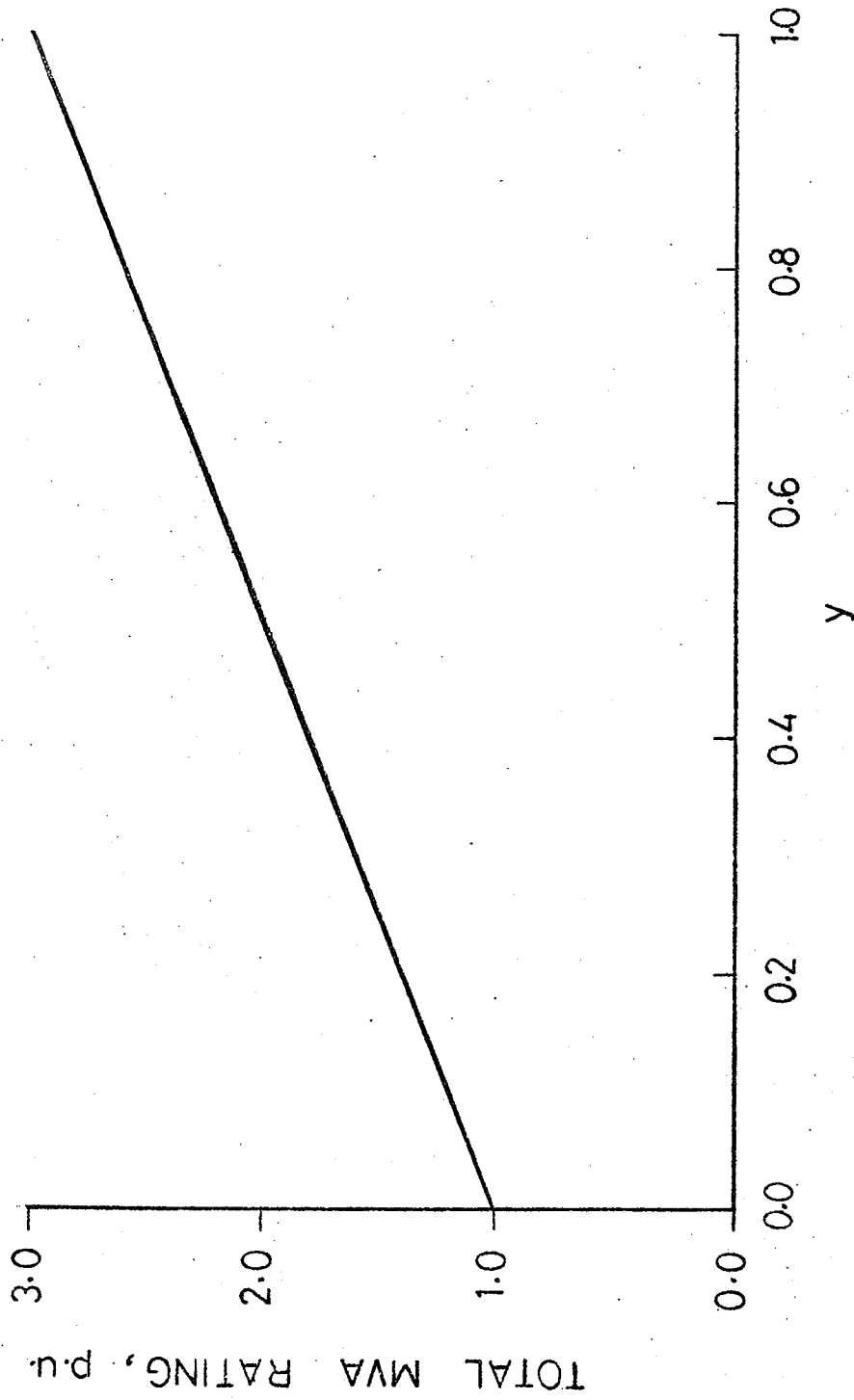


Figure 2.14 Total rating of reactors for various designs

The magnitude of the n th harmonic component of line current i_A is calculated using the following integration:

$$I_n = \frac{2}{\pi} \int_{\pi/2}^{3\pi/2} i_A(\omega t) \cos(n\omega t) d(\omega t) \quad (2.31)$$

where $I_A(\omega t)$ is given in Table 2.I. The detailed calculation of these currents is rather lengthy and gives rise to long expressions. The final simplified expressions are given in Table 2.II where the following substitutions are made:

$$f_1 = (n-1) \sin(n+1)\alpha \quad (2.32)$$

$$f_2 = (n-1) \sin\{(n+1)\alpha-120^\circ\} \quad (2.33)$$

$$f_3 = (n-1) \sin\{(n+1)\alpha+120^\circ\} \quad (2.34)$$

$$g_1 = (n+1) \sin(n-1)\alpha \quad (2.35)$$

$$g_2 = (n+1) \sin\{(n-1)\alpha+120^\circ\} \quad (2.36)$$

$$g_3 = (n+1) \sin\{(n-1)\alpha-120^\circ\} \quad (2.37)$$

Figures 2.15 to 2.24 show the magnitude of harmonic currents as a function of p.u. reactive power of the compensator. Figures 2.15, 2.16 and 2.17 correspond to the three cases considered (Cases 1 and 2 for known designs while Case 3 represents a reasonable example to illustrate the generalized proposed UM-Concept). Figures 2.18 to 2.24 are included to demonstrate the effect of increasing the parameter $y(=x_2/X)$ on the general behaviour of harmonics. The following important observations are to be made:

- (a) The peak values of all harmonics are the highest for Case 2 ($y=0, z=1$) and the lowest for the case with $y=1$. However, there is only little change in the harmonics for values of y from 0.4 to 1.0.

Table 2.11 Per-unit Fundamental and Harmonic Components of Line Current

OPERATING RANGE OF α FUNDAMENTAL, I_1 nth HARMONIC, I_n

$0 \leq \alpha \leq 30^\circ$	$1 - \frac{3y(1-z)}{\pi(3c_2-2yz)} (2\alpha - \sin 2\alpha)$	$\frac{4}{\pi} \cdot \frac{y(1-z)}{(3c_2-2yz)} \cdot \frac{(1-\cos 120^\circ n)}{n(n-1)} (f_1 - g_1)$
$30^\circ \leq \alpha \leq 60^\circ$	$1 - \frac{3yc_2\{\alpha c_1 - 2\sin 2\alpha\}}{2\pi c_1(3c_2-yz)} - \frac{3y(1-z)\alpha}{\pi(3c_2-2yz)} \left[\frac{2}{c_1} - \frac{3(1-y-z)^2}{2(3c_2-yz)} \right]$ $+ \frac{y^2 z [2\pi(1-z) - 3(2c_2-yz)\sin(120^\circ - 2\alpha)]}{\pi c_1(3c_2-yz)(3c_2-2yz)}$	$\frac{y(1-z)c_2}{\pi c_1(3c_2-yz)(3c_2-2yz)} \cdot \frac{1}{n(n-1)} \cdot \{ 2(1-\cos 120^\circ n) \left[\frac{2c_1(3c_2-yz)}{c_2} (f_1 - g_1) + 2z(f_2 - g_2) \right] \}$ $+ \frac{2z(3c_2-yz)}{c_2} [f_1 - g_1 - (n-1)\sin[(n+1)\alpha + 120^\circ n] + (n+1)\sin((n-1)\alpha + 120^\circ n)]$
$60^\circ \leq \alpha \leq 90^\circ$	$\frac{1}{c_1} \left\{ 1 + \frac{3c_2 y}{\pi(3c_2-yz)} \cdot (\pi - 2\alpha + \sin 2\alpha) \right\}$	$-z^2 [f_2 - g_2 - (n-1)\sin[(n+1)(\alpha - 120^\circ)] + (n+1)\sin((n-1)(\alpha - 120^\circ))] \}$
$90^\circ \leq \alpha \leq 120^\circ$	$\frac{1}{\pi c_1(c_4-z)} \{ \pi(2c_4-3z) - 3c_2(2\alpha - \sin 2\alpha) \}$	$\frac{4c_2 y}{\pi c_1(3c_2-yz)} \cdot \frac{(1-\cos 120^\circ n)}{n(n-1)} (f_1 - g_1)$
$120^\circ \leq \alpha \leq 150^\circ$	$\frac{1}{\pi c_1 c_4(c_4-z)} \{ \pi [2c_2(c_4-z) + c_4 c_5] + 3c_2 c_4 \sin 2\alpha - 3zc_3 \sin(2\alpha + 120^\circ) - 3\alpha [c_2(c_4-z) + c_1 c_4] \}$	$\frac{4c_2}{\pi c_1(c_4-z)} \cdot \frac{(1-\cos 120^\circ n)}{n(n-1)} (f_1 - g_1)$
$150^\circ \leq \alpha \leq 180^\circ$	$\frac{3}{\pi c_4} (2\pi - 2\alpha + \sin 2\alpha)$	$\frac{2}{\pi c_1 c_4(c_4-z)} \cdot \frac{1}{n(n-1)} \{ 2c_2(1-\cos 120^\circ n) [(c_4-z)(f_1 - g_1) - z(f_3 - g_3)] + z(c_4-z) [f_1 - g_1 - (n-1)\sin((n+1)\alpha + 120^\circ n) + (n+1)\sin((n-1)\alpha + 120^\circ n)] - z^2 [f_3 - g_3 - (n-1)\sin((n+1)(\alpha + 120^\circ)) + (n+1)\sin((n-1)(\alpha + 120^\circ))] \}$

- (b) Higher magnitudes of harmonics occur over a smaller operating range of reactive power as y increases from 0 to 0.4.
- (c) While many harmonic filters may be required for the known designs of Cases 1 and 2, because of lower harmonics generation, some of these may be unnecessary for the designs arising from the Generalized UM-Concept.
- (d) In the new designs where y takes a value >0.2 , an additional region of reactive power exists, in the neighbourhood of $\alpha = 90^\circ$, where the harmonic content is insignificant. This may be the preferred region for normal operation of the compensator which allows sufficient margin for excursions on either side. This region lies between 0.75 to 0.8 p.u. reactive power for the example of Case 3 ($y=0.3, z=0.7$) and approaches the mid operating range as y takes higher values.

In order to evaluate the influence of the alternatives offered by the new generalized concept from the harmonics point of view, an extensive study was made. Figures 2.25 and 2.26 summarize the peak values of the 5th and 7th harmonics respectively for some combinations of y and z . It is observed that as y is increased from 0 to 0.4 there is a sharp reduction in the peak value of the harmonics and for a given value of $y \leq 0.2$ as z is reduced the peak value of the harmonics are also reduced until z approaches 0.5. However with $y > 0.2$ as z is reduced the harmonic peaks increase and for $y > 0.4$ the reduction in the harmonic content is marginal. Consideration of peak value alone of a harmonic is not sufficient to illustrate their influence as can be seen from Figures 2.16 and 2.17. In Figure 2.16 the harmonic content is a flat topped function of the compensator reactive power implying, thereby, that a given value of harmonic is present over a

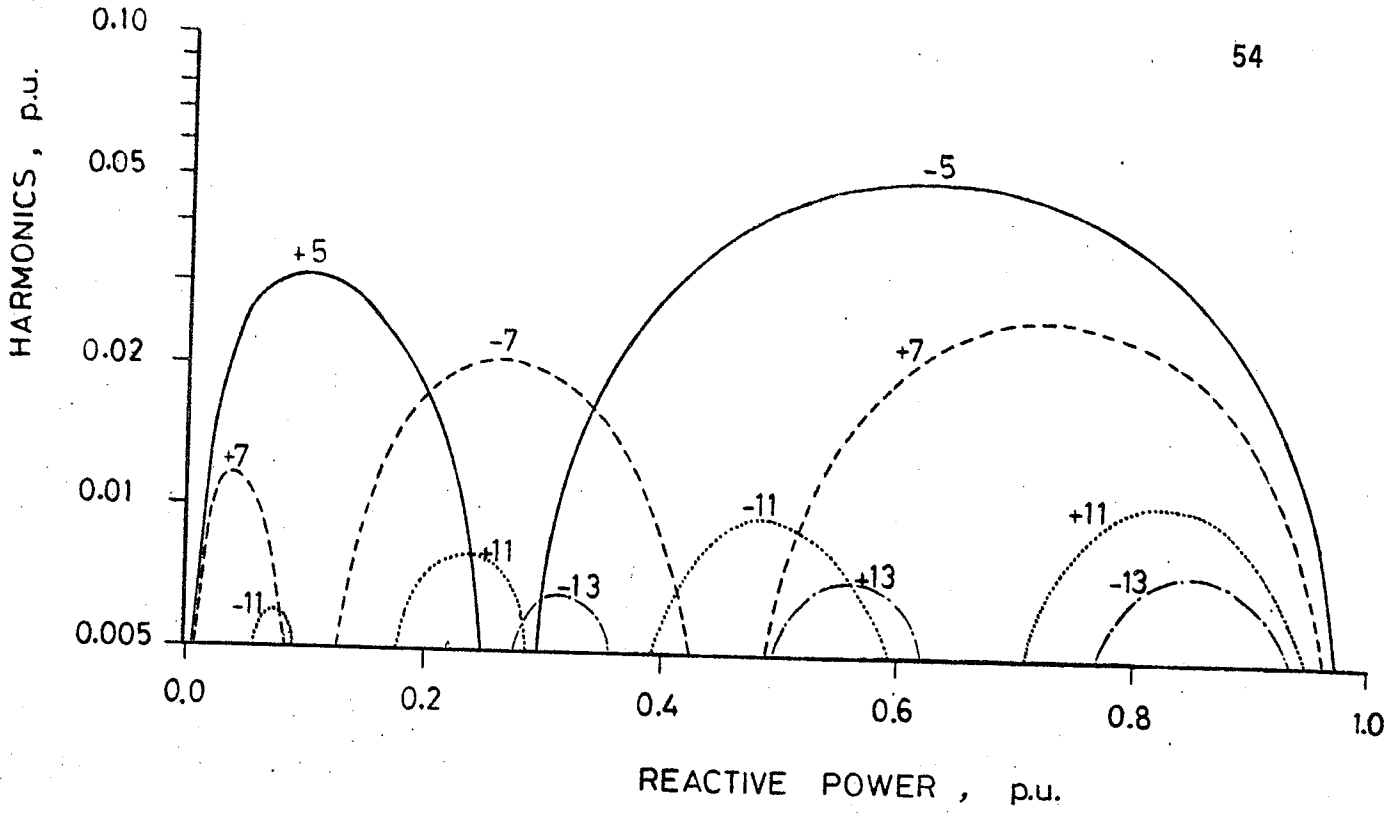


Figure 2.15 Magnitude of harmonics in line current for: $y = 0, z = 0$.

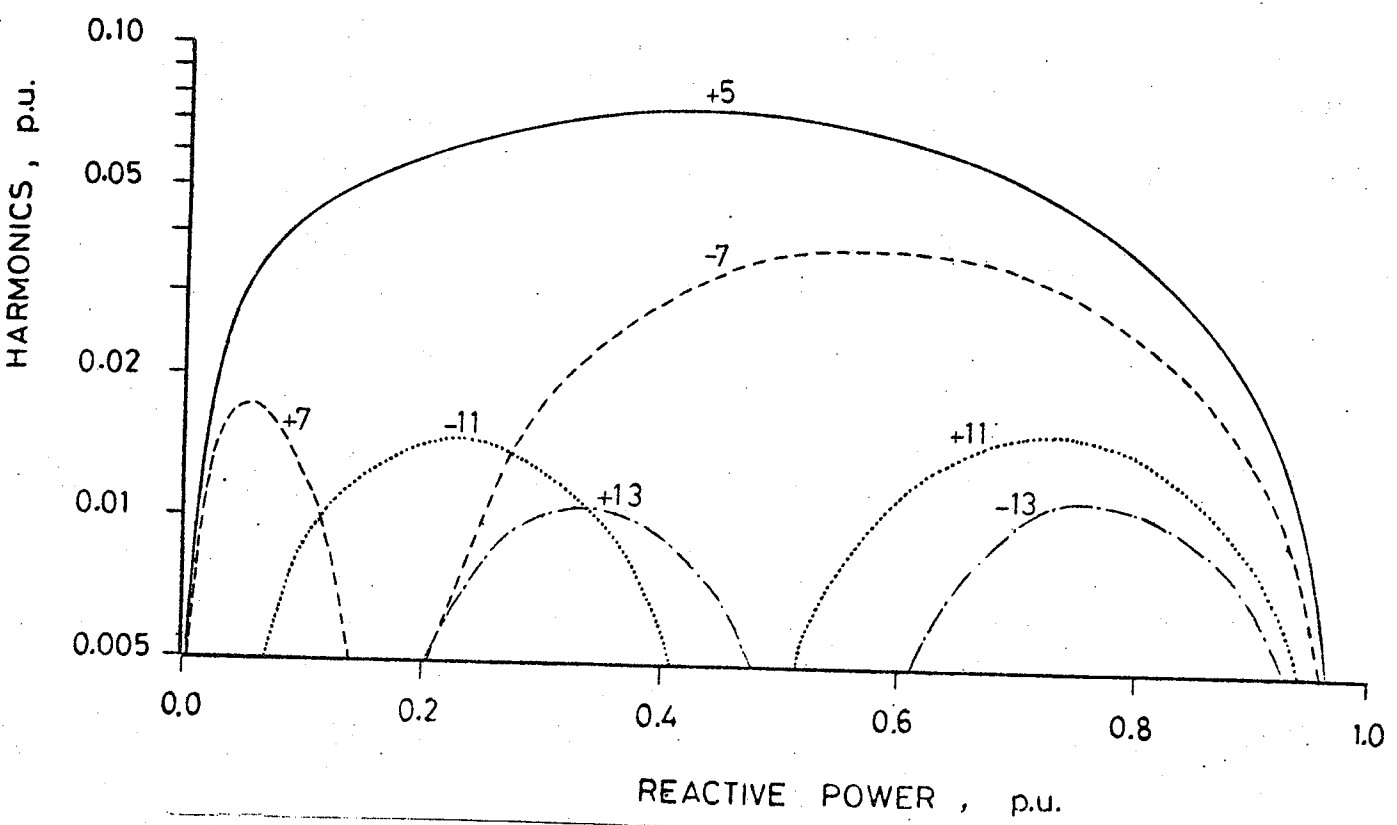


Figure 2.16 Magnitude of harmonics in line current for: $y = 0, z = 1$.

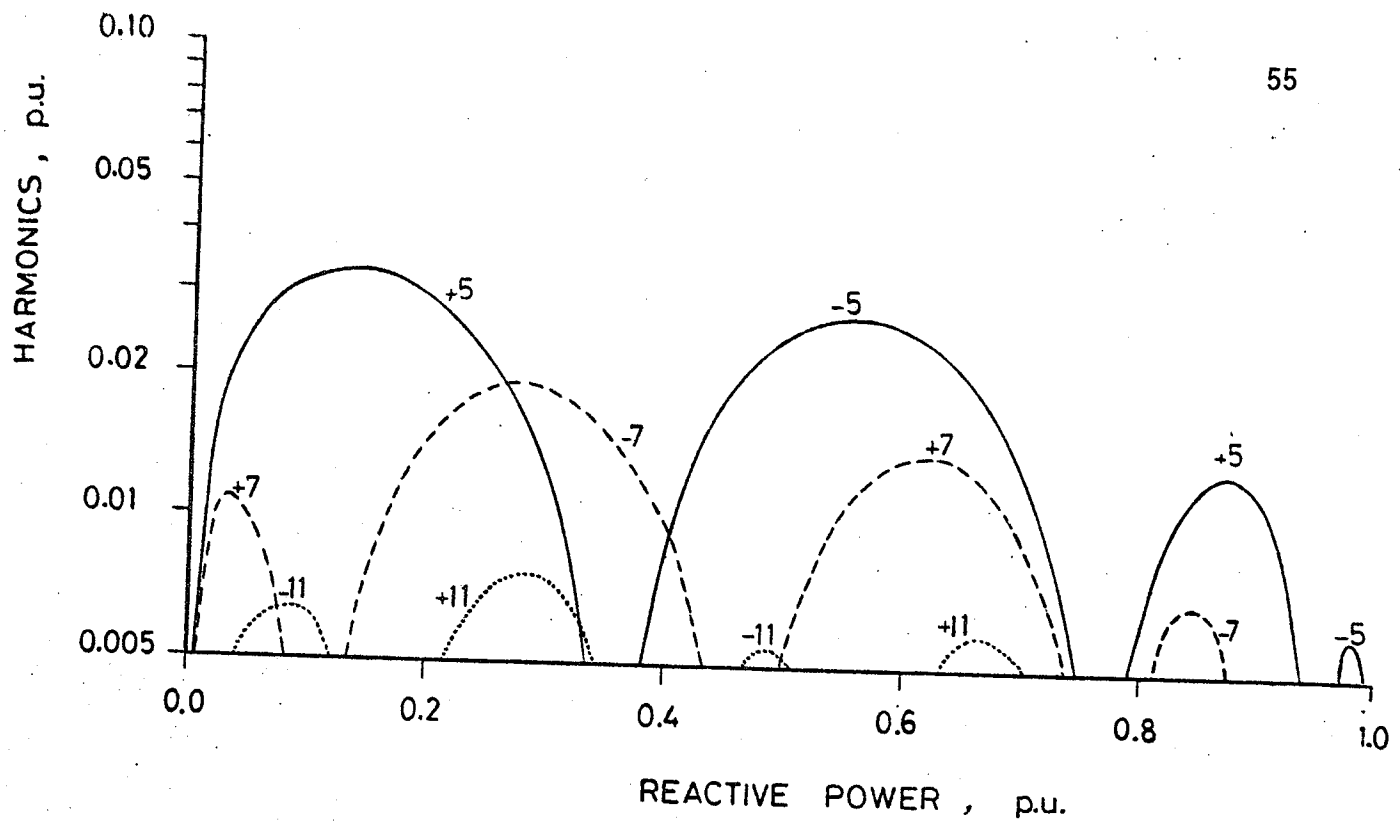


Figure 2.17 Magnitude of harmonics in line current for:
 $y = 0.3, z = 0.7$

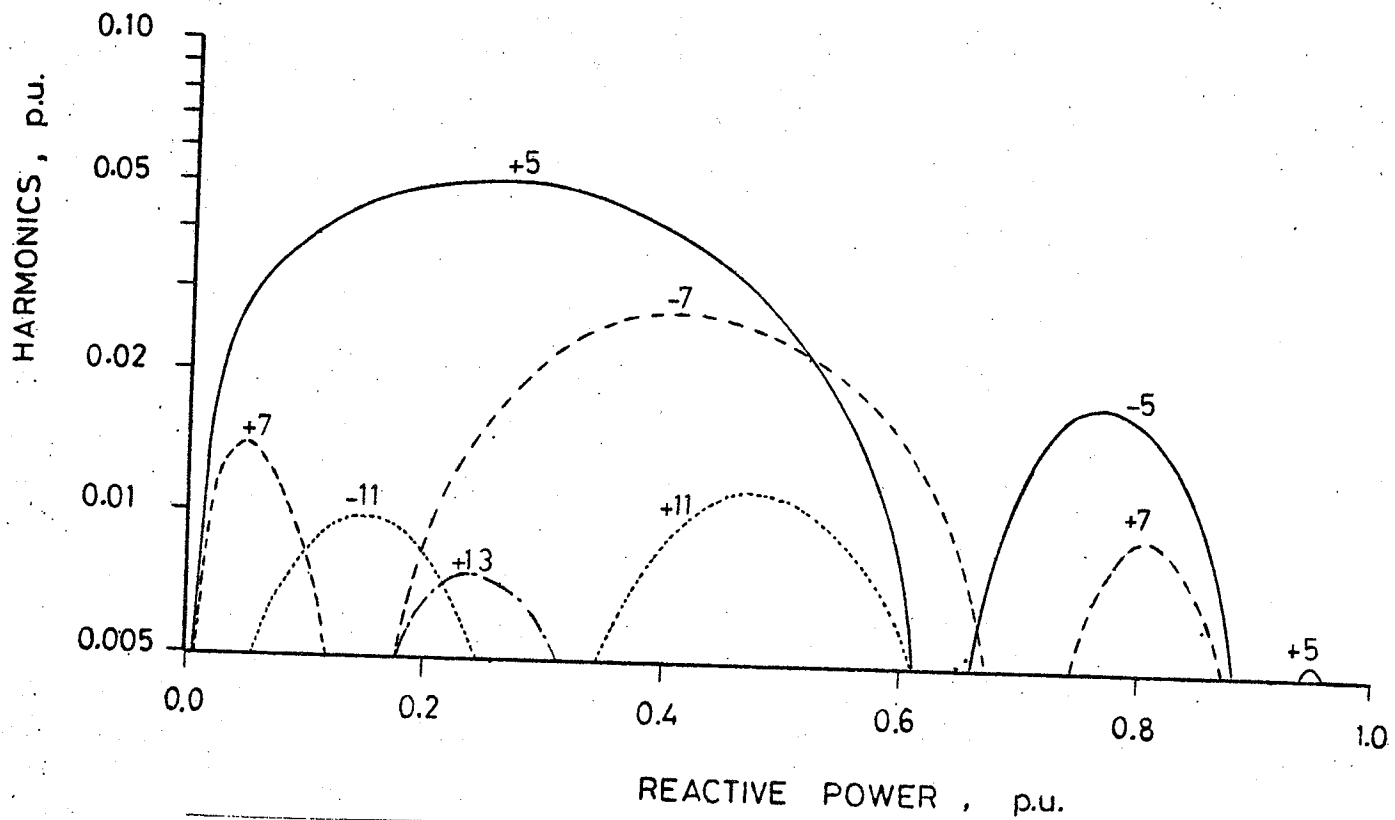


Figure 2.18 Magnitude of harmonics in line current for:
 $y = 0.1, z = 0.9$

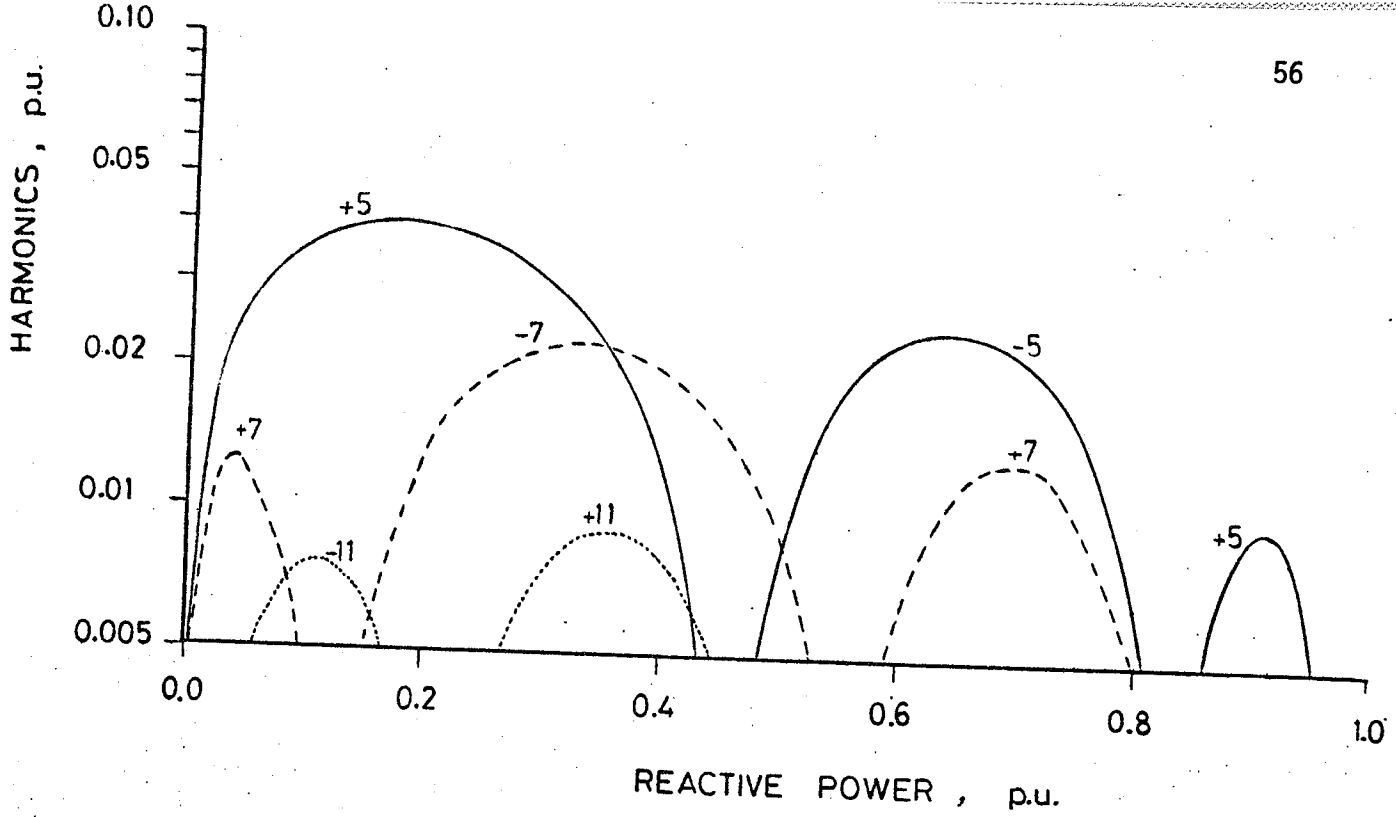


Figure 2.19 Magnitude of harmonics in line current for:
 $y = 0.2, z = 0.8$

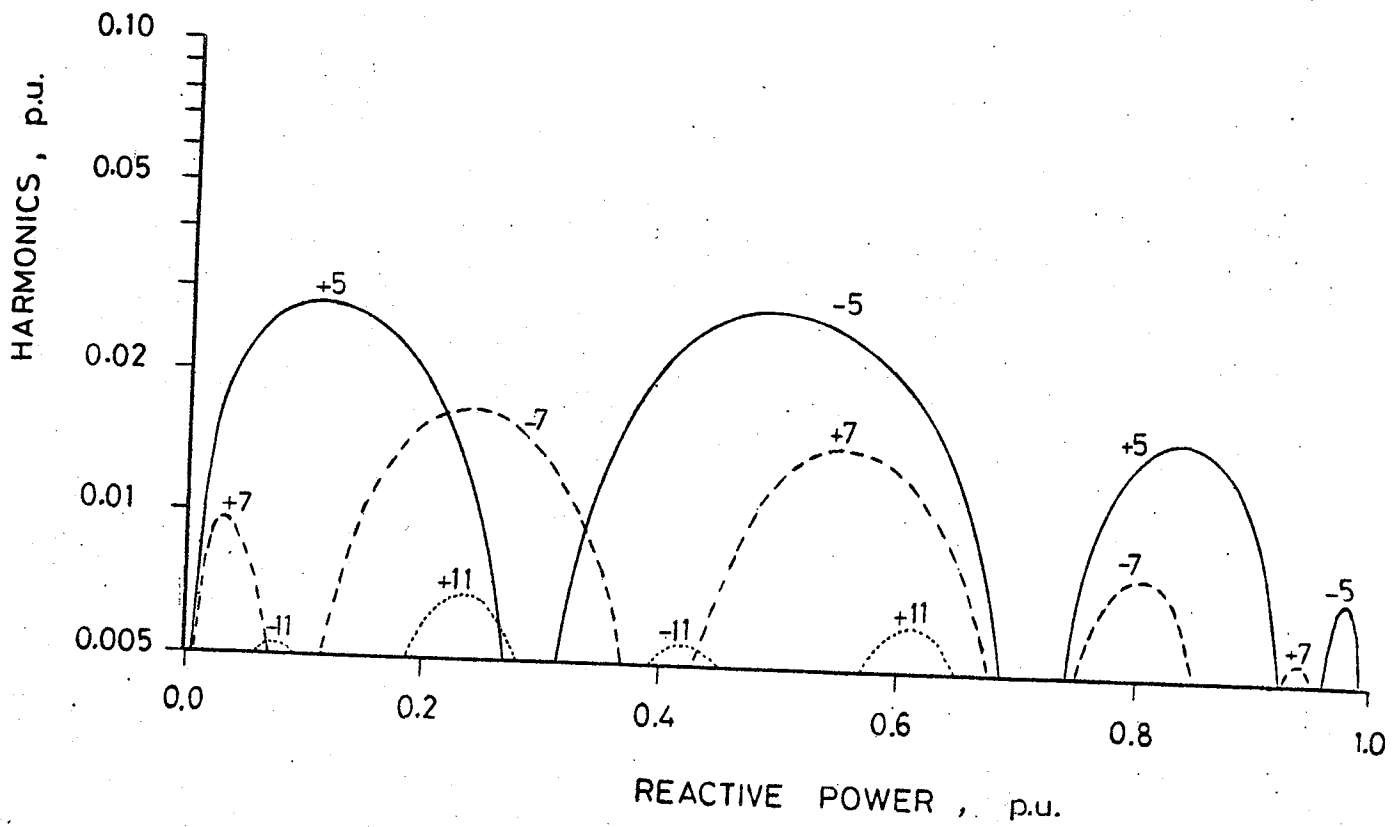


Figure 2.20 Magnitude of harmonics in line current for:
 $y = 0.4, z = 0.6$

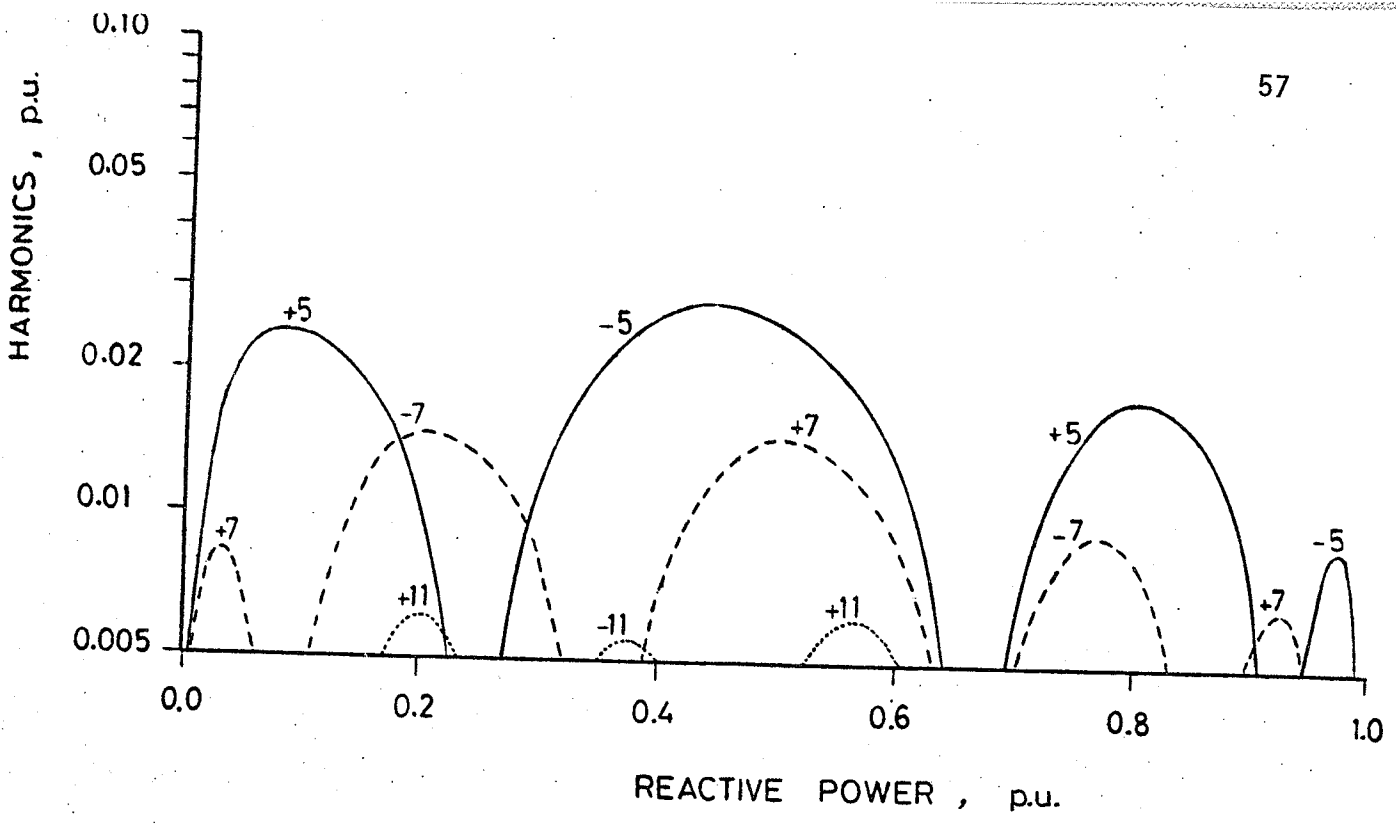


Figure 2.21 Magnitude of harmonics in line current for: $y = 0.5, z = 0.5$

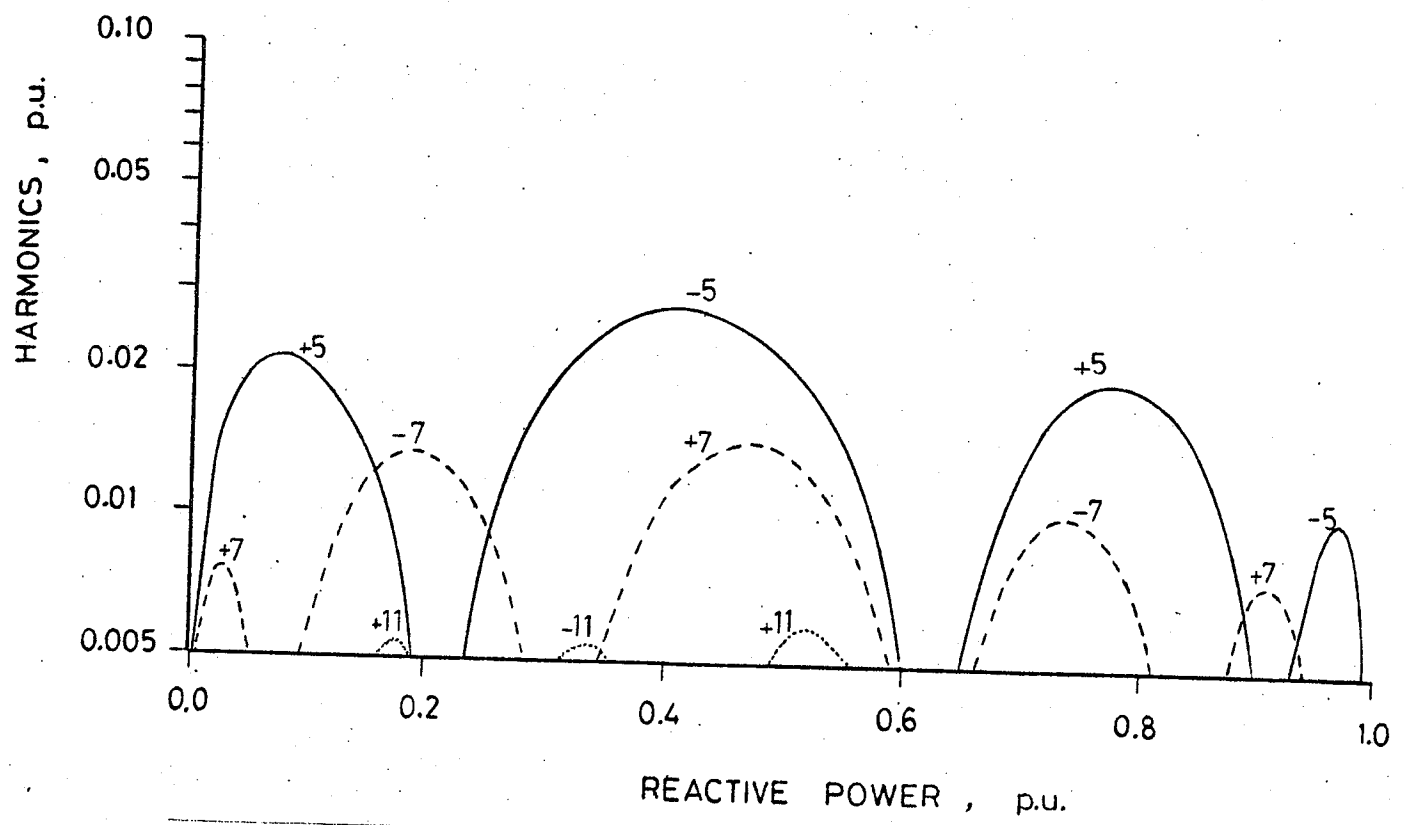


Figure 2.22 Magnitude of harmonics in line current for: $y = 0.6, z = 0.4$

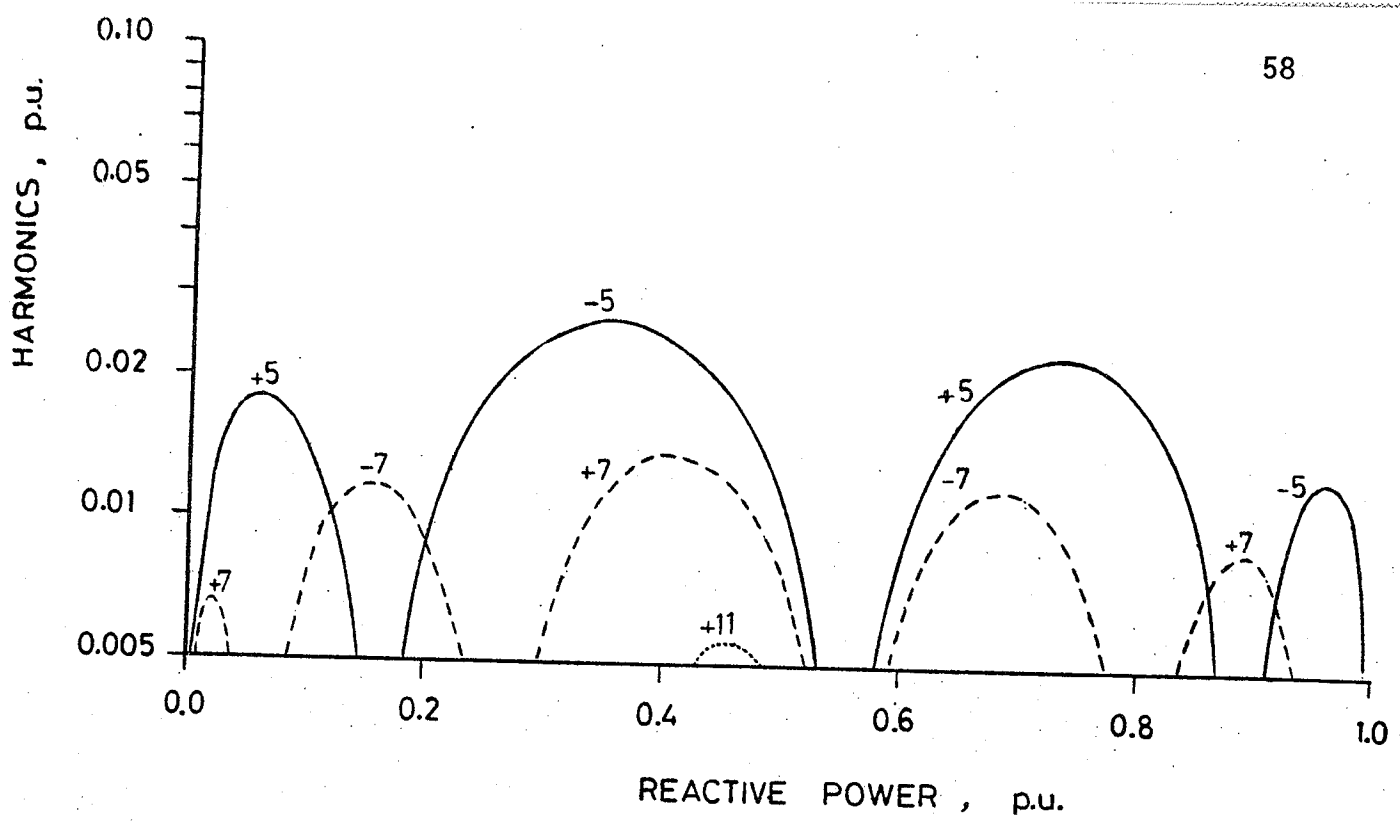


Figure 2.23 Magnitude of harmonics in line current for:
 $y = 0.8, z = 0.2$

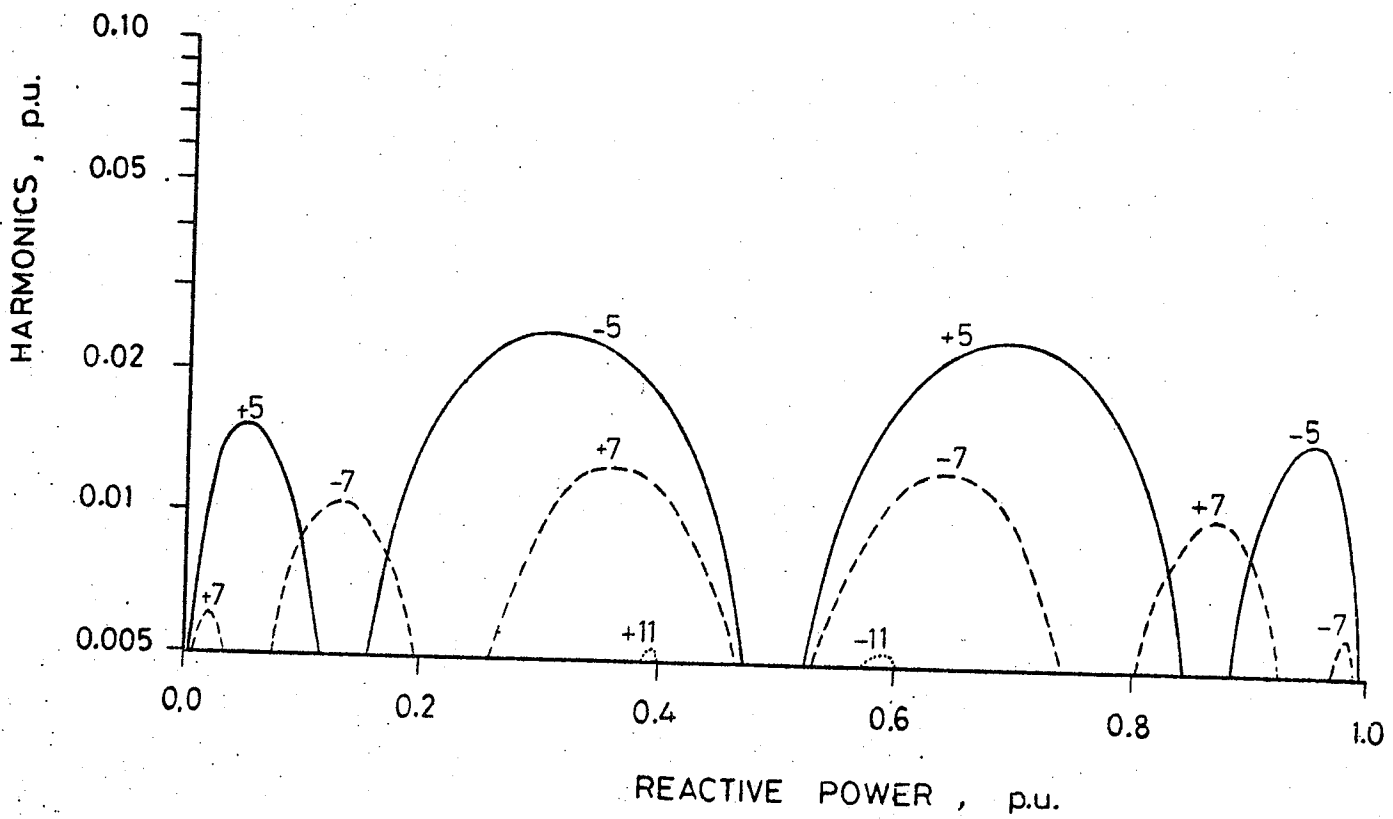


Figure 2.24 Magnitude of harmonics in line current for:
 $y = 1.0, z = 0.0$

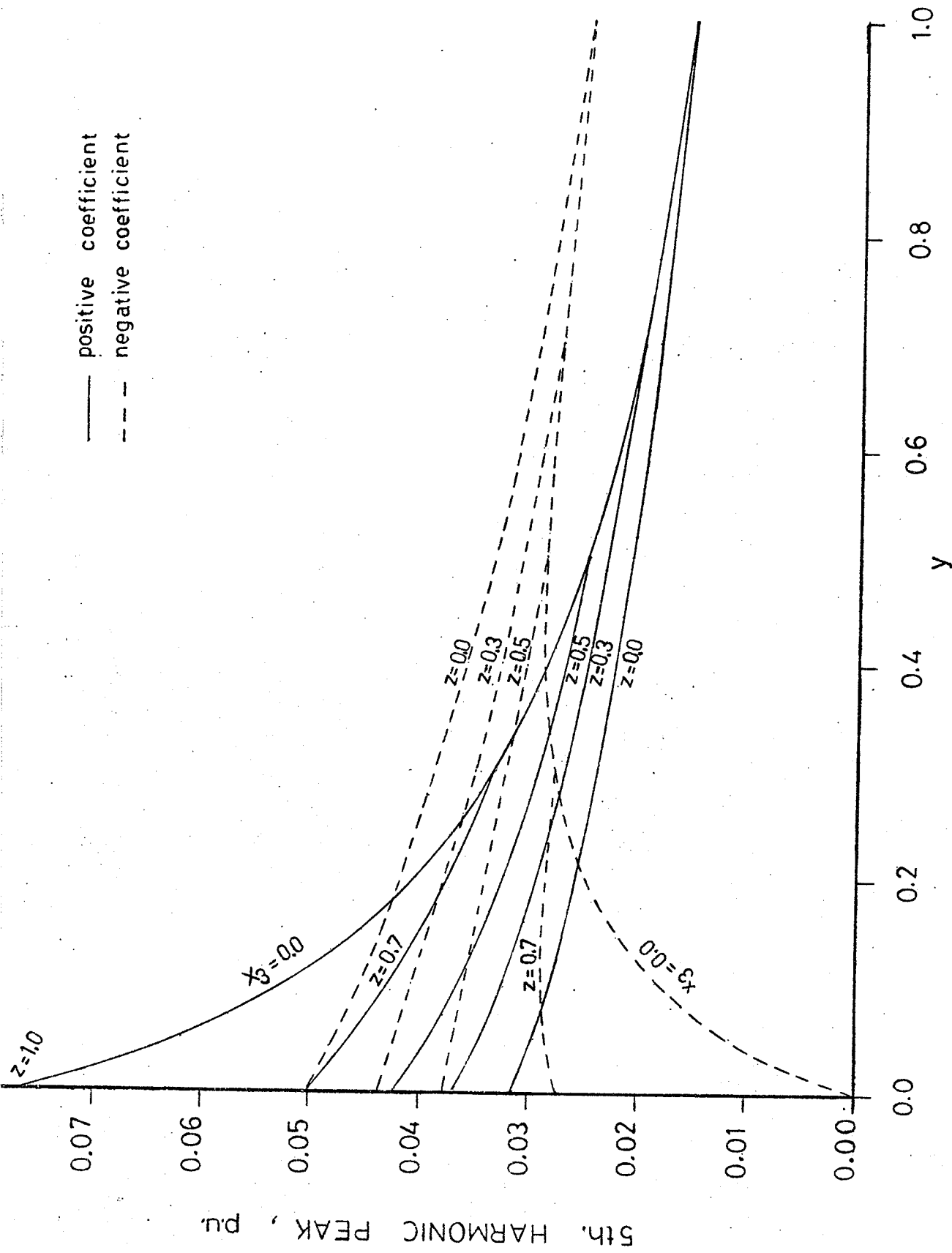


Figure 2.25 Peak value of the 5th harmonic current for various designs

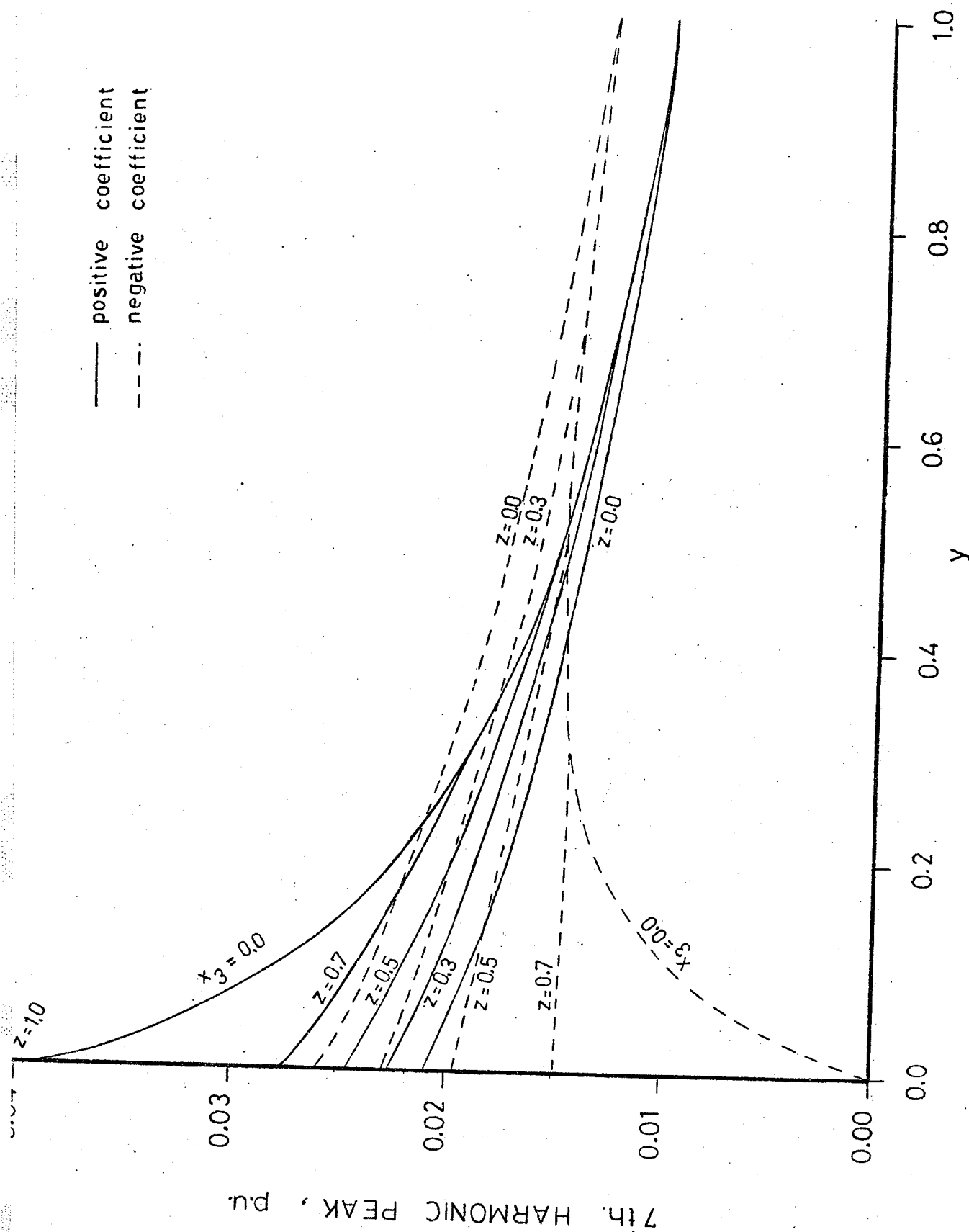


Figure 2.26 Peak value of the 7th harmonic current for various designs

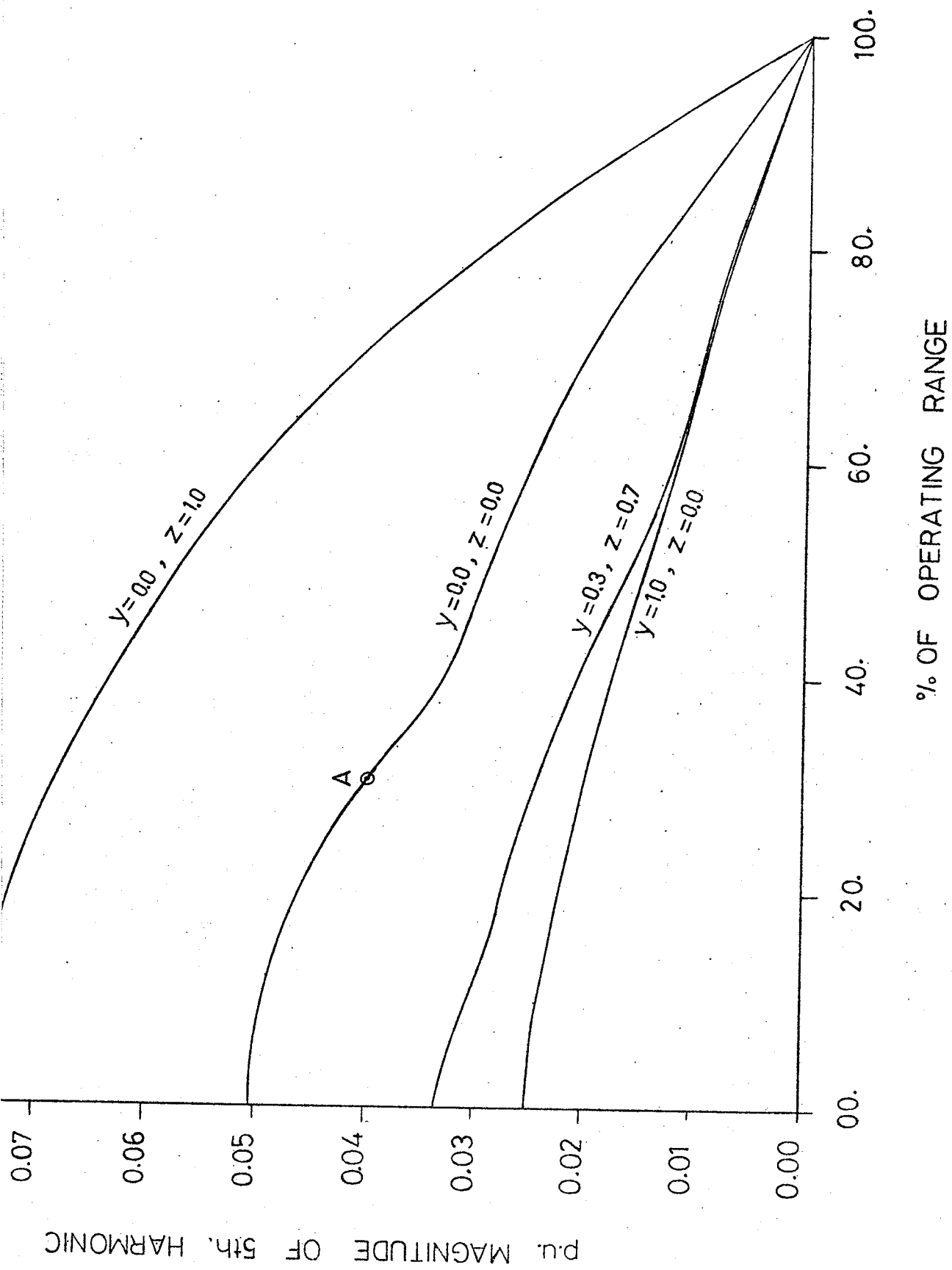


Figure 2.27 Presence of a 5th harmonic current magnitude over a percentage of the operating range for various designs

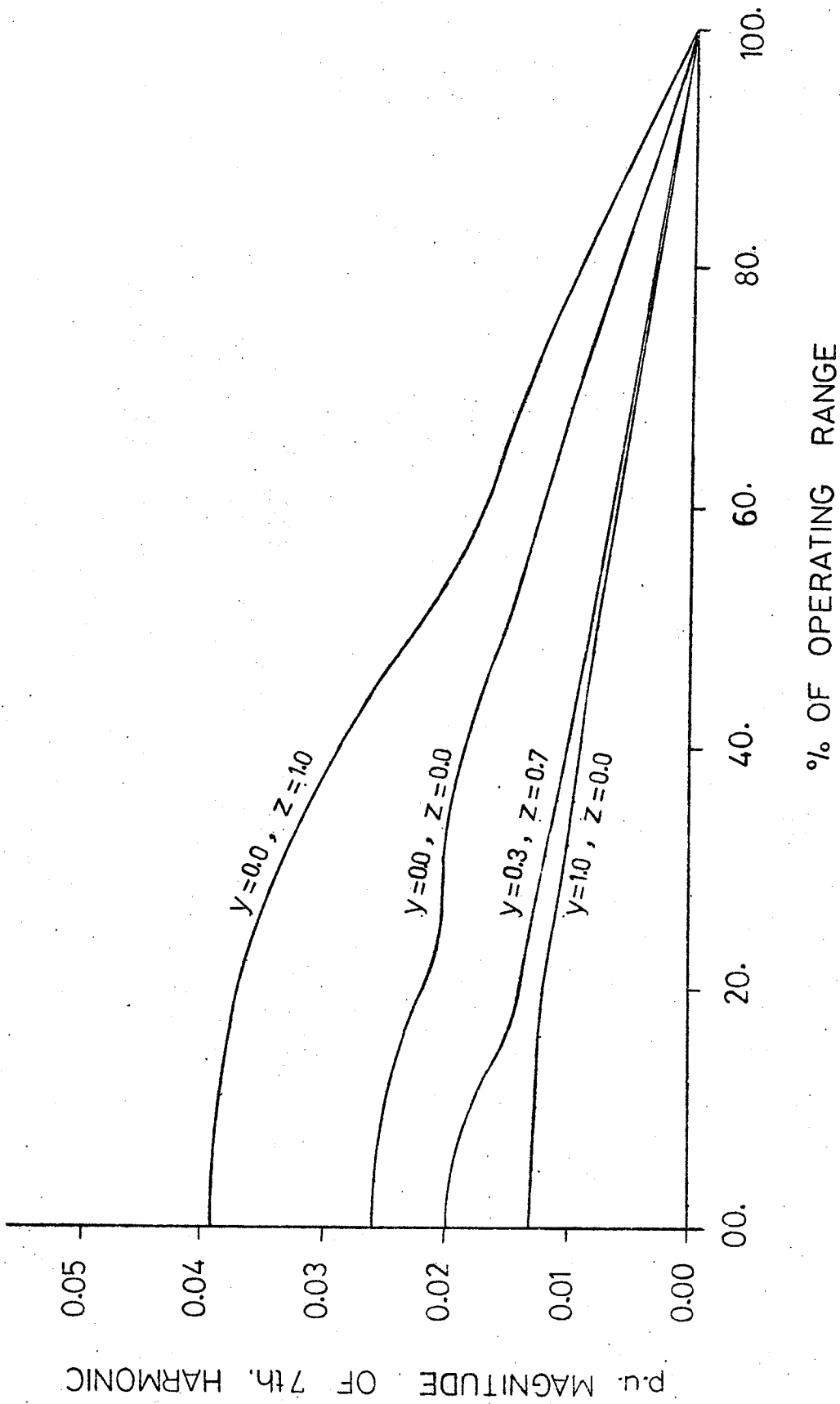


Figure 2.28 Presence of a 7th harmonic current magnitude over a percentage of the operating range for various designs

large operating range. On the contrary, a value of harmonic content exists over a much smaller range of reactive power in Figure 2.17.

A better evaluation of the harmonic content is, therefore, quantized in an alternative presentation in Figures 2.27 and 2.28 for the 5th and 7th harmonics respectively. For example, consider point A in Figure 2.27 (for $y=0$, $z=0$) it indicates that a 5th harmonic content of 0.04 p.u. exists for 30% of the VAR operating range of the compensator.

2.6 Overvoltage Transient Performance

For the application of static shunt VAR compensators the thyristor valves are invariably designed to withstand the transient overloadings, which are usually of many orders of magnitude above the steady state rating. In order to solve the issue of thyristor valve sizing for the proposed new designs in comparison to the available ones, the studies presented in this section have been carried out.

The purpose of this investigation is therefore to identify the worst case which would give rise to a maximum transient overloading of the thyristor valves and its extent when a reactor is subjected to overvoltages.

The prime cause for a bus overvoltage is a sudden rejection of load. During the first few cycles severe distortions in the 3-phase voltages usually occur which are influenced by system resonances. Hence, unless a system configuration is known in detail, it is difficult to predict the voltage waveforms after tripping a load. Since the major concern here is to study the transient overvoltage stresses on the thyristor valves of a number of alternative designs on a comparative basis, the exact waveforms of overvoltages are of less importance.

Under the circumstances it is reasonable to take a simplistic approach and represent the overvoltages in an orderly manner.

For this study a situation is considered where an overvoltage of 1.7 p.u. occurs on a bus and is maintained for a few cycles. Under this situation, in place of the line voltages jumping instantaneously from 1. to 1.7 p.u., it is assumed that each phase voltage changes from 1. to 1.7 p.u. value from its first zero crossing after the event and remains sinusoidal (Figure 2.29). Indeed the calculations show that this is a more severe condition as compared to overvoltages occurring instantaneously. The maximum overcurrent peak for sudden overvoltages turn out to be 5 to 10% lower, depending upon the value of y as compared to the overvoltage phenomenon described earlier, as can be seen in Figure 2.30.

It must be clearly understood that this description of overvoltages is neither defended to be realistic, nor should be misunderstood to imply a restriction on the analytical technique used to calculate the resulting overcurrents.

The overcurrents, as a consequence of the overvoltages, depend to a great extent firstly on the type of controller for the thyristor valves, and secondly on the setting of the compensator load, i.e. operating value of α prior to the occurrence of the overvoltage. Both above factors control the initial conditions and, hence, the d.c. offset of the transient currents.

The procedure adopted for the calculations of overcurrents is that at any time when a valve experiences an overvoltage of 1.25 p.u. (this setting can be altered; it has been chosen arbitrarily) an emergency firing pulse is supplied to it to put it into conducting mode. This

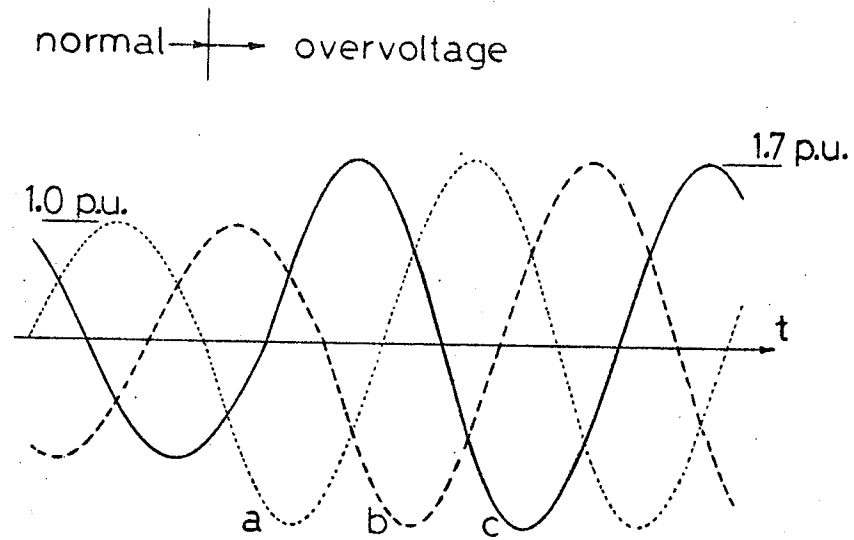


Figure 2.29 Description of the assumed overvoltage

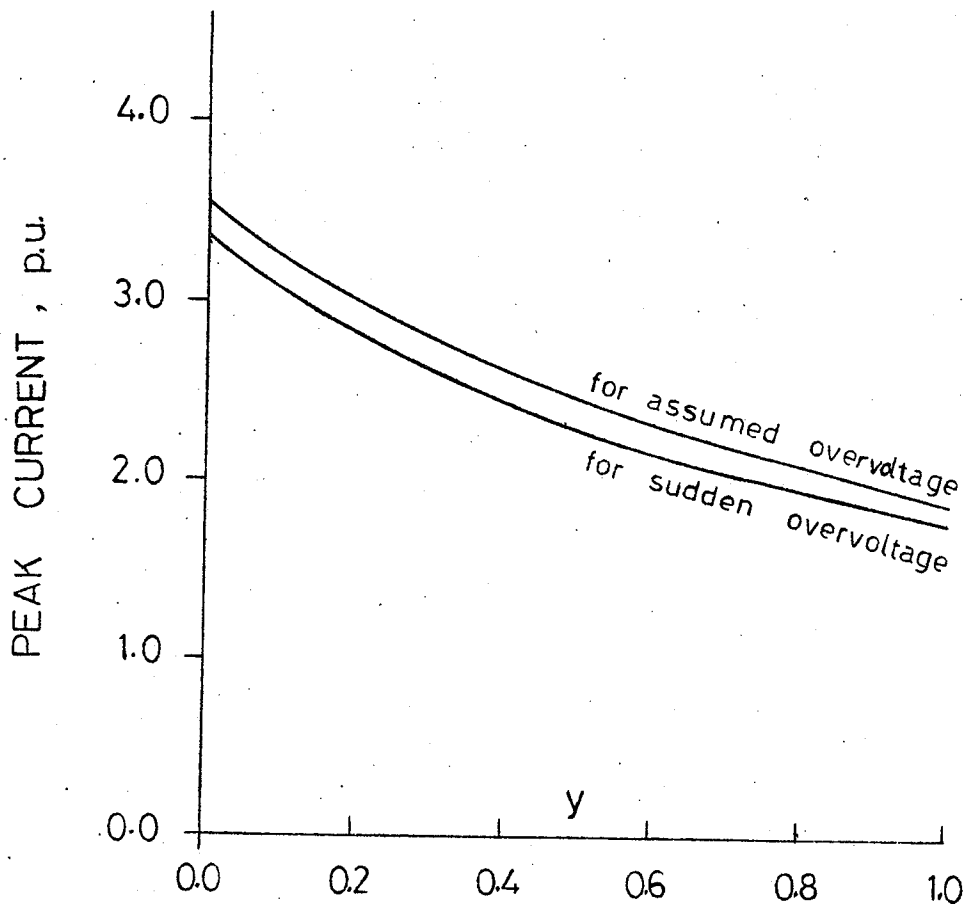


Figure 2.30 Maximum peak of transient valve current for sudden and assumed overvoltage (1.70 pu)

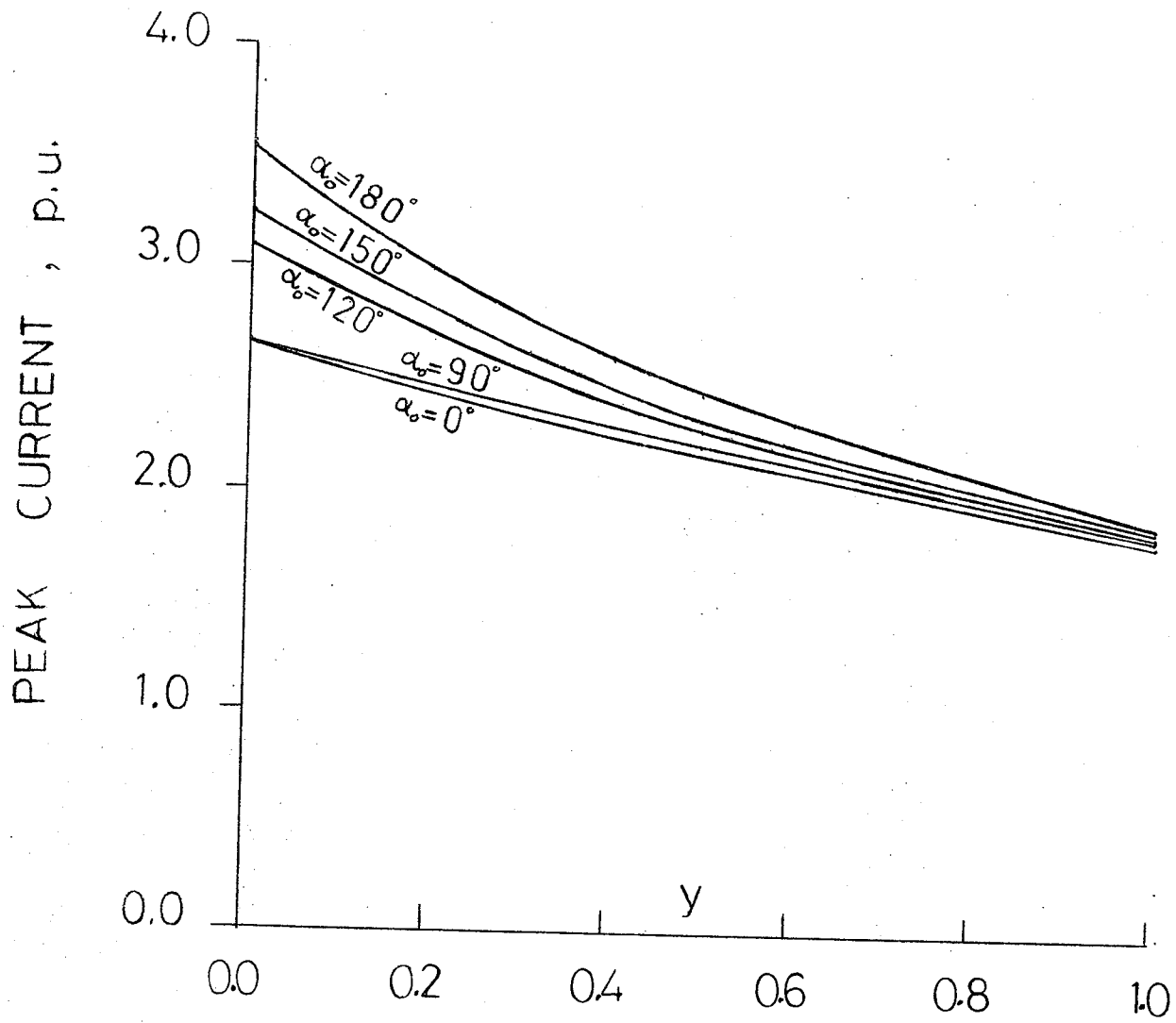


Figure 2.31 Maximum peak of transient valve current for different initial control angles

action can either be taken on an individual valve basis, or after the first emergency firing a continuous firing signal can be applied to all thyristor valves. The latter may be preferred because it provides a simpler and better protection strategy and is most effective in countering the overvoltages. Therefore, all results presented here correspond to a continuous firing scheme on all valves. In order to be able to make a comparative study between different designs an ideal connecting transformer was assumed with a total leakage reactance of 0.1 p.u.

In every time step the system current and voltage equations of Section 2.2 are simultaneously solved, using the criteria outlined in Section 2.3 whenever a new mode of operation arises, yielding new currents which are then used as initial values for the next time interval.

By conducting numerous numerical experiments it has been concluded that the worst case - the design case - is when overvoltages occur at a time when the thyristor controlled reactor is at no load, i.e. $\alpha_0 = 180^\circ$. Figure 2.31 shows the maximum peak current for any valve for different initial values of α for different designs (different values of y - the parameter z has no significant influence). In all, $\alpha_0 = 180^\circ$ is the worst case.

In fact this conclusion coincides with the results obtained by experiments on a reduced scale physical model for a specific design.³⁸ Figure 2.31 also illustrates the advantage of choosing a higher value of y .

Figures 2.32 (a,b and c) are for a known design, i.e., $y=0$, $z=0$. Figure 2.32 (a) shows the instantaneous voltages across the valves, $\alpha_0 = 180^\circ$ prior to emergency firing - triggered by voltage across

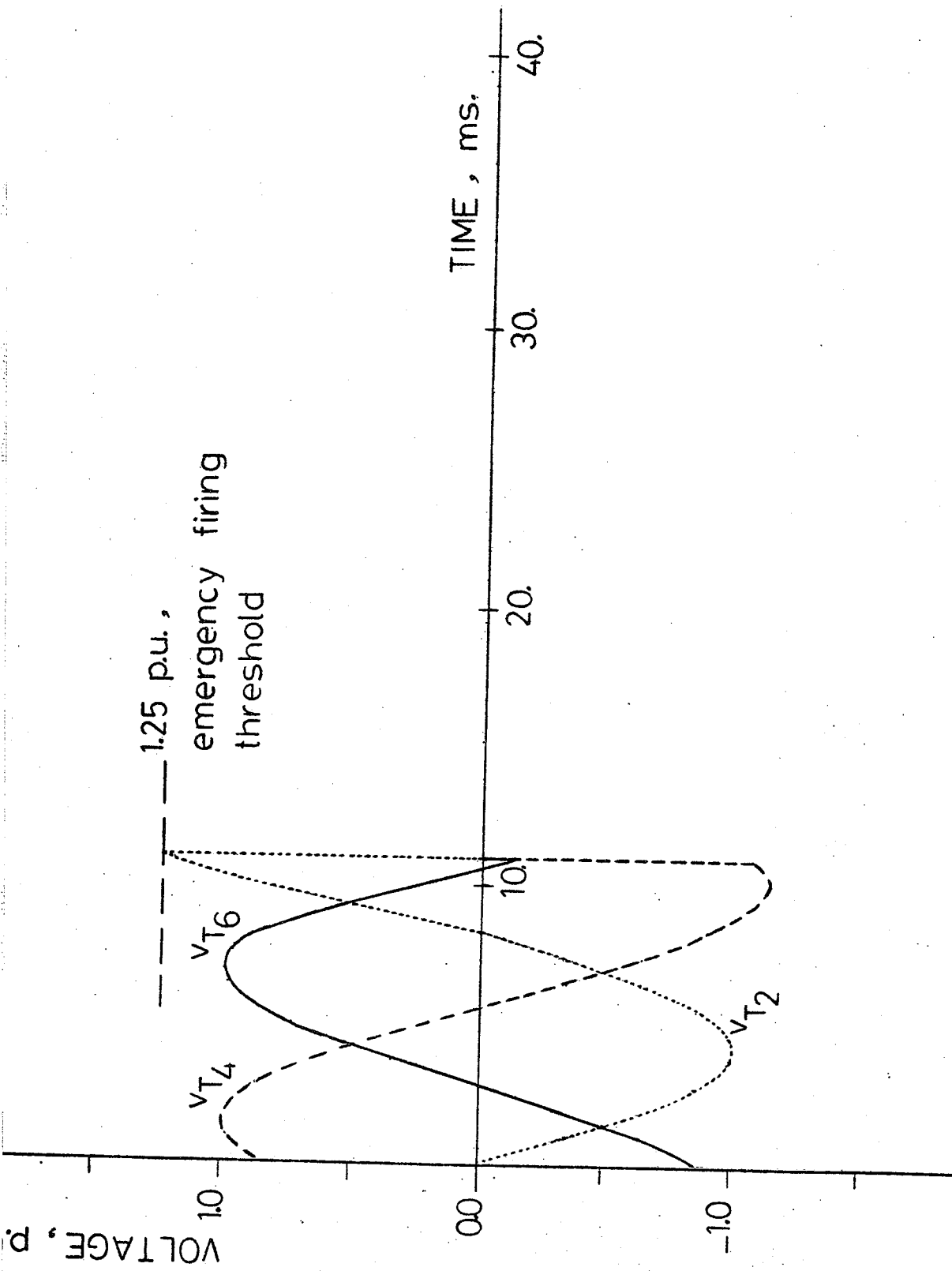


Figure 2.32 Transient performance subsequent to overvoltage for $\alpha_o = 180^\circ$, $y = 0$, $z = 0$
(a) valve voltages

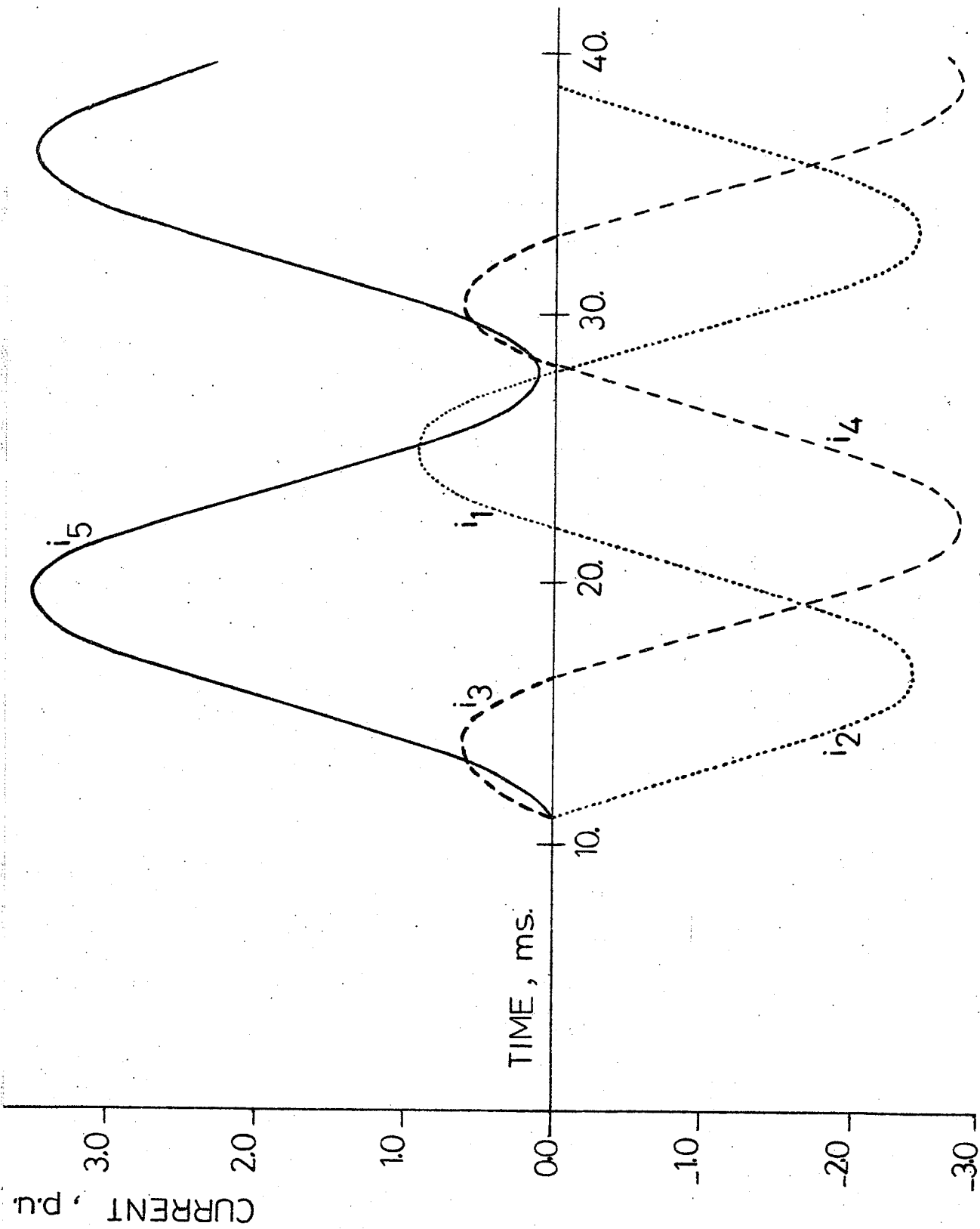


Figure 2.32 Transient performance subsequent to overvoltage for $\alpha_0 = 180^\circ, y = 0, z = 0$

(b) valve currents

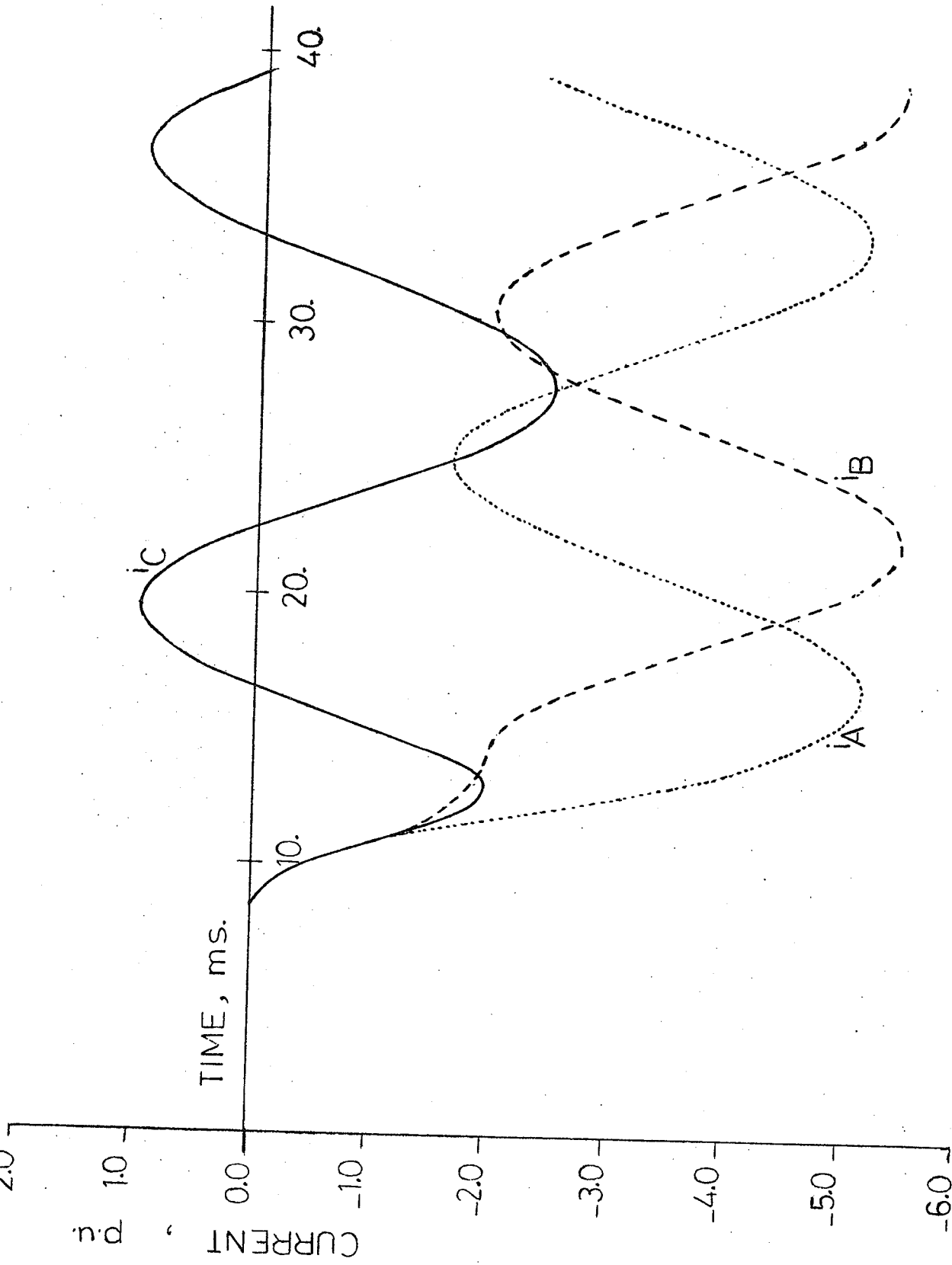


Figure 2.32 Transient performance subsequent to overvoltage
for $\alpha_0 = 180^\circ$
(c) line currents ($y = 0, z = 0$)

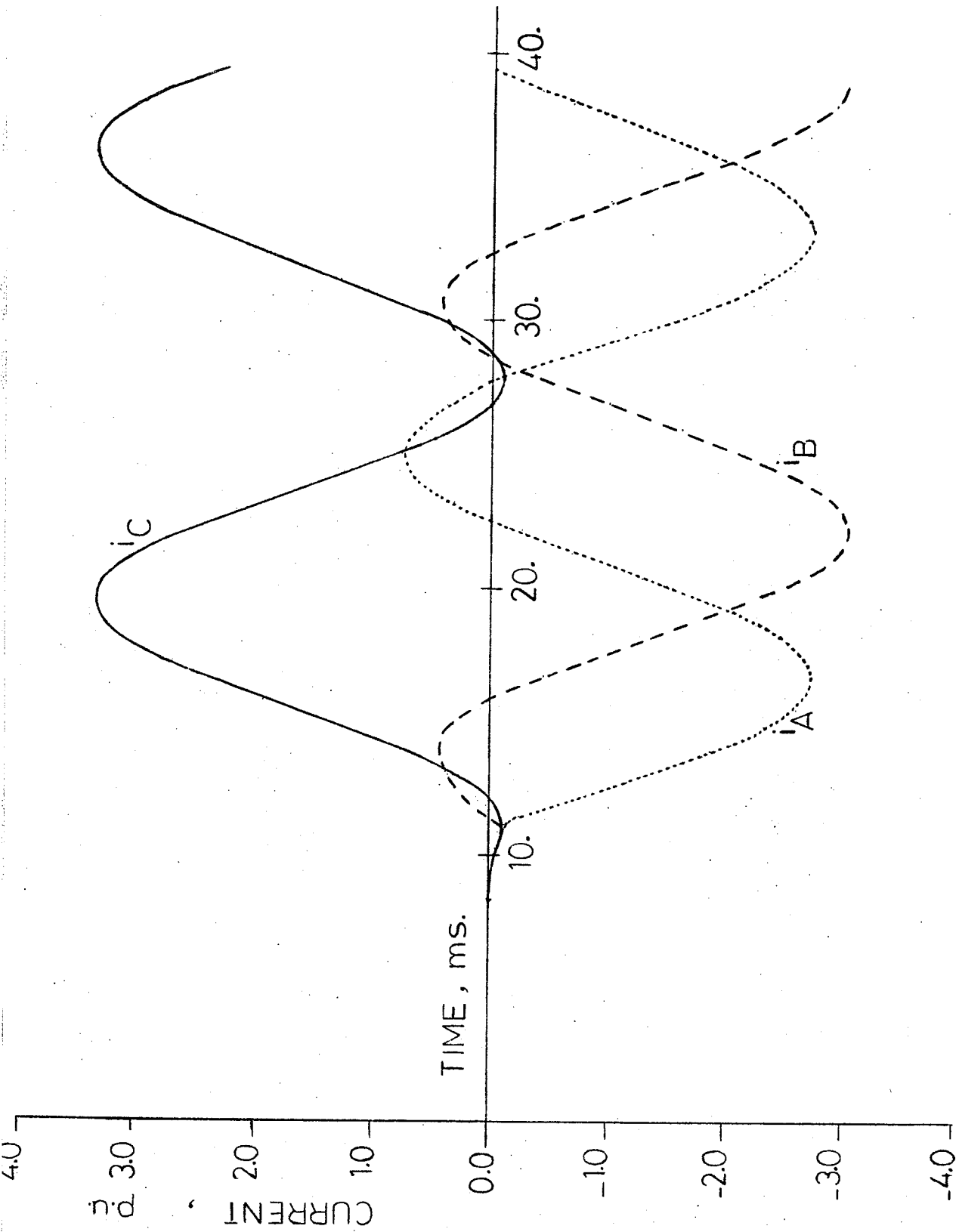


Figure 2.32 Transient performance subsequent to overvoltage
for $O_o = 180^\circ$
(d) line currents ($y = 0, z = 1.0$)

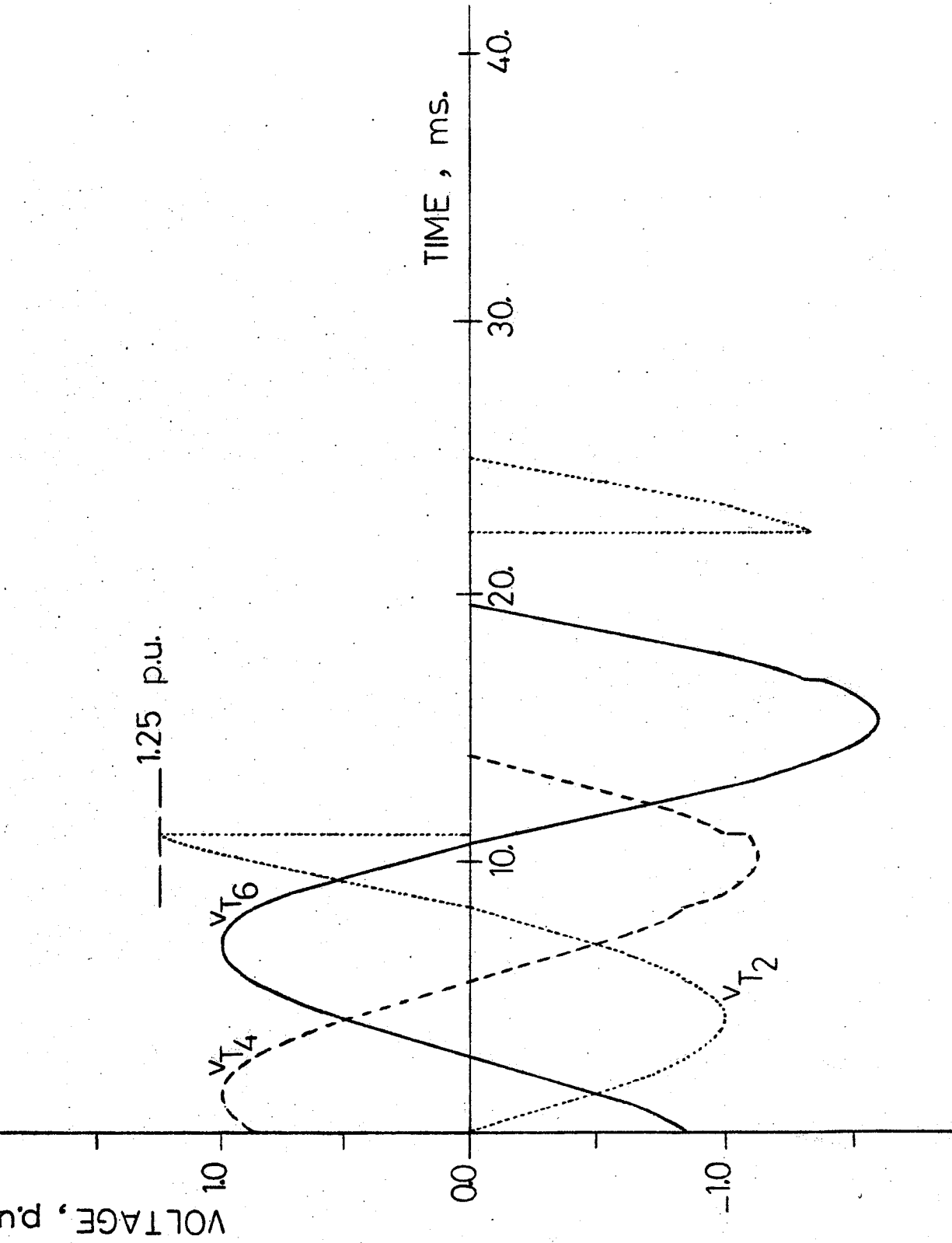


Figure 2.33 Transient performance subsequent to overvoltage
for $\alpha_0 = 180^\circ$, $y = 1$, $z = 0$
(a) valve voltages

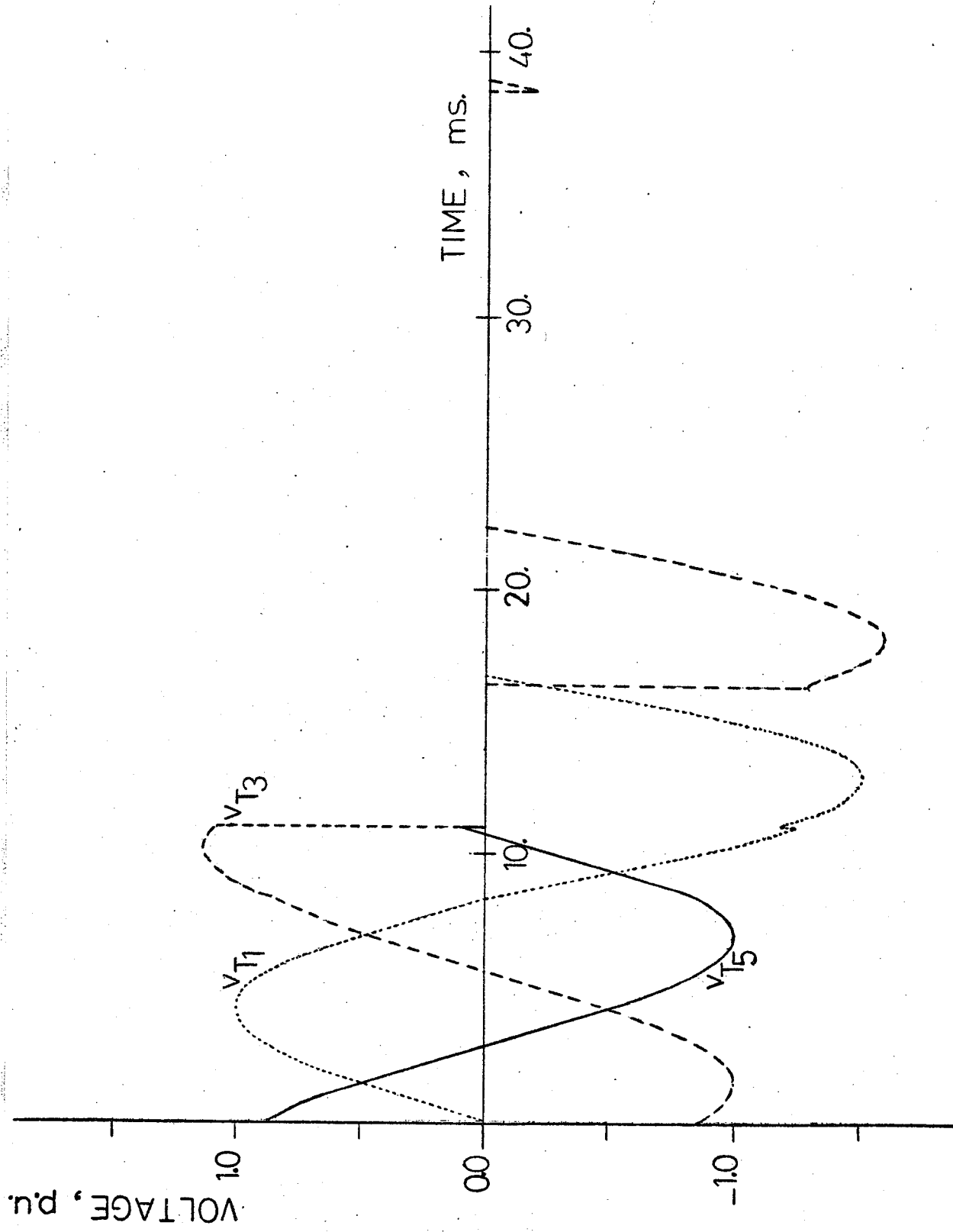


Figure 2.33 Transient performance subsequent to overvoltage
for $C_0 = 180^\circ$, $y = 1$, $z = 0$

(b) valve voltages

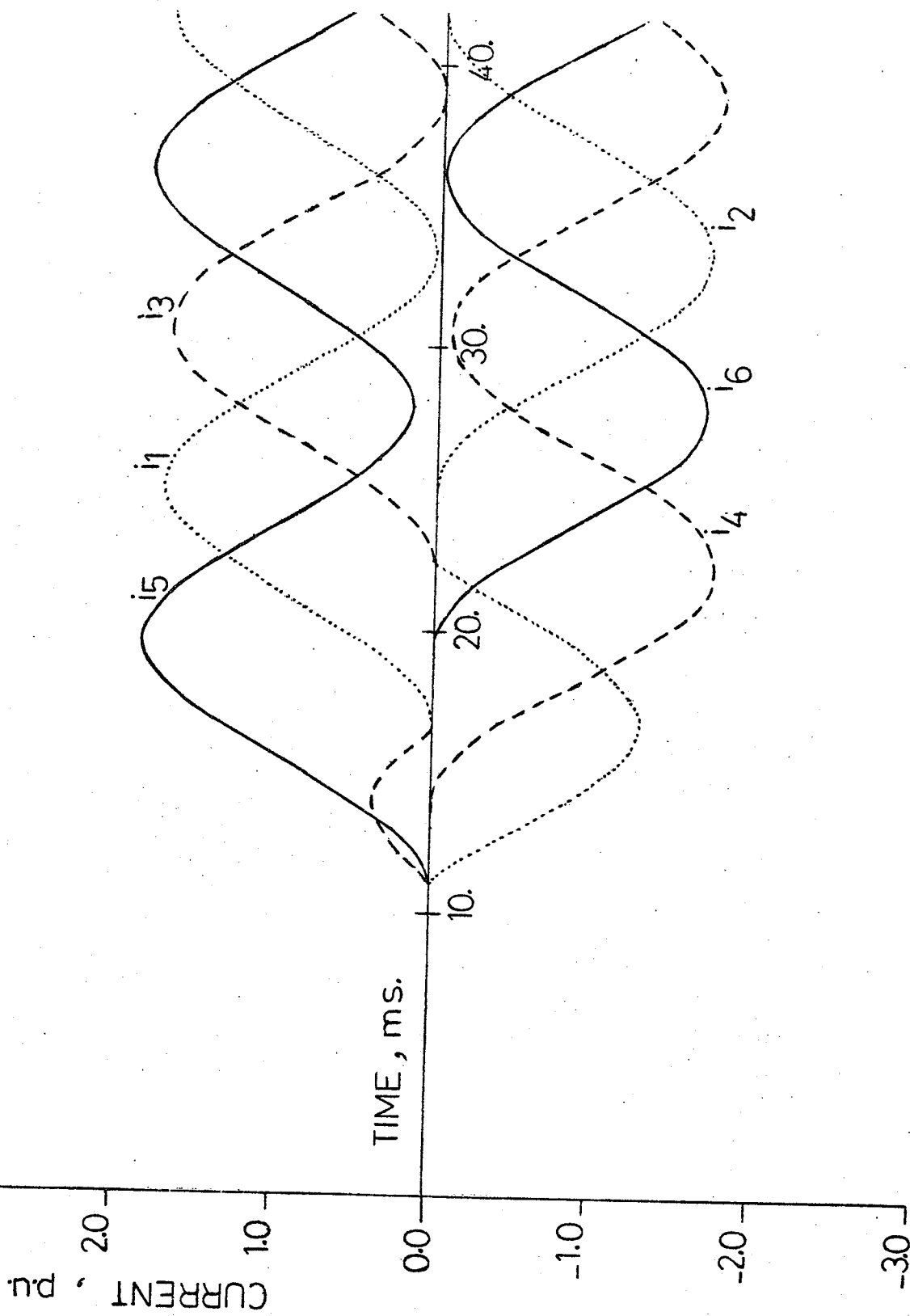


Figure 2.33 Transient performance subsequent to overvoltage for $\alpha_o = 180^\circ, \gamma = 1, z = 0$
(c) valve currents

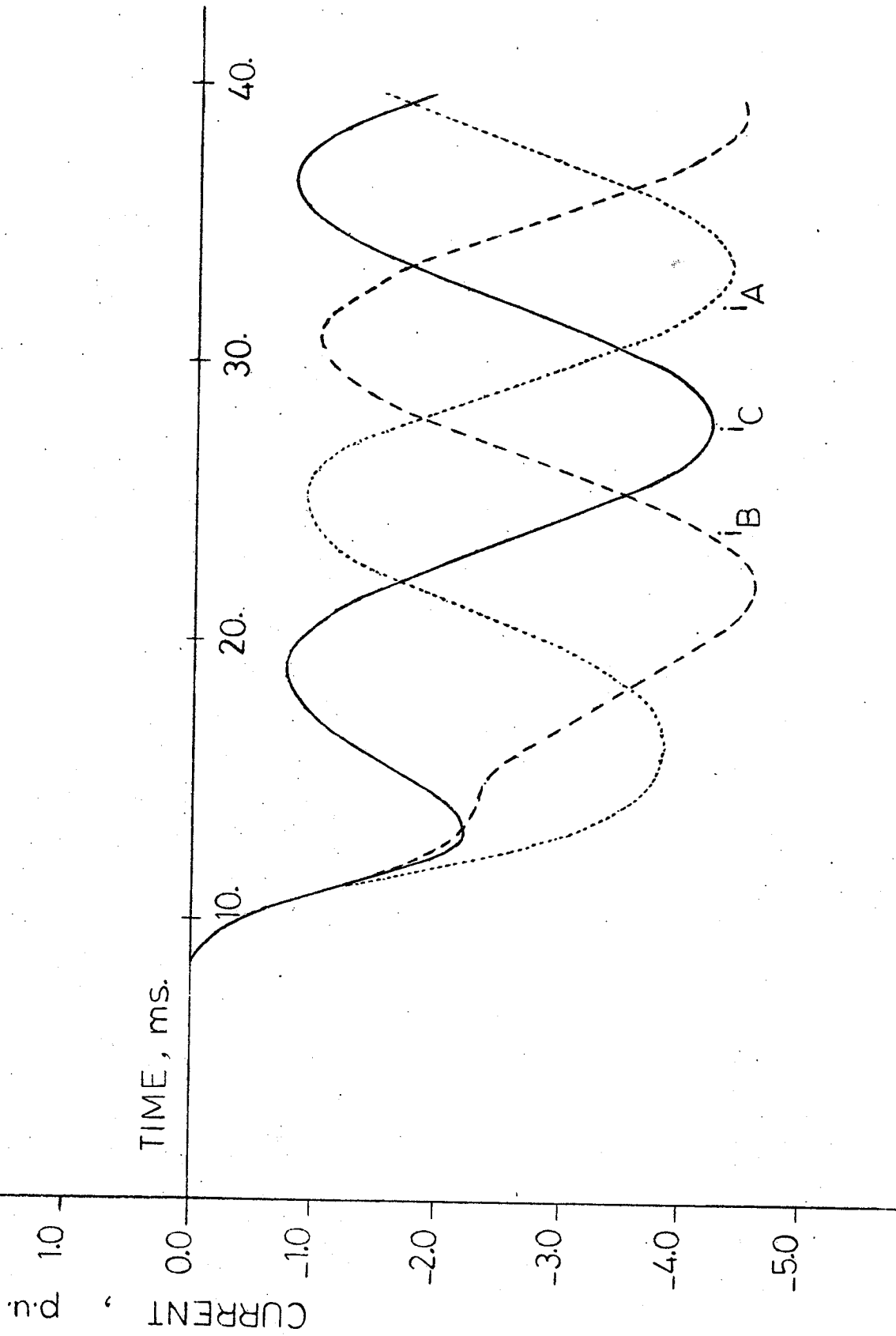


Figure 2.33 Transient performance subsequent to overvoltage
for $\alpha_o = 180^\circ$, $y = 1$, $z = 0$
(d) line currents

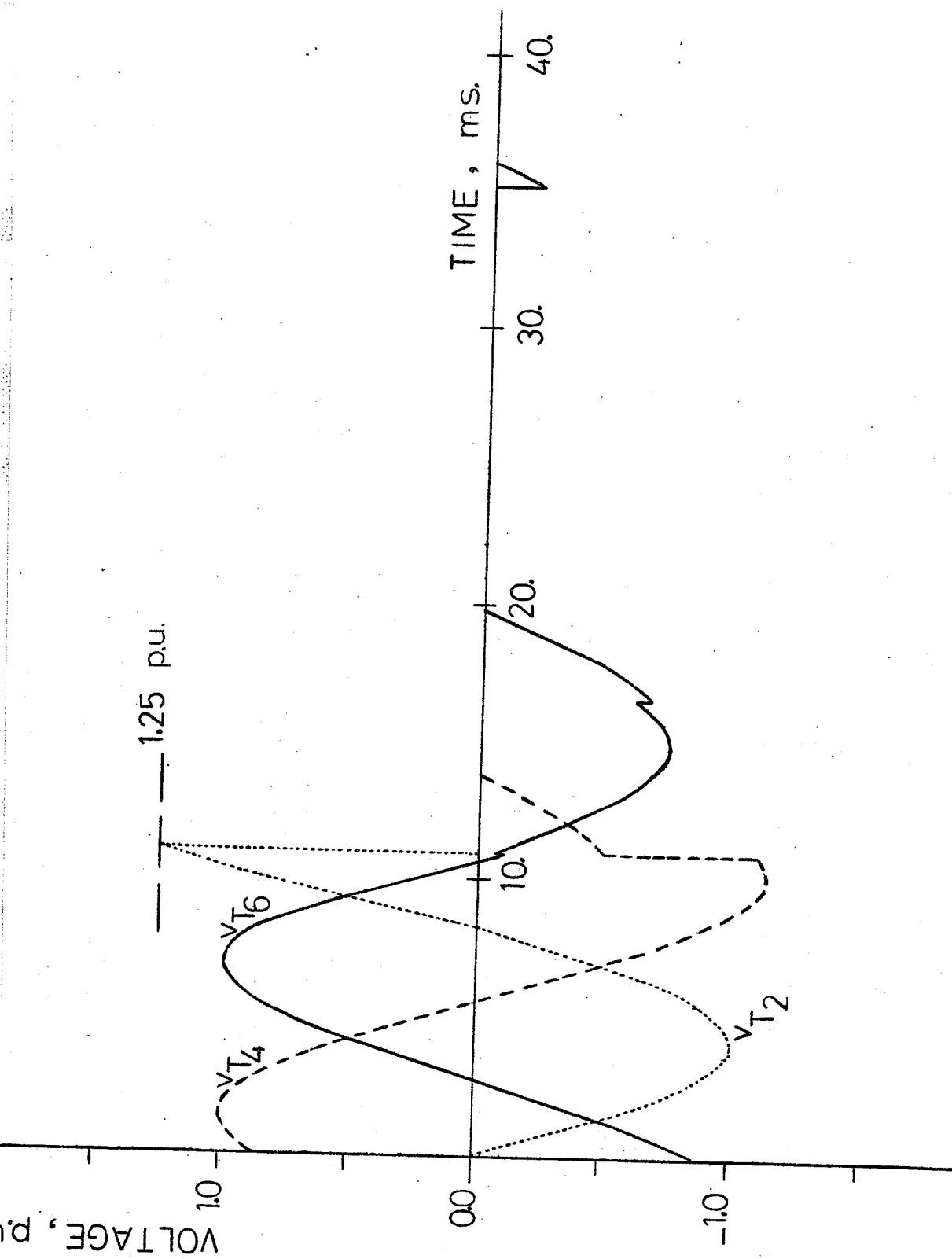


Figure 2.34 Transient performance subsequent to overvoltage
for $\alpha_0 = 180^\circ$, $y = 0.3$, $z = 0.7$
(a) value voltages

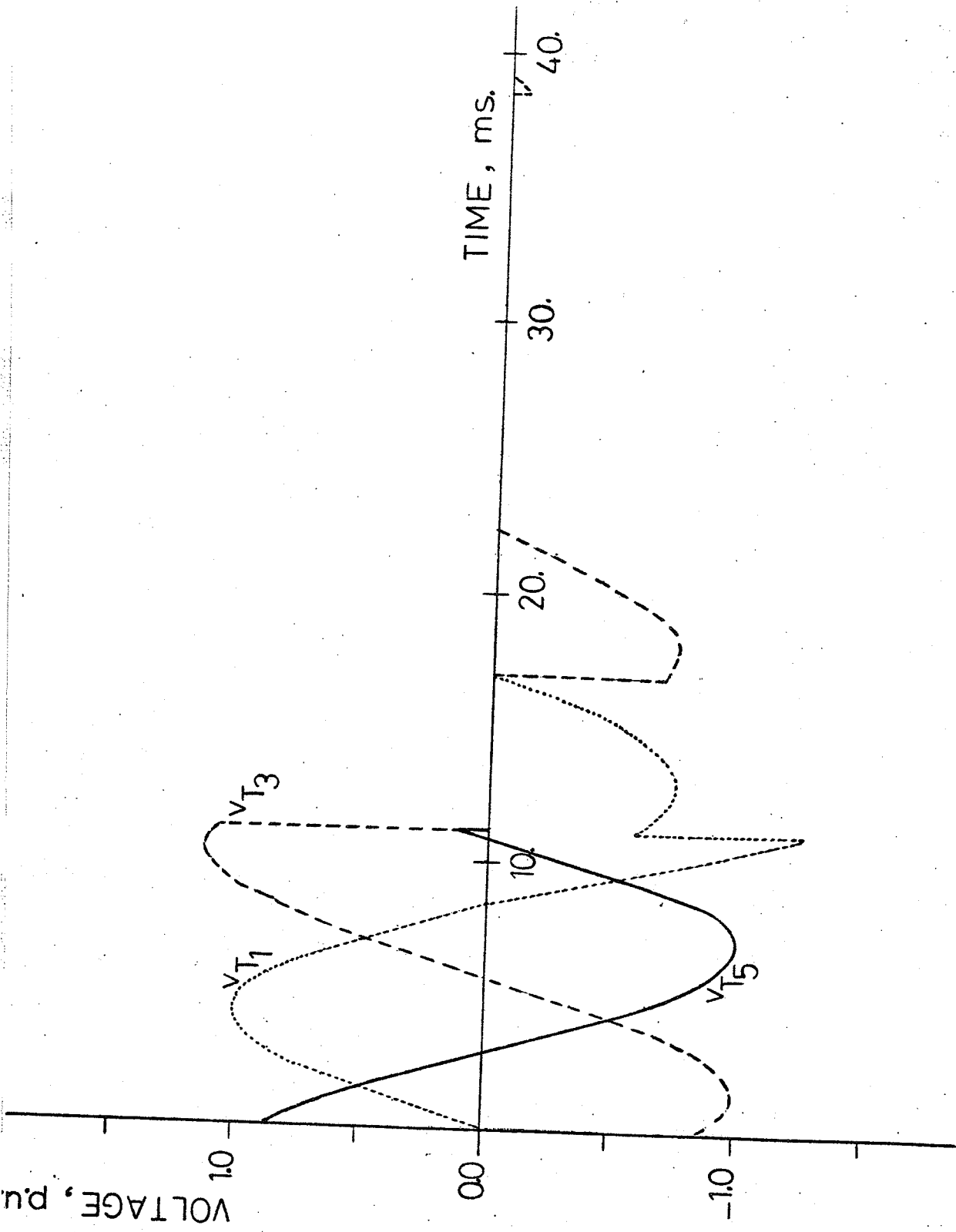


Figure 2.34 Transient performance subsequent to overvoltage for $\alpha_o = 180^\circ$, $\gamma = 0.3$, $z = 0.7$

(b) valve voltages

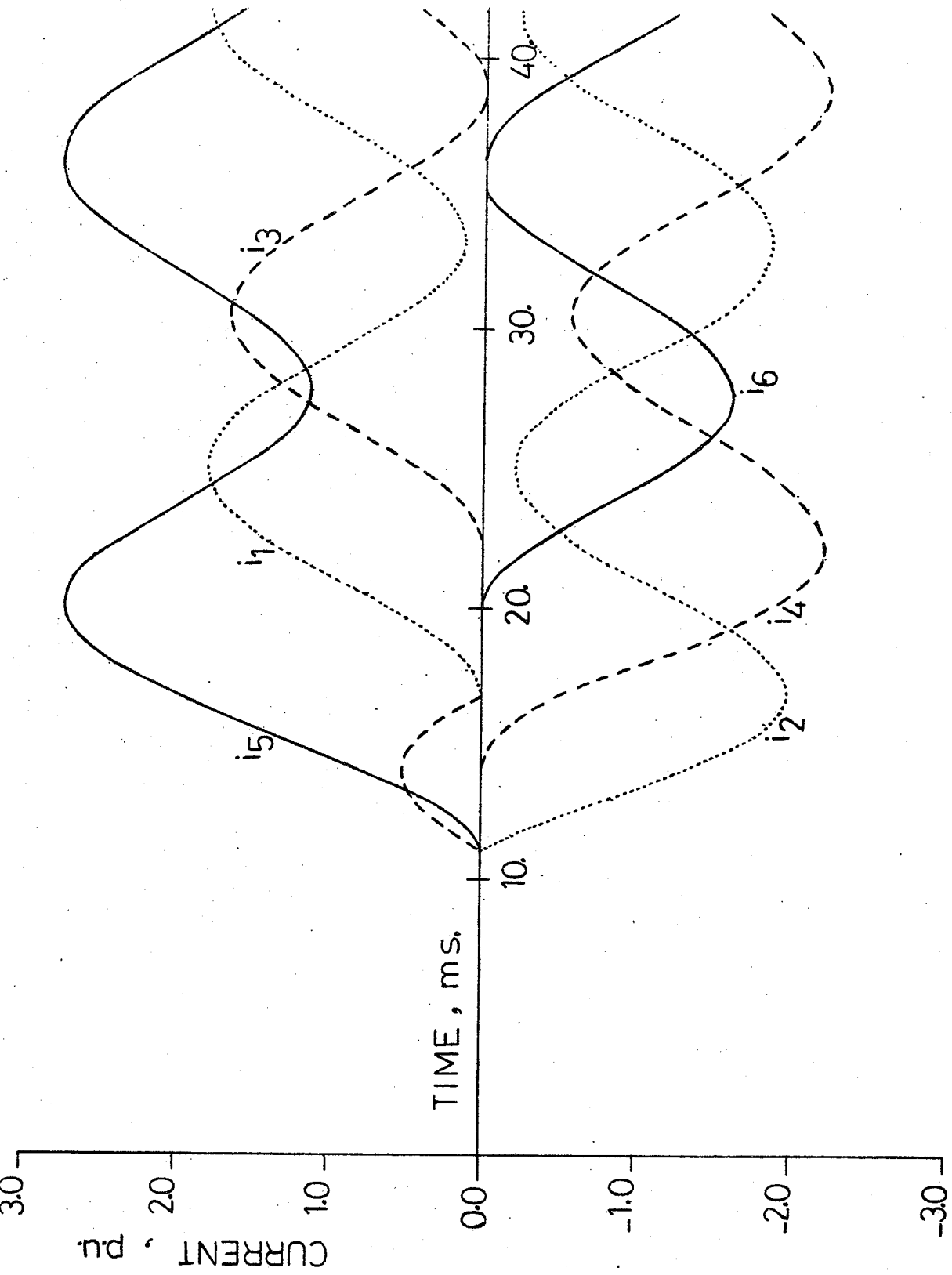


Figure 2.34 Transient performance subsequent to overvoltage for $\alpha_0 = 180^\circ$, $y = 0.3$, $z = 0.7$ (c) valve currents

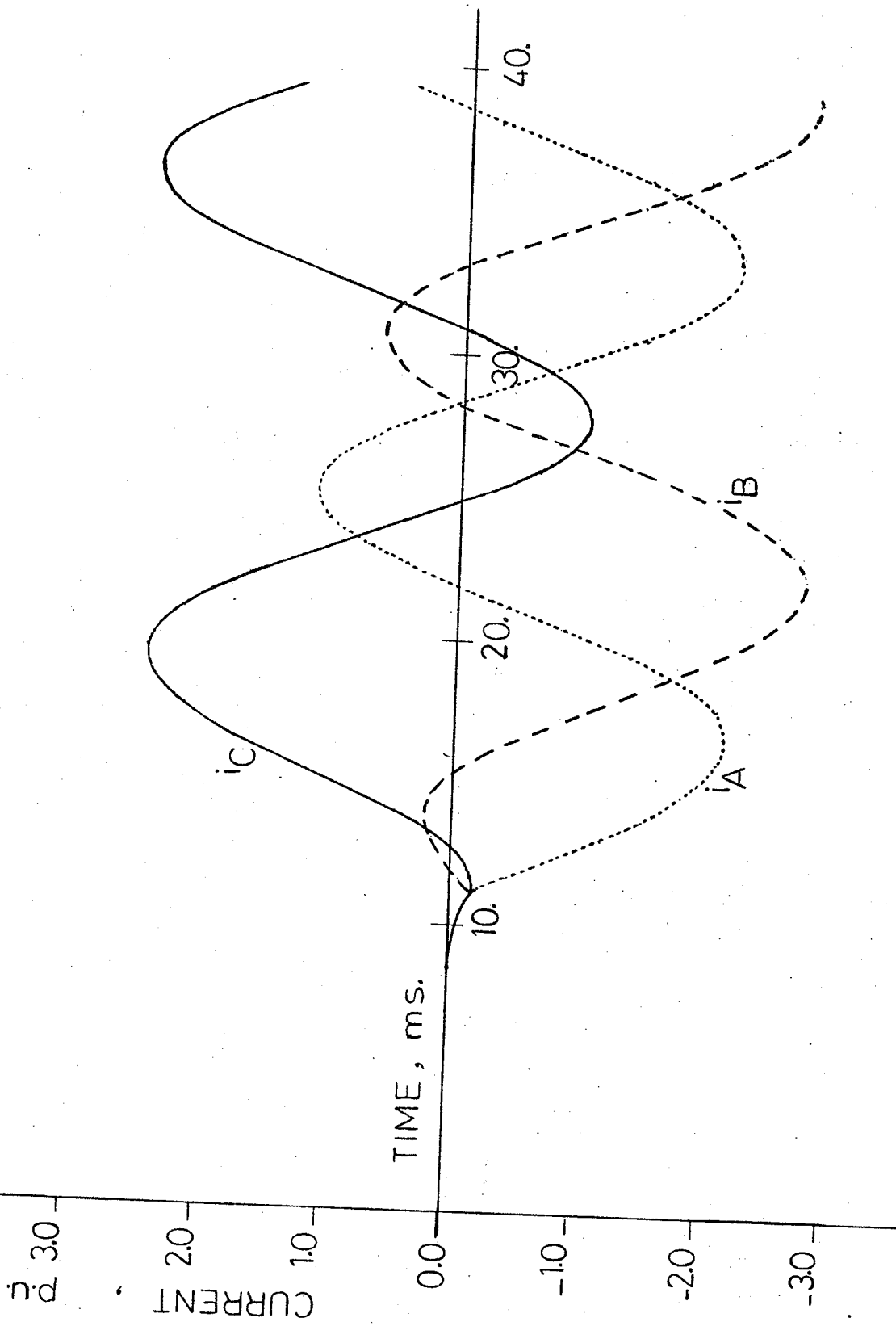


Figure 2.34 Transient performance subsequent to overvoltage
for $\alpha_o = 180^\circ$, $y = 0.3$, $z = 0.7$
(d) line currents

T_2 and is applied to all valves. Notice from the valve currents in Figure 2.32 (b) that the valve T_5 carries a peak current of 3.58 p.u. $[I_{base} = \frac{\hat{V}}{X}]$ and fails to extinguish. This can indeed happen to any one valve and hence each valve must be designed to withstand such a stress.

For the other known design where $y=0$ and $z=1$, the voltages across and currents through the valves subsequent to overvoltages are found identical to those shown in Figures 2.32 (a) and 2.32 (b).

Figures 2.33 (a), (b) and (c) are for another extreme in design for $y=1$, $z=0$. It must be realized that due to the reactors ($2x_2$) in series with each valve (Figure 2.3), unequal voltages appear across each valve. Further, one-half of the valves are not protected by the emergency firing during the first cycle because they are reverse biased. It is for this reason that modifications in the original concept were made to give the Generalized UM-Concept. It must, however, be noted that notwithstanding the overvoltages during one cycle, the transient over current peaks are indeed only about 50% (1.88 p.u.). Since valves must be sized for i^2t ratings the valve size could be almost $\frac{1}{4}$ th from current considerations alone. A part of this resulting saving in the number of parallel paths, or sizes of thyristors, can perhaps be reinvested by connecting a higher number of thyristors in series to withstand overvoltages and yet come out with a net saving. The final outcome depends to a great extent on the size of a compensator.

Figures 2.34 (a), (b) and (c) correspond to a more realistic design $y=0.3$, $z=0.7$ arising from the UM-Concept. In this case the maximum voltage coming across a valve is limited to 1.25 - emergency firing threshold level, as can be seen from Figure 2.34 (a) and (b) which reduces

to 0.75 p.u. on the non-conducting valve after emergency firing. The peak value of the valve currents at the same time are restricted well below 2.75 p.u. It should be noted here that the relative values of $\int i^2 dt$ works out to be of almost the same ratio as those of i peak.

A comparison of the results of Figures 2.32 and 2.34 brings out quite clearly that a great saving can be achieved in the thyristor valves for the proposed UM-designs in comparison to the known designs.

Table 2.III provides some important data for an easy comparison.

2.7 Guidelines for the Selection of an Optimum Design

In the previous sections it has been shown that many advantages are gained by selecting a thyristor phase controlled reactor design arising from the generalised UM-Concept. By choosing a non-zero value of y , it is possible to minimize harmonic generation, reduce the voltages appearing across the thyristors when they are in the off state, increase the control range and find a region for normal operation where the harmonic content is minimal and yet about which a margin exists on either side for making controlled adjustments. The above advantages occur at the cost of a slight increase in the total installed rating of the reactor components.

It was indicated in Section 2.3 that during the operation for $0 \leq \alpha \leq 90$ there are periods when both thyristors of a paralleled combination (per phase) conduct simultaneously, which result in a circulating current in the loop formed by two paralleled branches per phase. The influence of these circulating currents is that under steady state operation for $\alpha < 90^\circ$ the thyristors must cope with a higher $i^2 t$, i.e. junction heating.

TABLE 2.III
 A COMPARATIVE EVALUATION OF KEY PERFORMANCE
 INDICES OF VARIOUS DESIGNS

Performance Index	DESIGN DESCRIPTION			
	y=0, z=0	y=0, z=1	y=1, z=0	y=0.3, z=0.7*
1. Total rating of reactors, Q_r , p.u.	1.0	1.0	3.0	1.6
2. †Maximum peak of transient valve current p.u.	3.58	3.58	1.88	2.75
3. Maximum value of the 5th harmonic current p.u.	0.05	0.076	0.025	0.033
4. Control angle (α) range	90-180	120-180	0-180	0-180
4. †Maximum voltage across a thyristor valve, p.u.	1.25	1.25	1.7	1.25

* This is not an optimum design from the UM-Concept - it is used as an example.

† The figures refer to an assumed overvoltage situation of 1.7 p.u. when emergency firing level for thyristor valves is set at 1.25 p.u.

This requirement, in fact, influences the cooling system design for the thyristors and not the thyristor valve sizing as may otherwise be misunderstood.

When one considers overvoltages it is highly unlikely that the connecting transformers would stay linear. The system may, then, become a hybrid of saturated reactor and thyristor phase control. For realistic overvoltage studies, therefore, this fact must be taken into account. Designs with low leakage reactance transformers may, therefore, work out to be less effective than those with a high primary leakage reactance.

For selecting an optimum design perhaps the best criterion is to minimize cost. Following are the major components of a system which can be priced directly:

- (a) Connecting transformer;
- (b) Linear reactors;
- (c) Thyristor valves; and
- (d) Filters.

From the known designs two different points of view seem to emerge. While some manufacturers consider that the system cost can be minimized by using a standard transformer and having separate reactors, the others tend to think that it is better to have a high leakage reactance transformer to serve both functions. In the former the transformer must be specially designed because if the intent is not to operate the thyristor phase controlled reactors in a hybrid mode, the transformer must be designed for normal operation at a lower flux density. For a given value of y the options, therefore are to choose $z = (1-y)$ (reactor transformer), or $z=0$ (separate series reactors).

The total rating is, and hence the cost of reactors may turn out

to be, a simple linear function of y .

As the value of y is increased the harmonic content is reduced. This may, therefore, be the most important factor because it determines (a) the size of a filter, (b) the number of harmonics for which filters must be provided, and lastly it is always better to have a source which inherently generates little harmonics. Most people concern themselves with the harmonics which require filters. However it is of utmost importance to consider the harmonics which are not effectively filtered and which find their way through the lines. Hence in cost optimization, while the cost of filters is taken into account, a penalty function must be added for harmonic level in general.

The selected value of y has another significant influence on the cost of thyristor valves. The results of Figure 2.31 are very informative in this regard ($\alpha_0 = 180^\circ$ design case). Since i^2t function influences sizing (including parallel paths) the worst peak current provides a good indication. Higher values of y not only reduce the loading, but also ensure that all thyristors are nearly equally stressed, whereas this is not the case for the known designs.

When a reliable cost function for the above discussed factors is available an optimum system configuration can be determined.

Most of the results presented in this chapter are for designs which have $y+z=1$. This is not a necessary condition but may be most desirable from cost optimization considerations because $y+z \neq 1$ implies that all x_1 , x_2 and x_3 values are non-zero. It may be desirable to have $x_3=0$ and incorporate the required reactance value in the leakage reactance of the connecting transformer or use a standard transformer and get the remaining reactance adjusted in x_2 .

2.8 Modeling for System Studies

For power system studies by digital simulation, it is required to represent the thyristor phase controlled reactor adequately. The basic requirements of a good model are:

- (a) to provide a correct relation between device terminal voltage and current (or reactive power),
- (b) to be suitable for easy application in available digital programs with minimum modifications, and
- (c) to be simple and accurate enough for all practical purposes over widest possible operating range.

Here, a simple model is suggested which satisfies such conditions. As shown in Figure 2.35 the model is an inertia-less generator of source voltage E_T connected to the terminal bus through a fixed reactance X per phase. The constraints on E_T are that it always stays in phase with the terminal bus voltage V_T and is a controlled function of the conduction angle α .

For system dynamics studies, the concern mainly lies in the reactive power flow from a VAR compensating device. Therefore, it is sufficient to take into account the power frequency current component of the device. From the model in Figure 2.35;

$$I = \frac{V_T - E_T}{jX} = I_1(\text{p.u.}) \frac{V_T}{X} \quad (2.38)$$

$$\text{or } E_T = V_T(1 - I_1(\text{p.u.})) = V_T f(\alpha) \quad (2.39)$$

where, the p.u. fundamental current I_1 is given in Table 2.II as an explicit function of control angle α for any arrangement of reactors.

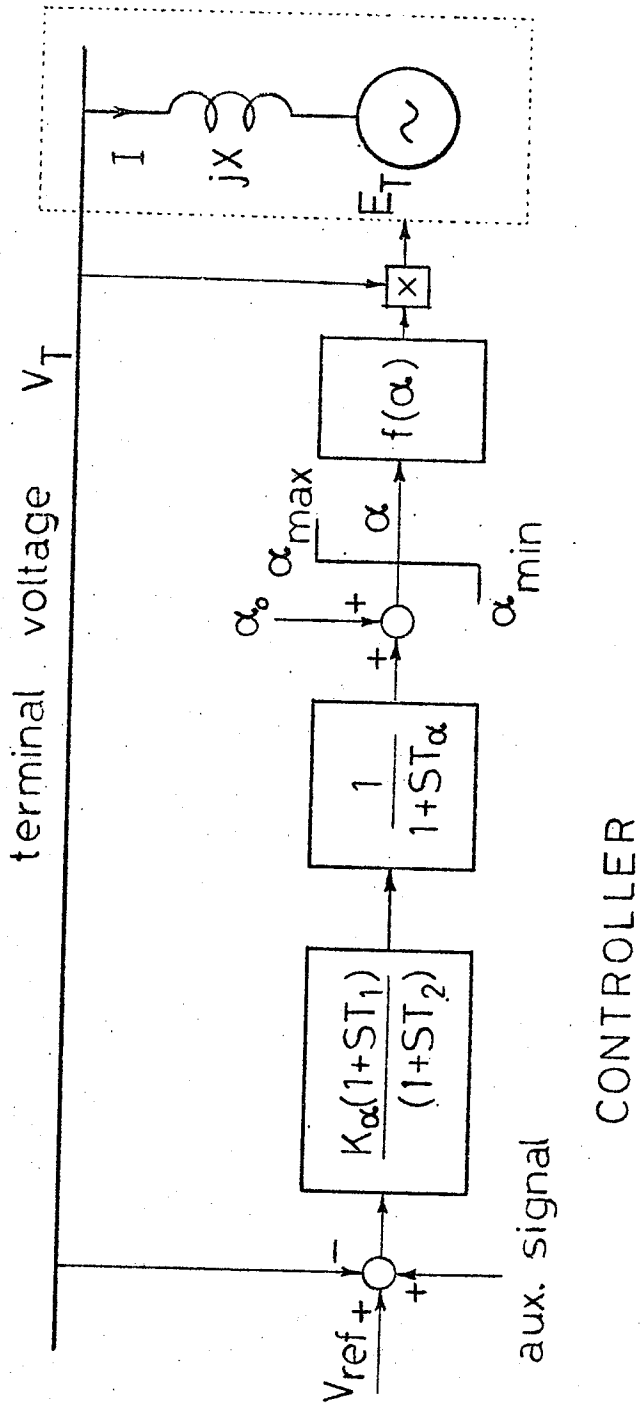


Figure 2.35 System model of a thyristor controlled reactor

For special cases of design:

(a) $y = 0, z = 0,$

$$E_T = V_T \left[\frac{2\alpha - \sin 2\alpha}{\pi} - 1 \right] \quad \text{for } \pi/2 \leq \alpha \leq \pi \quad (2.40)$$

(b) $y = 0, z = 1,$

$$E_T = V_T \left[\frac{3\{2\alpha + \sin(2\alpha + 120^\circ)\}}{2\pi} - 2 \right] \quad \text{for } 2\pi/3 \leq \alpha \leq 5\pi/6 \quad (2.41)$$

$$E_T = V_T \left[\frac{3(2\alpha - \sin 2\alpha)}{2\pi} - 2 \right] \quad \text{for } 5\pi/6 \leq \alpha \leq \pi \quad (2.42)$$

(c) $y = 1, z = 0,$

$$E_T = V_T \left[\frac{2\alpha - \sin 2\alpha}{2\pi} \right] \quad \text{for } 0 \leq \alpha \leq \pi \quad (2.43)$$

This model is most suited for digital programs where modern techniques of direct solution of power system networks are employed.

For harmonic studies under steady-state conditions, the primary concern generally lies in investigating the effect of harmonic currents, generated by the static VAR controlling device, on the ac system rather than on the device itself. The effect of the harmonics will vary as a function of system parameters and such variables as the proximity of telephone lines, etc. The model described earlier can be readily used for these studies by replacing I_1 (p.u.) by the n th harmonic current I_n (p.u.) given in Table 2.II .

chapter three

STATIC REACTIVE POWER CONTROL WITH HVDC SYSTEMS

3.1 Reactive Power Control at ac/dc Junction Terminal

Transmission of power through any dc scheme involves the necessity of a correct balance and therefore of generation and control of reactive power on the ac side of the converter terminal by an economical and reliable means.

The operation of a HVDC converter causes harmonic currents injection into the ac system while the ac system must supply the reactive power necessary for the commutation process. The harmonic currents so generated are short circuited by means of series resonant filters which also provide some capacitive reactive power at the fundamental frequency.^{4,6,53-57}

It is usual to provide complete compensation, by terminal equipment, for the steady-state reactive power demand of a HVDC converter to avoid high I^2R losses associated with the transmission of reactive power.⁷² This means that the ac system is only called upon to deliver (or accept) real power under steady-state conditions.

Unfortunately, transient regulating phenomena taking place in a converter give rise to large changes in reactive power demand (as will be shown in Section 3.2) which has to be supplied from or to the 3-phase system. If the system is strong (i.e. of low impedance or in other words, the a.c. system short circuit level is in excess of the ratio of converter full load MVar to the permitted per-unit voltage regulation) at the interconnecting point to the HVDC station, reactive power compensation

is almost exclusively striven for by utilizing fixed capacitors and filter circuits.⁷¹ If the ac system has an appreciable internal impedance at fundamental frequency, however, the above procedure does not provide an optimum solution partly because in the event of a sudden disturbance in the reactive power balance at the converter bus high terminal voltage fluctuations will occur. The design of the thyristor converter valves to withstand such overvoltage fluctuations is quite costly.^{59,60} Thus a reduction of load rejection overvoltages is vital for the HVDC converter station design as well as the station insulation level.

For these reasons a fast controllable reactive power compensating system is required and the filter circuits are designed for the smallest possible capacitive VAr's at fundamental frequency.⁶¹

The synchronous compensator is the conventional solution.⁴ It can regulate the reactive power in a stepless manner, provide a good amount of damping and minimize the ac voltage angle fluctuations thus reducing the possibility of commutation failure in an inverter terminal. It, however, increases the short circuit level and has inherently slow response. Also, it has its own stability problems.

An investigation was carried out to study stability problems using only synchronous compensators and a combination of synchronous and static compensators.

The system shown in Figure 3.1 (a) was examined for a temporary loss of all dc (real and reactive) power. A recovery time of 100 msec. was assumed, for all cases, in which the dc power is restored gradually to its normal prefault value. The results for different periods of dc load rejection are summarized in Figure 3.1 (b) for various reactive

power compensation schemes. The results clearly show a favorable effect of using static VAr compensation without increasing the system short circuit level.

The case indicated by point A in Figure 3.1 (b) was tested for unstable operation on the dc simulator of IREQ.⁶² It was also confirmed that when a static compensator (of 20% slope) was added the system was stable.

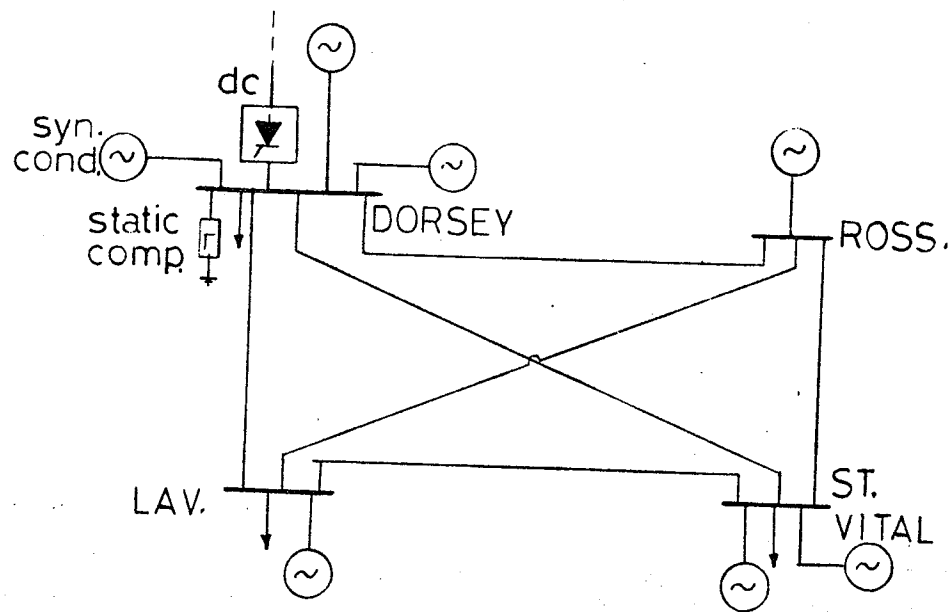
3.2 Short-Term Regulation Characteristics of ac/dc Junction Terminal

There are two important aspects, as mentioned earlier, of controlling the momentary reactive power balance at the ac/dc interconnecting terminal. First, the reactive power has a significant effect on the dynamic overvoltages which are of vital concern for dc converters especially those employing thyristor valves and also for the ac system equipments. The second aspect concerns the effect on the stability particularly of a weak ac system.

Previous attempts to investigate the HVDC/AC junction VAr characteristics were made either for long-term duty or under the assumption of constant ac system voltage or by oversimplifying dc and/or ac system models.^{59, 67, 68, 73-76} In view of the above aspects, this section provides an accurate study of the reactive load short-term regulation characteristics of the ac/dc junction terminal as affected by the parameters of the ac system, compensating equipment, filters and dc link controls.

The expression short-term duty indicates the temporary conditions occurring during the period when sudden changes, such as a load step on the HVDC system or a voltage dip on the three-phase system, are stabilized.

a)



b)

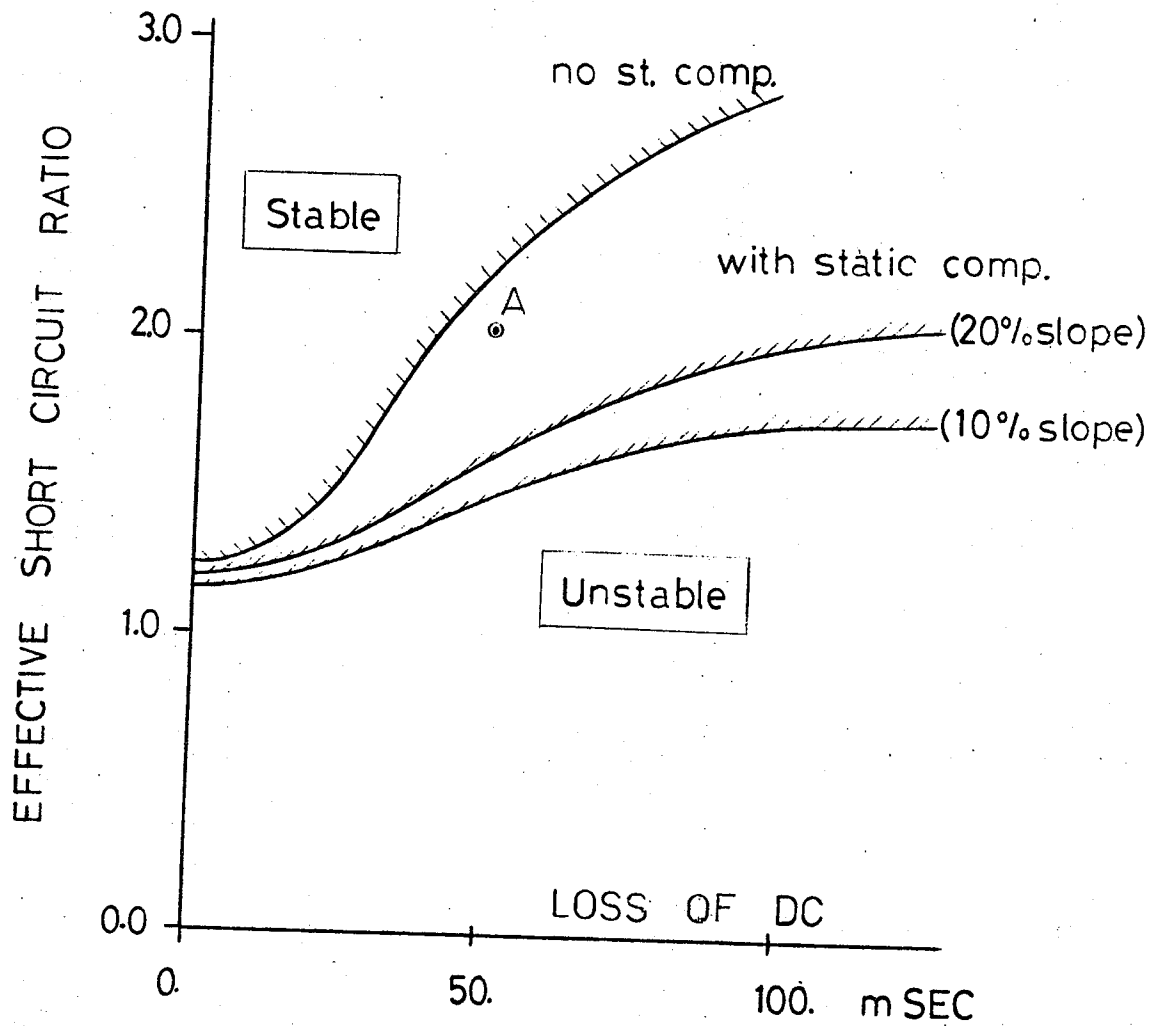


Figure 3.1 (a) system model
(b) synchronous compensators stability regions

The time taken to stabilize such a temporary phenomenon depends largely on the response time of the regulating unit (transformer tap changer, time constant of generator or synchronous compensator) which depending on the magnitude of the surge, may be in the region of 10 msec. to 10 sec.⁶¹ Short-term operation thus closes the gap between transient phenomena and long-term duty.

As the reactive load of the static converter and also that of the compensating media are dependent upon the 3-phase voltage (and vice versa) and the 3-phase voltage depends on the momentary reactive load balance, there is no satisfactory means of separating the HVDC from the ac system for calculation.

In order to study the reactive load response of the HVDC terminal in short-term duty it is necessary to treat the static converter, compensating media and 3-phase network as a single entity.

Obviously, combining these partial systems to form an overall system makes it difficult to obtain an overall picture of the phenomena because of various parameters involved.

In this study the analysis of the interaction phenomena between dc and ac system variables is carried out by means of reasonable assumptions and appropriate representation of the parameters in order to promote understanding of the control and regulation manoeuvres which can improve operation.

The following considerations are based on the equivalent circuit for an HVDC inverter terminal station in a 3-phase network as shown in Figure 3.2.

The ac system is simulated by an ideal voltage supply (V_b) behind a reactance (X_e) and a shunt damping resistor (R_ℓ) in parallel with a load reactance (X_ℓ). A total impedance angle of 75° at fundamental frequency with this representation may provide a realistic representation of the ac system load damping and lines, transformers and generators reactances. These measures seem acceptable and justified for gaining qualitative information about the power frequency phenomena.^{42,58}

The reactive power compensating system (synchronous or static) is represented by a voltage source (E_T) behind a reactance (X_S). (See Section 2.8 for the static compensator)

The current harmonics filter circuits are replaced by a capacitor for compensating part of the reactive power at fundamental frequency. This simplification is acceptable for the time span involved and believed to cause negligible error.⁶¹

The inverter terminal with its converter transformer leakage reactance is faithfully simulated in the computer programme on which the following results are based. The smoothing reactor ensures a smoothed direct current (I_d) and is matched to the HVDC conditions. The derivation of the piecewise linearized system equations used in the computer program is given as follows:

Using a suitable per-unit system for the dc quantities,⁵⁹ the following equations govern the system model shown in Figure 3.2.

$$P_d = P + P_\ell - \frac{E_T V_a}{X_S} \sin(\theta_s - \theta) \quad (3.1)$$

$$P_d = V_d I_d \quad (3.2)$$

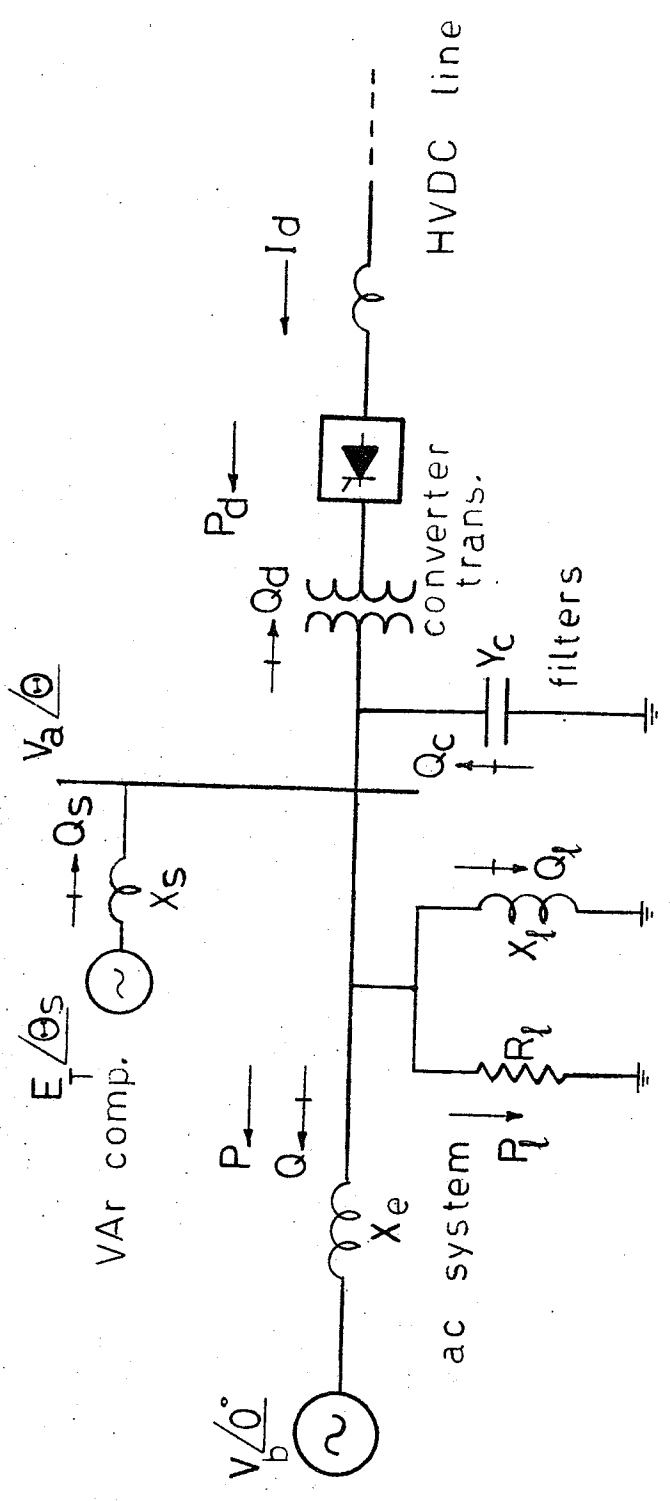


Figure 3.2 Equivalent circuit diagram of a HVDC inverter terminal station in a 3-phase system

$$Q_d = Q_s + Q_c - Q_\ell - Q \quad (3.3)$$

$$\cos \phi = \frac{V_d}{V_a TN} \quad (3.4)$$

$$Q_d = P_d \tan \phi \quad (3.5)$$

$$V_d = V_a TN \cos \gamma + R_c I_d \quad (3.6)$$

where:

$$P = \frac{V_a V_b}{X_e} \sin \theta$$

$$P_\ell = V_a^2 / R_\ell$$

$$Q_s = \frac{V_a}{X_s} [E_T \cos (\theta_s - \theta) - V_a]$$

$$Q_c = V_a^2 Y_c$$

$$Q_\ell = V_a^2 / X_\ell$$

$$Q = \frac{V_a}{X_e} (V_a - V_b \cos \theta)$$

T = converter transformer taps

X_c = p.u. commutating reactance/bridge

N = number of dc bridges in series

$$R_c = -\frac{\pi}{6} NX_c$$

γ = extinction angle of inverter valves.

The piece-wise linearization of the above equations gives:

$$a_1 \Delta V_a + a_2 \Delta P_d + a_3 \Delta \theta + a_4 \Delta \theta_s = 0 \quad (3.7)$$

$$b_1 \Delta I_d + b_2 \Delta V_d + b_3 \Delta P_d = 0 \quad (3.8)$$

$$c_1 \Delta V_a + c_2 \Delta Q_d + c_3 \Delta \theta + c_4 \Delta \theta_s = 0 \quad (3.9)$$

$$d_1 \Delta V_a + d_2 \Delta V_d + d_3 \Delta \phi = 0 \quad (3.10)$$

$$e_1 \Delta Q_d + e_2 \Delta P_d + e_3 \Delta \phi = 0 \quad (3.11)$$

$$f_1 \Delta V_a + f_2 \Delta V_d + f_3 \Delta I_d + f_4 \Delta \gamma = 0 \quad (3.12)$$

(provided that all angles are in radians)

The values of the coefficients in the above equations are:

$$a_1 = (P_d + P_\ell) / V_a$$

$$a_2 = -1.0$$

$$a_3 = Q_d + V_a^2 \left(\frac{1}{X_e} + \frac{1}{X_s} + \frac{1}{X_f} - Y_c \right)$$

$$a_4 = -Q_s - V_a / X_s$$

$$b_1 = -V_d$$

$$b_2 = -I_d$$

$$b_3 = 1.0$$

$$c_1 = Q_d / V_a + V_a \left(Y_c - \frac{1}{X_s} - \frac{1}{X_e} - \frac{1}{X_\ell} \right)$$

$$c_2 = -1.0$$

$$c_3 = P_\ell - P_d$$

$$c_4 = -V_a E_T \sin(\theta_s - \theta) / X_s$$

$$d_1 = TN \cos \phi$$

$$d_2 = 1.0$$

$$d_3 = V_a TN \sin \phi$$

$$e_1 = 1.0$$

$$e_2 = -\tan \phi$$

$$e_3 = -P_d / \cos^2 \phi$$

$$f_1 = TN \cos \gamma$$

$$f_2 = -1.0$$

$$f_3 = R_c$$

$$f_4 = V_a TN \sin \gamma$$

For a static compensator $\Delta \theta_s = \Delta \theta$ whereas for a synchronous compensator $\Delta \theta_s$ is assumed to be zero. For a given value of $\Delta \gamma$, Equations 3.7 to 3.12 are solved simultaneously, for a small change of ΔP_d . Values of V_a , θ , θ_s , I_d , V_d , Q_d and ϕ are then updated and used as initial conditions for the next change in ΔP_d .

The rated reactive load (Q_d) of the static converter is about 53% of the rated active load transmitted (P_d) and corresponds to a displacement factor of 0.88 without taking the compensating equipment into account, i.e. measured direct at the converter transformer terminals. This applies under the assumption that the static converter transformer is supplied with a sinusoidal rated voltage, which is assured by the filter circuits, and with a rated load at the inverter at nominal extinction angle (γ) of 18° .

In contrast to ac transmission, with HVDC, real power can be adjusted by means of grid control acting on the current or on the voltage, or on a combination of both. An economically most suitable method of power reduction is determined by the amount and duration of the reduction in conjunction with the requirements regarding the reactive load balance. When protracted long-term duty is involved it would be preferable to introduce a current reduction because of the significance of the transmission losses, whereas in the case of short-term power reduction it is advantageous to reduce the voltage or at least make a combined reduction of voltage and current.

Figures 3.3 and 3.4 show the ac fundamental frequency voltage rise during short-term dc load shedding for a system with a short circuit ratio of 2.0 (including synchronous compensator).

Filter capacitive VAR compensation is 50% of inverter VAR consumption at rated load and ac voltage.

In order to avoid complicated charts, the parameters used in Figure 3.3 are extinction angle (γ) and dc current (I_d), whereas dc voltage (V_d) and advance angle (β) are used in Figure 3.4. The dotted line represents the ac voltage angle (θ) variations.

Inverter reactive load characteristics for the same case are shown in Figure 3.5.

It is noticed that the reactive power consumption of the inverter reduces, somewhat more than proportionately to the active power. Large reduction of Q_d affects the network in that the reactive power supplied by the compensation devices no longer flows to the same extent to the static dc converter equipment, but instead, part of it has to be absorbed

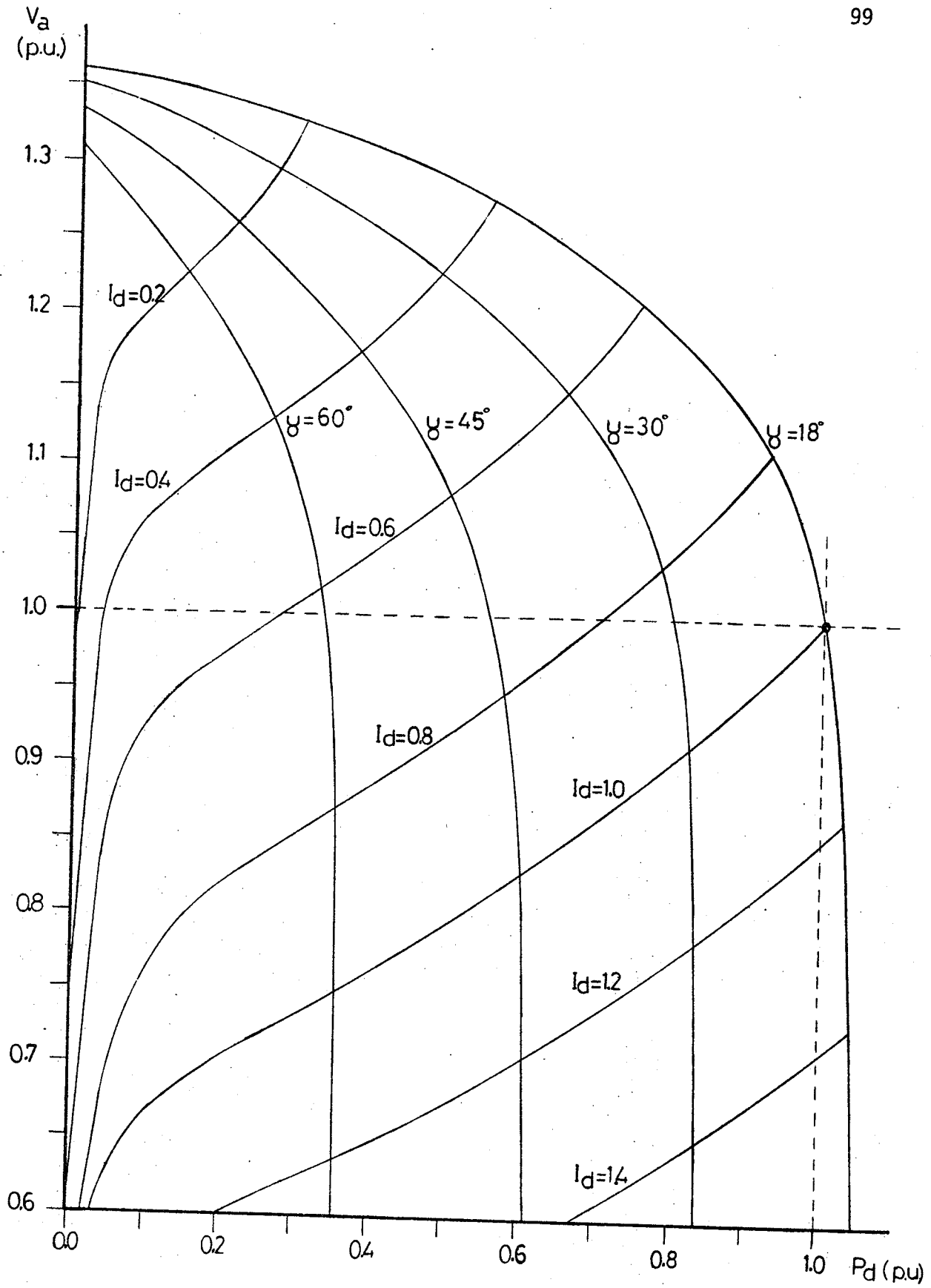


Figure 3.3 Short-term inverter regulation characteristics
(S.C.R. = 2.0)

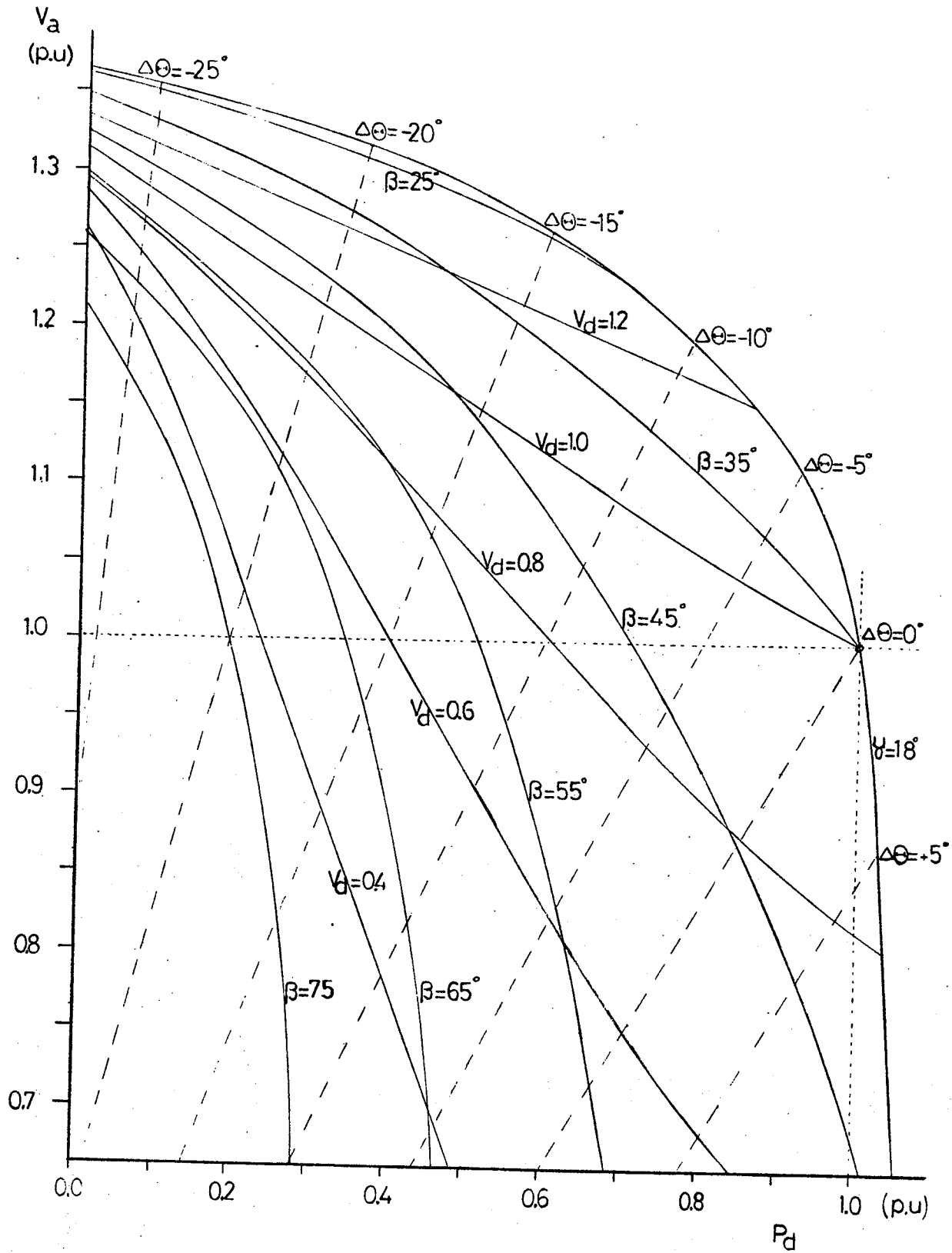


Figure 3.4 Short-term inverter regulation characteristics (S.C.R. = 2.0)

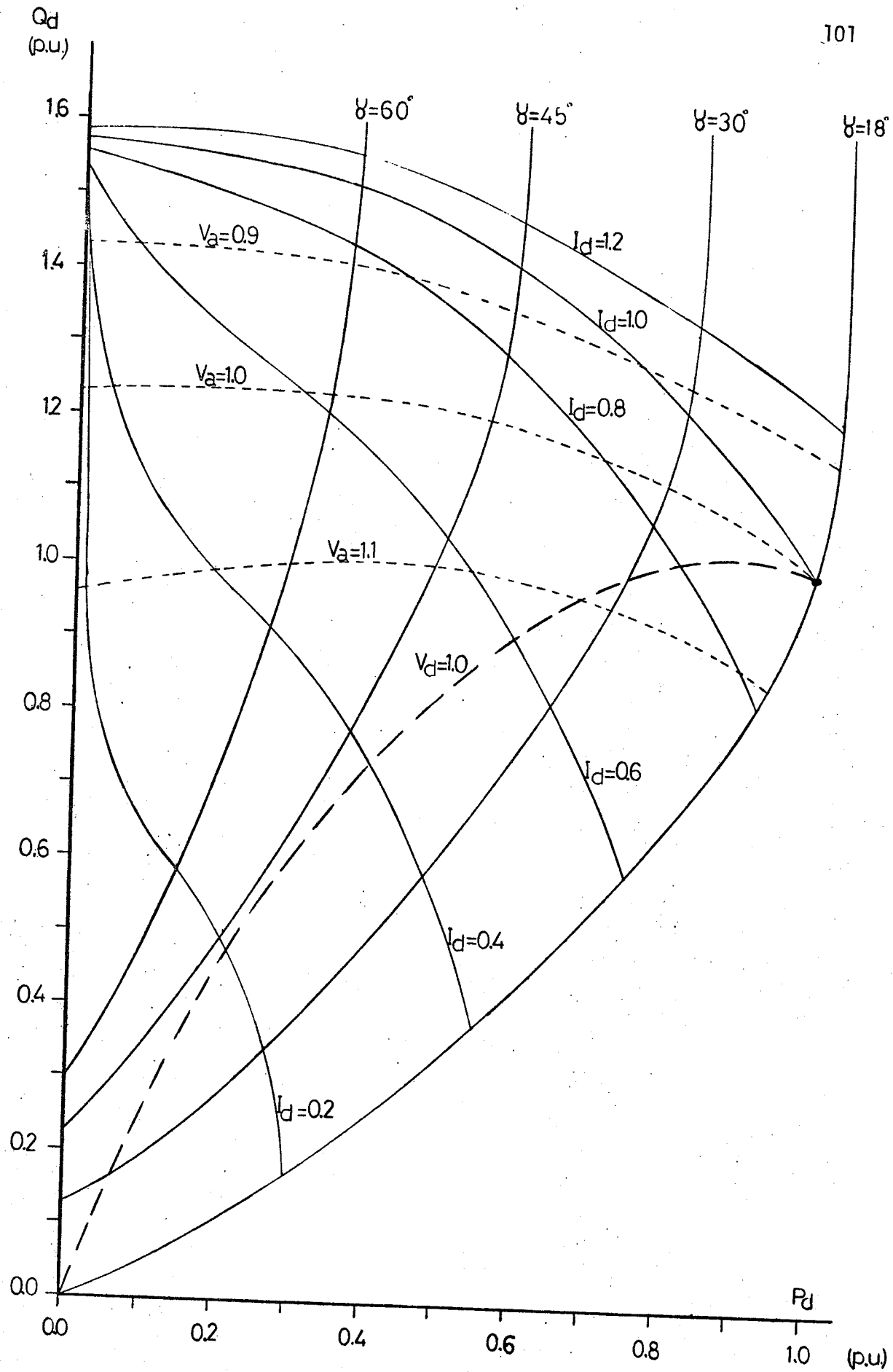


Figure 3.5 Short-term inverter reactive load characteristics
(S.C.R. = 2.0)

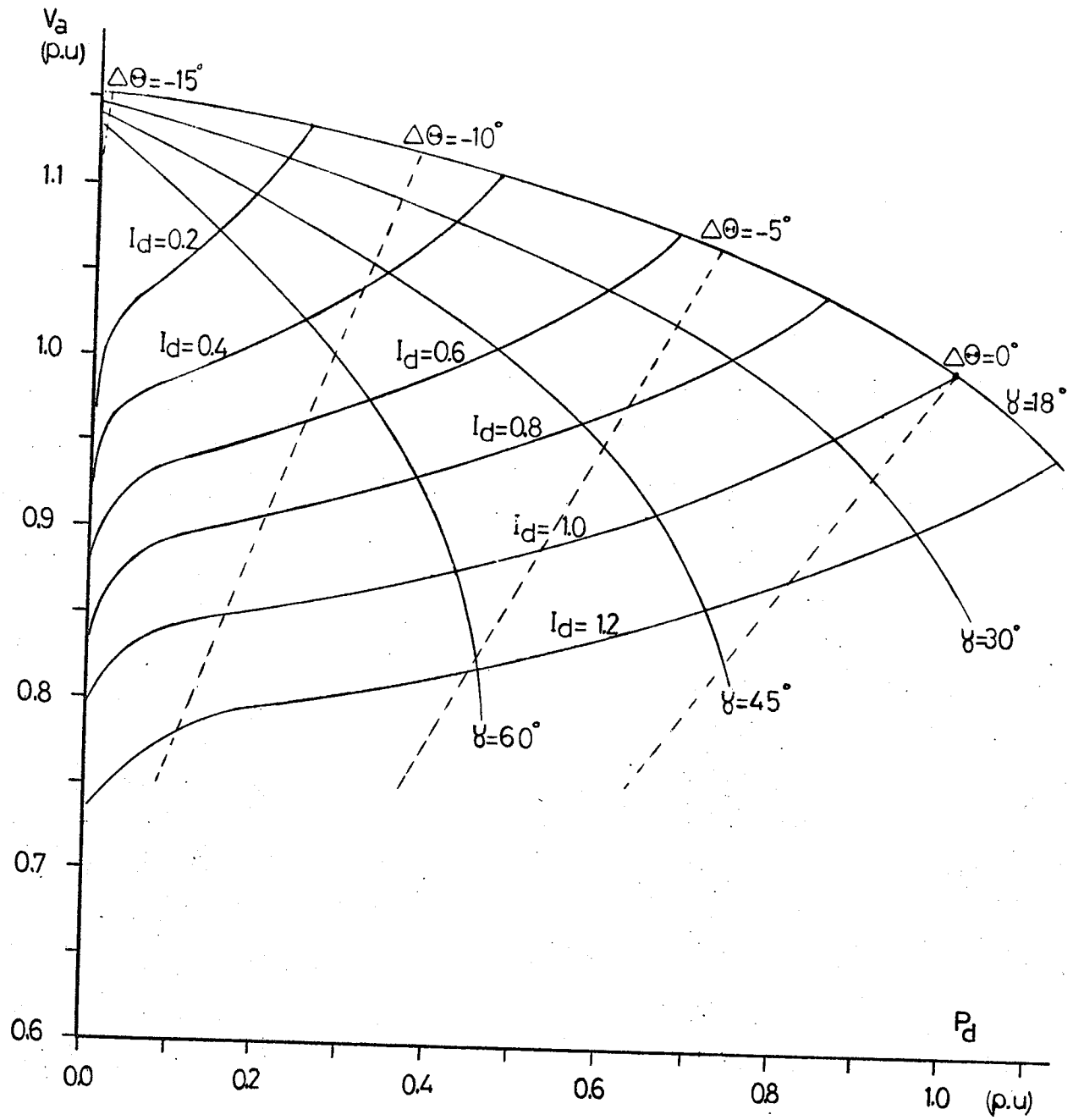


Figure 3.6 Regulation characteristics for S.C.R. = 40

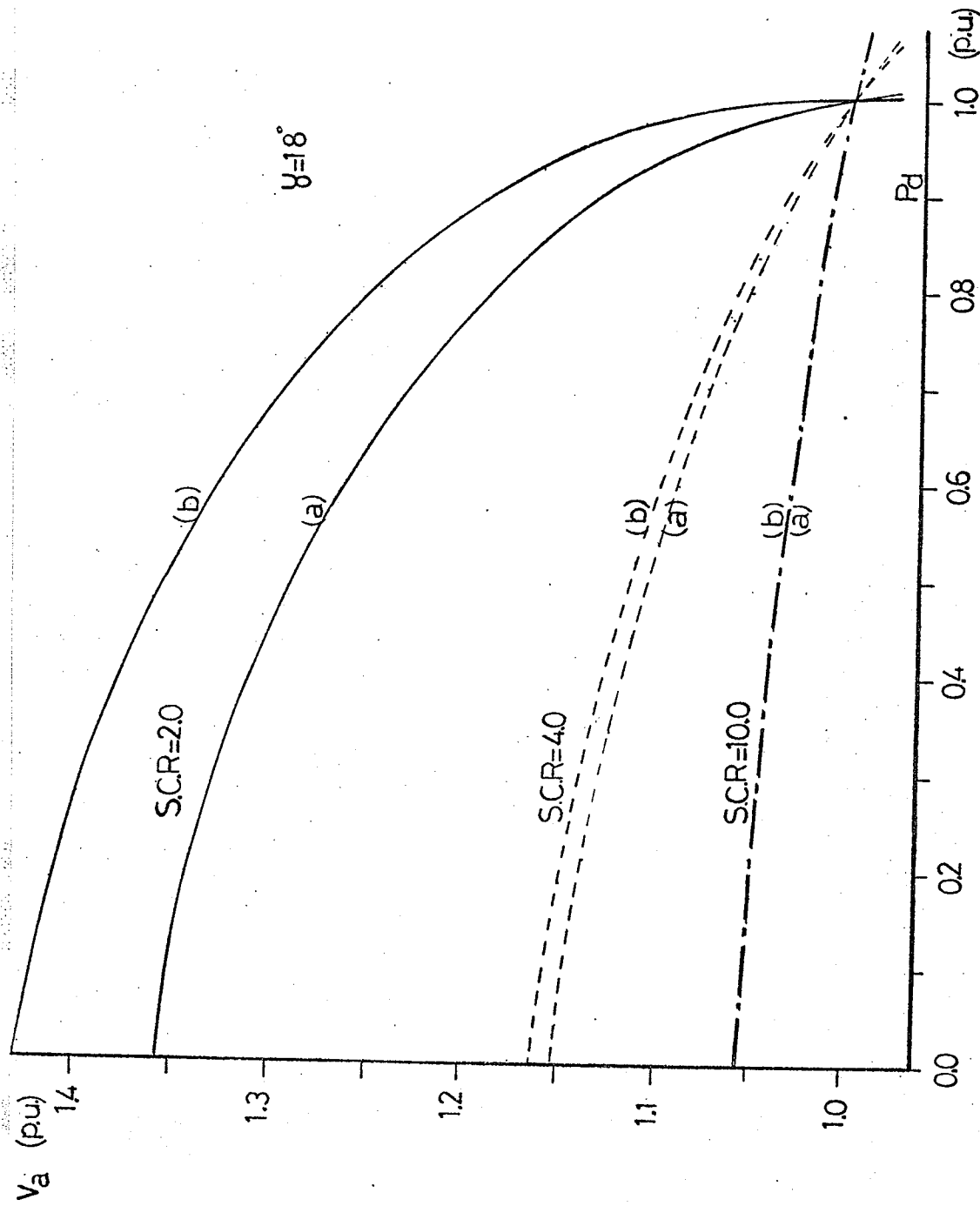


Figure 3.7 Short-term regulation characteristics for different values of short circuit ratio

(a) for $Q_{co} = 0.5$ p.u. (b) for $Q_{co} = 1.0$ p.u.

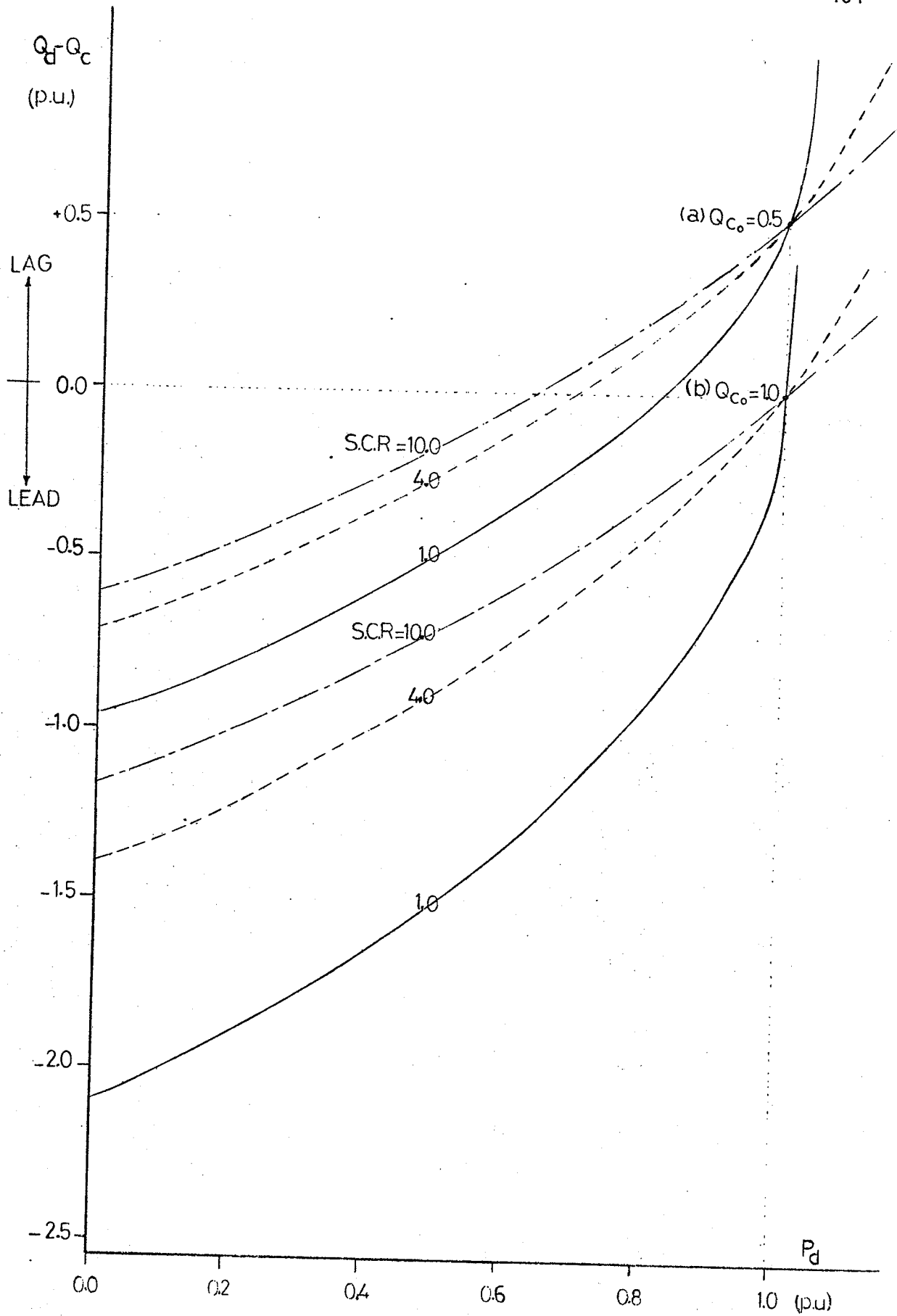


Figure 3.8 Reactive power characteristics for an inverter terminal with constant extinction angle of 18°

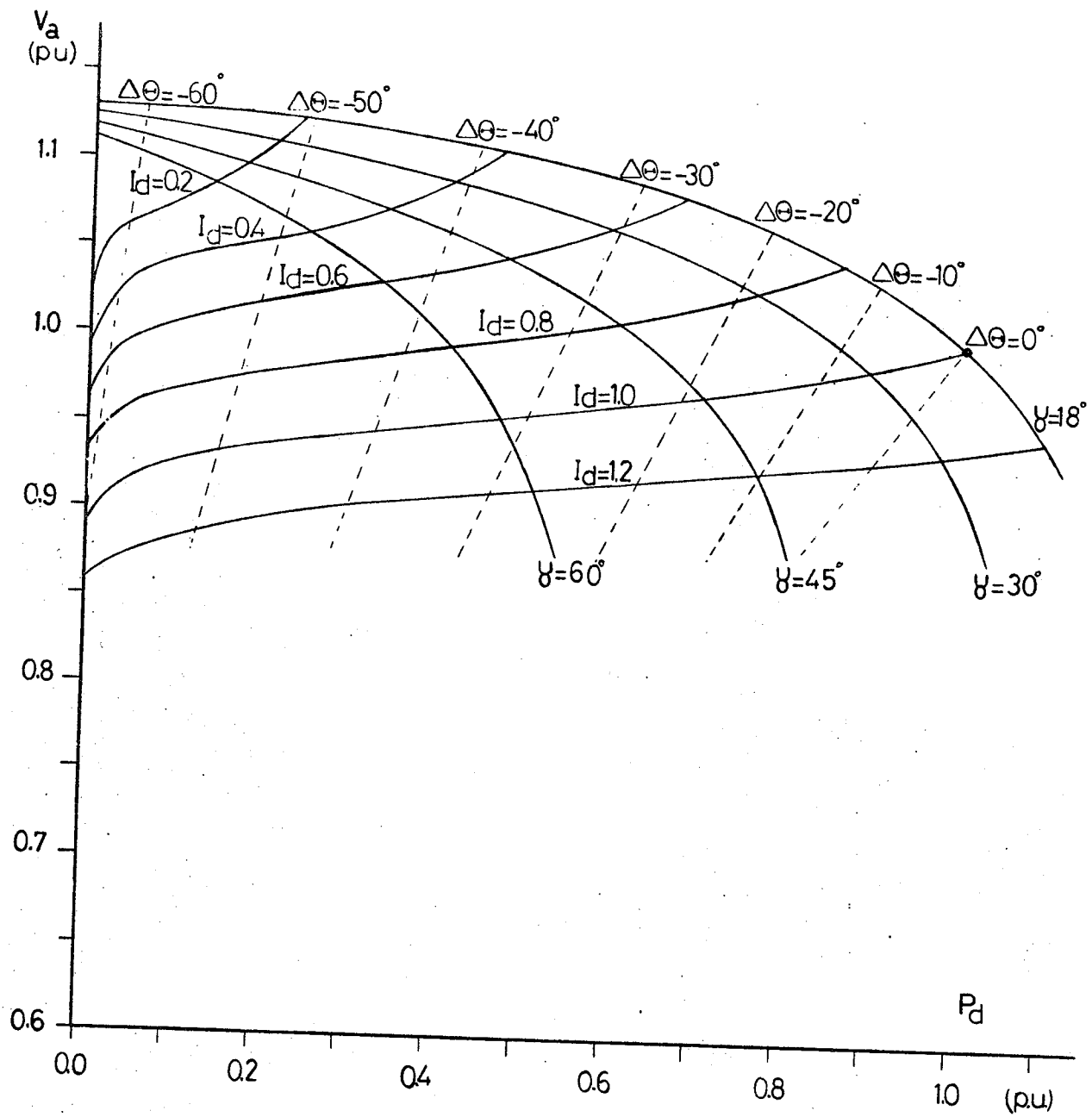


Figure 3.9 Short-term regulation characteristics with a system S.C.R. = 1.0 and a static compensator of 10% reactance slope

by the network. The result is an increase in ac system voltage. In short-term duty, the higher system voltage causes a further reduction in the commutating reactive load and also a rise in the capacitor reactive supply which increases as the square of the voltage.

Both of these effects tend to raise the ac system voltage. The rise is more pronounced in weak networks as compared to that in strong ones. (Figure 3.6.)

Besides the system reactance influence on the short-term regulation phenomena, the installed capacitor MVar has an additional effect.^{61,77} Figures 3.7 and 3.8 show a comparison of system regulation characteristics as affected by different short circuit ratios and filter capacitive VAr compensation. The higher the capacitor rating, for weak ac systems, the higher the regulation.

If a static compensator is installed in place of a synchronous compensator, with the system short circuit ratio as low as unity, the regulation characteristics are as shown in Figure 3.9. The ac voltage rise, for a short-term complete load rejection, with constant extinction angle control in this case, is about 13% as compared with 36% and 15% for a system using synchronous compensators with overall short circuit ratios of 2.0 and 4.0 respectively.

The system shown in Figure 3.2 was simulated using a transient stability program (see Appendix A). The ac terminal voltage time response for a case when the dc power order, acting upon dc current, is reduced by 50% is shown in Figure 3.10. A high dynamic overvoltage is experienced when a synchronous compensator is used for VAr control at the inverter terminal (curve i). The amount of overvoltage is substantially reduced

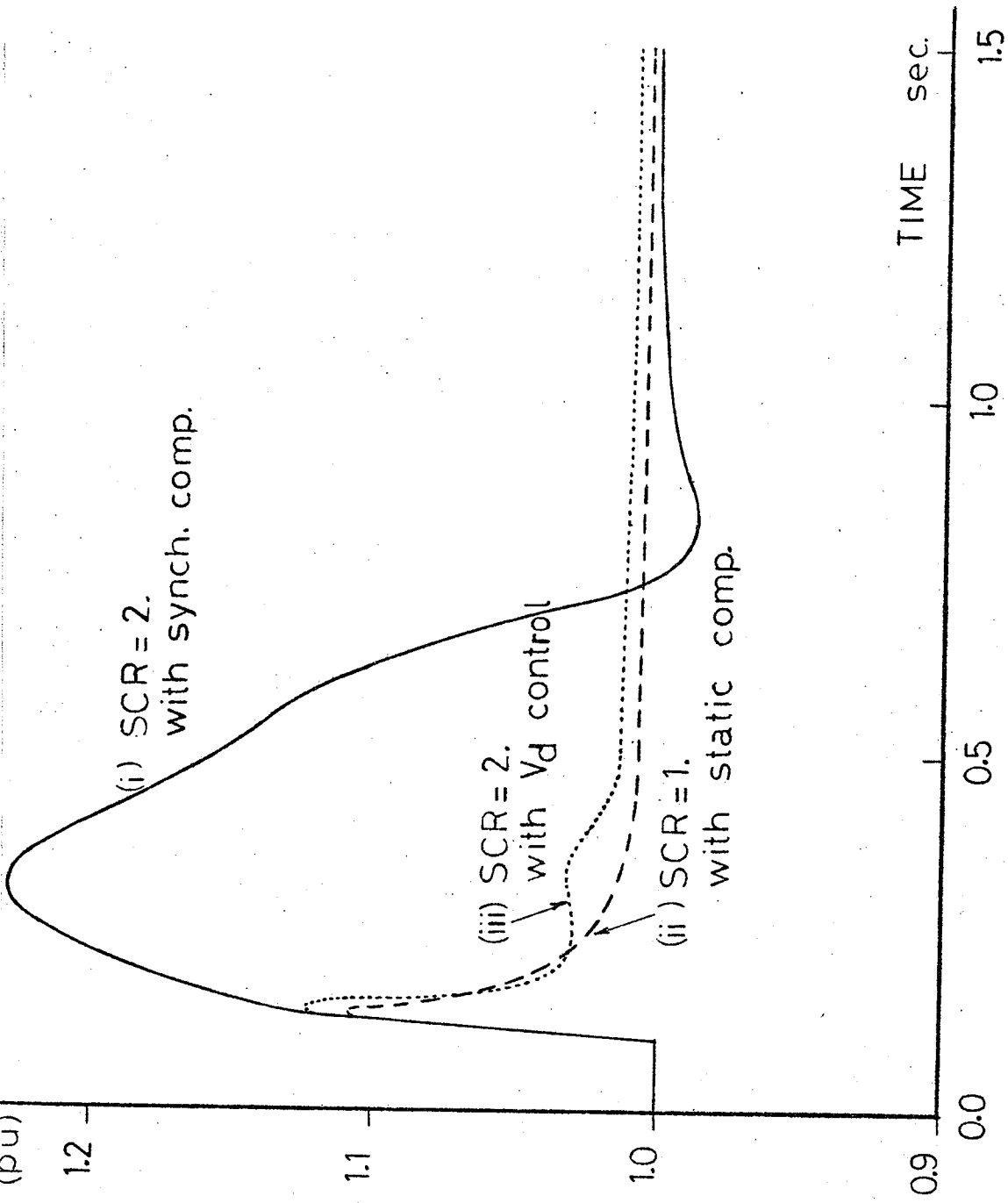


Figure 3.10 AC terminal voltage time response for a 50% dc load rejection

when, in place of a synchronous compensator, a static VAr compensator (of slope 20%) is used (curve ii). However, when the dc voltage is temporarily reduced, by advancing the extinction angle, through a voltage controller (as shown in Figure A.2) it gave an overall favorable terminal effects (curve iii) similar to those when a static compensator was used.

Therefore, it is evident that, firstly, control of the ac voltage at a dc terminal by means of a static VAr compensating equipment, without increasing system short circuit ratio, is feasible and, secondly, the usual type of dc terminal control, i.e. constant extinction angle control with basically constant dc voltage, does not give a reasonable performance, in the short-term duty, for an interconnected weak ac system. These two aspects are dealt with in the next two sections respectively.

3.3 Application of Thyristor Controlled Reactors at the Terminals of HVDC Systems

An extensive effort was devoted to investigate the extent to which static VAr compensating systems (including thyristor controlled reactors) can affect the overall system behaviour when applied at the terminals of HVDC schemes⁷⁹ (including multiterminal) in practical networks.

Because of the generalized nature and large size of the problem, a complete large scale load flow and transient stability program was developed.⁸⁰ The unique features of this digital program include:

(a) HVDC Systems:

- A general model to simulate two and multi-terminal schemes with parallel converter stations connected in any configuration,
- ability to simulate diode rectifiers and non-converter dc buses (with dc loads or generations),

- independent terminal controls (for both rectifiers and inverters) for; constant dc current, constant dc power or constant firing (or extinction) angle modes,
- variety of pole controllers to enhance ac system performance such as frequency damping and ac voltage controls,
- a generalized master controller with the flexibility to simulate extra special transfer functions,
- provisions for dc power or current order changes, blocking, deblocking and automatic simulation of long-term commutation failures and recovery from them.

(b) Static VAr Compensating Systems:

- saturated reactors with, or without, transient effects of slope correcting capacitors,
- transductors with dc controlled saturation,
- thyristor phase controlled reactors,
- thyristor switched capacitor banks.

(c) Synchronous Alternators Systems:

- classical machine model,
- transient machine model,
- subtransient machine models (round rotor or salient pole),
- standard and static exciters, voltage regulators and stabilizers,
- hydraulic turbines and standard steam turbines and governors.

(d) System Solution:

- loads are represented by a combination of constant impedance and current sources while synchronous machines and static compensators are represented as constant current sources to avoid increasing number of unknown variables,^{101,102}

- sparsity techniques to reduce storage and increase efficiency of calculations.^{81,105,106}

One version of the program is currently used by Manitoba Hydro Electric Board and Furnas Power Utility in Brazil. A summary and a mathematical background of the program are included in Appendix A.

For a large system model representing the MAPP power pool with an ac/dc hybrid transmission link tying the areas of Manitoba, North Dakota and Nebraska (MANDAN)⁸² as shown in Figure 3.11, various VAR compensation schemes were studied. Figures 3.12 and 3.13 show respectively the ac voltage at the ac/dc interconnecting point at Fargo and a machine rotor angle in North Dakota for a 3-cycle, 3-phase fault in North Dakota cleared by tripping an ac line to Fargo. The results in Figures 3.12 and 3.13 clearly demonstrate the positive effects a thyristor controlled reactor can have to maintain system voltage (of a system with low short circuit ratio) and to damp system oscillations.

For a three-terminal dc alternative (shown in Figure 3.14), similar results were obtained as shown in Figures 3.15 and 3.16.

3.4 AC Voltage Control Using a HVDC Converter Terminal

The asynchronous nature of the dc link does not appreciably increase the fault level of the ac system to which it is connected.⁵⁸ Moreover, the dc converter with different types of control policies can have important effects on an ac system performance.^{63,65}

It is relatively easy to design controls for a dc link connected to a strong ac system. When the link real and reactive powers are small compared to those of the ac system, the link operation and maloperation due to, for example, dc line faults, load rejection or commutation failure will have small effect on the ac system and in turn, ac system disturbances caused by the dc link are not simultaneously reflected back on

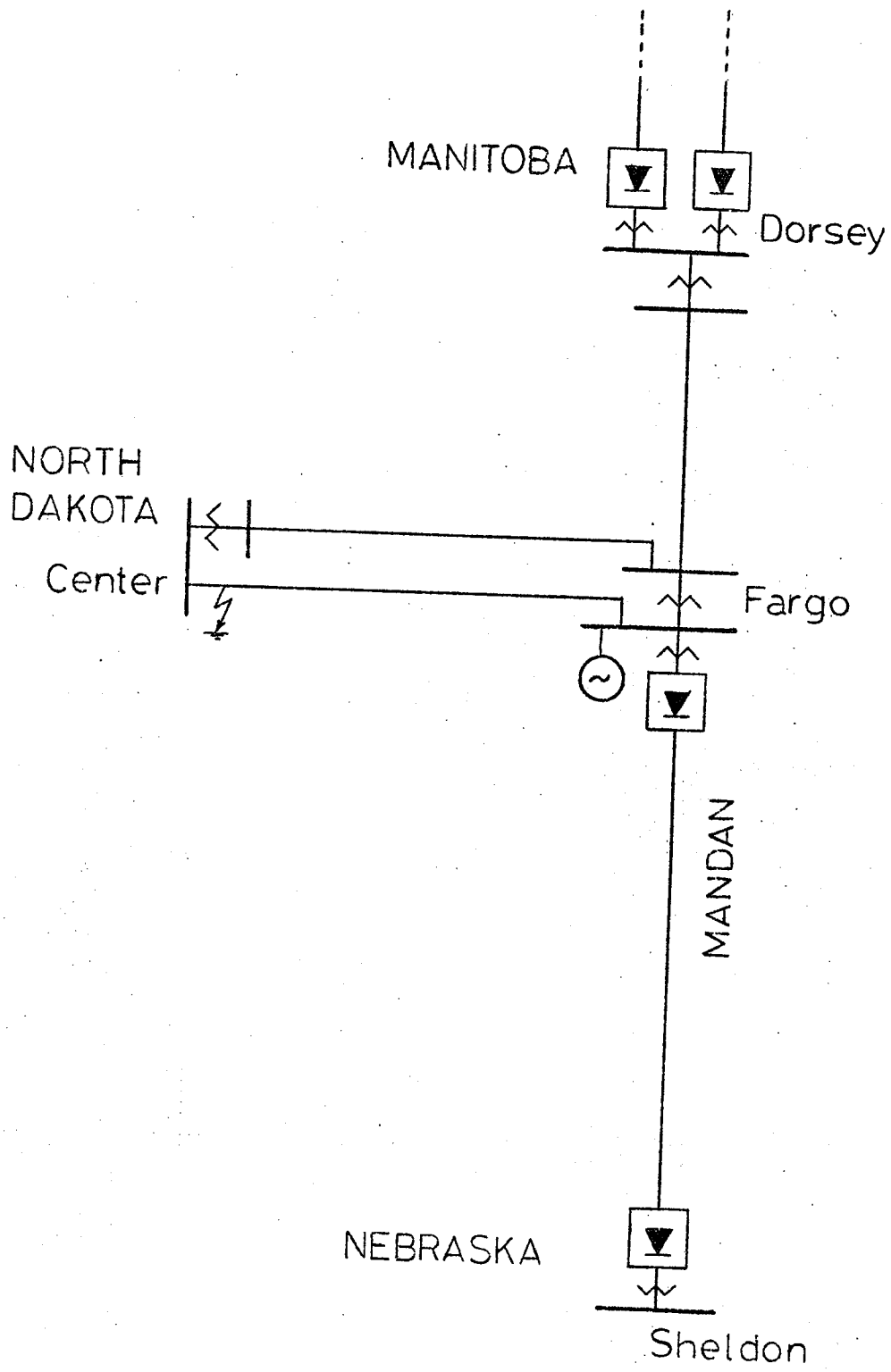


Figure 3.11 MANDAN Transmission scheme, ac/dc alternative

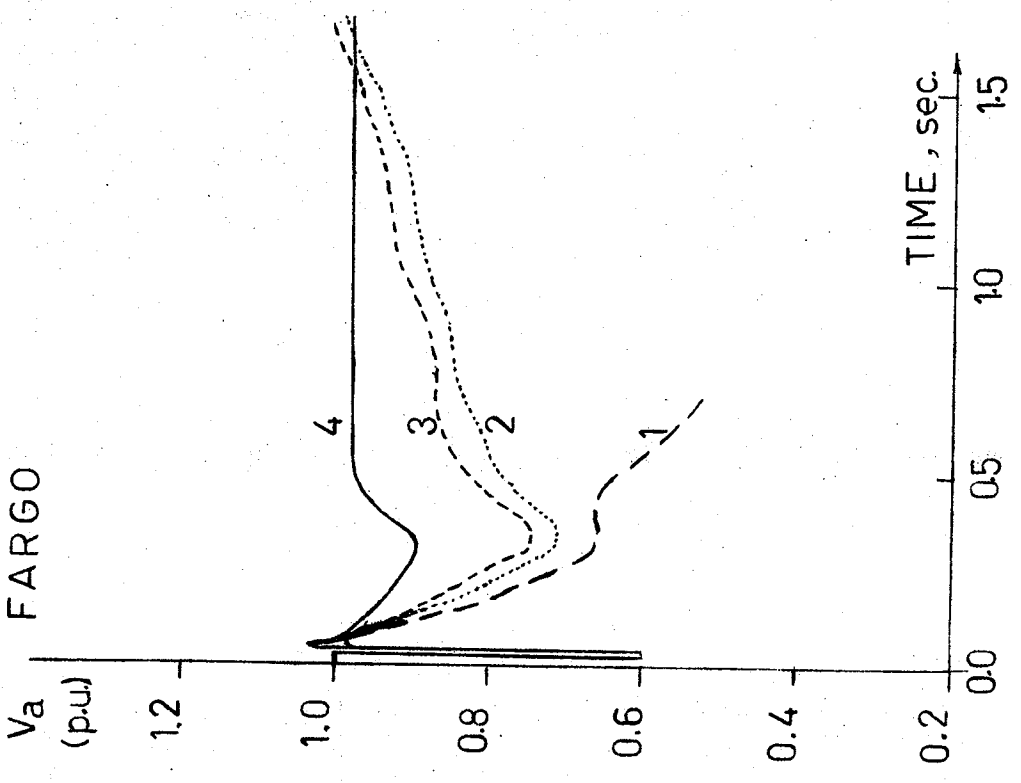


Figure 3.12 AC voltage at Fargo for a 3- ϕ fault at Center

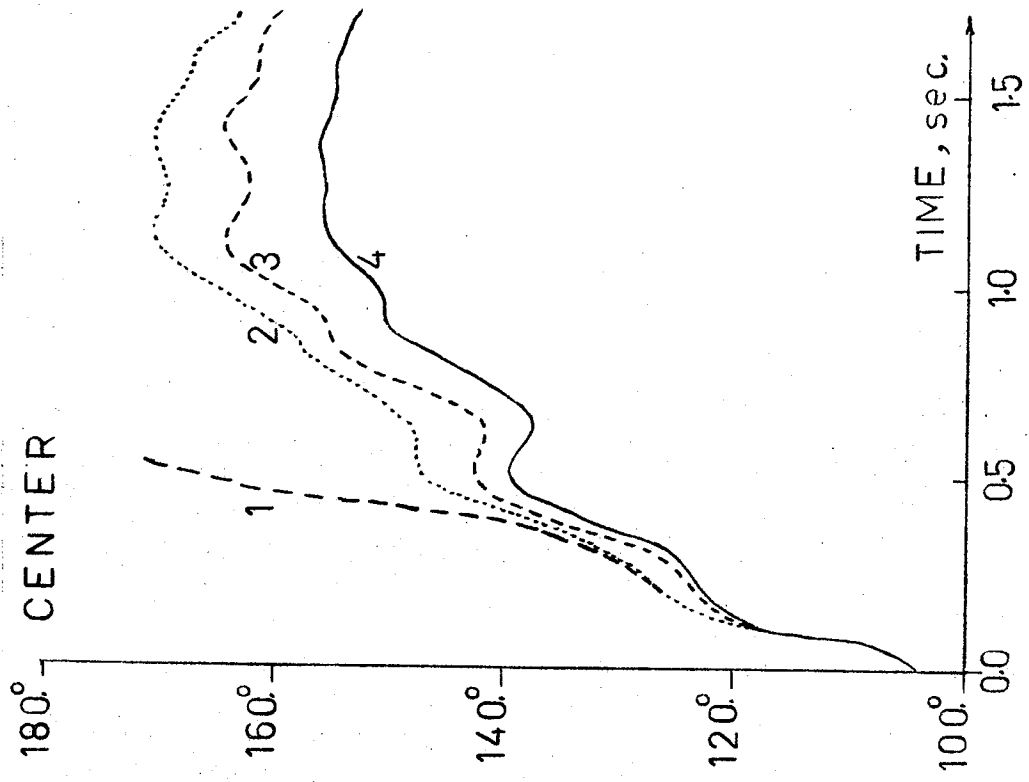


Figure 3.13 Machine rotor angle at Center

VAr Compensation at Fargo:

- (1) Two synchronous compensators (SCR = 2.7)
- (2) Three synchronous compensators (SCR = 3.1)
- (3) Four synchronous compensators (SCR = 3.5)
- (4) Two syn. compensators & 300 MVAR static comp.

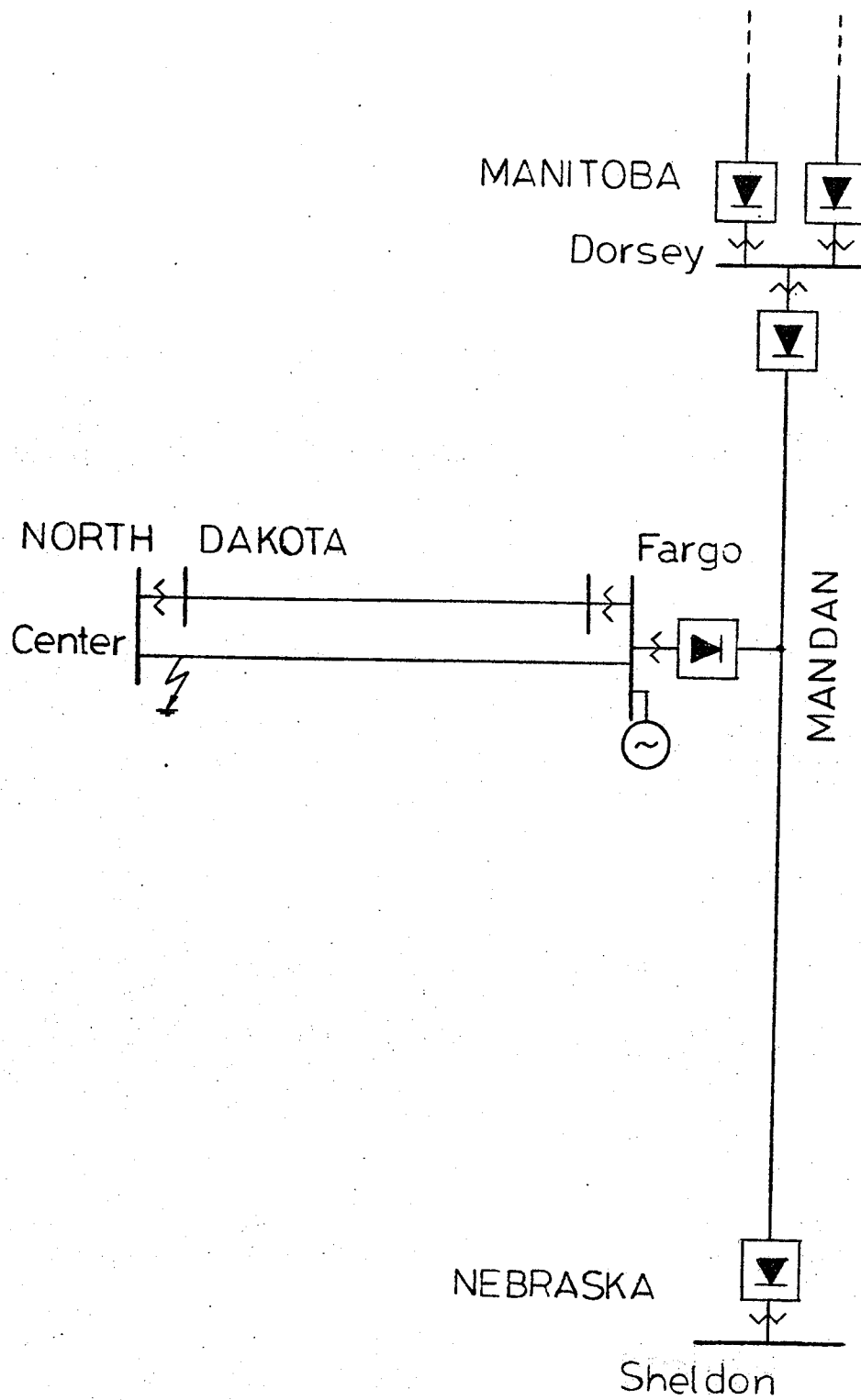


Figure 3.14 MANDAN Transmission scheme, dc alternative with tapping at Fargo

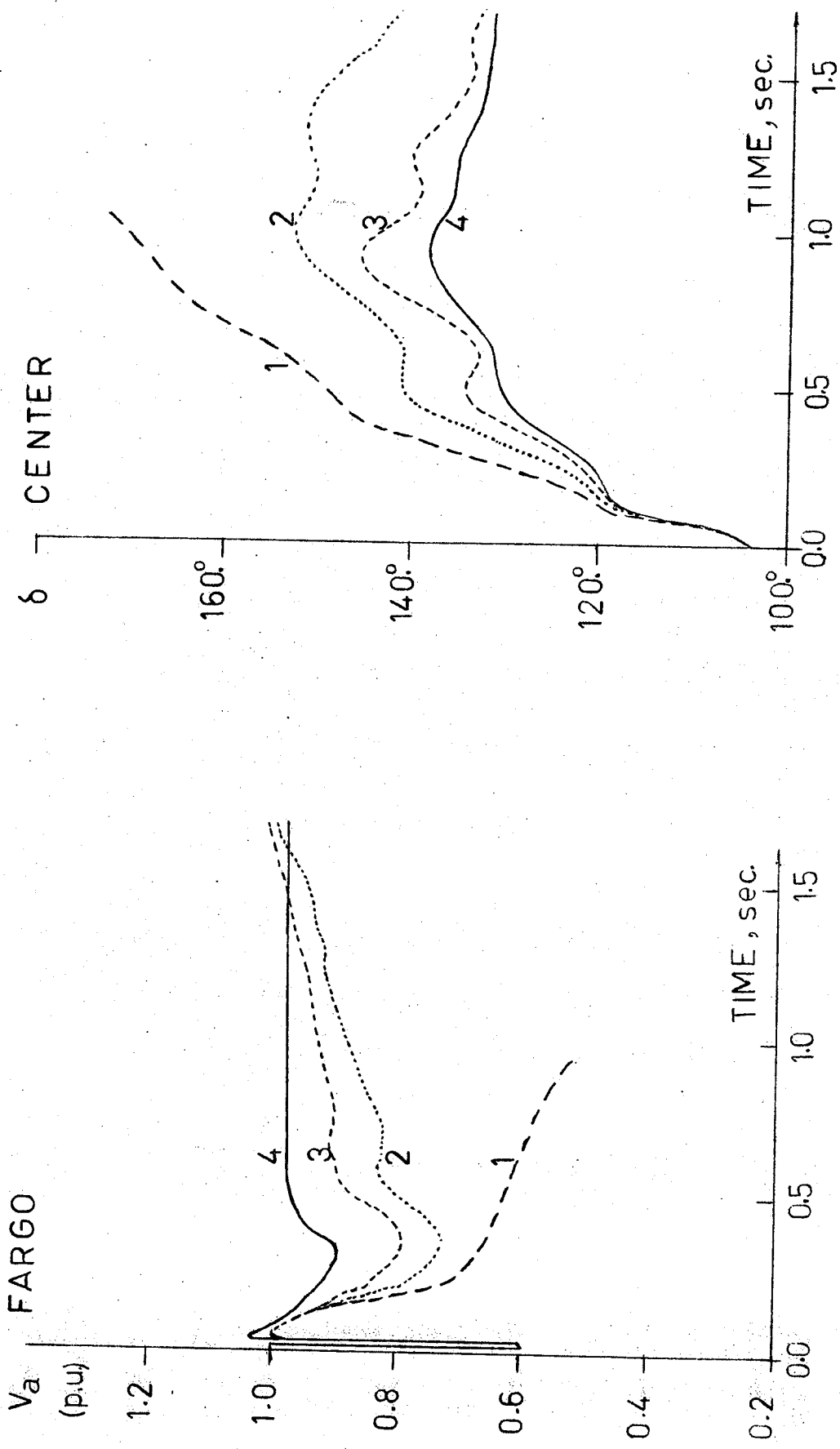


Figure 3.15 AC voltage at Fargo for a 3-Ø fault at Center

Figure 3.16 Machine rotor angle at Center

Var Compensation at Fargo:

- (1) One synchronous compensator (SCR = 2.6)
- (2) Two synchronous compensators (SCR = 3.1)
- (3) One syn. compensator & 100 MVar static comp.
- (4) 300 MVar static compensator (SCR = 2.1)

the dc link operation.⁶⁷⁻⁷¹

Problems are encountered increasingly as the short circuit ratio is reduced.⁵⁵

One of the ideas most often put forth is to enhance the performance and to improve damping the oscillations of an ac system by modifying the power of the HVDC terminal in response to changes in various parameters of the interconnected ac network, such as frequency and phase angle at a certain bus.⁶⁶⁻⁶⁹ Other parameters such as power through a tie line or other important line or transformer in a system or the angle across such a line may be used in certain situations.⁶⁵

However this action can be extended to control also the reactive power flow and consequently the ac voltage adjacent to the dc terminal.⁶⁰ A HVDC converter, which can be looked at as a huge static VAR compensator, absorbs reactive power according to:

$$Q_d = |P_d| \tan \phi$$

when

$$V_d = V_a \cos \phi \quad \text{in p.u.}$$

Therefore by changing the dc voltage, the reactive power demand of the dc converter can be highly affected (as was shown in Figure 3.5).

A study was carried out to investigate the possibility of such a new method of ac voltage control via advancing the firing (or extinction) angle, as well as damping system oscillations via dc current modulation of a HVDC terminal at an ac bus with multiple dc infeed.

For the system shown in Figure 3.17, the main principle for controlling the Dorsey ac voltage is based upon using the MANDAN dc Dorsey rectifier as the dc voltage controlling (rather than dc current controlling) terminal, i.e. with minimum delay angle α_{\min} under steady-state

operation, and the firing angle α (and consequently the dc voltage) changing according to the ac bus voltage under transient conditions. Generally this control action is quite similar to a thyristor controlled reactor static VAr compensation system. Also, this fast control is local and does not depend on the telecommunication channels since the dc current (controlled by the other terminals) can remain unchanged. However, it should be pointed out that this control method is only effective as long as the HVDC converter is free from any faults or commutation failures. In the event of a dc fault, commutation failure or complete blocking an external VAr controller may still be required as was discussed previously.

Four different control strategies were examined for the Dorsey MANDAN dc terminal (of Figure 3.17) in a case when dc BP1 is permanently blocked:

- i. conventional constant dc voltage and no frequency damping,
- ii. conventional constant dc voltage and frequency damping acting on dc current,
- iii. variable dc voltage and no frequency damping,
- iv. variable dc voltage and frequency damping acting on dc current.

For the conventional mode of operation (cases i and ii) the Dorsey rectifier delay angle α is adjusted in order to keep the dc current equal to the current order, which can change if frequency damping control is used, while the dc voltage is kept constant by the Sheldon inverter terminal (Figure 3.18). However, for the variable dc voltage control strategy (case iii) the Dorsey rectifier delay angle α is advanced - causing a temporary dc voltage reduction - in order to maintain the ac rms voltage during the swing while the dc current is controlled

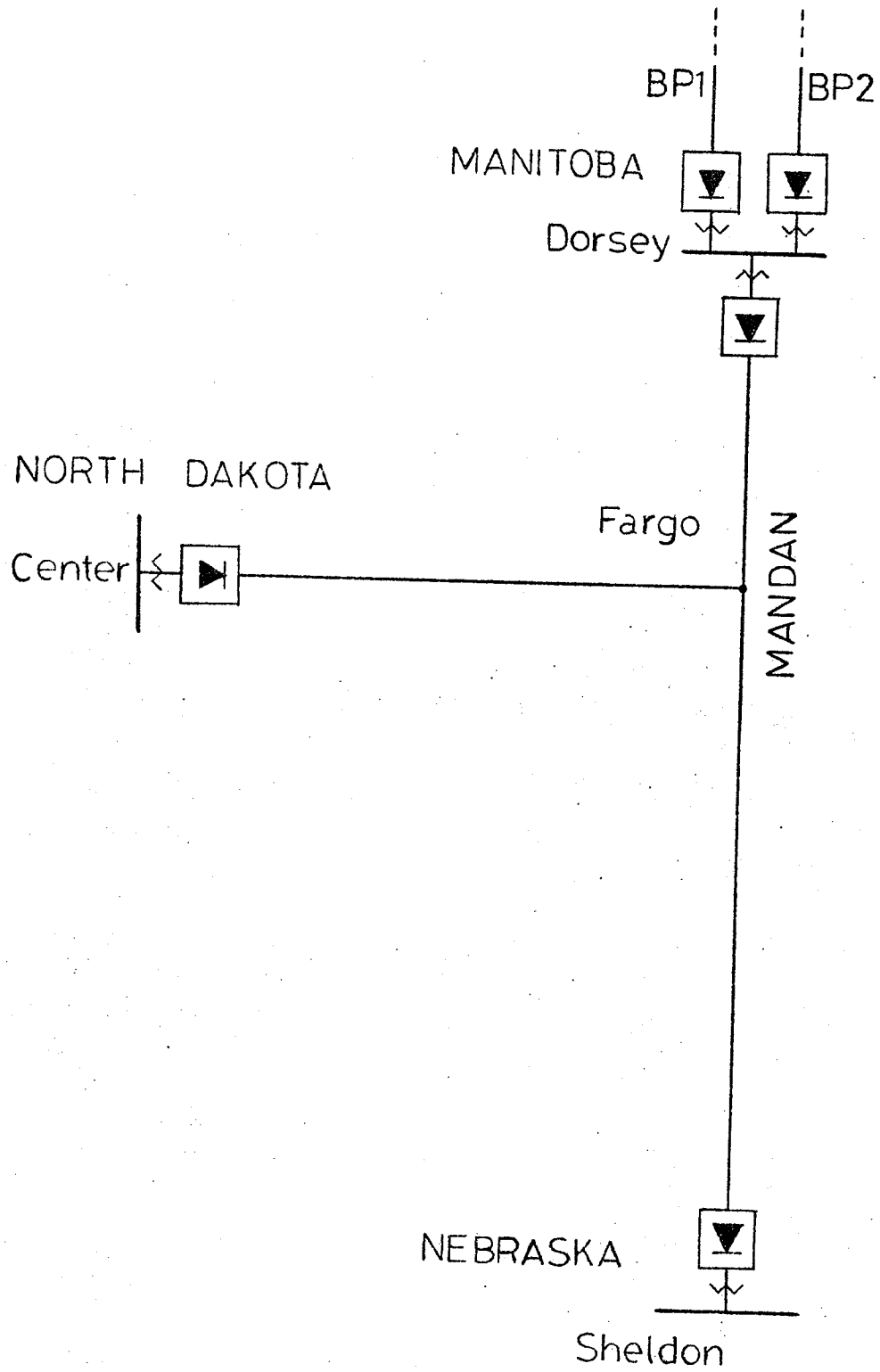


Figure 3.17 A 3-Terminal HVDC alternative for MANDAN Transmission scheme

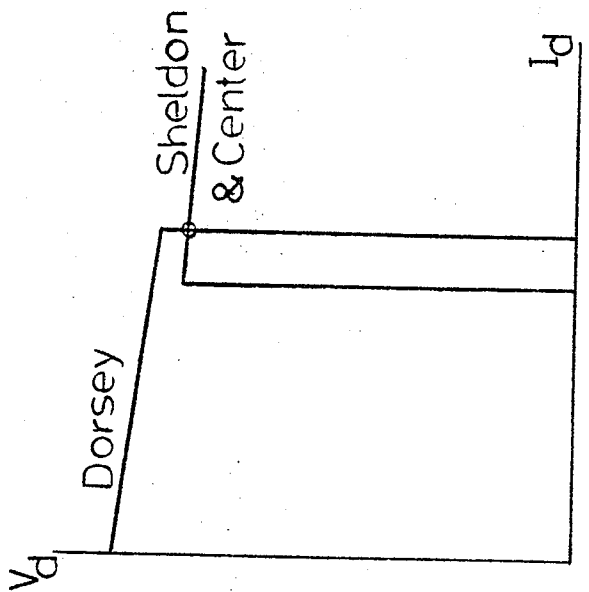


Figure 3.18 Steady state characteristics for Dorsey rectifier with dc current control

case (i) no frequency damping,
 case (ii) with frequency damping.

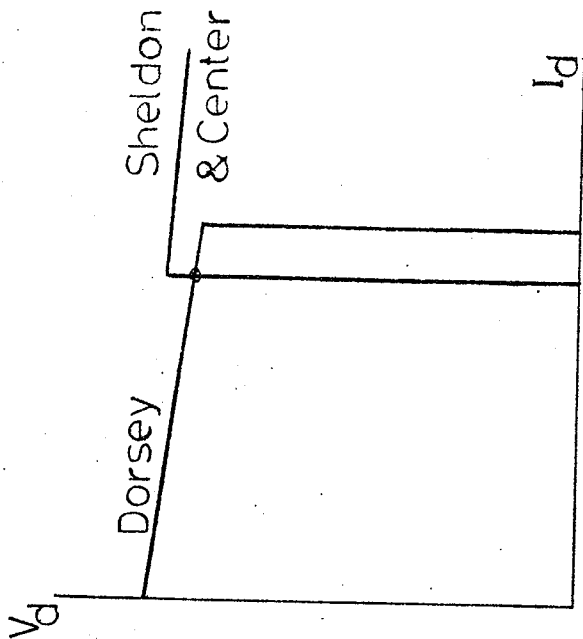


Figure 3.19 Steady state characteristics for Dorsey rectifier with dc voltage control

case (iii) no frequency damping,
 case (iv) with frequency damping.

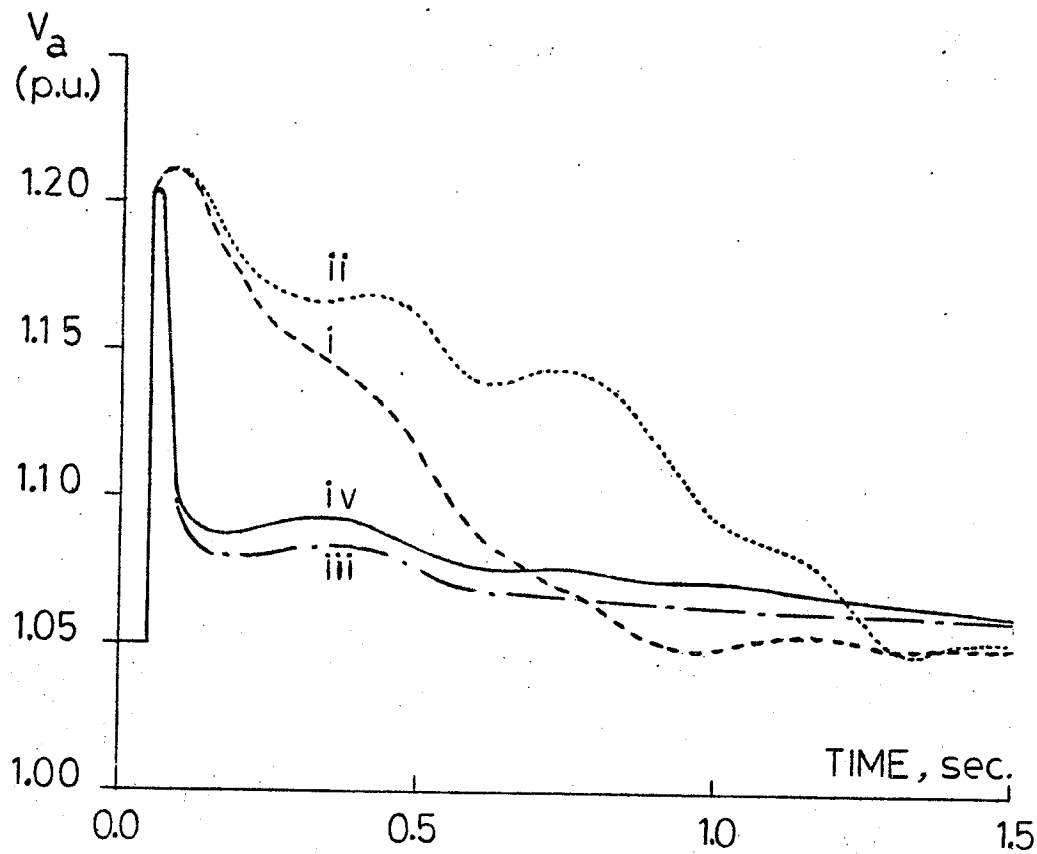


Figure 3.20 AC voltage at Dorsey following blocking of BP1

- (i) Dorsey Rectifier with current control
- (ii) Dorsey Rectifier with current control & frequency damping
- (iii) Dorsey Rectifier with voltage control
- (iv) Dorsey Rectifier with voltage control & frequency damping

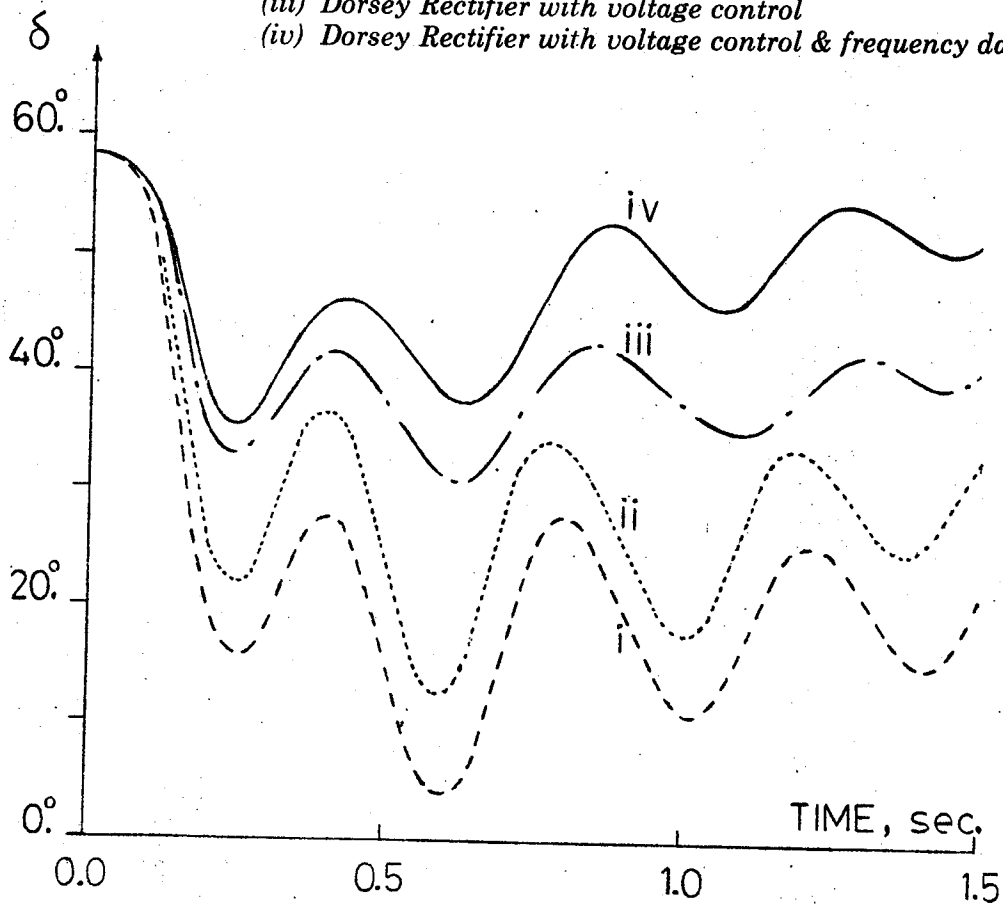


Figure 3.21 Machine rotor angle at Dorsey following blocking of BP1

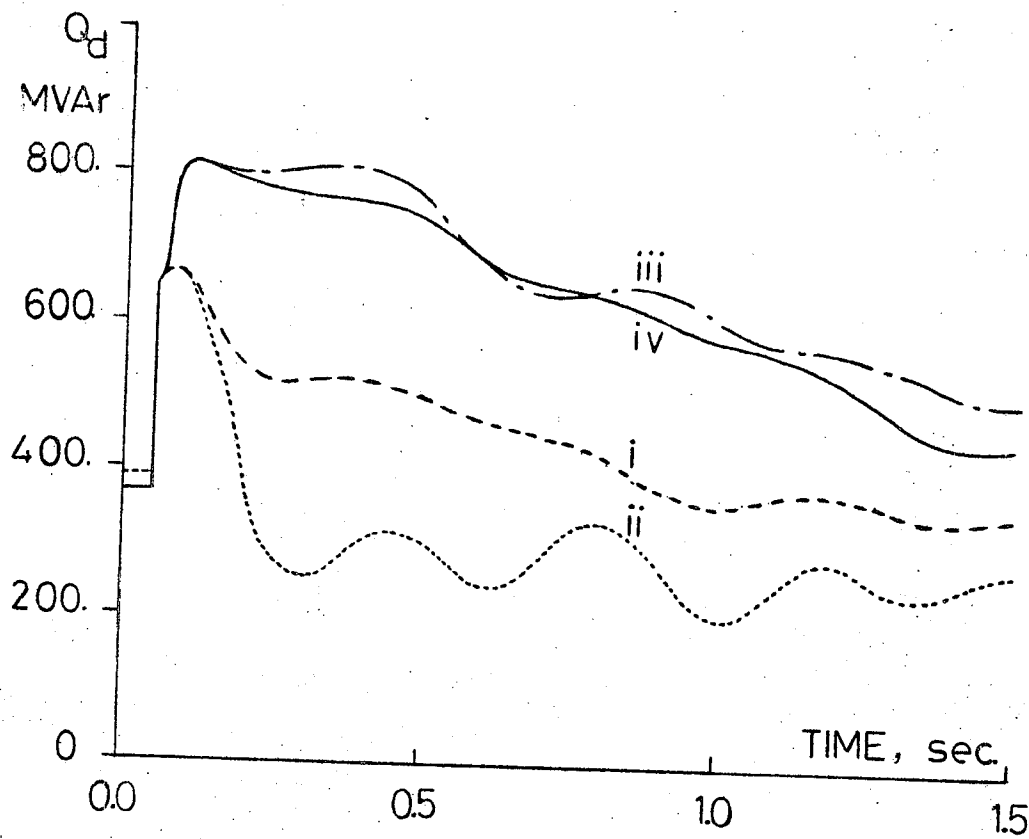


Figure 3.22 Ractive power absorbed by MANDAN rectifier at Dorsey

- (i) Dorsey Rectifier with current control
- (ii) Dorsey Rectifier with current control & frequency damping
- (iii) Dorsey Rectifier with voltage control
- (iv) Dorsey Rectifier with voltage control & frequency damping

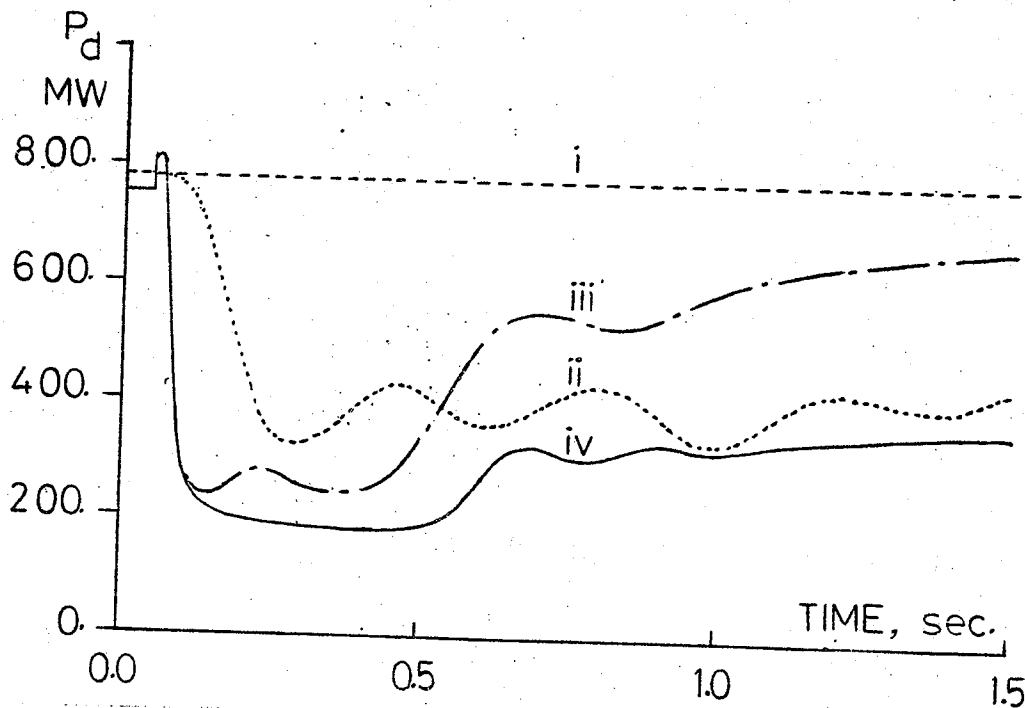


Figure 3.23 DC power of MANDAN rectifier at Dorsey

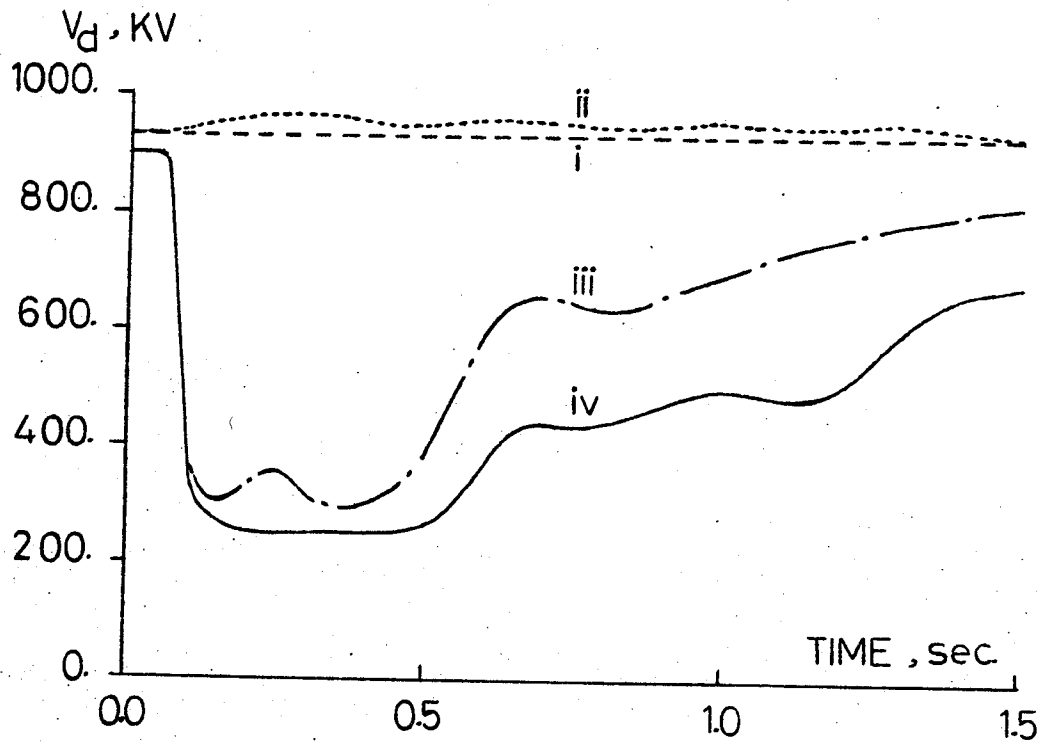


Figure 3.24 DC voltage of MANDAN rectifier at Dorsey

- (i) Dorsey Rectifier with current control
- (ii) Dorsey Rectifier with current control & frequency damping
- (iii) Dorsey Rectifier with voltage control
- (iv) Dorsey Rectifier with voltage control & frequency damping

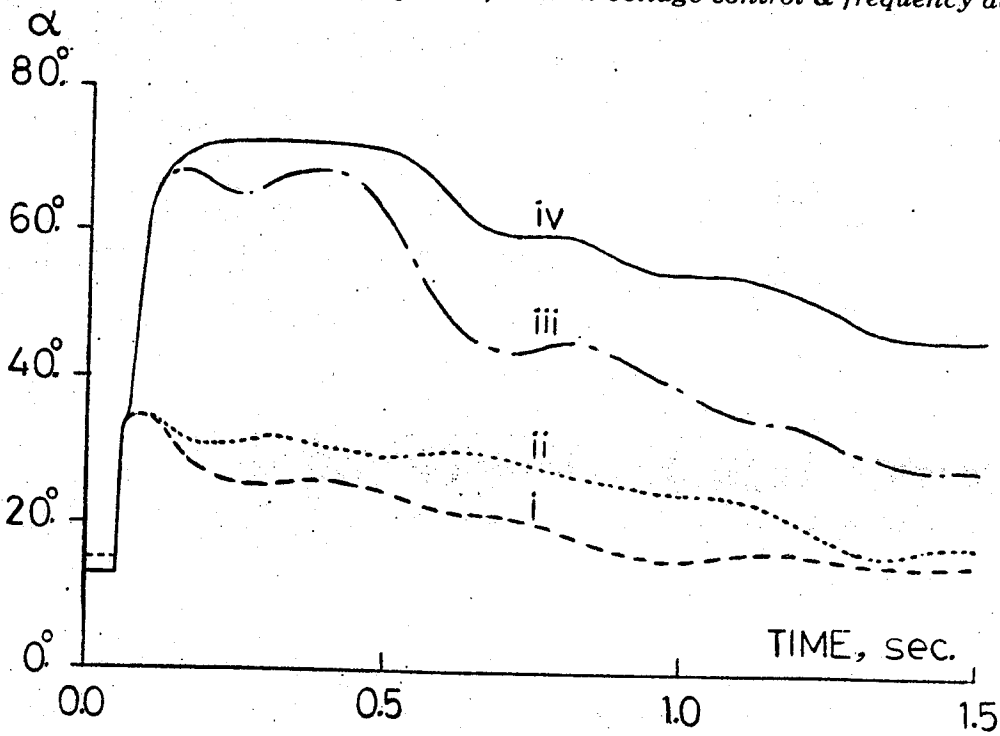


Figure 3.25 Firing angle of MANDAN rectifier at Dorsey

by the Sheldon inverter (Figure 3.19). For case (iv) the same strategy is employed at Dorsey but with an additional frequency damping control applied on the dc current order of the Sheldon terminal via telecommunication channels.

Figure 3.20 shows the ac rms voltage at Dorsey following the blocking of BP1 for control strategies (i) to (iv). The fast control of the dynamic voltage is evident for cases (iii) and (iv) whereas a case of sustained overvoltages can occur when the conventional frequency damping control (ii) is used. Figure 3.21 shows the rotor angle of a machine at Dorsey. The reactive power absorbed by the Dorsey MANDAN terminal is shown in Figure 3.22 whereas the dc power, dc voltage and firing angle are shown in Figures 3.23, 3.24 and 3.25 respectively. It is worth noting that better damping of system frequency oscillation can be achieved if dc current modulation is used, besides the ac voltage control (as in case iv), even with a high telecommunication time lag of up to 0.5 second. If dc current modulation is used, instead, with conventional constant dc voltage control (as in case ii) a serious dynamic overvoltage situation can arise unless more reactive power compensators are employed.

3.5 Conclusions

- (1) Application of a thyristor controlled static VAR compensator at a dc converter terminal in a two or multi-terminal scheme provides a reliable and economical alternative to the synchronous compensator.
- (2) Without increasing the short circuit ratio, a static VAR compensator can improve short-term voltage regulation characteristics of a dc converter connected to a weak ac system.

- (3) If synchronous compensators, already exist at a HVDC converter, a static compensator can avoid their instability on account of a dc load rejection.
- (4) A temporary operation of a trouble free HVDC terminal under variable dc voltage control strategy, through a fast acting local firing (or extinction) angle controller, is feasible to limit ac dynamic over-voltages.

*chapter four*APPLICATION OF THYRISTOR CONTROLLED REACTOR SYSTEMS
WITH SUPER CONDUCTING GENERATORS4.1 Introduction

The state of current activities in the development of prototypes of superconducting-field alternators and the interest in their analytical investigations suggest quite clearly that this new breed of alternators would be operational in the near future in sizes bigger than the biggest turbo-alternators available as of now. It is likely that the first few units commissioned would lie in the 1-3 GW range, but it appears reasonable to think that much bigger sizes would be seriously considered once field experience is gained.⁸³⁻⁸⁹

Quite apart from the novelty of the internal designs of the superconducting alternators, there are features of their dynamic performance which differ greatly from their conventional counterparts. One such feature, which is of prime interest for this investigation, stems from the application of a superconducting field winding. The novel field winding has a negligible resistance and therefore its field time constant is exceptionally large. It lies typically in the range of 300-800 s. Therefore, there is at first the question of incorporating features which would ensure a good voltage regulation performance. The implication of this statement is that the excitation voltage ceiling must be raised grossly if field current must be changed rapidly in spite of the large field time constant. Increasing the limits of excitation voltage, by a

few tens to hundreds of times, in itself may not pose a serious enough problem from the insulation point of view. However, high values of di_f/dt may not be acceptable for the superconducting field system. Limits on the excitation voltage, thus imposed, may not guarantee a satisfactory dynamic performance. Further, the fast changes in the field current are also influenced by coupled electrical circuits formed by the damping and screening shields of the machine. Hence field forcing by larger voltage ceiling does not appear to be a simple matter.

An alternative approach to ensure the same end effects obtained by fast field excitation changes, is adopted by proposing a fast acting thyristor controlled static reactive power compensator connected at the terminals of the superconducting alternator. In this scheme the field system can be either supplied with a fixed voltage or better still by a simpler conventional type regulator which takes care of only major steady state field current adjustments.

As a matter of interest, this superconducting machine system has a close analogy to an HVDC terminal. For both systems, conventional VAR controls (synchronous compensator in case of a HVDC terminal and field forcing in case of a superconducting machine) cannot provide a fast means of changing the reactive power level at the terminals. The application of static VAR compensator at the terminals of either system provides a satisfactory solution.

From system point of view the studies for both systems are similar albeit responses are different. The HVDC system has been investigated in Chapter 3 while this chapter is devoted to the superconducting machine system.

4.2 System Under Study

Figure 4.1 shows the system under study in which a superconducting alternator having separate screening and damping shields is connected through a transformer and a transmission line to an infinite bus. The alternator is modelled by Park's equations using lumped parameters. The skin effect in the shields and other conductors is ignored. In addition, the shields and field system are regarded to form a rigid mechanical system on the shaft.⁸³⁻⁸⁶

In order to evaluate the technical merits of the new proposal, the following studies have been carried out:

- (a) load rejection performance,
- (b) small signal dynamic stability and eigenvalue analysis,
- (c) large signal transient stability.

For load rejection studies a local load has been connected at the machine terminal bus.

In all the studies the machine performance with either internal field forcing control or external control by a static compensator at its terminals was investigated. It has generally been found that the alternator has better performance when a static compensator is used at its terminal bus.

For field forcing studies the generator is regarded to be equipped with an excitation controller, the voltage limits of which can be preset. For the investigations of the proposed alternative, of a static compensator at the terminals of the alternator, the range of controlled reactive power flow from the compensator has been, where necessary, offset by connecting a capacitor bank in parallel with the controlled reactor.

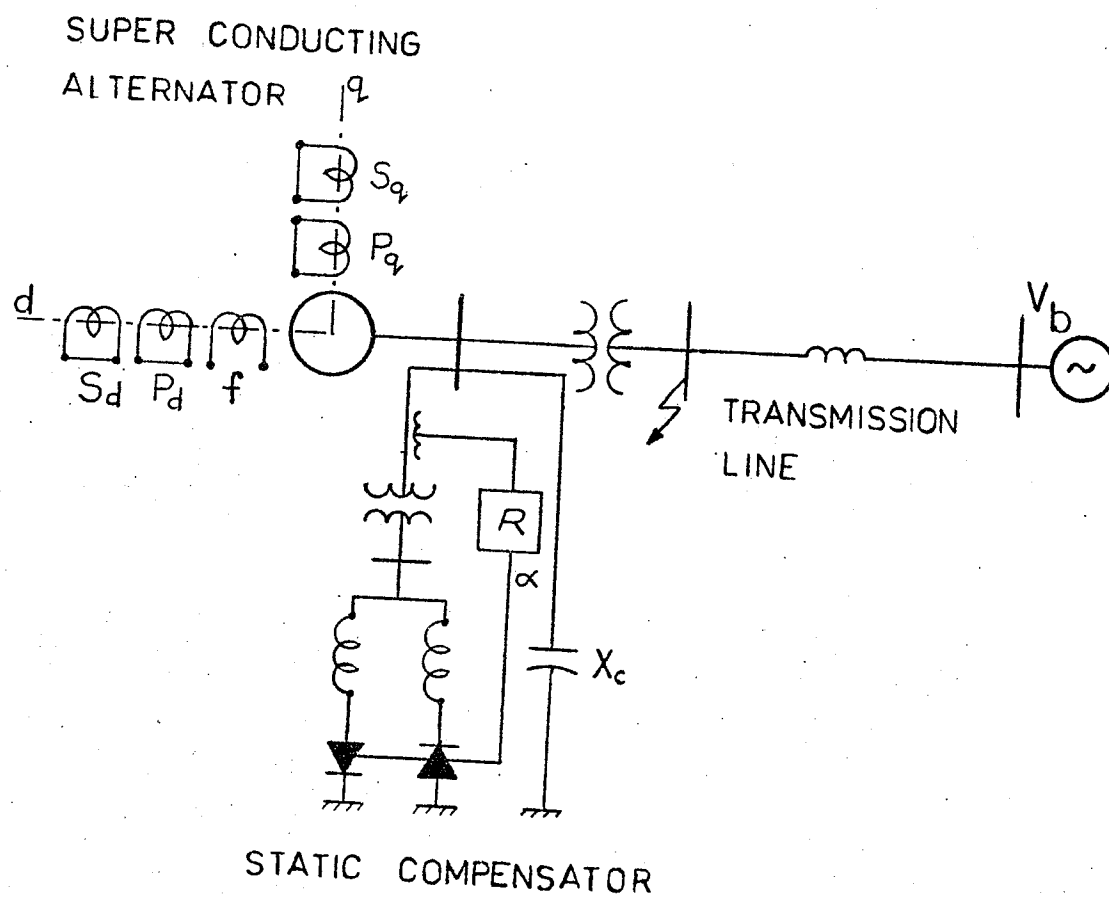


Figure 4.1 Super-conducting machine system

It has been relatively easy to incorporate auxiliary stabilizing signals in the compensator. Hence, in order to make meaningful comparison with the field forcing technique similar stabilizing signals are also incorporated in its controller.

4.3 Mathematical Modelling

4.3.1 Super Conducting Alternator

Basic equations of the superconducting alternator with two fixed shields are: ⁸⁵

$$e_d = p \frac{\psi_d}{\omega_0} - \frac{\omega}{\omega_0} \psi_q - R_a i_d$$

$$e_q = p \frac{\psi_q}{\omega_0} + \frac{\omega}{\omega_0} \psi_d - R_a i_q$$

$$e_f = p \psi_f + R_f i_f$$

$$0 = p \psi_{sd} + R_{sd} i_{sd}$$

$$0 = p \psi_{sq} + R_{sq} i_{sq}$$

$$0 = p \psi_{pd} + R_{pd} i_{pd}$$

$$0 = p \psi_{pq} + R_{pq} i_{pq}$$

(4.1)

Flux linkages in (4.1) are represented in terms of machine currents and reactances by (4.2) and (4.3).

$$\begin{bmatrix} \psi_d \\ \psi_f \\ \psi_{sd} \\ \psi_{pd} \end{bmatrix} = \begin{bmatrix} -X_d & X_{md} & X_{md} & X_{md} \\ -X_{md} & X_f & X_s & X_p \\ -X_{md} & X_s & X_s & X_s \\ -X_{md} & X_p & X_s & X_p \end{bmatrix} \begin{bmatrix} i_d \\ i_f \\ i_{sd} \\ i_{pd} \end{bmatrix} \quad (4.2)$$

$$\begin{bmatrix} \psi_q \\ \psi_{sq} \\ \psi_{pq} \end{bmatrix} = \begin{bmatrix} -X_q & X_{mq} & X_{mq} \\ -X_{mq} & X_s & X_s \\ -X_{mq} & X_s & X_p \end{bmatrix} \begin{bmatrix} i_q \\ i_{sq} \\ i_{pq} \end{bmatrix} \quad (4.3)$$

$$\text{where } X_f = \frac{X_{md}^2}{X_d - X_d'} , \quad X_s = \frac{X_{md}^2}{X_d - X_d''} , \quad X_p = \frac{X_{md}^2}{X_d - X_d'''} .$$

Electromagnetic torque produced by the alternator is

$$T_e = \psi_d i_q - \psi_q i_d \quad (4.4)$$

and the swing equation of the alternator is

$$p\delta = (\omega - \omega_0) \quad (4.5)$$

$$\text{and } p\omega = \frac{\omega_0}{2H} (T_m - T_e) \quad (4.6)$$

4.3.2 Static Compensator

The harmonics generated by the compensator are ignored assuming that they are filtered satisfactorily and that the filters do not affect the system performance. In fact the biasing capacitor connected in parallel with the controlled reactor could be an integral part of a double tuned filter which is predominantly capacitive at power frequency.

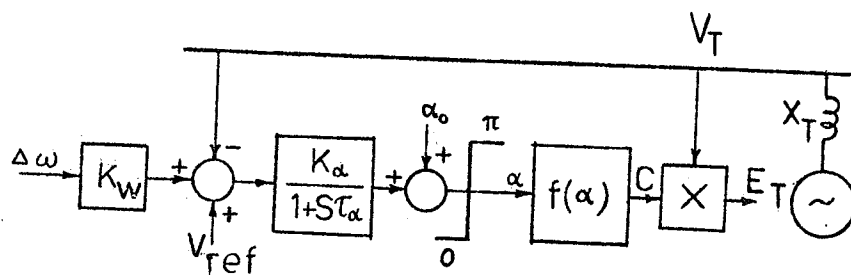


Figure 4.2 Thyristor-controlled reactor model

As shown in Figure 4.2, the controlled reactor is represented by an inertialess voltage source E_T behind a fixed reactance X_T . The magnitude of E_T is controlled but it always stays in phase with the terminal bus voltage V_T and is given by

$$E_T = C V_T \quad (4.7)$$

where

$$C = \frac{2\alpha - \sin 2\alpha}{2\pi} \quad (\text{from Eq. 2.43}) \quad (4.8)$$

and α is the firing angle of thyristors.

A single time constant and gain is used to represent the firing control system of the thyristors. The value of α is obtained as a function of the terminal voltage and frequency;

$$p\alpha = \{\alpha_0 - \alpha + K_\alpha [(V_{ref} - V_T) + K_W (\omega - \omega_0)]\} / \tau_\alpha \quad (4.9)$$

where

$$0 \leq \alpha \leq \pi$$

and α_0 is obtained by solving equation (4.10) for a given reactive power Q_r absorbed by the reactor

$$2\alpha_0 - \sin 2\alpha_0 = 2\pi \left\{ 1 - \frac{Q_r X_T}{V_T^2} \right\} \quad (4.10)$$

The tie line, local load, controlled reactor and capacitor algebraic equations are:

$$\begin{aligned} e_d &= V_b \sin \delta - \frac{\omega}{\omega_0} X_e (i_q - i_{qL} - i_{rq} - i_{cq}) \\ e_q &= V_b \cos \delta + \frac{\omega}{\omega_0} X_e (i_d - i_{dL} - i_{rd} - i_{cd}) \end{aligned} \quad (4.11)$$

where compensator currents are:

$$\begin{aligned} i_{rd} &= \frac{\omega_0}{\omega} (1-C) \frac{e_q}{X_T}; \\ i_{rq} &= - \frac{\omega_0}{\omega} (1-C) \frac{e_d}{X_T}; \\ i_{cd} &= - \frac{\omega_0}{\omega} \frac{e_q}{X_C}; \\ i_{cq} &= \frac{\omega_0}{\omega} \frac{e_d}{X_C}; \end{aligned} \quad (4.12)$$

Compensator terminal voltage is:

$$V_T = \sqrt{e_d^2 + e_q^2} \quad (4.13)$$

From (4.11) and (4.12)

$$\begin{aligned} e_d &= V_b' \sin \delta - \frac{\omega}{\omega_0} X_e' (i_q - i_{qL}) \\ e_q &= V_b' \cos \delta + \frac{\omega}{\omega_0} X_e' (i_d - i_{dL}) \end{aligned} \quad (4.14)$$

where

$$V_b' = V_b / C', \quad X_e' = X_e / C'$$

and

$$C' = 1 + (1-C) \frac{X_e}{X_T} - \frac{X_e}{X_C} \quad (4.15)$$

4.3.3 Governor

For the investigation of all cases presented here a governor of 5 s time constant is used for the superconducting alternator, without any stabilizing signals, in order to establish effectively the damping action of the proposed scheme.

Equation (4.6) is therefore modified to

$$p\omega = \frac{\omega_0}{2H} \{T_m - T_e + \Delta T_m\} \quad (4.16)$$

where

$$p\Delta T_m = \frac{1}{\tau_h} \left\{ K_h \left(\frac{\omega - \omega_0}{\omega_0} \right) - \Delta T_m \right\} \quad (4.17)$$

4.3.4 Excitation Control for Field Forcing

For field forcing studies, a voltage regulator with an auxiliary stabilizing signal is considered as shown in Figure 4.3. Field voltage is therefore governed by the equation;

$$pV_f = \{V_{f_0} - V_f + K_e [(V_{ref} - V_T) + K_w (\omega - \omega_0)]\} / \tau_e \quad (4.18)$$

and in this case

$$C' = 1 - \frac{X_e}{X_c} \quad \text{in Eqn. (4.15)}$$

4.3.5 System Mathematical Model for Large Disturbances

By substituting e_d and e_q from Equation (4.14) and flux linkages from Equations (4.2 & 4.3) into machine equation (4.1) and neglecting the resistances and $p\psi_d$ and $p\psi_q$ terms, as is usual for such studies,⁸⁵ the flux linkage equations of the super conducting alternator system can be written as:

$$\begin{bmatrix} 0 \\ 0 \\ p\psi_f \\ p\psi_{sd} \\ p\psi_{pd} \\ p\psi_{sq} \\ p\psi_{pq} \end{bmatrix} = \begin{bmatrix} \omega(X_d + X'_e) & 0 & -\omega X_{md} & -\omega X_{md} & -\omega X_{md} & 0 & 0 \\ 0 & -\omega(X_q + X'_e) & 0 & 0 & 0 & \omega X_{mq} & \omega X_{mq} \\ 0 & 0 & -\frac{X_f}{\tau_f} & 0 & 0 & 0 & 0 \\ 0 & 0 & 0 & -\frac{X_s}{\tau_s} & 0 & 0 & 0 \\ 0 & 0 & 0 & 0 & -\frac{X_p}{\tau_p} & 0 & 0 \\ 0 & 0 & 0 & 0 & 0 & -\frac{X_s}{\tau_s} & 0 \\ 0 & 0 & 0 & 0 & 0 & 0 & -\frac{X_p}{\tau_p} \end{bmatrix} \begin{bmatrix} i_q \\ i_d \\ i_f \\ i_{sd} \\ i_{pd} \\ i_{sq} \\ i_{pq} \end{bmatrix} + \begin{bmatrix} \omega_0 V'_{bq} \\ \omega_0 V'_{bd} \\ \frac{V_f}{\tau_f} \\ 0 \\ 0 \\ 0 \\ 0 \end{bmatrix} \quad (4.19)$$

where,

$$V_f = e_f \left(\frac{X_{md}}{R_f} \right)$$

$$V'_{bd} = V'_b \sin \delta + \frac{\omega}{\omega_0} X'_e i_{qL} \quad (4.20)$$

$$\text{and } V'_{bq} = V'_b \cos \delta - \frac{\omega}{\omega_0} X'_e i_{dL}$$

Other differential equations of system components are given separately in Equations (4.5), (4.9), (4.16), (4.17) and (4.18).

For large disturbances, the system differential equations are solved simultaneously using the 4th order Runge-Kutta numerical technique to yield new values of machine rotor flux linkages, δ , ω , α or V_f and ΔT_m . Stator flux linkages are calculated by assuming:

$$\psi_d = \frac{\omega_0}{\omega} e_q \quad \text{and} \quad \psi_q = -\frac{\omega_0}{\omega} e_d \quad (4.21)$$

where terminal voltage components e_d and e_q are calculated from Equation (4.14) using the previous values of stator current.

New values of rotor currents are then calculated using the inverse of reactance matrices in Equations (4.2) and (4.3).

Equation (4.19) is used to obtain new values of stator current components. Machine electrical torque and terminal voltage are then computed using Equations (4.4) and (4.13) respectively.

4.3.5 Linearized Small Signal Model

The state equations of the above non-linear system are organized in the form:

$$\dot{x} = f(x) \quad (4.22)$$

which are then linearized about an operating point giving

$$\Delta \dot{x} = A \Delta x \quad (3.23)$$

The linearized state equation matrix A is given in Equation (4.25) and the state vector Δx is given by:

$$\Delta x = \{\Delta \delta \quad \Delta \omega \quad \Delta \Psi_f \quad \Delta \Psi_{sd} \quad \Delta \Psi_{pd} \quad \Delta \Psi_{sq} \quad \Delta \Psi_{pq} \quad \Delta T_m \quad \Delta y\}^T \quad (4.24)$$

where

$\Delta y = \Delta \alpha$ in the case of static compensator and

$\Delta y = \Delta V_f$ in the case of field forcing.

$$A = \begin{bmatrix}
 0 & 1 & 0 & 0 & 0 & 0 & 0 & 0 & 0 & 0 \\
 \frac{C_1 F_1 + C_2 B_1}{M} & \frac{C_1 F_3 + C_2 B_3}{M} & 0 & 0 & 0 & 0 & 0 & 0 & 0 & 0 \\
 0 & 0 & \left(-\frac{2B_4}{M} + \frac{\psi_q X_{md}}{X_s X_d^{ii} \tau_s}\right) & 0 & 0 & 0 & 0 & 0 & 0 & \frac{1}{M} \\
 0 & 0 & \frac{-X_f}{\tau_f(X_f - X_p)} & 0 & \frac{X_f}{\tau_f(X_f - X_p)} & 0 & 0 & 0 & 0 & 0 \\
 \frac{B_1 X_{md}}{X_d^{ii} \tau_s} & \frac{B_3 X_{md}}{X_d^{ii} \tau_s} & 0 & \frac{B_4 X_{md}}{X_d^{ii} \tau_s} - \frac{X_s}{\tau_s} & 0 & 0 & 0 & 0 & 0 & 0 \\
 0 & 0 & \frac{-X_p}{\tau_p(X_p - X_f)} & \frac{-X_p}{\tau_p(X_p - X_f)} & \frac{-X_p}{\tau_p(X_p - X_f)} & 0 & 0 & 0 & 0 & 0 \\
 \frac{X_{mq} F_1}{X_q^{ii} \tau_s} & \frac{X_{mq} F_3}{X_d^{ii} \tau_s} & 0 & 0 & 0 & 0 & 0 & 0 & 0 & 0 \\
 0 & 0 & 0 & 0 & 0 & 0 & 0 & 0 & 0 & 0 \\
 0 & -\frac{K_h}{\tau_h \omega_0} & 0 & 0 & 0 & 0 & 0 & 0 & 0 & 0 \\
 S_5 & S_6 & 0 & 0 & 0 & 0 & 0 & 0 & 0 & 0 \\
 & & & & & & & & & S_7 \\
 & & & & & & & & & S_8 \\
 & & & & & & & & & S_9
 \end{bmatrix} \quad (4.25)$$

where, $M = \frac{H}{2\omega_0}$

The constants of the small signal model contained in matrix A are,

$$B_1 = -\frac{V'_{bo}}{B_{11}} \sin \delta_o$$

$$B_2 = \frac{(V'_{bo} \cos \delta_o + X'_e i_{do})}{B_{11}} \frac{(1 - \cos 2\alpha_o)}{\pi} \frac{X'_e}{X_T}$$

$$B_3 = -\frac{(\psi_{do} - X'_e i_{do})}{B_{11}}$$

$$B_4 = \frac{X'_e X_{md}}{X_s X_d'' B_{11}}$$

where,

$$B_{11} = 1 + \frac{X'_e}{X_d''}$$

$$C_1 = \frac{\psi_{do}}{X_d''} + i_{do}$$

$$C_2 = -\left(\frac{\psi_{qo}}{X_d''} + i_{qo}\right)$$

$$F_1 = -\frac{V'_b \cos \delta_o}{F_{11}}$$

$$F_2 = -\frac{(V'_b \sin \delta_o - X'_e i_{qo})}{F_{11}} \left(\frac{1 - \cos 2\alpha_o}{\pi}\right) \left(\frac{X'_e}{X_T}\right)$$

$$F_3 = -\frac{(\psi_{qo} - X'_e i_{qo})}{F_{11} \omega_o}$$

$$F_4 = \frac{X'_e X_{md}}{F_{11} X_s X_q''}$$

where

$$F_{11} = 1 + \frac{X'_e}{X_q''}$$

$$D_1 = B_1 e'_{qo} - F_1 e'_{do}$$

$$D_2 = B_3 e'_{qo} - F_3 e'_{do} + \frac{(\psi_{do} e'_{qo} - \psi_{qo} e'_{do})}{\omega_o}$$

$$D_3 = B_4 e'_{qo}$$

$$D_4 = - F_4 e'_{do}$$

$$D_5 = B_2 e'_{qo} - F_2 e'_{do}$$

where,

$$e'_{do} = \frac{e_{do}}{V_{To}} ; e'_{qo} = \frac{e_{qo}}{V_{To}}$$

For thyristor controlled scheme;

$$S_1 = C_1 F_2 + C_2 B_2$$

$$S_2 = 0.0$$

$$S_3 = B_2 X_{md}/X_d'''$$

$$S_4 = F_2 X_{mq}/X_q'''$$

$$S_5 = - K_\alpha D_1 / \tau_\alpha$$

$$S_6 = - K_\alpha (D_2 - Kw) / \tau_\alpha$$

$$S_7 = - K_\alpha D_3 / \tau_\alpha$$

$$S_8 = - K_\alpha D_4 / \tau_\alpha$$

$$S_9 = - (K_\alpha D_5 + 1) / \tau_\alpha$$

For field forcing scheme;

$$S_1 = 0$$

$$S_2 = X_f / X_{md}$$

$$S_3 = S_4 = 0.0$$

$$S_5 = -K_e D_1 / \tau_e$$

$$S_6 = -K_e (D_2 - K_w) / \tau_e$$

$$S_7 = -K_e D_3 / \tau_e$$

$$S_8 = -K_e D_4 / \tau_e$$

$$S_9 = -1.0 / \tau_e$$

Also

$$B_2 = 0.0, F_2 = 0.0$$

4.3.7 System Parameters

The values of various system parameters considered in the studies are:

Alternator

$$X_d = 0.5, X'_d = 0.3, X''_d = 0.25, X'''_d = 0.15, \text{all in p.u.}$$

$$\tau_f = 300, \tau_{pd} = \tau_{pq} = 2.0, \tau_{sd} = \tau_{sq} = 0.5, \text{all in s.}$$

$$H = 3.0 \text{ s}$$

$$V_{ref} = V_{T0} = 1.0$$

$$X_q = X_d, X'_q = X'_d, X''_q = X''_d \text{ and } X'''_q = X'''_d$$

Transformer

$$x_{tr} = 0.15 \text{ p.u.}$$

Transmission Line

$$x_{tL} = 0.216 \text{ p.u.}$$

$$x_e = x_{tr} + x_{tL} = 0.366$$

Thyristor controlled Reactor

$$X_T = 1.8 \text{ or } 0.2 \text{ p.u.,}$$

$$\tau_\alpha = 0.05\text{s}, K_\alpha = 20.0$$

Biasing Capacitor

$$X_C = 2 \text{ or } 4 \text{ p.u.}$$

Governor

$$K_h = 20.0, \tau_h = 5.0\text{s}$$

Voltage Regulator (for field forcing)

$$K_e = 600.0, \tau_e = 0.05\text{s}$$

4.4 Load Rejection Study

In this study the machine is assumed to be operating, under normal operating conditions, at given values of real and reactive power with a local load at its terminals. A load rejection is simulated by setting components of load current to zero.

A sudden loss of a lagging power factor load of $(0.6 + j0.7)$ p.u. at the generator terminals has been simulated for the case when the generator was overexcited $(0.8 + j0.8)$ p.u. The resulting overvoltages of this severe condition, as shown in Figure 4.4, is characterized by

an almost instantaneous rise at the instant of load rejection followed by a more gradual rise.⁴⁵⁻⁴⁷ By using conventional field forcing techniques⁸⁴⁻⁸⁶ (either with a limited ceiling voltage of ± 20.0 p.u. or unlimited ceiling voltage) it takes more than 4.0 seconds to damp voltage oscillations and to bring terminal voltage deviation close to 3%. However, the thyristor controlled reactor brings down the terminal voltage to its initial rms value of 1.0 p.u. from the dynamic overvoltage value of 1.12 p.u. within a time less than 0.2 seconds. If a constant field voltage, with no voltage regulation, is assumed, the terminal voltage in this case stays at a steady value of 1.10 p.u.

Figures 4.5, 4.6 and 4.7 show, respectively, the dynamic response of the generator with regard to speed deviation $\Delta\omega$ rad/sec, p.u. field voltage V_f and the p.u. reactive power Q_r of the thyristor controlled reactor. From Figure 4.5 it is observed that there is hardly any difference in the rotor speed deviation for all cases without a static compensator, while there is an improvement in the response when the thyristor controller is provided with a supplementary stabilizing signal ($K_w = 0.1$).

4.5 Small Signal Dynamic Stability

Two basic cases are examined for the stability performance of the superconducting alternator:

- (1) Employing Field forcing,⁸⁴⁻⁸⁸ and
- (2) Employing a static compensator at the terminals.⁹⁰ The case of an alternator with neither control, that is operating on constant field voltage, is trivial and hence not considered any further. For both

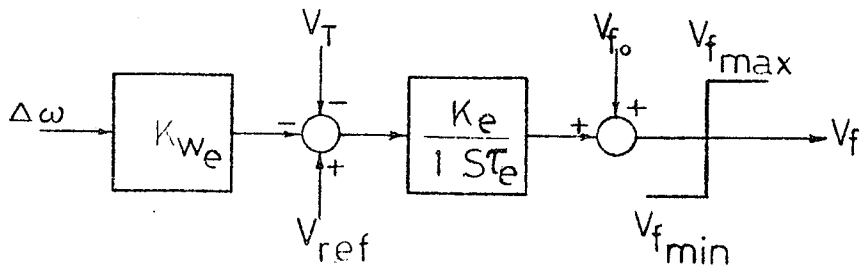


Figure 4.3 Voltage regulator for field forcing

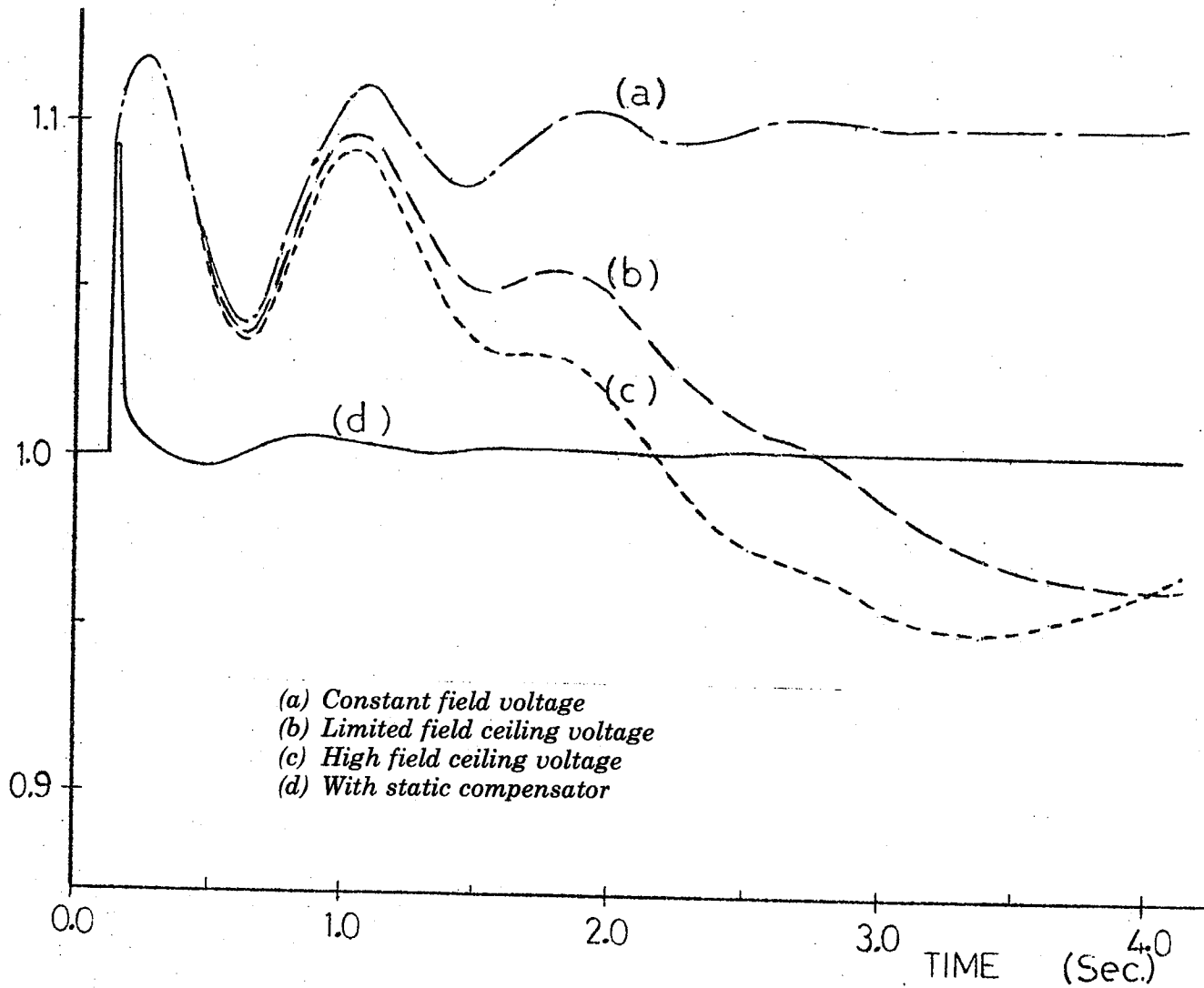


Figure 4.4 Terminal voltage response following load rejection

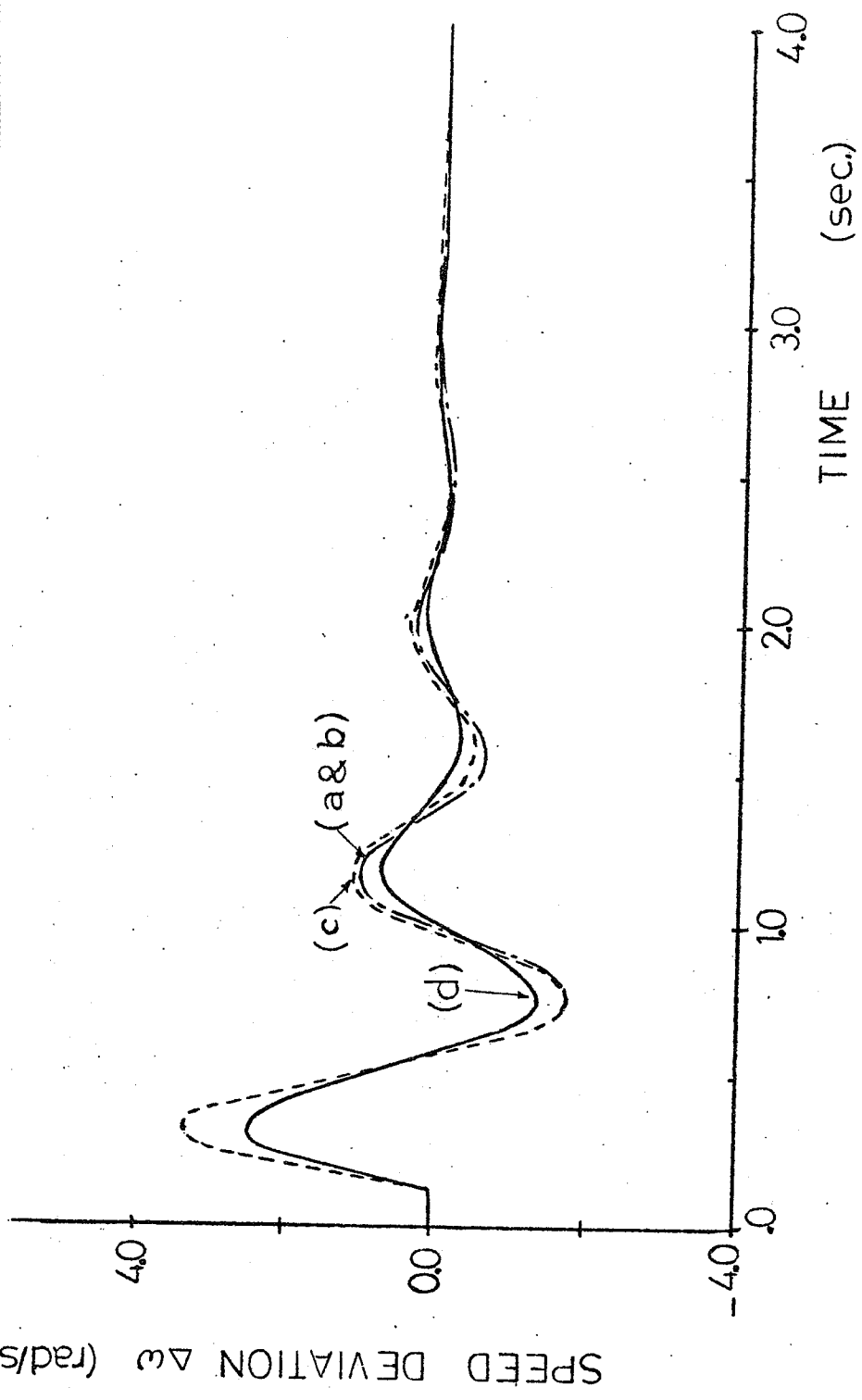


Figure 4.5 Machine rotor speed deviation following load rejection

- (a) Constant field voltage
- (b) Limited field ceiling voltage
- (c) High field ceiling voltage
- (d) With static compensator

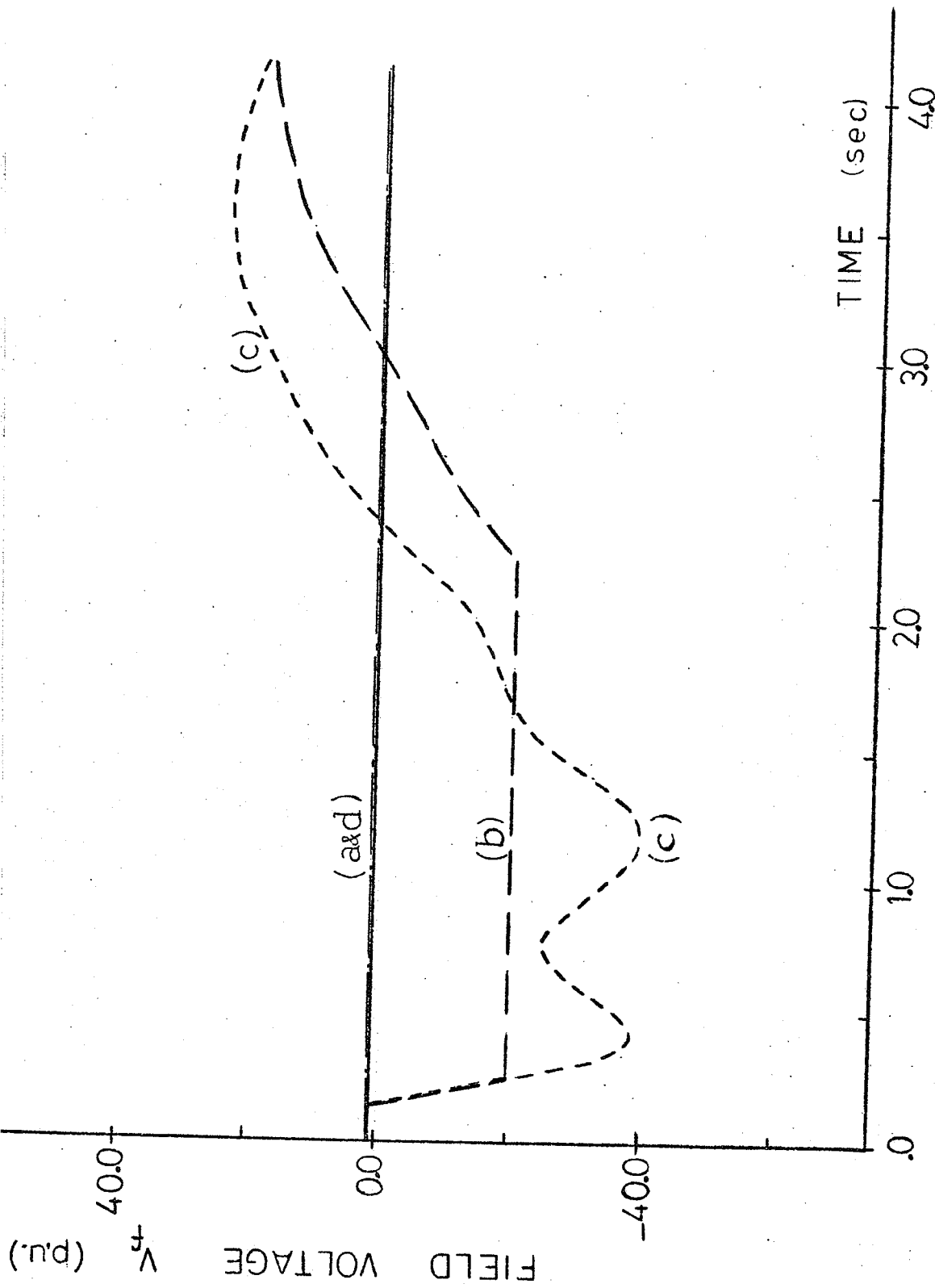


Figure 4.6 Field voltage response for various control methods

- (a) Constant field voltage
- (b) Limited field ceiling voltage
- (c) High field ceiling voltage
- (d) With static compensator

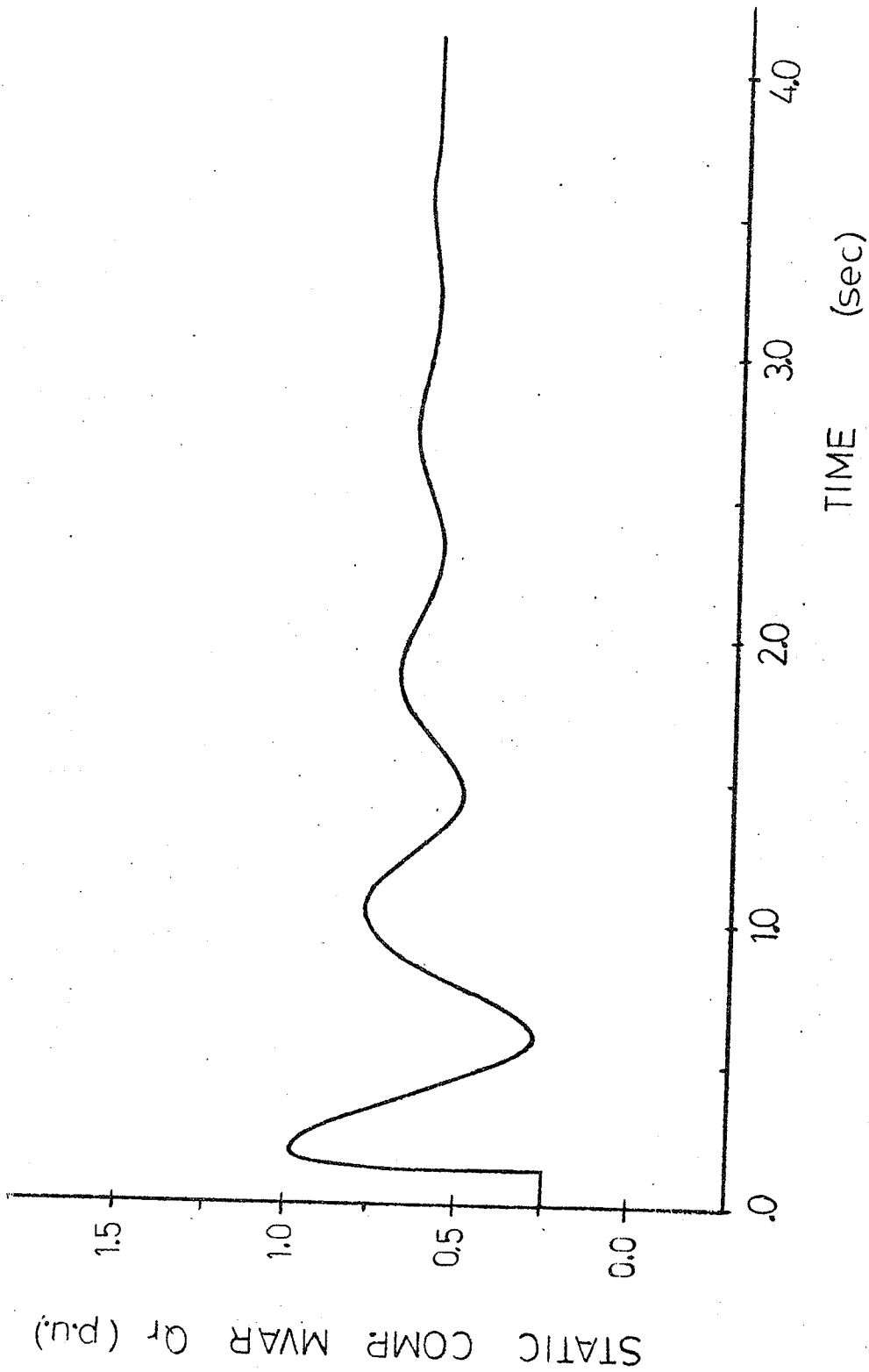


Figure 4.7 Reactive power absorbed by the static compensator

above modes of operation, cases are examined when a stabilizing signal is and is not employed. The level of stabilizing signal used in the study has not been optimized because the prime concern here is to evaluate, on a comparative basis, the superiority of an operating mode. However, in some results influence of the changes in the stabilizing signal gain is demonstrated.

The eigenvalues of Matrix A (Equation 4.25) are calculated for certain system parameters at the particular operating point. Figures 4.8 and 4.9 show the dominant eigenvalues (with positive imaginary part) in the complex S-plane for a variety of combinations of the time constants of the screening (primary) and damping (secondary) shields. The results of Figures 4.8 (a) and 4.9 (a) show clearly that when no stabilizing signal is used regions of distinct instability exist for very high values of τ_s , as well as for combinations of very low values of τ_s with very high values of τ_p . These extremes have to be avoided. Comparing these results with Figures 4.8 (b) and 4.9 (b) show a general improvement in the dynamic stability.

The results of Figures 4.8 and 4.9 are for a lagging load condition of $0.8 + j0.6$ p.u. on the generator. It has been found that the eigenvalues are not highly sensitive to variations in the reactive power loading.

Figures 4.10 (a) and 4.10 (b) have been drawn to show quite clearly the damping effect of the application of a static compensator. The results in form are similar to those presented by Lawrenson et al⁸⁷ and should be useful for the designer of the alternator while choosing the time constants of the shields. If a static compensator is to be

employed at the terminals of the alternator a considerable flexibility in choosing the time constants of the shields exists especially considering the required damping. This may assist greatly in incorporating good screening. A comparison of Figures 4.10 (b) and 4.10 (c) shows that by increasing the gain (K_w) of the stabilizing signal a significant improvement is not likely to continue indefinitely with the increasing values of K_w .

Figures 4.11 show the dynamic response ($\Delta\omega$ vs time) predicted by the results of small signal analysis for a step change of 0.04 rad in the machine load angle (δ). In Figure 4.11 (a) the time constants of the shields ($\tau_p = 0.5$ s, $\tau_s = 0.2$ s) are chosen in a feasible range providing near maximum damping associated with reasonably good screening. Comparisons of traces 1 with 2 and 3 with 4 show clearly the influence of additional damping signal for each of the two — namely field forcing and external static compensator controls. Comparison of trace 2 with 3 shows that with the same level of stabilizing signal static compensator provides better damping and a higher frequency of oscillation thereby ensuring that the oscillation disappear faster.

Since for load rejection results screen time constant of $\tau_p = 2.0$ s and $\tau_s = 0.5$ s were used comparisons such as offered by the results of Figure 4.11 (a) are made in Figure 4.11 (b). The influence of the size of static compensator was also studied by choosing different values of X_T . As would be expected it was confirmed that a higher compensator rating would be more effective in enhancing the stability. The size of the compensator is therefore a case for an optimization study, influenced by inherent damping available from the alternator, desired system damping and the compensator cost.

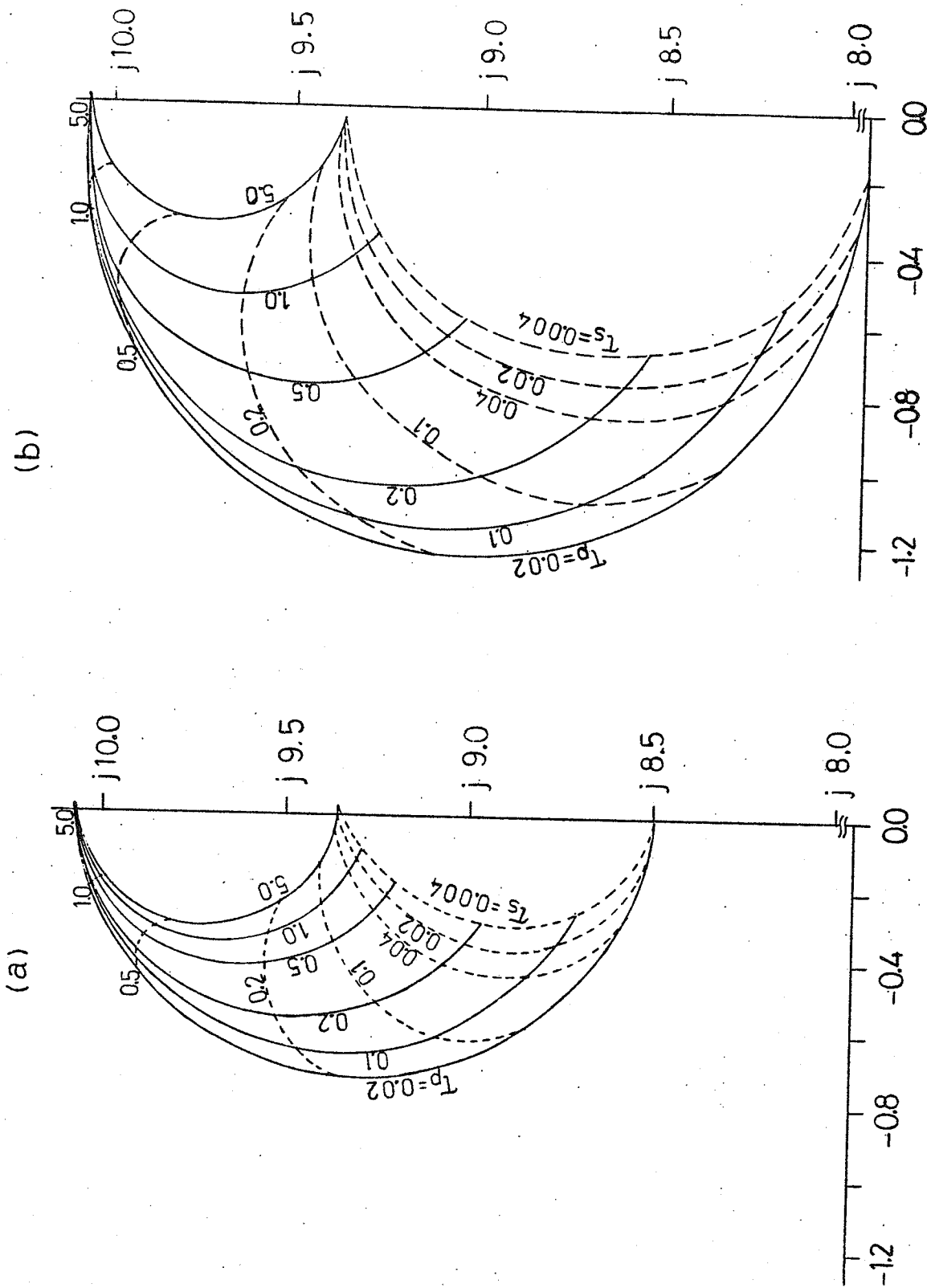


Figure 4.8 Dominant eigenvalues in τ_p and τ_s with field forcing:
 (a) for stabilizer gain $K_{we} = 0.0$
 (b) for stabilizer gain $K_{we} = 0.1$

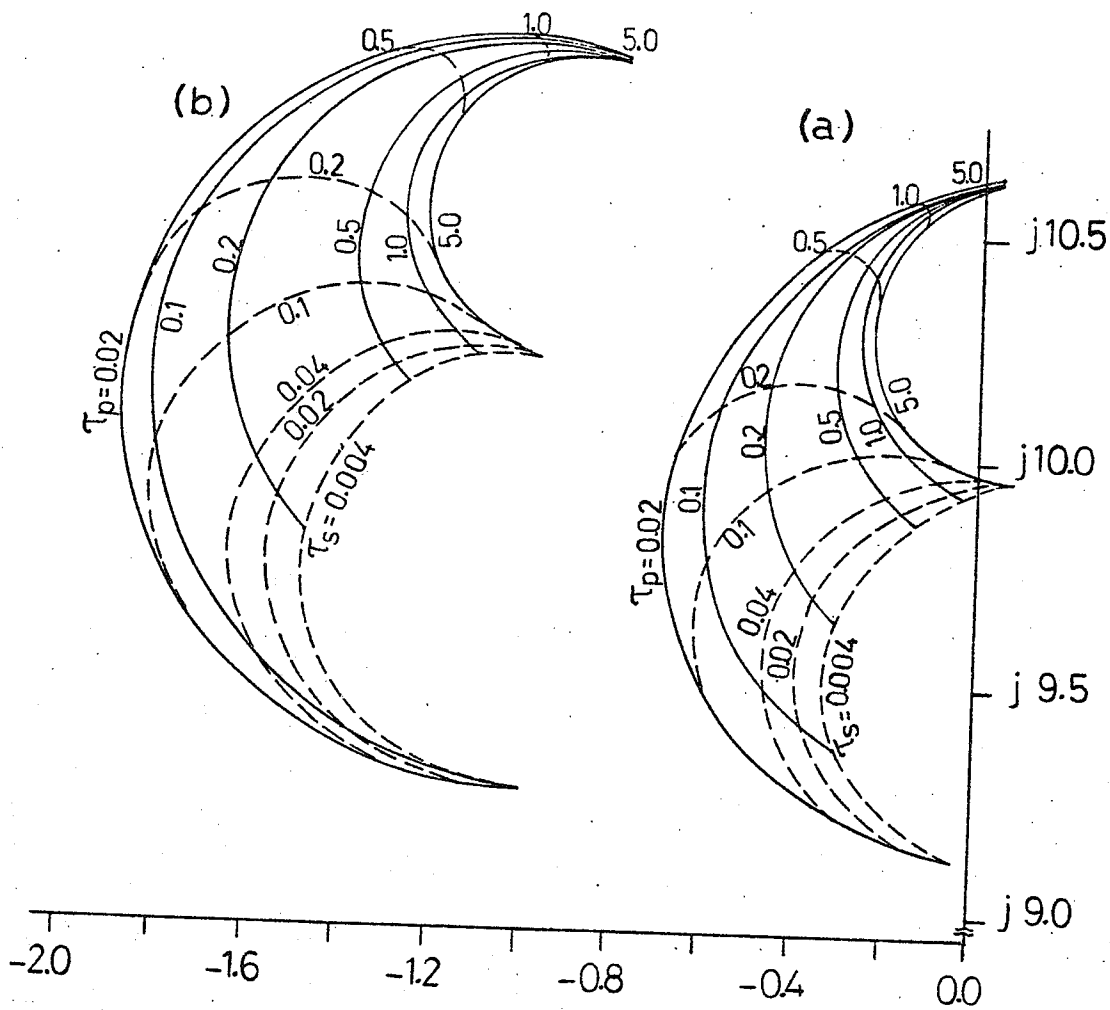


Figure 4.9 System dominant eigenvalues for variations in τ_p and τ_s with static compensator:
 (a) for stabilizer gain $K_w = 0.0$
 (b) for stabilizer gain $K_w = 0.1$

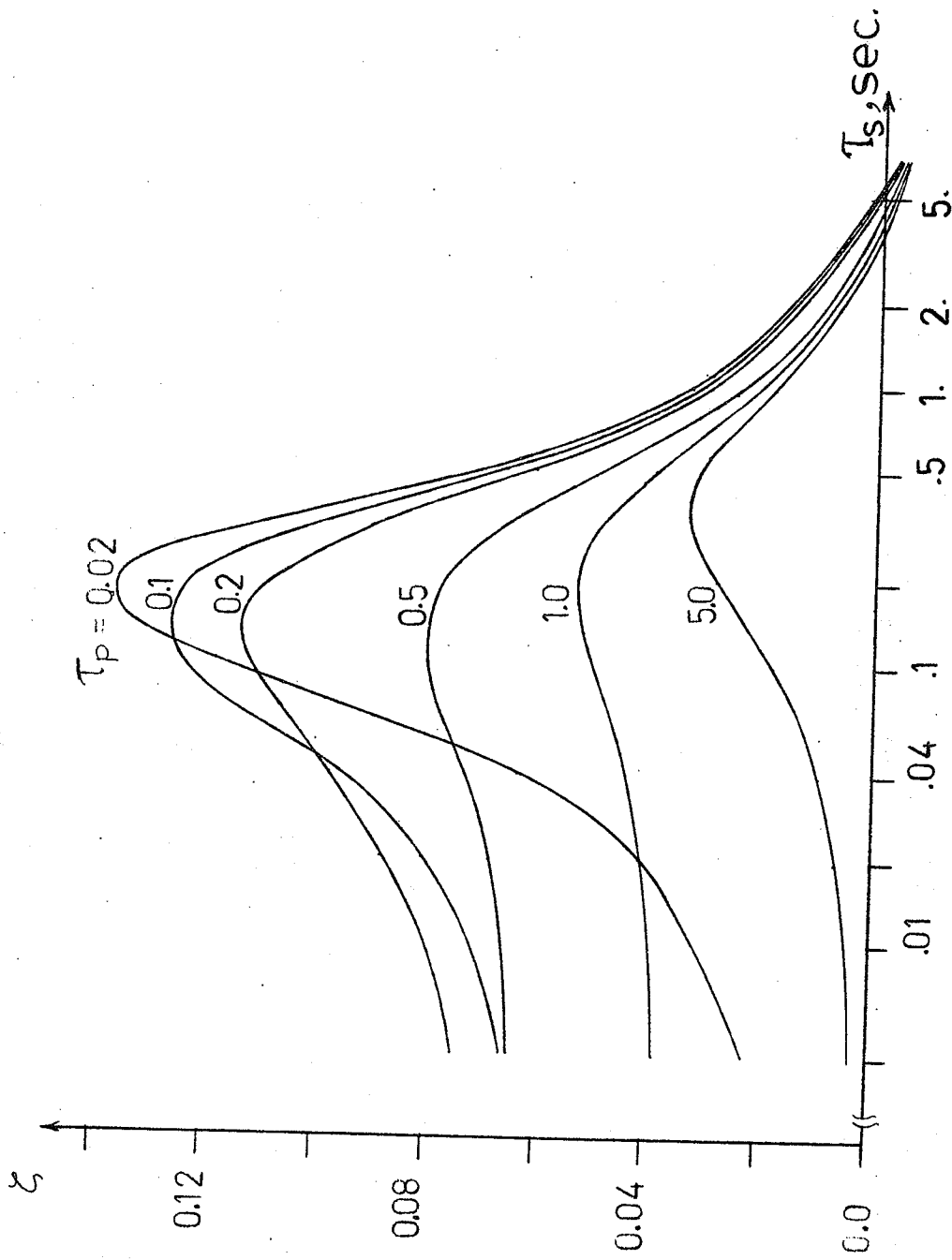


Figure 4.10 System damping with:
 (a) Field forcing, $K_{we} = 0.1$

$$\zeta = \tan^{-1} (\text{Real/Imaginary components of dominant eigenvalue})$$

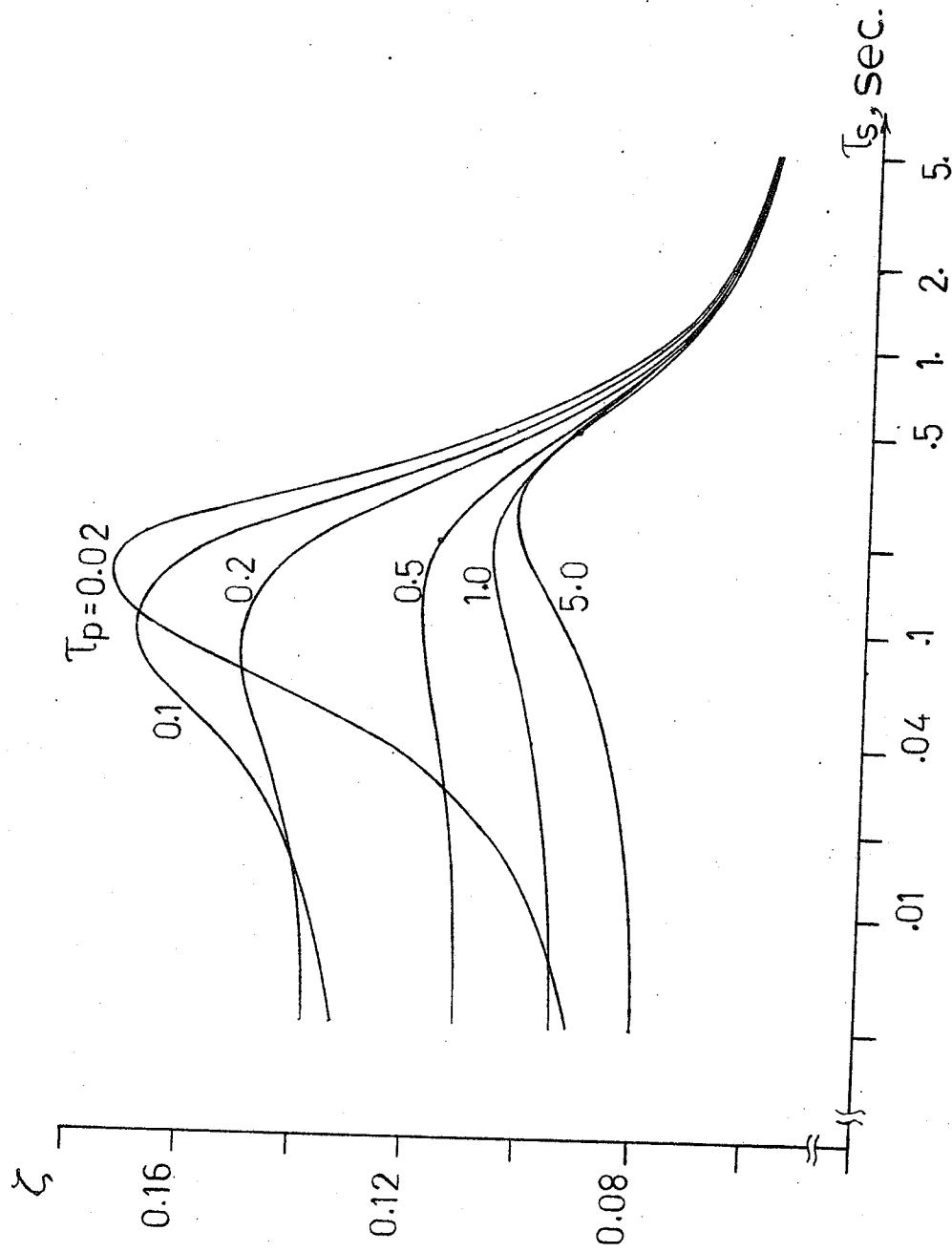


Figure 4.10 System damping with:

(b) Static compensator, $K_w = 0.1$

$\zeta = \tan^{-1}(\text{Real/Imaginary components of dominant eigenvalue})$

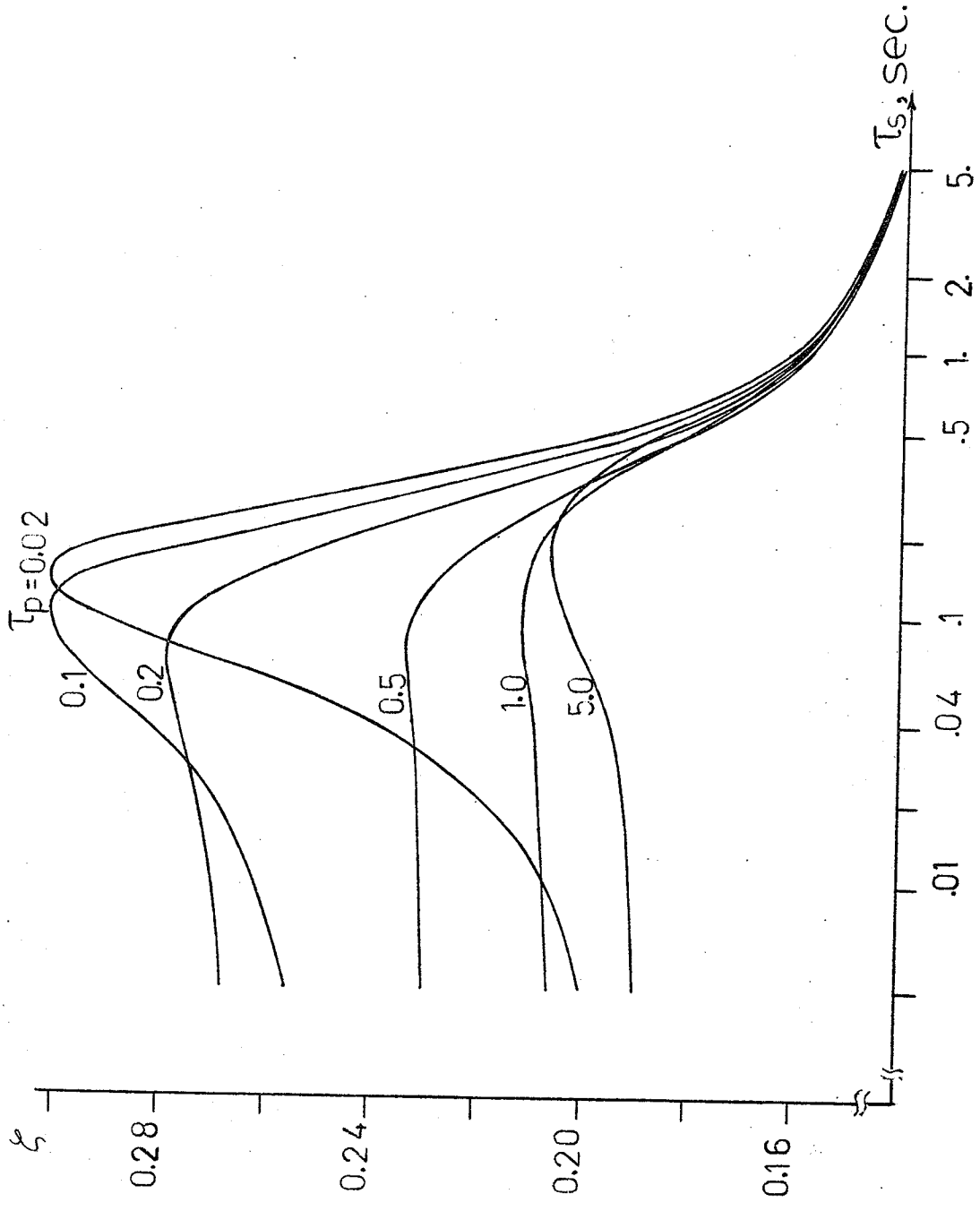


Figure 4.10 System damping with:

(c) Static compensator, $K_w = 0.2$

$\zeta = \tan^{-1}$ (Real/Imaginary components of dominant eigenvalue)

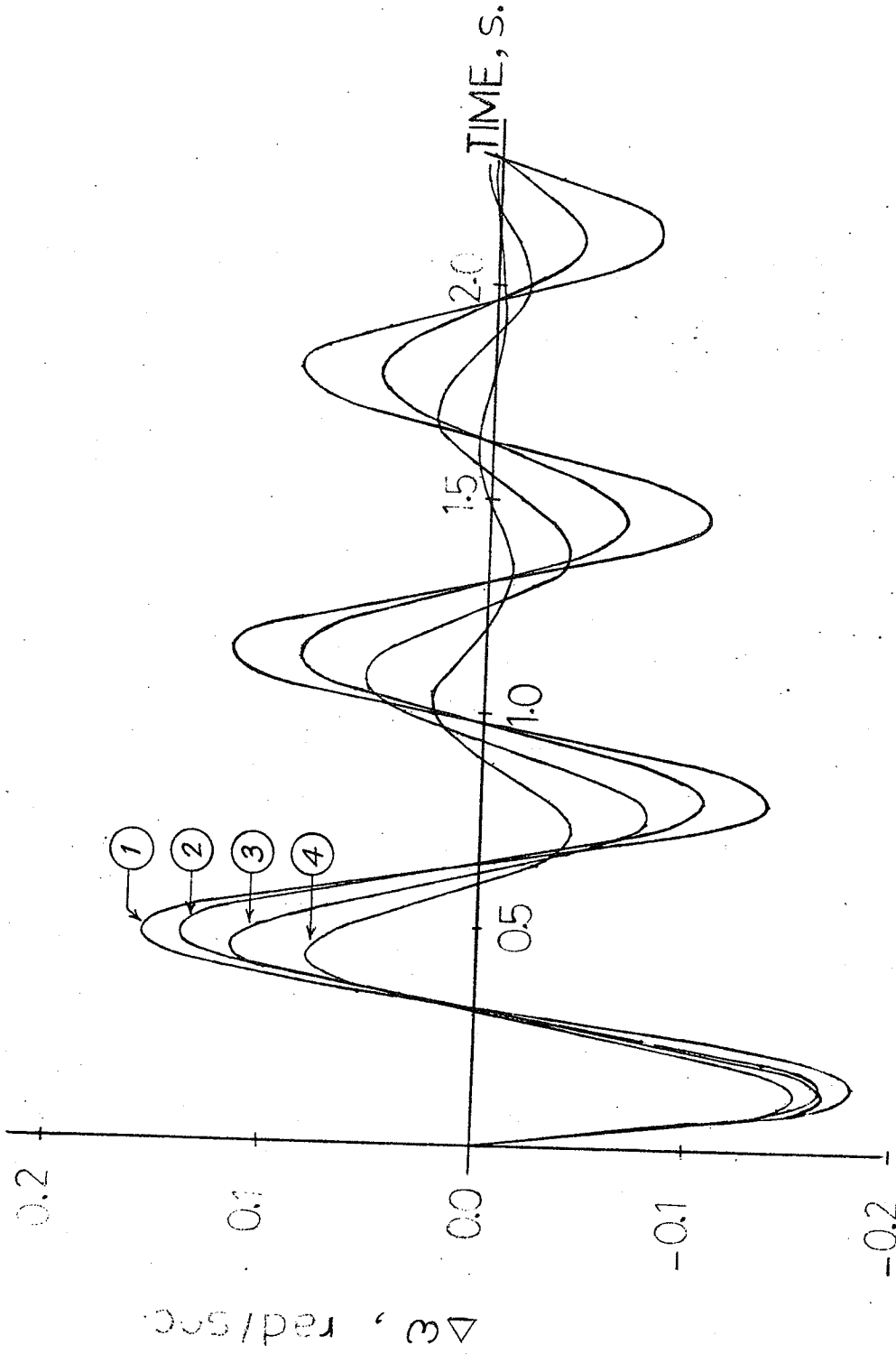


Figure 4.11 Small signal dynamic response for:
 (a) $\tau_p = 0.5$, $\tau_s = 0.2$

- (1) Field forcing, $K_{we} = 0.0$
- (2) Field forcing, $K_{we} = 0.1$
- (3) Static compensator, $K_w = 0.1$
- (4) Static compensator, $K_w = 0.2$
- (5) Field forcing, $K_{we} = 0.2$

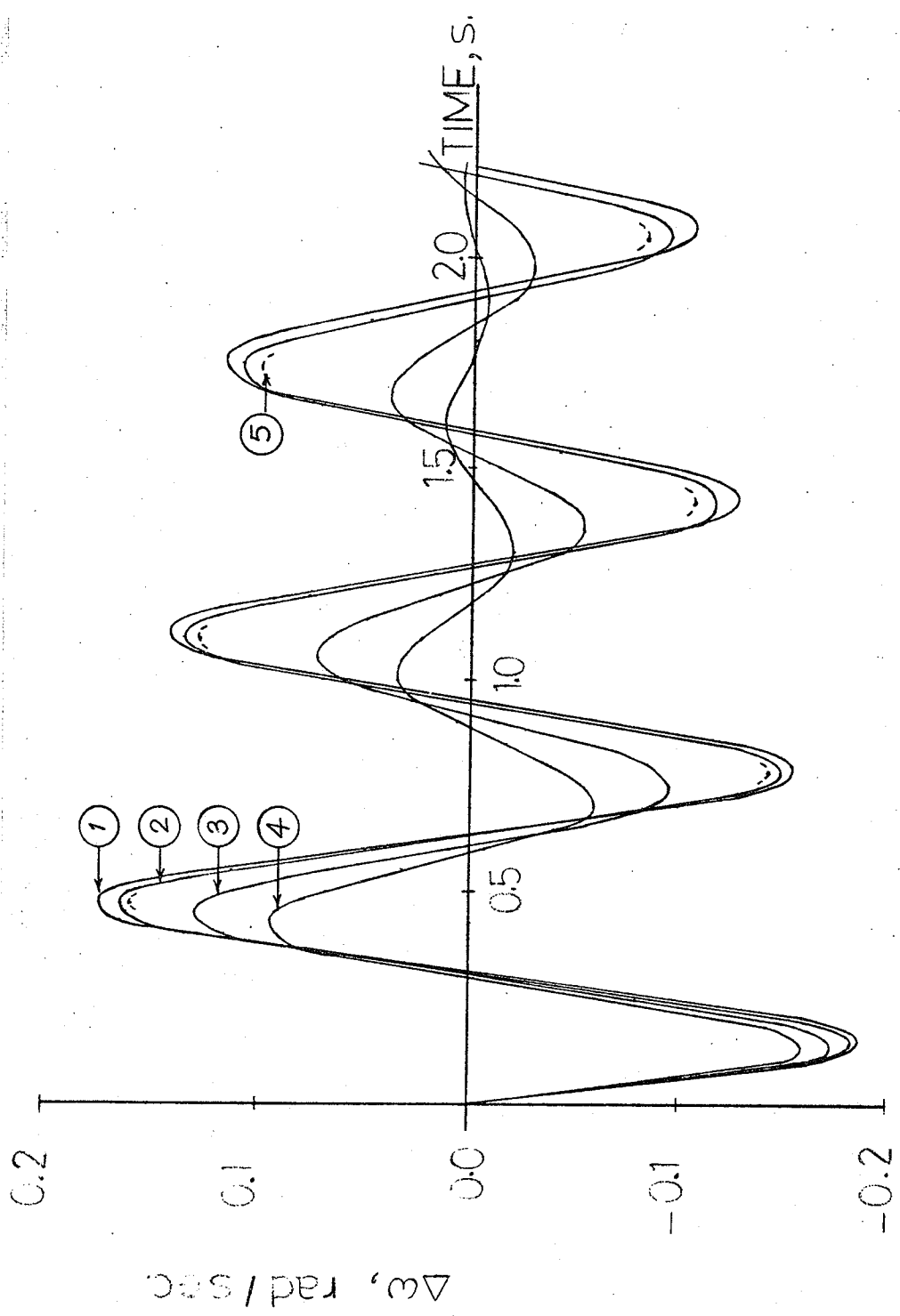


Figure 4.11 Small signal dynamic response for:

(b) $\tau_p = 2.0, \tau_s = 0.5$

- (1) Field forcing, $K_{we} = 0.0$
- (2) Field forcing, $K_{we} = 0.1$
- (3) Static compensator, $K_w = 0.1$
- (4) Static compensator, $K_w = 0.2$
- (5) Field forcing, $K_{we} = 0.2$

4.6 Large Signal Transient Stability

For the transient stability study of the superconducting alternator a 3-phase fault was applied at the sending end of the transmission line. In order to have an adequate severity of the disturbance the fault was cleared after 0.10 s. In this section only the results for a lagging p.f. transmitted power of $(0.8 + j0.6)$ prior to the fault, are presented. For these results screen time constants of $\tau_p = 2.0$ s and $\tau_s = 0.5$ s are used.

Figure 4.12 shows the variation of rotor angle δ with time for a number of operating conditions. It is to be noted that field forcing alone provides a very poor damping and when a stabilizing signal is incorporated in the excitation system the excursions in the field current are rather high (Figure 4.13) with the possibility of unacceptable values of di_f/dt . In comparison when a static compensator is employed at the terminals of the alternator with the same stabilizing signal, damping is far superior with or without the application of a capacitor in parallel with the controlled reactor. Figure 4.14 shows the total p.u. MVar supplied by the compensator. The capacitor rating if chosen comparable to the reactor, as in one set of results ($X_c = 2$ p.u., $X_T = 1.8$ p.u.), permits reactive power variation in principally positive (capacitive) direction as compared to only negative (inductive) obtained without the capacitor. None of these options are optimum. By choosing $X_c = 4.0$ p.u. reactive power variation in both directions, almost equally, is possible. Since in this case a limited size of static compensator is chosen, which is reasonable from cost considerations, the compensator operates in a bang-bang mode. Figure 4.12 also shows a highly damped performance when

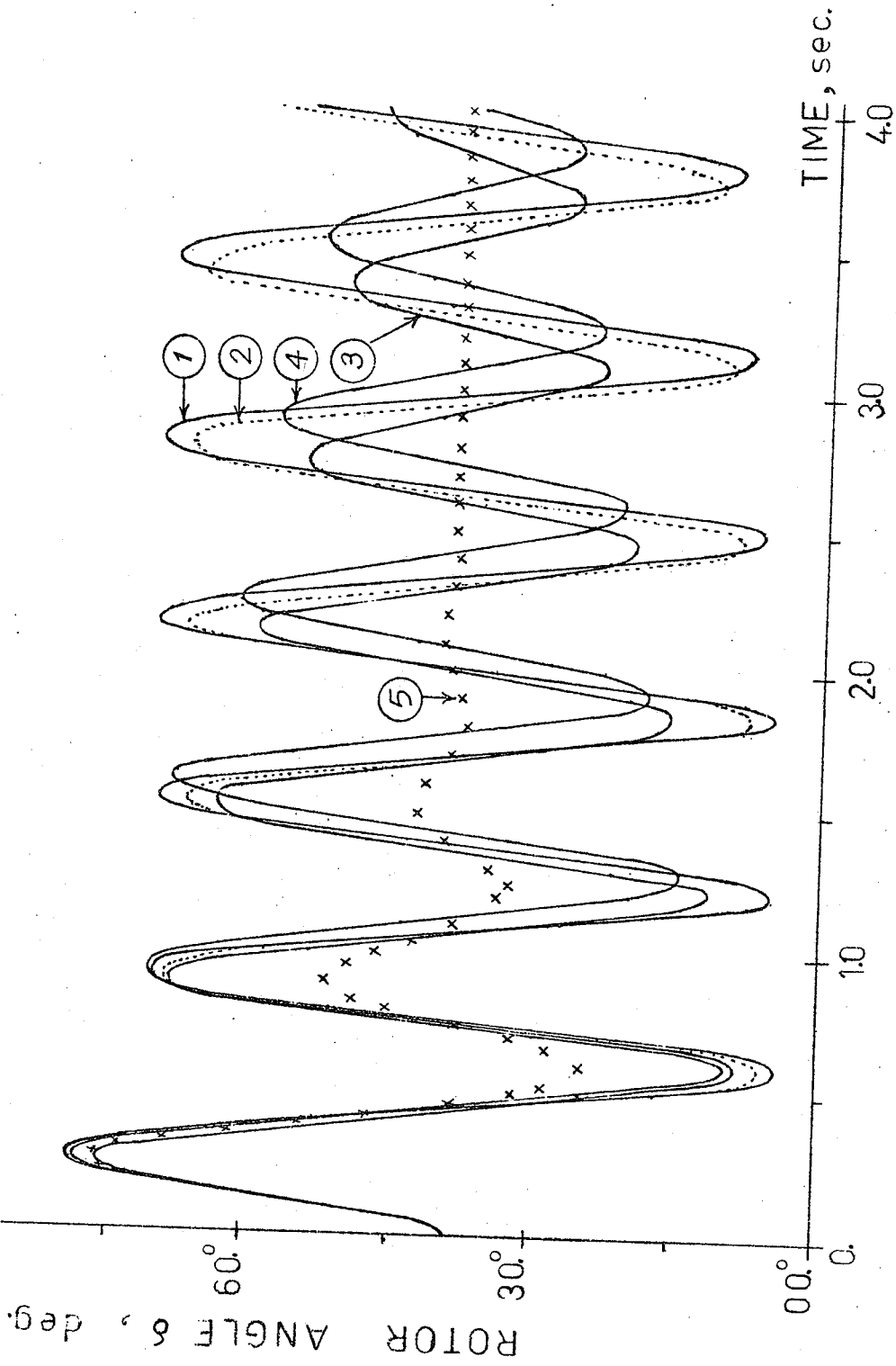


Figure 4.12 Variation in rotor angle for 3-phase fault,
 $\tau_p = 2.0$, $\tau_s = 0.5$

- (1) Field forcing, $K_{we} = 0.0$
- (2) Field forcing, $K_{we} = 0.1$
- (3) Static compensator, $K_w = 0.1$ with parallel capacitor
- (4) Static compensator, $K_w = 0.1$ without capacitor
- (5) Static compensator, $X_T = 0.2$ with capacitor

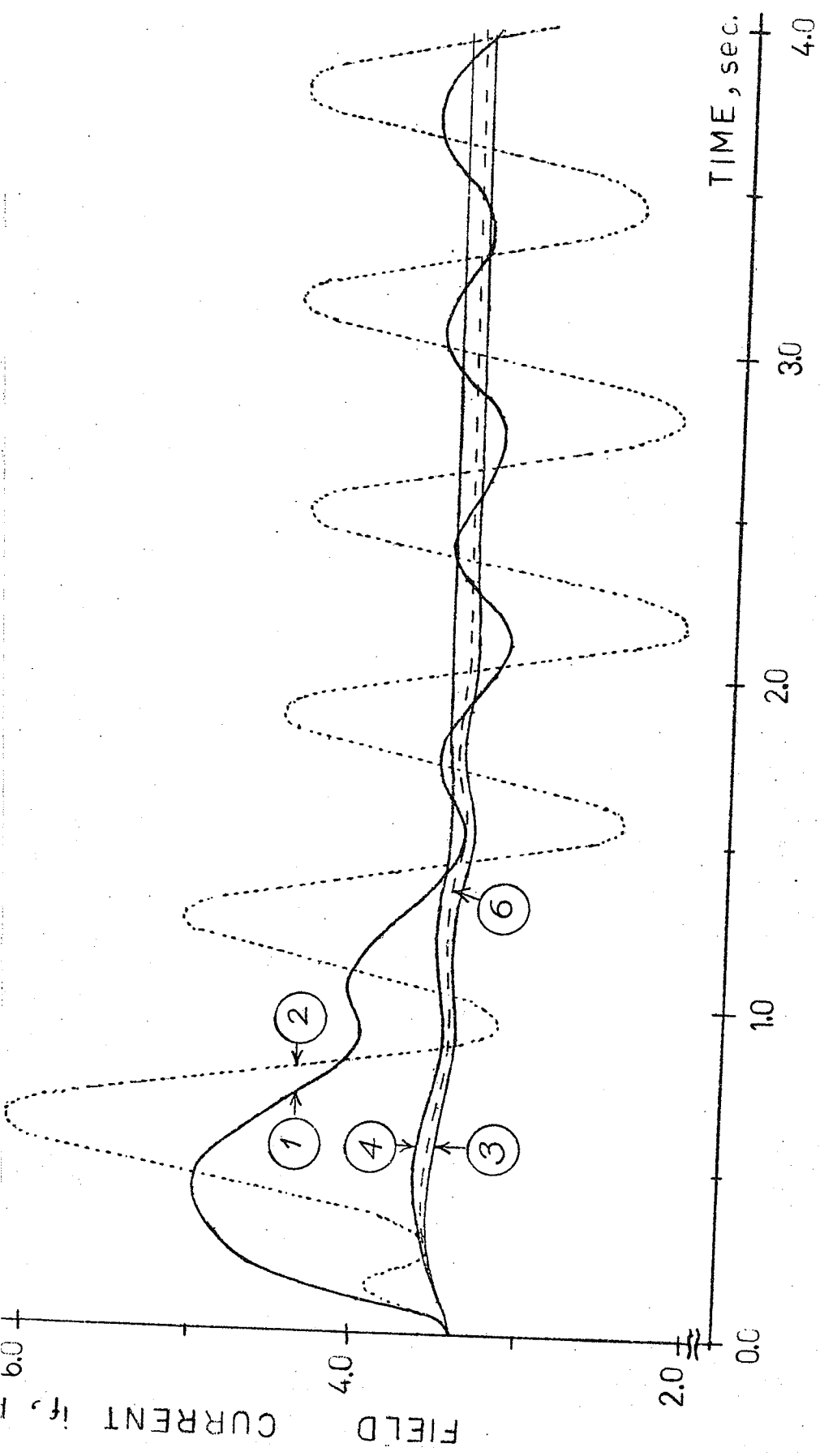


Figure 4.13 Variation of field current for 3-phase fault

- (1) Field forcing, $K_{we} = 0.0$
- (2) Field forcing, $K_{we} = 0.1$
- (3) Static compensator, $K_w = 0.1$ with parallel capacitor
- (4) Static compensator, $K_w = 0.1$ without capacitor
- (5) Static compensator, $X_T = 0.2$ with capacitor
- (6) Static compensator, $K_w = 0.1$, $X_c = 4.0$

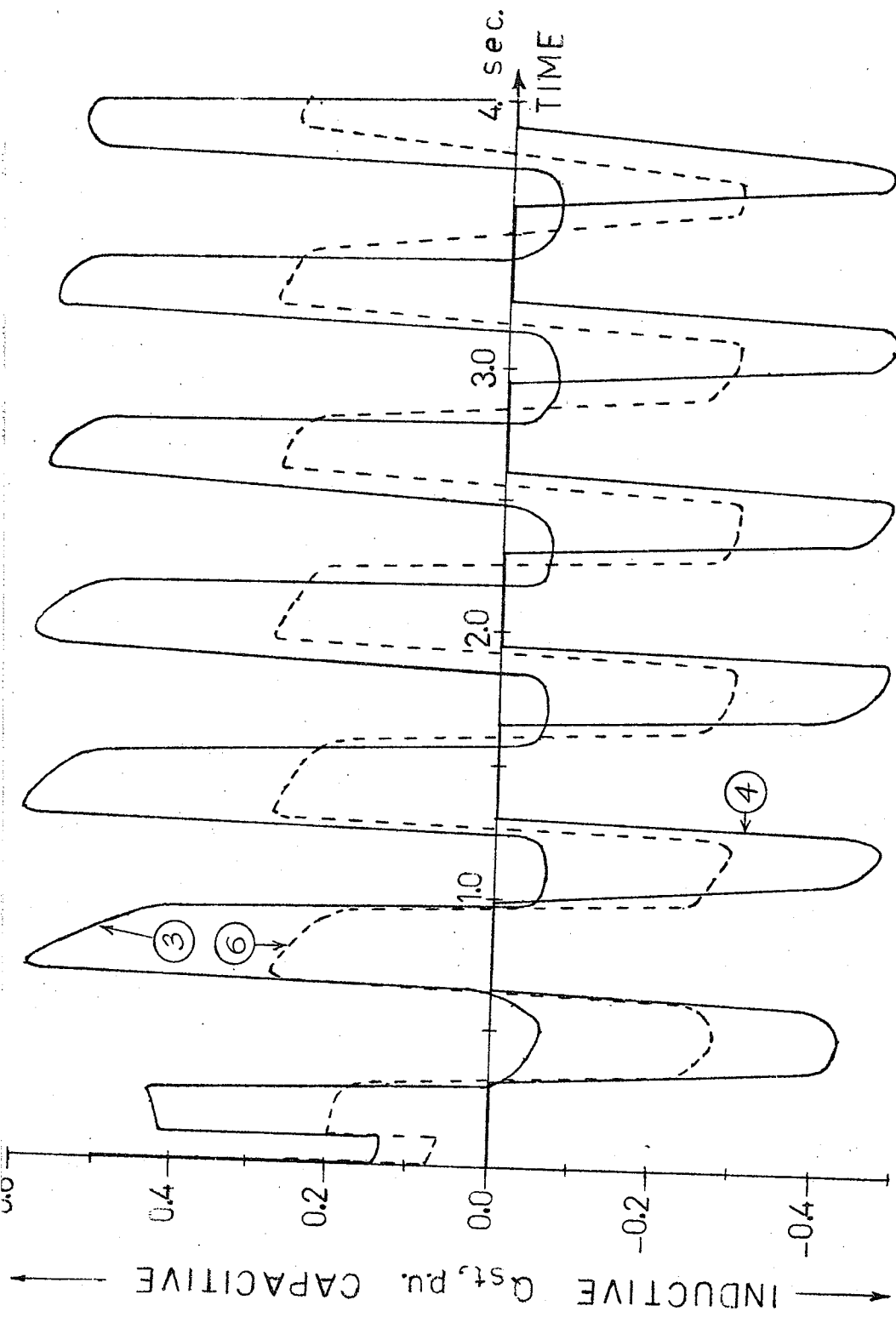


Figure 4.14 Variation in the total reactive power of the compensator

- (3) Static compensator, $K_w = 0.1$ with parallel capacitor
- (4) Static compensator, $K_w = 0.1$ without capacitor
- (5) Static compensator, $X_T = 0.2$ with capacitor
- (6) Static compensator, $K_w = 0.1$, $X_c = 4.0$

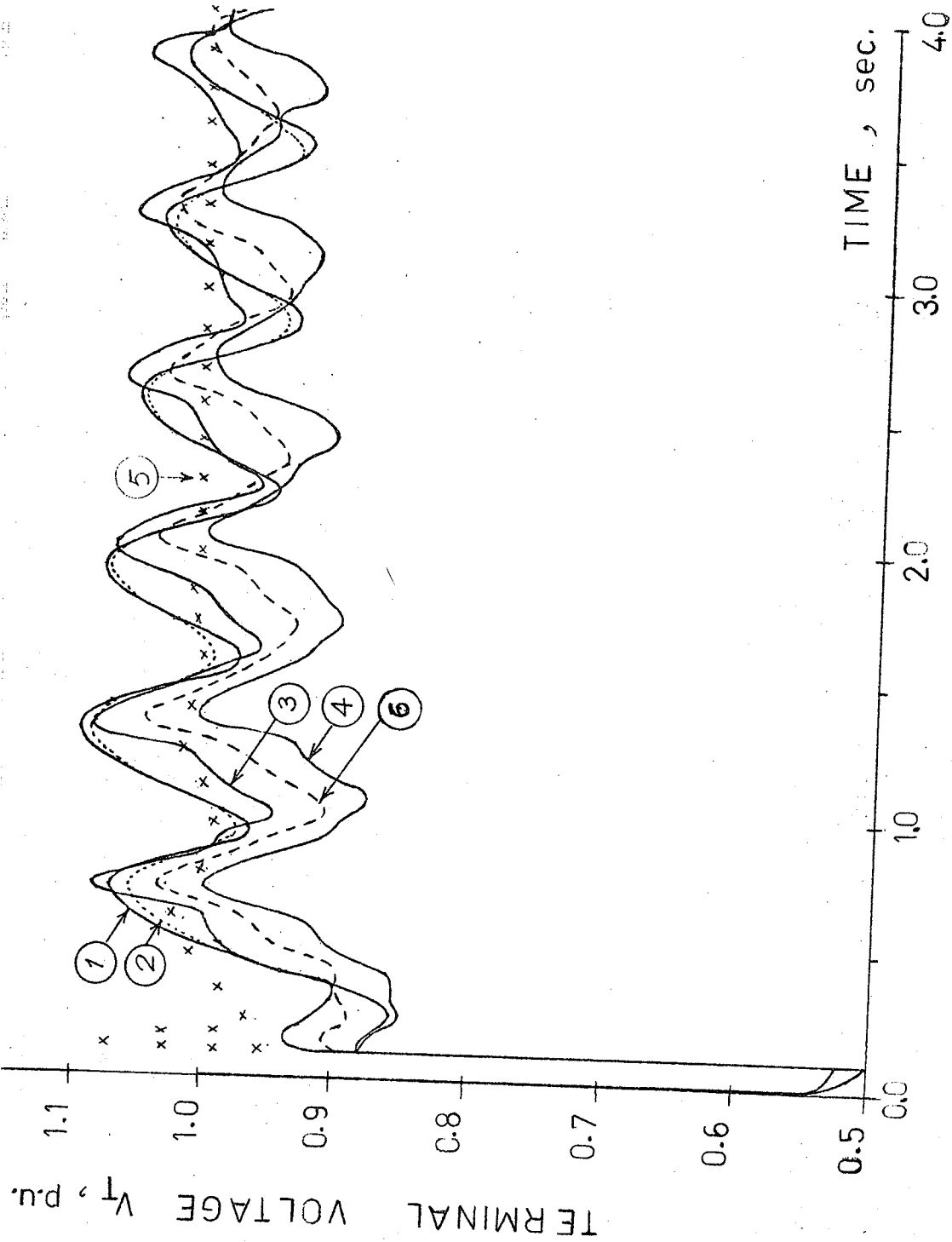


Figure 4.15 Variation in the generator terminal voltage

- (1) Field forcing, $K_{we} = 0.0$
- (2) Field forcing, $K_{we} = 0.1$
- (3) Static compensator, $K_w = 0.1$ with parallel capacitor
- (4) Static compensator, $K_w = 0.1$ without capacitor
- (5) Static compensator, $X_T = 0.2$ with capacitor
- (6) Static compensator, $K_w = 0.1$, $X_c = 4.0$

a very large compensator is used which may be hard to justify on economic grounds.

Figure 4.15 is included to show the influence on terminal voltage during and subsequent to the fault. Examine the case, where a controlled reactor is employed ($X_T = 1.8$) but without a shunt capacitor. The voltage variation is least in this case because the compensator now provides the highest level of reactive power absorption capability. Other results can be easily interpreted in a similar way.

4.7. Conclusions

- (1) Application of a thyristor controlled reactor VAR compensator at the terminals of a superconducting alternator provides an attractive alternative to the field forcing technique which must otherwise be employed to control its dynamic performance.
- (2) Auxiliary stabilizing signals can be easily incorporated in the static compensator control circuit which greatly improve the damping and stabilizing aspects of the alternator performance.
- (3) Static compensators provide an external control and damping for the superconducting alternator and hence permit a greater freedom in the inherent design by allowing, for example, a better screening at the cost of a poorer damping.
- (4) Field forcing technique provides basically an internal control and therefore may interfere with the screening requirement and may thus have to be constrained.
- (5) Since the suitability of static compensators at the terminals of superconducting alternators has been shown for controlling voltage

during load rejection as well it appears to offer an overall good engineering solution.

- (6) When the rating of the static VAr compensator is limited to a smaller value (for economic considerations) it operates primarily in bang-bang control mode and therefore in place of a continuous controller a switching controller with fixed inductor and capacitor component is feasible.

chapter five

MAJOR CONTRIBUTIONS

The major contributions achieved in this thesis are as follows:

1. A general concept for thyristor phase controlled reactors is developed which provides a whole new range of attractive alternatives to the existing designs. The novelty of the proposed design arises from the considerable savings that can be achieved on account of ;
 - (a) reduction of harmonics generated,
 - (b) possibility of completely avoiding the need for many harmonic filters, and
 - (c) reduction of thyristor valves overcurrent stresses due to transient overvoltages.
2. A general analysis is developed and simple algebraic expressions are obtained for the currents and voltages of various components of thyristor phase controlled reactors under different operating values of control angle α .
3. The feasibility of using static methods for reactive power control (thyristor controlled reactors or dc converter control) is demonstrated to enhance the performance of a weak ac system connected to a HVDC terminal.
4. The application of a thyristor controlled reactor at the terminals of a superconducting generator is proposed and fully analysed.
5. A large scale load flow and transient stability digital program is developed with unique features for simulation of multiterminal HVDC schemes and static VAR compensators and for ac/dc network solution.

Suggestions for Future Work

1. Studying the influence of copper losses and non-characteristic harmonics generation, of the proposed thyristor controlled reactor, on the selection of an optimum design.
2. Investigating the feasibility of using an economical bang-bang VAR controller at the terminals of a HVDC converter or a superconducting generator.
3. Expansion of the transient stability program to include the sub-transient response of a HVDC scheme (of any configuration) under various dc fault conditions.

Appendix A

POWER SYSTEM DIGITAL SIMULATION PROGRAM

(A Load Flow and Transient Stability Program for Power Systems with Multi-Terminal HVDC Schemes and Static VAr Compensators)

A.1 General

Because of the economic and technical advantages offered by HVDC and static VAr compensation facilities in the future expansion of power systems, their adequate representation, besides other normally used components, in load flow and transient stability programs is of great value.

In all available transient stability programs, the solution of HVDC networks - usually limited to two terminal schemes - is performed alternately with the ac system solution.^{91,92} However, such a method does not guarantee, in some critical cases, the convergence of the overall system solution. The reason behind this is that the solution is dependent upon system conditions, i.e. a large number of iterations would be expected for solution of a weak ac system under or post fault conditions. A non converged solution can occur when the system is marginally stable.

Two methods of solution techniques can overcome this problem. A direct inclusion of HVDC schemes model into the ac system equations to form a combined Newton's ac/dc solution is one method.⁸⁰ The other is a direct solution of the ac system with the HVDC schemes treated as non-linear loads at their ac/dc interconnecting points.

Both methods are adopted in this program. The former method forms the basis for one version while the latter is used in a large scale version due to its high efficiency. The flow chart in Figure A.1 describes the general arrangement for the stability portion of the program.

A.2 Generalized HVDC System Model

A general model is used for HVDC schemes in either two or multi-terminal operation.⁹³⁻⁹⁸

Three types of dc buses are identified: rectifiers, inverters or non-converter dc buses. Input data for rectifiers and inverters include minimum and maximum set values for firing, or extinction, angle ($\theta_{(min)}$ and $\theta_{(max)}$).

For each dc bus, the facility for steady state control exists with three options:^{96,97}

- constant dc voltage control (category 'k' bus)
- constant dc current control (category 'l' bus)
- constant dc power control (category 'm' bus)

Input data for these controls include the desired or setting value, i.e. $V_{d(set)}$ and $\theta_{(set)} = \theta_{(min)}$, $I_{d(set)}$ or $P_{d(set)}$ respectively.

A diode rectifier will be of category 'k' with $\theta_{(min)} = \theta_{(max)} = 0$.

During steady-state simulation (load flow), Newton's method is utilized to solve the equations representing any HVDC scheme in the form:

$$F = A \Delta X \quad (A.1)$$

where F is the residual vector and ΔX is the change in the dc variables:

$$\Delta X = [\Delta I_d \quad \Delta V_d \quad \Delta \cos \theta \quad \Delta T \quad \Delta \phi]^T \quad (A.2)$$

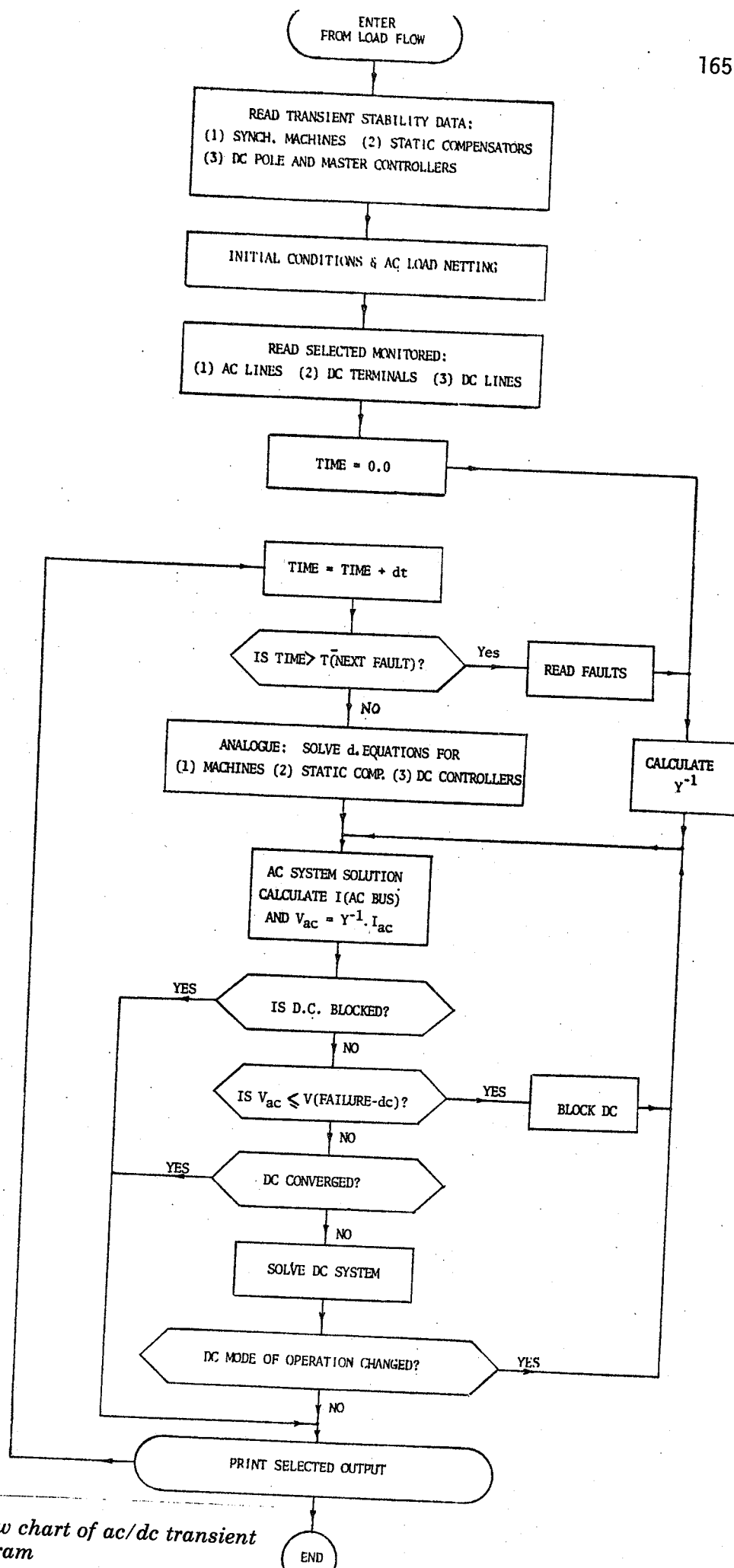


Figure A.1 Simplified flow chart of ac/dc transient stability program

where θ is the firing angle for a rectifier or the extinction angle for an inverter and

$$\phi = \tan^{-1} (Q_d/|P_d|)$$

Residual vector F depends upon the mode of control as follows: (using same p.u. dc system equations of Section 3.2 and Reference [97]).

Control Mode	k	l	m	
Residue F	Const. dc Voltage	Const. dc Current	Const. dc Power	
F_c	$\cos\theta_{(set)} - \cos\theta$	$I_{d(set)} - I_d$	$P_{d(set)} - P_d$	(A.3)
F_t	$V_{d(set)} - V_d$	$0.97V_a T N \cos\theta_{(min)}$ $-V_d$	$0.97V_a T N \cos\theta_{(min)}$ $-V_d$	(A.4)
F_p	$V_d - V_a T N \cos\phi$			(A.5)
F_v	$V_d - V_a T N \cos\theta + R_c I_d$			(A.6)
F_g	$\Sigma [G] V_d - I_d$			(A.7)

Assuming the conductance matrix $[G]$ to contain the following sub-matrices:

$$[G] = \begin{bmatrix} g_{k,k} & g_{k,l} & g_{k,m} \\ g_{l,k} & g_{l,l} & g_{l,m} \\ g_{m,k} & g_{m,l} & g_{m,m} \end{bmatrix} \quad (A.8)$$

Subscripts k, l or m denote the category of a dc bus. To avoid complications arising from the existence of zero diagonal elements in matrix A of Equation (A.1), the following step-by-step solution is developed to calculate elements of ΔX .

$$\Delta Vd_k = Ft_k$$

$$\Delta Id_k = Fc_l$$

$$\begin{bmatrix} \Delta Id_k \\ \Delta Vd_l \\ \Delta Vd_m \end{bmatrix} = \begin{bmatrix} -1 & g_{k,l} & g_{k,m} \\ 0 & g_{l,l} & g_{l,m} \\ 0 & g_{m,l} & (g_{m,m} + Pd_m/Vd_m^2) \end{bmatrix}^{-1} \begin{bmatrix} -Fg_k - g_{k,k} Ft_k \\ -Fg_l - g_{l,k} Ft_k + Fc_l \\ -Fg_m - g_{m,k} Ft_k + Fc_m/Vd_m \end{bmatrix}$$

For terminals of category 'k':

$$\Delta \cos \theta = Fc$$

$$\Delta T = (Fv + Ft - Va TN Fc + Rc \Delta Id)/VaN \cos \theta$$

$$\text{and } \Delta \phi = - (Fp + Ft + (Fp-Vd) \Delta T/T)/VaTN \sin \phi$$

For dc buses of category 'm':

$$\Delta Id = Fc/Vd - Pd \Delta Vd/Vd^2$$

For terminals of category 'l' or 'm':

$$\Delta T = (\Delta Vd + 0.97 Rc \Delta Id - Ft)/0.97 VaN \cos \theta_{(min)}$$

$$\Delta \cos \theta = (Fv + \Delta Vd + Rc \Delta Id - VaN \cos \theta \Delta T)/VaTN$$

$$\text{and } \Delta \phi = -(Fp + Ft + (Fp-Vd) \Delta T/T)/VaTN \sin \phi$$

The dc variables X are then modified by ΔX and used as initial values for next iteration until F approaches very small value. At the end of each dc iteration, however, violations for the upper and lower limits of converter transformer taps T and firing or extinction angles θ are corrected.

For transient stability simulation, each terminal in a HVDC scheme, will operate in either a constant current $Id_{(set)}$ or a constant angle $\theta_{(set)}$ mode according to its operating constraints and ac voltage condition. In this case, the converter transformers taps are considered

to be fixed at their steady state values. The equations for F_c , F_p , F_v and F_g in A.3 to A.7 still hold for categories k and l with $F_t = 0.0$.

The step-by-step solution of dc variables ΔX is then given by:

$$\Delta \cos \theta = F_{c_k}$$

$$\Delta I_{d_l} = F_{c_l}$$

$$\begin{bmatrix} \Delta V_{d_k} \\ \Delta V_{d_l} \end{bmatrix} = \begin{bmatrix} g_{k,k} + 1/R_{c_k} & g_{k,l} \\ g_{l,k} & g_{l,l} \end{bmatrix}^{-1} \begin{bmatrix} -F_{g_k} + (V_a T N F_c - F_v)_k / R_{c_k} \\ -F_{g_l} + F_{c_l} \end{bmatrix}$$

For terminals of category 'l' :

$$\Delta \cos \theta = (F_v + R_c F_c + \Delta V_d) / V_a T N$$

For dc buses of category 'k' :

$$\Delta I_d = F_g + \Sigma [G] \Delta V_d$$

For all terminals:

$$\Delta \phi = -(F_p + \Delta V_d) / V_a T N \sin \phi$$

Two possible control strategies, with their operating constraints, are accommodated for HVDC system representation; namely, current-margin and limiting-voltage control methods, through local terminal controls overseen by a central controller. Each dc terminal, except one predetermined terminal in every HVDC scheme assigned as a non-power controlled station is provided, independently, with various pole controllers to enhance the ac system performance. DC power modulation, through changing dc current order setting, is provided for frequency damping while reactive power absorbed by the dc terminal can also be modified, through firing or extinction angle, to control the ac voltage. Power order modulation at the non-power controlled terminal is provided via remote control through any other terminal in the dc scheme.

A functional diagram of various local and central controllers is shown in Figure (A.2).

Provisions for dc power order changes, blocking, deblocking and simulation of long term commutation failure and recovery from it are included in dc system dynamics. The deblocking (or starting) process is taken care of through the transfer function of power order, whereas simulation of recovery from commutation failure assumes a fast dc voltage recovery and a ramp dc current over a preset period.

A.3 Generalized Static VAR Systems Model

A unified model is used for all types of static VAR compensating systems. The model, as shown in Figure A.3, is an inertialess source, of controlled voltage magnitude E behind a fixed reactance X_S . E is always in phase with terminal voltage V_T . Different parameters of the model depend upon the specific type of static compensator as follows:

- Saturated Reactors:⁵

X_S = reactance of the saturated reactor (plus its step up transformer leakage if any)

$$V_{cont} = V_T$$

V_{ref} = knee voltage of the saturated reactor E_0

$$K = 1/(1 - X_C/X_S)$$

$$T_1 = T_{cc}$$

$$T_3 = K T_{cc}$$

$$T_2 = T_4 = T_c = 0.0$$

$$h_0 = 0.0$$

$$A = V_T(1 - \text{sign}(k))$$

$$B = -V_{cp} X_s / X_c$$

$$f(h) = V_T + h \quad \text{for } h > B$$

or

$$f(h) = E_0 \quad \text{for } h \leq B$$

where;

X_c = reactance of the slope correcting series capacitor

T_{cc} = an approximate slope correction time lag

V_{cp} = slope correcting capacitor protection voltage level.

No auxiliary signals or any other external controllers are permitted with saturated reactors.

- Transductors

X_s = equivalent total transient reactance of the fully saturated reactors

V_{cont} = ac voltage of controlled bus

V_{ref} = desired ac voltage of controlled bus

k, T_1, T_2, T_3 and T_4 = parameters of dc current controller

T_c = time lag of the dc control winding

$$A = 2\pi$$

$$B = 0.0$$

h_0 = initial saturation level

$$f(h) = V_T (2\pi - h + \sin(h)) / 2\pi$$

- Thyristor Phase Controlled Reactors and Transformer Reactors

Model parameters are given in Section 2.8.

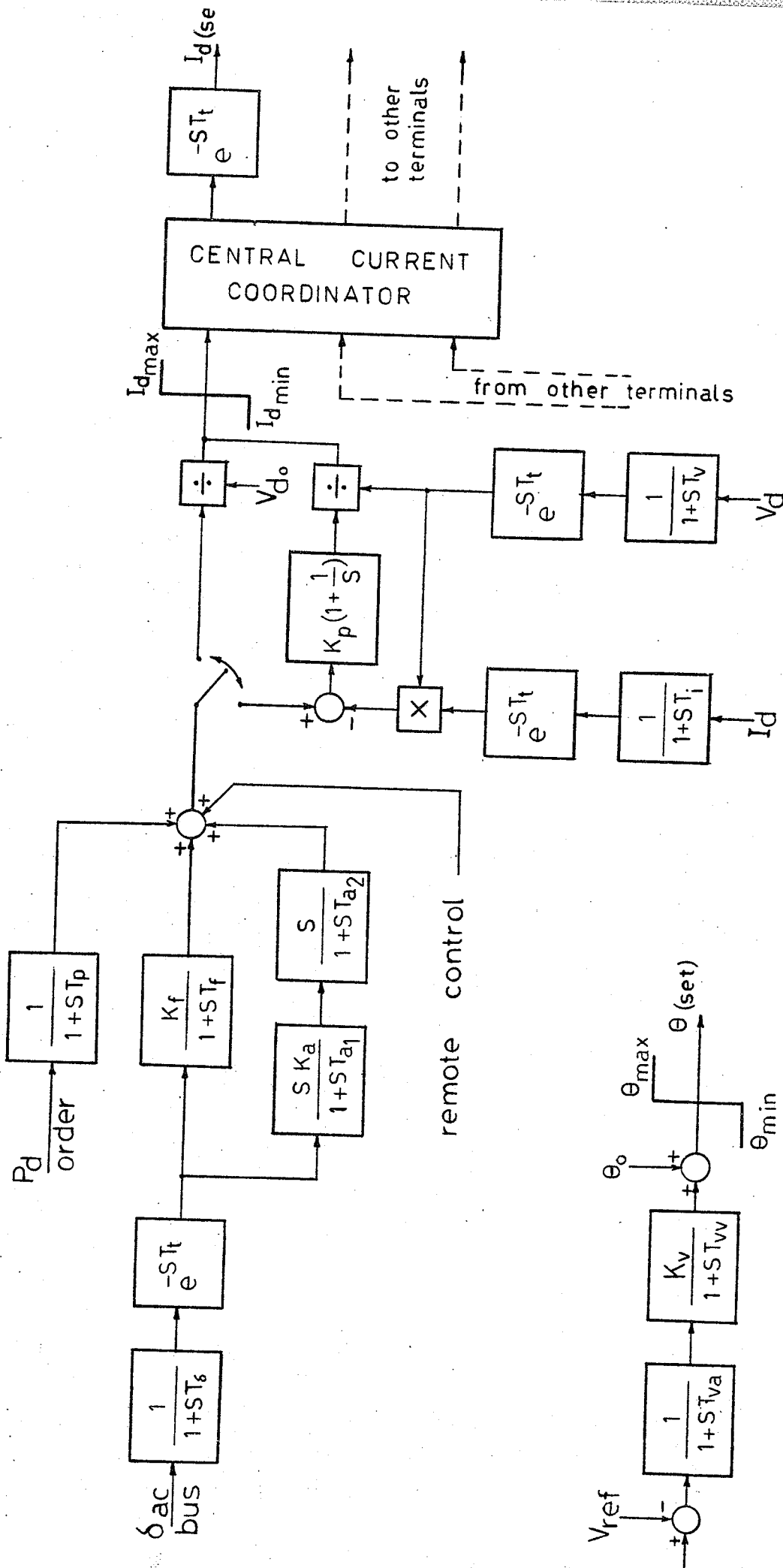


Figure A.2 Functional diagram of local and central controllers of a HVDC scheme

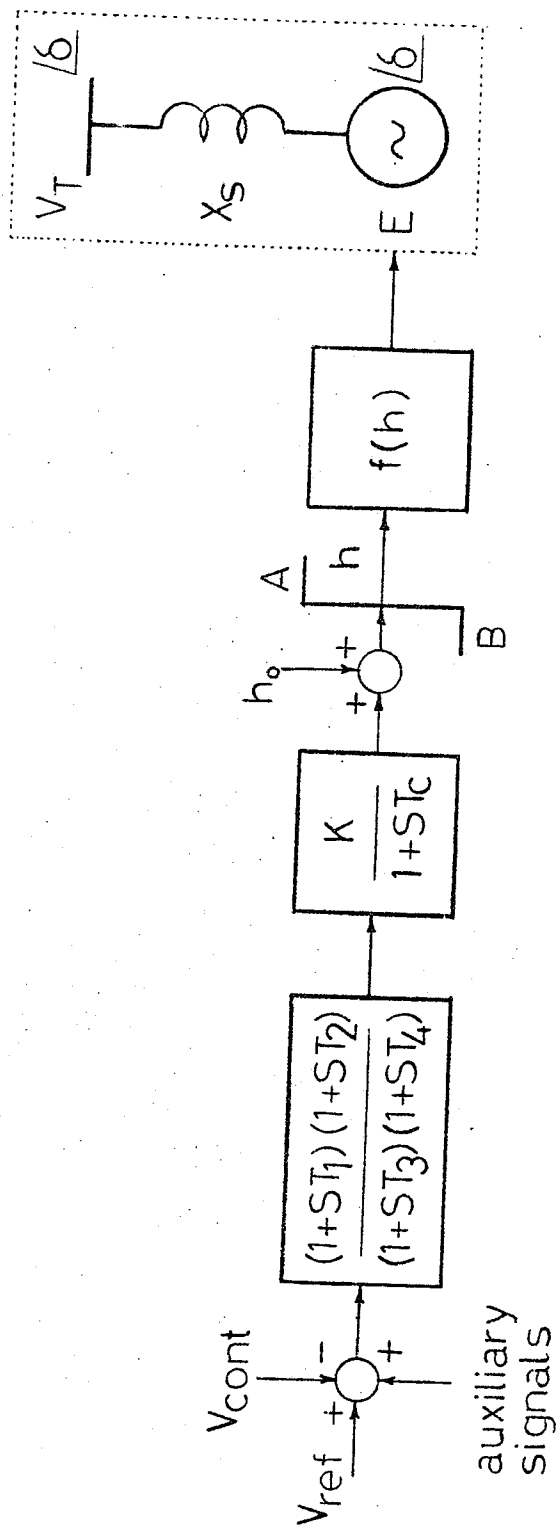


Figure A.3 Generalized model for static VAR Compensators

- Thyristor Switched Capacitor Banks

X_s = total reactance of all capacitor banks

V_{cont} = ac voltage of controlled bus

V_{ref} = desired ac voltage of controlled bus

k, T_1, T_2, T_3 and T_4 = parameters of controller

$A = 1.0$

$B = 0.0$

h_0 = initial fraction of connected capacitor banks to the total number of banks M

$f(h) = V_T(1 + Mh/M)$ (for discrete control)

A.4 Synchronous Machines Model

The subtransient model of round rotor machines is used as a general model of which other types of machine models (subtransient salient-pole, transient and classical) are considered special cases.⁹⁹

Machine saturation is also contained within the machine model.^{99,100}

Different types of exciters models with or without stabilizers as well as governor models (hydraulic or steam turbines) are provided for every synchronous machine.

A.5 System Solution

For the version where ac system is solved by Newton's method,⁸⁰ the ac system of equations is in the form:^{103,104}

$$\begin{bmatrix} \Delta P \\ \Delta Q \end{bmatrix} = \begin{bmatrix} J1 & J2 \\ J3 & J4 \end{bmatrix} \begin{bmatrix} \Delta \delta \\ \Delta V_a/V_a \end{bmatrix}$$

where $J1, J2, J3$ and $J4$ are elements of the Jacobian matrix and ΔP and ΔQ are residues of real and reactive power at each bus. The dc system

of equations, given in Section A.1, are modified to take into account the change in the ac voltage V_a . The dc equations are then directly included in ac system to give the combined Newton's solution for the integrated ac/dc system in the form;

$$\begin{bmatrix} \Delta P' \\ \Delta Q' \end{bmatrix} = \begin{bmatrix} J_1 & J_2' \\ J_3 & J_4' \end{bmatrix} \begin{bmatrix} \Delta \delta \\ \Delta V_a/V_a \end{bmatrix}$$

where the convergence of $\Delta P'$ and $\Delta Q'$ guarantees the convergence of both ac and dc systems.

The modifications to the residual vector and Jacobian matrix elements of the ac buses (i, j, \dots) interconnected to the dc converters (k, l, \dots) with current margin control strategy are:

$$\Delta P_i' = \Delta P_i - V_d I_s + F_d F_g$$

$$\Delta Q_i' = \Delta Q_i - Q_d I_s / I_d + F_e F_g + F_b F_p$$

$$J_2'(i, i) = J_2(i, i) + (F_{d_k} G'(k, k)^{-1} + V_{d_k}) a_k$$

$$J_2'(i, j) = J_2(i, j) + F_{d_k} G'(k, l)^{-1} a_l$$

$$J_4'(i, i) = J_4(i, i) + Q_{d_k} (1 - C_f^2) + (Q_d / I_d + F_e G'(k, k)^{-1}) a_k$$

$$J_4'(i, j) = J_4(i, j) + F_{e_k} G'(k, l)^{-1} a_l$$

where,

$$C_f = \cos \phi, \quad C_t = \cos \theta$$

$$F_b = Q_d / TV C_f (1 - C_f^2)$$

$$F_p = V_d - TV C_f$$

For a constant current mode converter '1':

$$I_s = I_d(\text{set})$$

$$F_d = I_d, \quad a = 0.0$$

$$F_e = -F_b + Q_d / V_d$$

For a constant angle mode converter 'k':

$$C_s = \cos \theta \text{ (set)}$$

$$I_s = -(V_d - TV C_s) / R_c$$

$$F_d = I_d - V_d / R_c$$

$$F_e = -F_b + Q_d (1 / V_d - I_d / R_c)$$

$$a = TV C_t / R_c$$

$$G'(k, k) = G(k, k) + 1 / R_{c_k}$$

For the dc network:

$$F_g = -[G']^{-1} (I_s - [G] V_d)$$

At the end of each iteration the dc converters mode of operation is determined according to their operating constraints and the ac voltage.

For the other version of the program where the ac system is directly solved by inverting the admittance matrix (using bi-factorization¹⁰¹⁻¹⁰² method)¹⁰⁵⁻¹⁰⁶ the dc system is considered as a non-linear load at the inter-connecting ac buses. The real and reactive power of this equivalent non-linear load depends on the mode of operation of each terminal and are calculated directly as follows (using same terminology):

$$\cos \theta_k = \cos \theta \text{ (set)}$$

$$I_{d_1} = I_d \text{ (set)}$$

$$\begin{bmatrix} V_{d_k} \\ V_{d_1} \end{bmatrix} = \begin{bmatrix} g_{k,k} + 1/R_{c_k} & g_{k,1} \\ g_{1,k} & g_{1,1} \end{bmatrix}^{-1} \begin{bmatrix} V_a T_N \cos \theta_k / R_{c_k} \\ I_{d_1} \end{bmatrix}$$

For terminals '1' with constant current control:

$$\cos \theta = (V_d + R_c I_d) / V_a T_N$$

For terminals 'k' with constant angle control

$$I_d = \Sigma [G] V_d$$

for terminals 'k' and 'l'

$$\cos \phi = V_d/V_a \text{ TN}$$

$$P_d = V_d I_d$$

$$Q_d = |P_d| \tan \phi$$

A.6 Computer Application

This program has been written in Fortran IV for execution on IBM 370 computer system. The execution time is linearly dependent on the size of the system being analyzed. For a given system the program generally takes approximately 50% execution cpu time as compared to programs employing Gauss-Sidel solution techniques.

BIBLIOGRAPHY

Note: References marked with * are of the author's publications.

1. CIGRE Working Group 31-01 "Static Shunt Devices for Reactive Power Control," CIGRE Paper No. 31-08, 1974.
2. Elgerd, O. I. "Electric Energy Systems Theory," McGraw-Hill, 1971.
3. Weedy, B. M. "Electric Power Systems," John Wiley, 1970.
4. Calderbank, H. A. and Ralls, J. S. "Reactive Compensation for DC Transmission with Particular Referent to Synchronous Compensators," IEE Conference on HVDC, 1966, Publication No. 22, Part I, pp. 268-269.
5. CIGRE Working Group 31-01 "Modeling of Static Shunt VAR Systems for System Analysis," Electra, No. 51, 1977, pp. 45-74.
6. Tarnawecky, M. Z. "HVDC Transmission and Advanced HVDC Transmission," (Graduate Courses), University of Manitoba, 1975.
7. Kimbark, E. W. "Improvement of Power System Stability by Changes in the Network," IEEE Trans., Vol. PAS-88, 1969, pp. 773-781.
8. Farouk, A. M. Rizk and Hamdi, M. E. El-Shair. "Power Frequency Overvoltages on Long Overhead Lines with a Special Reference to the Aswan-Cairo 500 KV Transmission System," CIGRE, 1966, Report No. 412, pp. 1-14.
9. Dobsa, J. and Huber, F. "Shunt Reactors with and without Loadable Secondary Windings," Brown Boveri Review 59, 1972, No. 8, pp. 410-415.
10. Johnston, D. L. and Johnson, I. B. "EHV Shunt Reactors," Transmission Systems Engineering Conference, 1975, Rev. 10/20/75.
11. Electrical Review, "Arc Connection of Reactor at 500 KV," December, 1964.
12. Becker, H., et al. "Three Phase Shunt Reactors with Continuously Controlled Reactive Current," CIGRE Paper No. 31-13, 1972.
13. Kuchumov, L. A., et al. "Voltage Regulation in Networks by a Controlled Static Compensator with Parametric Regulation," Electric Technology USSR, No. 10, 1973.
14. Friedlander, E. "Static Network Stabilization," GEC Journal, 1966, pp. 58-64.

15. Dixon, G. F., et al. "Static Shunt Compensation for Voltage Flicker Suppression," IEE Conference Report Series No. 8, 1964, pp. 45-61.
16. Friedlander, E. and Jones, K. M. "Saturated Reactors for Long Distance Bulk Power Lines," Electrical Review, 27th June, 1969, pp. 940-943.
17. Friedlander, E. and Garrard C. "Long Distance Power Transmission by Alternating Current," Engineering, January, 1942.
18. Friedlander, E. "Static Network Stabilization - Recent Progress in Reactive Power Control," GEC Journal, Vol. 33, No. 2, 1966.
19. Friedlander, E. and Young, D. "AC Saturated Reactors for Power System Stability," Electrical Review, January, 1965.
20. Young, D. "Voltage Fluctuations and Their Suppression," ERA Distribution Conference, Edinburgh, October, 1967.
21. Thanawala, H. and Young, D. "Saturated Reactors - Some Recent Applications in Power Systems," Energy International, Vol. 7, No. 11, 1970.
22. Ralls, K. J. "Recent Developments in the Application of Saturated Reactors in Transmission and Distribution Systems," British Technical Symposia, Argentina, Nov. 1970.
23. Banks, R., et al. "Application to EHV Transmission of Static Compensators Using Saturated Reactors," IEEE Canada Communication and EHV Conference, Nov., 1972, pp. 153-154.
24. Electrical Review, "Reactive Compensation for Electrical Power," 17 August, 1973.
25. Armstrong, W. and Montgomery, D. "Saturated Reactors Aid Long Distance AC Line Planning," Engineering International, July, 1975.
26. Snider, L. A. "Saturated Reactors for Voltage Control," CEA Spring Meeting, Toronto, March, 1973.
27. Ainsworth, J. D., et al. "Long Distance AC Transmission Using Static Voltage Stabilizers and Switched Linear Reactors," CIGRE Paper No. 31-01, 1974.
28. Thanawala, H. L., et al. "The Application of Static Shunt Reactive Compensators in Conjunction with Line Series Capacitors to Increase the Transmission Capabilities of Long AC Lines," CIGRE Paper No. 31-09, 1976.

30. Richert, K., Schweickardt, H. E. "Application of Controllable Reactor Compensators in AC Systems," BBC Brown Boveri Publication No. CH-E201623E.
31. Reichert, K., Kauferle, J. and Glavitsch, H. "Controllable Reactor Compensator for More Extensive Utilization of High Voltage Transmission Systems," CIGRE Paper No. 31-04, 1974.
32. Brown Boveri Review. "Static and Electronic Regulated Phase Compensators Above 100 MVA," 1973.
33. Herbst, W., et al. "Controllable Static Reactive Power Compensation of H.V. Systems," Brown Boveri Review 9/10-1974.
34. Erche, M., Hettler, H. P. and Povh, D. "Performance of Static Compensators," IEEE Conference, Montreal, 1976, pp. 350-353.
35. McAlister, G. M. "Application of Static Devices for Power System Voltage Control," IEEE Western Canada Tour Paper, November, 1975.
36. Moran, R. J., Titus, C. H., Tice, J. B. "Solid State Converters for Power System Voltage Control," Proceedings of the American Power Conference, 1975.
37. Motto, J. W., Orange, D. P., and Otto, R. A. "The Static VAR Generator and Alternative Approaches to Power System VAR Compensation," Proceedings of the American Power Conference, 1975.
38. Mathur, R. M. "A Study of the Overvoltage Performance of the BBC Controllable Reactor: with Special Reference to the Design for Laurentides," Report BBC, Baden, 1 November, 1976.
39. Frank, H. "Power-factor Correction with Thyristor-controlled Capacitors," ASEA Journal, Vol. 44, No. 8, 1971.
40. Olwegard, A., Ahlgren, L., and Frank, H. "Thyristor Controlled Shunt Capacitors for Improving System Stability," CIGRE Report No. 32-20, 1976.
41. Woodford, D. A. and Tarnawecy, M. Z. "Compensation of long Distance AC Transmission Lines by Shunt Connected Reactance Controllers," IEEE Trans., Vol. PAS-94, No. 2, 1975, pp. 655-662.
42. Ainsworth, J. D., et al. "Application of Saturated Reactors to AC Voltage Stabilization for HVDC Transmission and Other Large Convertors," IEEE PES Summer Meeting & EHV/UHV Conference, 1973, Paper No. 73, pp. 431-434.
43. Miller, R. L. "Automatic Control of the E1 Chocon Power Transmission System," IEE HVDC and/or AC Power Transmission Conference Publication No. 107, 1973, pp. 92-113.

- *44. Hammad, A. E. "Reactive Power Shunt Compensation for 500 KV Line Between Dorsey and Forbes," Manitoba Hydro, Tech. Memo, March, 1976.
- *45. Mathur, R. M., Dash, P. K. and Hammad, A. E. "Application of a Fast Acting Static Reactive Power Compensator at the Terminals of a Superconducting Generator," Paper 1-50, World Electrotechnical Congress, Moscow, 1977.
- *46. Dash, P. K., Mathur, R. M. and Hammad, A. E. "Improvement of Performance of a Superconducting Turbo Generator Through Use of a Controllable Reactive Power Compensator," Electrical Machines and Electromechanics: An International Quarterly, Vol. 2, 1977, pp. 73-86.
- *47. Dash, P. K., Hammad, A. E., and Mathur, R. M. "Application of a Thyristor Controlled Reactor at the Terminals of a Superconducting Alternator," IEEE Int. Electrical & Electronics Conference, Toronto, 1977, Paper No. 77192.
- *48. Hammad, A. E., and Mathur, R. M. "A New Generalized Concept for the Design of Thyristor Phase Controlled VAR Compensators - Part I: Steady State Performance," to be presented at the IEEE, PES Summer Meeting, 1978 and published fully in Trans. of PAS.
- *49. Mathur, R. M. and Hammad, A. E. "A New Generalized Concept for the Design of Thyristor Phase Controlled VAR Compensator - Part II: Transient Performance," to be presented at the IEEE, PES Summer Meeting, 1978 and published fully in IEEE Trans. on PAS.
- *50. Hammad, A. E. and Mathur, R. M. "A New Thyristor Controlled VAR Compensator Design," Paper submitted to the IEEE Canadian Conference on Communications and Power, Montreal, 1978.
51. Beriger, C., Etter, P., Hengsberger, J., and Thiele, J. "Design of Water-Cooled Thyristor Valve Groups for Extension of Manitoba Hydro HVDC System," CIGRE Paper No. 14-05, 1976.
52. Gyugyi, L. and Otto, R. A. "Static Shunt Compensation for Voltage Flicker Reduction and Power Factor Correction," American Power Conference, 1976.
53. Adamson, C. and Hingorani, N. G. "High Voltage Direct Current Power Transmission," Garraway Ltd., 1960.
54. Cory, B. J., et al. "High Voltage Direct Current Convertors and Systems," Macdonald: London, 1965.
55. Kauferle, J., et al. "HVDC Stations Connected to Weak AC Systems," IEEE Trans., Vol. PAS-89, No. 7, 1970, pp.1610-1617.

56. Lips, H. P. "Aspects of multiple infeed of HVDC Inverter Stations into a Common AC System," IEEE Trans., Vol. PAS-92, 1973, pp. 775-778.
57. Bower, J. B., et al. "Reactive Power Requirements of AC Systems and AC/DC Convertors," IEE Conference on DC Transmission, 1966, No. 20.
58. Gavrilovic, A. "Large DC Infeeds Relative to AC Systems: Considerations of Higher Voltages and Thyristors," IEE Conference on EHV Trans., 1968.
59. Gavrilovic, A. and Taylor, D. G. "The Calculation of the Regulation Characteristics of DC Transmission System," IEEE Trans., Vol. PAS-83, 1964, pp. 215-223.
60. Kauferle, J. and Beriger, C. "Possibilities to Control the AC Busbar Voltage by the Reactive Power of an HVDC Terminal," IEE Conference, Publication No. 107, 1973, pp. 75-79.
61. Beriger, C. "Reactive Load at HVDC Terminals," Brown Boveri Review 60 (1973), pp. 95-99.
62. Thio, C. "Effects of 500 KV Line upon Dorsey D.O.V. Compensation," Manitoba Hydro, May, 1976.
63. Machida, T. "Improving Transient Stability of AC System by Joint Usage of DC System," IEEE Trans., Vol. PAS-85, No. 3, 1966.
64. Haywood, R. W. and Patterson, W. A. "Applications of Control on the Eel River and Nelson River HVDC Schemes to Enhance Operation of Interconnected System," CIGRE Paper No. 14-04, 1976.
65. Haywood, R. W. and Ralls, K. J. "Use of HVDC for Improving AC System Stability and Speed Control," Manitoba Power Conference, June, 1971, pp. 779-803.
66. Becker, W. and Hochstetler, W. "HVDC Transmission System Connected to an Isolated Hydro Power Station," IEE Conference, Publication No. 107, 1973, pp. 237-241.
67. Kanngiesser, K. W. and Lips, H. P. "Control Methods for Improving the Reactive Power Characteristic of HVDC Links," IEEE Trans., Vol. PAS-89, No. 6, 1970, pp. 1120-1125.
68. Althaus, B., et al. "Control Methods for Improving the Reactive Power Characteristic of HVDC Inverter Stations," IEE Conference HVDC and/or AC, 1973, pp. 60-64.
69. Breuer, G. D., et al. "The Dynamic Performance of AC Systems with HVDC Transmission Links," CIGRE Paper No. 14-02, 1976.

70. Kirkham, H. and Mosher, C. "Control of Real and Reactive Power to HVDC System to Stabilize AC System - Part I and Part II," IEE Conference Publication No. 107, 1973, pp. 65-74.
71. Sucena, J. P., et al. "Stability of a DC Transmission Link Between Strong AC Systems," IEE Proc., Vol. 120, No. 10, 1973, pp. 1233-1241.
72. Vithayathil, J. J. "Experience with Harmonic Problems at Celilo HVDC Station," IEE Conference Publication No. 107, 1973, pp. 6-10.
73. Hayashi, T., et al. "Voltage Regulation Characteristics of AC-DC Interconnecting Point and Its Suppression Method." Elec. Eng. in Japan, Vol. 93, No. 4, 1973.
74. Machida, T. "Effect of DC System Upon Generator Terminal Voltage Rise at Remote Load Interruption," Direct Current, Vol. 2, No. 2, 1970.
75. Yoshida, Y. "Development of a Calculation Method of AC Voltage Stability in HVDC Transmission Systems," Elec. Eng. in Japan, Vol. 94, No. 2, 1974.
76. Yoshida, Y. and Machida, T. "AC Voltage Stability on AC-DC Power Transmission System," IEEE Conf. Paper No. 75 195-3, 1975.
77. Friedlander, E. "Features of a Static Reactive Power Supply for Polyphase Inverters," IEE Conference on HVDC, Publ. No. 22, Part I, No. 54, 1966, pp. 270-274.
78. Lips, H. P. and Ring, H. "The Performance of AC Systems with Predominant Power Supply by HVDC Inverters, (and discussion by Dougherty, J, Thio, C. V. and Woodford, D. A.), IEEE Trans., Vol. PAS-94, No. 2, 1975.
- *79. Hammad, A. E., Woodford, D. A. and Mathur, R. M. "AC Voltage Control at an HVDC Terminal," Paper submitted to the IEEE Canadian Conference on Communications and Power, Montreal, 1978.
- *80. Hamad, A. E. "A Transient Stability Program for a Power System with Multi-Terminal HVDC Networks and VAR Static Compensators," IEEE International Conference and Exposition, Toronto, 1977, Paper No. 77075.
- *81. Wexler, A. and Hammad A. E. "Solution of Large Sparse Systems in Design and Analysis," G-MTT International Microwave Symposium, Palo Alto, California, May 1975.
82. Tishinski, W. J. and Rice, D. A. "MANDAN Transmission Considerations," CIGRE Study Committee No. 14 Meeting and Colloquium, Winnipeg, June 1977.

83. Jefferies, M. J., et al. "Prospect for Superconducting Generators in the Electrical Utility Industry," IEEE Transaction on Power Apparatus and Systems, Vol. PAS-92, 1973, pp. 1659-1669.
84. Einstein, T. H. "System Performance Characteristics of Superconducting Alternators for Electric Utility Power Generation," IEEE Transaction on Power Apparatus and Systems, PAS-94, 1975, pp. 310-319.
85. Furuyama, M. and Kirtley, J. L. "Transient Stability of Superconducting Alternators," *ibid*, PAS-94, 1975, pp. 320-328.
86. Kirtley, J. L. and Furuyama, M. "A Design Concept for Large Superconducting Alternators," *ibid*, PAS-94, 1975, pp. 1264-1269.
87. Lawrenson, P. J., et al. "Damping and Screening in the Synchronous Superconducting Generator," Proceedings IEE, Vol. 123, No. 8, 1976, pp. 787-794.
88. Bratoljic, T., Fursich, N., and Lorenzen, H. W. "Transient and Small Perturbation Behaviour of Superconducting Turbo-generators," IEEE Transaction, PAS-96, No. 4, 1977, pp. 1418-1429.
89. Woodson, H. H., et al. "The application of Superconductors in the Field Winding of Large Synchronous Machines," IEEE Trans., Vol. PAS-90, 1971.
- *90. Mathur, R. M., Dash, P. K. and Hammad, A. E. "Transient and Small Signal Stability of a Superconducting Turbogenerator Operating with Thyristor Controlled Static Compensator," Paper submitted to the IEEE, PES Summer Meeting, 1978.
91. Breuer, G. D., Luini, J. F. and Young, C. C. "Studies of Large AC/DC Systems on the Digital Computer," IEEE Transactions on Power Apparatus and Systems, Vol. PAS-85, November, 1966.
92. Carter, G. K., Grund, C. E., Happ, H. H. and Pohl, R. V. "The Dynamics of AC/DC Systems with Controlled Multiterminal HVDC Transmission," IEEE, Vol. PAS-96, 1977, pp. 402-413.
93. Kanngiesser, K. W., Bowles, J. P., Ekstrom, A., Reeve, J. and Rumpf, E. "HVDC Multiterminal Systems," CIGRE Paper 14-08, Paris, 1974.
94. Foerest, R., Heyner, G., Kanngiesser, K. and Waldmann, H. "Multiterminal Operation of HVDC Converter Stations," IEEE Transactions on Power Apparatus and Systems, Vol. PAS-88, No. 7, July, 1969.
95. Reeve, J. and Carr, J. "Review of Techniques for HVDC Multiterminal Systems," IEE Int. Conference, Publication, HVAC/DC Transmission, London, 1973.

96. Fahmy, G., Reeve, J., and Stott, B. "Load Flow in Multiterminal HVDC Systems" CIGRE, 14-75 (SC) 08, Johannesburg, October, 1975.
97. Reeve, J., Fahmy, G. and Stott, B. "Versatile Load Flow Method for Multiterminal HVDC Systems," IEEE, Vol. PAS-96, 1977, pp. 925 - 933.
98. Reeve, J., Rose, I. A. and Carr, J. "Central Computer Controller for Multiterminal HVDC Transmission Systems," IEEE, Vol. PAS-96, 1977, pp. 934 - 944.
99. Carter, G., et al, "Input Validation and Output Management for Power Flow and Stability," PICA, 1977.
100. Schulz, R. P. "Synchronous Machine Modelling," Paper C72616-1, IEEE PES Summer Meeting, July 1972.
101. Dandeno, P. L. and Kundur, P. "A Non-iterative Transient Stability Program Including the Effects of Variable Load-voltage Characteristics," IEEE, Vol. PAS-92, 1973, pp. 1478 - 1483.
102. Brown, H. E., et al. "Transient Stability Solution by an Impedance Matrix Method," IEEE, Vol. PAS-84, 1965, pp. 1204 - 1212.
103. Tinney, W. F. and Hart, C. E. "Power Flow Solution by Newton's Method," IEEE, Vol. PAS-86, 1967, pp. 1449 - 1460.
104. Stagg, G. W. and El-Abiad, A. H. "Computer Methods in Power Systems Analysis," McGraw-Hill Co., N.Y. 1968.
105. Tinney, W. F. and Walker, J. W. "Direct Solution of Sparse Network Equations by Optimally Ordered Triangular Factorization," Proceedings IEEE, 1967, pp. 1801 - 1809.
106. Zollenkopf, K. "Bi-Factorization - Basic Computational Algorithm and Programming Techniques," Large Sparse Sets of Linear Equations, Edited by J. K. Reid, Academic Press, 1971, pp. 75 - 96.